WIPP Library

March 27, 1995

Systems Prioritization Method - Iteration 2 Baseline Position Paper:

Rock Mechanics: Creep, Fracture, and Disturbed Rock Zone (DRZ)

D.E. Munson, D.J. Borns, M.K. Pickens,
D.J. Holcomb, and S.E. Bigger

Sandia National Laboratories
Albuquerque, NM 87185

ABSTRACT

The Rock Mechanics Program is important to the establishment of a radioactive waste repository in salt because rock mechanics deals with the prediction of creep closure and eventual encapsulation of the waste. The intent of this paper is to give the current status of the program. This program consists of three major modeling efforts: continuum creep, fracture, and the disturbed rock zone. These models, together with laboratory material parameters, plastic flow potentials, initial and boundary input data, and other peripheral information forms the predictive technology. The extent to which the predictive technology is validated against in situ test data adds certainty to the method. Application of the technology is through simulations of the test results, design, or performance using numerical codes. In summary, the predictive capabilities are technically sound and reasonable. The current status of the program is that which would be advanced for compliance.

950322

CONTENTS

1.0 INTRODUCTION 1

2.0 CREEP 5
2.1 Constitutive Model 7
2.2 Flow Potential 15
2.3 Material Parameters 15
2.4 Stratigraphy and Initial Conditions 16
2.5 Numerical Codes 16
2.6 Remarks 17
2.7 Continuum Creep Data to Analysis Guide 18

3.0 FRACTURE 21
3.1 Fracture Constitutive Model 22
3.2 Fracture Model Parameters 23
3.3 Numerical Code MDCF Model Incorporation 24
3.4 Discrete Fracture - Fracture Mechanics Approach 24
3.5 Discrete Fracture - Local Approach 27
3.6 Remarks 27
3.7 Fracture Model Data to Analysis Guide 27

4.0 DISTURBED ROCK ZONE (DRZ) 29
4.1 Process Model of DRZ 29
4.2 Kinetics of Healing 30
4.3 Permeability Relationship to Damage 30
4.4 Peripheral Inputs 31
4.5 DRZ Characterization 31
4.6 Remarks 32
4.7 DRZ Process Model to Analysis Guide 33

5.0 SUMMARY 35

6.0 REFERENCES 37

Figures

1. Tertiary creep curve schematic with continuum model noted. 6
2. Plan view of the *in situ* tests in the WIPP facility. 8
3. Local stratigraphy at the WIPP horizon. 9
4. Calculated and measured closures of Room D and Room B. 12
5. Comparison of calculated and measured Room Q closures. 13
6. Deformation mechanism map for salt. 14
7. Comparison of in situ ultrasonic equivalent of damage against MDCF model calculation. 25
8. Predicted damage around a TRU test panel room. 26

Tables

I. Rock Mechanics Models 2
II. Relevant Performance Assessment (PA) References 2
III. Rock Mechanics Program Support Correlations 4
IV. Parameter Values for the M-D Model 11
V. Continuum Creep Data and Analysis Guide 19
VI. Fracture Model Data and Analysis Guide 28
VII. DRZ Process Model Data and Analysis Guide 33

ACRONYMS

CFR	Code of Federal Regulations
DC	Direct Current
DRZ	Disturbed Rock Zone
EATF	Engineered Alternatives Task Force
EM	Electromagnetic
MD	Multimechanism Deformation (model)
MDCF	Multimechanism Deformation Creep Fracture
NAS	National Academy of Sciences
PA	Performance Assessment
WIPP	Waste Isolation Pilot Plant

1.0 INTRODUCTION

An important aspect of radioactive waste disposal is the ability of the repository to ensure public safety through isolation of the waste from the accessible environment until the waste is no longer radioactive. The fact that salt slowly deforms or "creeps" with time and that fractures in salt heal under load suggests that in a radioactive waste repository in a natural salt formation the rooms would eventually creep closed and encapsulate the waste, isolating it from the accessible environment for the relevant regulatory time period. The technical question concerns the need to know exactly how and when this creep process occurs with respect to other possible events so that we may state with reasonableness that repository safety is ensured. To answer this concern, a predictive technology is required. The technology is based on establishing a mathematical equation which simulates the known salt behavior as accurately as possible based on laboratory data and validated against measured short-term *in situ* data. This mathematical equation or constitutive model can then be used to answer the important questions about the repository condition far into the future—in other words to predict the behavior. The description of this predictive technology and its technical basis follows.

The disposal of radioactive waste imposes unique engineering requirements in that it is necessary to predict the behavior of the repository perhaps as much as 10,000 years. Even though the rock mechanics processes discussed here will occur on a faster time scale, usually a few hundred years, the only way such predictions can be made is through calculations based on an understanding of the behavior obtained over a relatively short interval of contemporary observation. Predictive calculations such as these require three elements: a *model*, which is a mathematical description of the behavior; *material parameters*, which are the values (numbers) relating an individual material to the behavior; and a calculational method, which may be an analytic method but which is often a computer program or *numerical code*. Together with other important peripheral information, these three fundamental elements form a predictive technology. The subject of this paper is essentially a discussion of the specific models and predictive technology developed for the Rock Mechanics Program under the auspices of the Waste Isolation Pilot Plant (WIPP) Project.

In the Rock Mechanics Program, there are both discrete material response models and process models. A list of these models and an evaluation of their status is given in Table I. Although the discrete material behavior model may be quite complicated, it is always related to one type of material, such as salt. The process model is actually a collection of several types of other models, assembled to describe a more complicated physical situation, such as the behavior of a disturbed rock zone (DRZ) which forms around underground openings. For example, in this case, the process model must include, at least, models that determine the

Table I. Rock Mechanics Models

Phenomenon	Model	Status
Creep	Multimechanism Deformation (M-D) Model	Technically Sound, Validated Against In Situ Data
Fracture	M-D Coupled Fracture (MDCF) Model	Technically Sound, Partially Validated Against In Situ Data
DRZ	Process Model (involving several models)	Still in Development, Usable

formation of microfractures, the creep closure, the potential healing of microfractures, and the relation between fracture and permeability.

The Rock Mechanics Program considers *creep*, the time-dependent deformation of salt; *fracture*, the time-dependent development of creep-induced microfracture formation and damage; and the *disturbed rock zone* (DRZ), the region adjacent to the excavated openings affected by the development of damage with attendant changes in permeability. The understanding of the rock mechanical or structural response of the underground excavations in the salt is one of the critical applied engineering areas of study for the WIPP Program. It is utilized either (1) directly through performance calculations of repository room and shaft closure or (2) indirectly through the prediction of coupled behavior of room contents under concurrent gas generation, the crushed salt backfill, the compaction of crushed salt seal components, the formation of the DRZ adjacent to rooms and seals, and the potential increases in permeability and eventual healing adjacent to seal locations. The full array of fundamental behaviors or processes covered by the Rock Mechanics Program are given in Table II (Rechard et al., 1989; WIPP PA, 1992a,b).

Table II. Relevant Performance Assessment (PA) References

Phenomenon or Process	PA (1992) Reference
Creep Closure	Vol. 2 p. 2-55 (2.3.5) Vol. 3 p. A109
Seal System Performance* DRZ	Vol. 2 P. 2-45 (2.3.2) Vol. 2 p. 2-45 (2.3.2.2) and p. 2-42 (2.3.1)
Compaction Processes* (e.g., back stress development, etc.)	Vol. 2 p. 2-28 (2.3.2.3)
Fracture (propagation)	Vol 2 p. 2-42 (2.3.1)

* Not part of Rock Mechanics Program but included for completeness.

In those cases where the understanding of individual process has progressed sufficiently, the constitutive models and the associated material parameters have been specified. In addition, to establish the relevance to performance assessment and regulatory requirements, the appropriate reference is made to the Performance Assessment documentation (WIPP PA, 1992a,b). However, mathematical definition of individual models, parameter lists, and databases are too extensive to repeat here, but will be summarized by example throughout the paper as appropriate.

The basis for the mechanical performance of a radioactive waste repository was initially defined by the National Academy of Sciences, Committee on Waste Disposal (NAS, 1957) based on the ability of rooms in natural salt deposits to creep closed with time and ensure the isolation of the waste for sufficient time to render it harmless. The NAS recommended a natural deposit of salt for three reasons: (1) its thermal properties, (2) its physical properties (e.g., creep deformation), and (3) the very existence of the salt deposit for hundreds of millions of years demonstrates its isolation from circulating groundwater and the stability of the geologic formation in which it is located. For non-heat producing waste, such as that proposed for the WIPP, only the last two reasons pertain. Because the Rock Mechanics (Creep, Fracture, and DRZ) Program incorporates processes affecting total repository performance (e.g., room and seal performance, migration pathways, etc.), this program bears on compliance issues in both *40 CFR 191* and *40 CFR 268.6*. With the citations in the 92 PA document, further specific references to the regulations will not be made, except for well defined cases.

As a result of the basic NAS premise and the subsequent regulations, the principal direct application of the models developed by the Rock Mechanics Program is the calculation of the creep closure of the rooms and shafts, with or without contributions from the development of the DRZ. In addition to providing the primary compliance evaluation of the creep closure of the repository to ensure the encapsulation of the waste, the general application of the constitutive models and results of the Rock Mechanics Program directly and indirectly support technical goals of other WIPP programs. The most direct support is of the Disposal Room and Drift Systems and the Seal Design and Modeling Programs, as shown in Table III. The Rock Mechanics Program also provides indirect support to other programs of the WIPP Project, although these will not be discussed here.

As is evident, the current status of the three elements of the Rock Mechanics Program are in fact statements of the rock mechanics *program position* and the technology base that would currently support any formal compliance submittal.

Table III. Rock Mechanics Program Support Correlations

Activity	Creep	Fracture	DRZ
Repository Creep Closure	X		
Room and Drift Systems			
Backfill	X		
Waste	X		
Disposal Room	X	X	X
Eng. Alt. Sys. Analy.	X		
Seal Design and Modeling			
Components	X	X	X
Seal and System Design	X	X	X
Small-Scale Seal Test	X	X	X
Large-Scale Seal Test			
Large-Seal Brine Inflow	X	X	X
Salado Permeability vs. Stress	X	X	X

The three major areas of the Rock Mechanics Program will be discussed separately because they represent somewhat discrete but closely related efforts at different stages of development. In each area, a brief status summary is given which will be indicative of the technical soundness and level of validation of the model involved. Significant aspects of the model development, parameter evaluations, and data will be traced through important references, and in some cases will be included in the paper. The major consequences for compliance are noted for each model area.

2.0 CREEP

As previously noted, one of the advantages of placing radioactive waste in natural salt deposits is that the salt undergoes time-dependent deformation or creep and therefore will eventually close the repository rooms and encapsulate the waste. Even in more complex situations, such as concurrent gas generation, the mechanical or structural response of the repository or shaft is governed by the creep of the salt. In fact, the mechanical behavior of salt, as expressed by creep, is one of the fundamental inputs to the design and performance assessment of the repository and seal systems. It has already proven influential in repository design through structural evaluation of several room configurations (Krieg et al., 1980). In this regard, it is critical that the creep process be adequately understood and properly described to permit reasonable long-term predictions of the repository performance required by the regulatory standards.

A simple representation of a standard creep curve is given in Figure 1, which shows the strain as a function of time for a specimen under a constant stress and temperature. This figure indicates the customary decomposition of the curve into a steady-state creep and transient creep components. Also, two different creep curves are indicated, one with tertiary creep behavior as marked by an accelerated creep rate caused by progressive failure of the material, and one denoted as a continuum creep curve matching the continuum creep model in which the tertiary behavior is suppressed. Tertiary creep contains all of the aspects of the development of the DRZ, in that the early stage of tertiary creep is caused by the generation of microfractures; as the microfractures increase, grow, and coalesce to form discrete cracks in the late stage of tertiary creep, the material ultimately fails.

The detailed technology that permits the prediction of the structural response consists of a constitutive model for creep, the material parameters for all of the materials in the site stratigraphy, and a numerical code for calculation of the response of the repository structure. In addition, because the actual stress fields involved are three-dimensional, there must be a flow potential which describes the deformation of salt in response to a three-dimensional stress state. Two other inputs are required: the stratigraphy which gives the materials and elevations of the bedded layers in the natural salt (evaporite) deposit, and the initial stress condition.

The constitutive model of salt creep, the experimentally determined parameter values, and the numerical codes required for simulation of WIPP structural problems, at the current stage of development, are well established on technically sound principles and data. At this

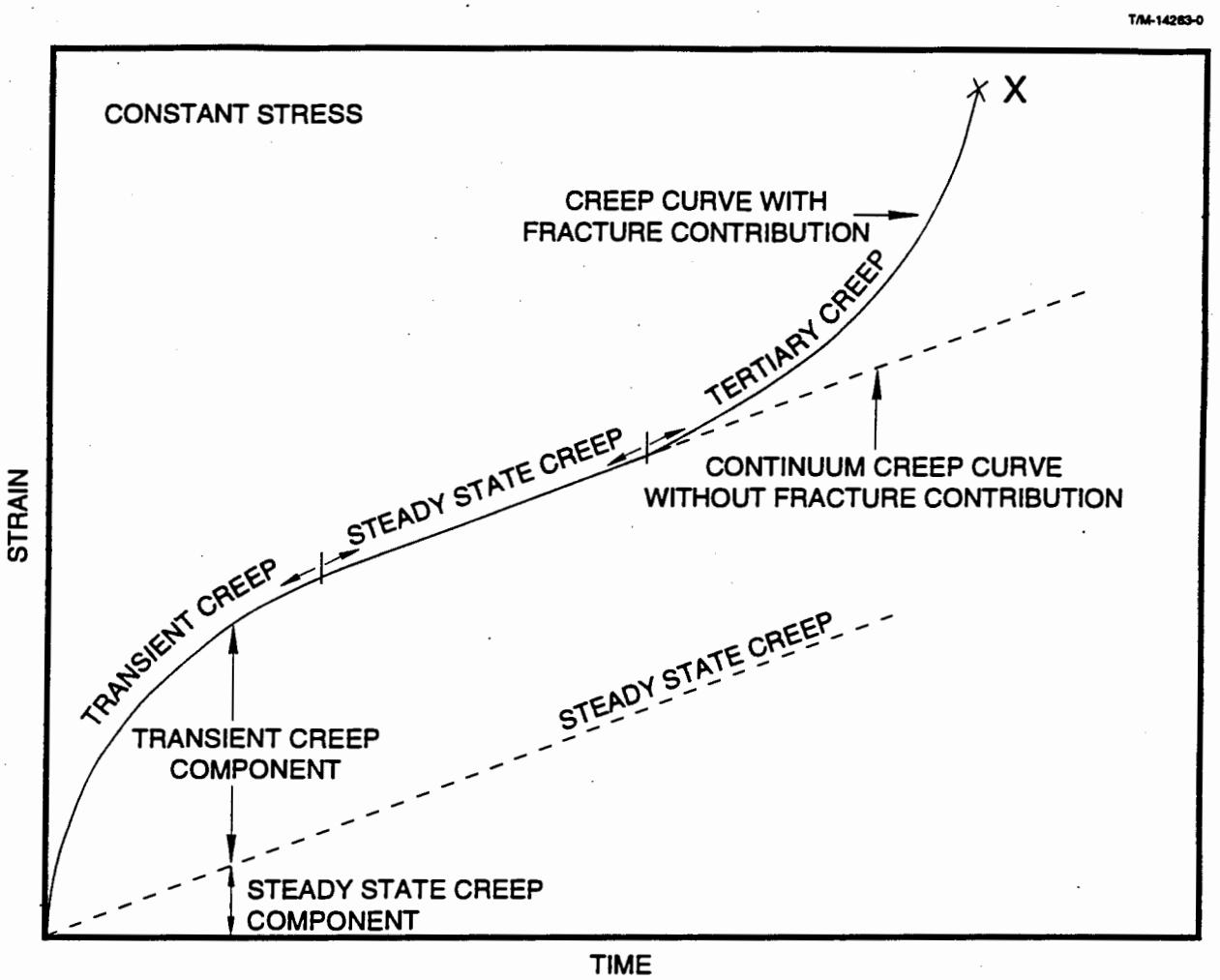

Figure 1. Tertiary creep curve schematic with continuum model and fracture contribution noted.

time, the creep predictive technology is the most sound and best validated of the models and technologies of the Rock Mechanics Program. However, to establish site-specific compliance criteria and demonstrate compliance with general regulatory criteria, completion of ongoing efforts in several areas will potentially assist in demonstrating regulatory compliance. Briefly, these are the determination of the creep parameter distribution functions for argillaceous salt, further definition of the fast probability integration methodology, additional improvements in calculational speed of the codes, probabilistic evaluation of room and shaft closure, and some minor additional improvements in the current three-dimensional code capability.

2.1 Constitutive Model

During the course of the project, two constitutive models of continuum creep have been used for performance assessment: the multimechanism deformation steady-state creep response with workhardening/recovery transient creep model (Munson et al., 1989a), and a steady-state, reduced modulus model (Morgan et al., 1986).

The model that produces very reasonable agreement with the extensive in situ test data and is proposed as the new reference model is the multimechanism deformation steady-state creep response with workhardening/recovery transient (M-D) model. Room closures (as required by *40 CFR 268.6(b)(3)* and *40 CFR 268.6(b)(5)* and environmental performance standard *40 CFR 264.601*) as measured from a number of *in situ* tests have been successfully predicted using this model, together with the recommended updated stratigraphy (Munson et al., 1989a). The agreement between calculated and measured room closures is typically better than 10%, with the longest current comparison of 3.5 years. This indicates that the model and predictive technology may be valid within acceptable uncertainty (Munson and DeVries, 1991). A plan view of the WIPP underground together with designations of the *in situ* test rooms is given in Figure 2. The updated stratigraphy is as shown in Figure 3. The simulations included both heated (Room B) and unheated (Room D and G) single rooms, a multiple room complex (Rooms A), a cylindrical room (Room Q) and a shaft (Air Intake Shaft - Shaft V), a cylindrical pillar (Room H), and the computationally complicated, three-dimensional, intermediate-scale borehole test (Rooms C). As a result of the success of this model in simulating the room closure of a range of significantly different room and shaft geometries, which implies different stress fields, using a single reference set of parameters (see Table IV), suggests that this model is reasonable for WIPP use (WIPP PA, 1992a,b). As examples of the ability of this model, and associated predictive technology, the calculated and measured vertical and horizontal closures of Rooms D and B, both isolated 5.5-m-square cross-section rooms some 5.5 m above the WIPP horizon, but with the latter heated after one year, are shown in Figure 4 (Munson et al., 1990a).

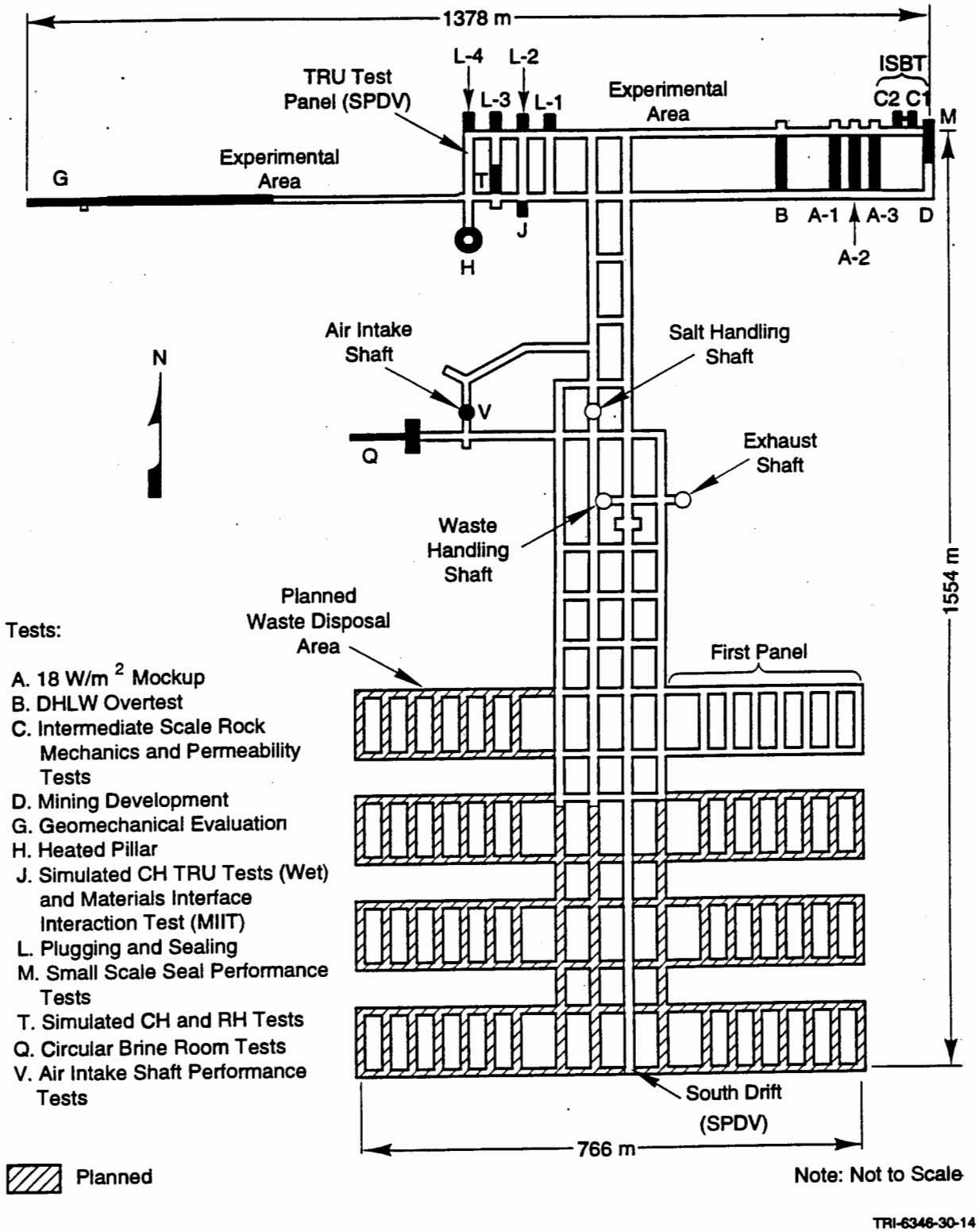

Figure 2. Plan view of the *in situ* tests in the WIPP facility.

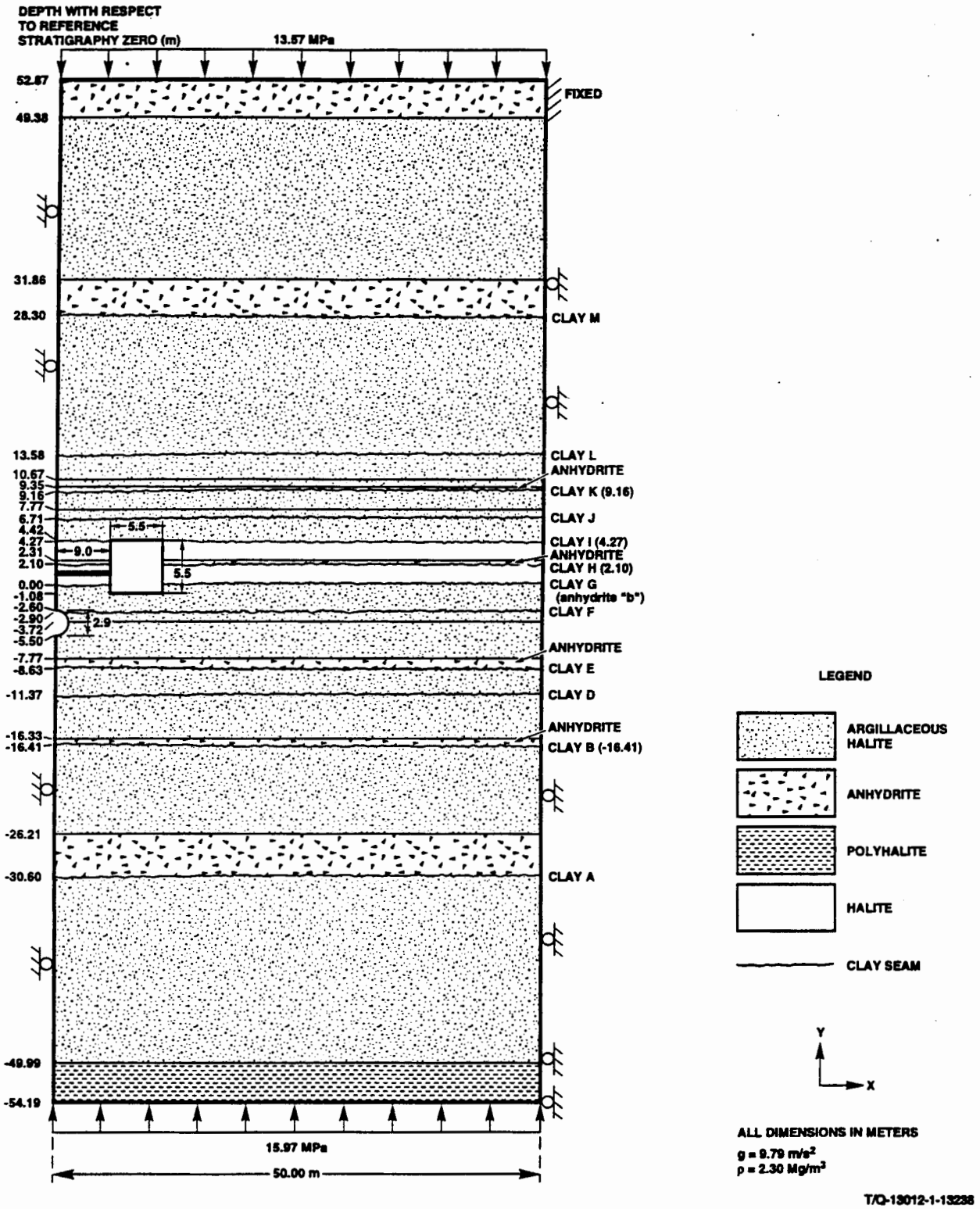

Figure 3. Local stratigraphy at the WIPP horizon.

Agreement between measured and calculated closure is within 10% except for the vertical closure of Room B where progressive roof failure leads to a high apparent measured closure rate. The continuum creep model does not include fracture and cannot simulate the roof response once fracture becomes a significant mechanism. In Figure 5, the comparison is shown between calculated and measured horizontal and vertical closures (Munson et al., 1993) for the entirely different geometry of Room Q. This room is a horizontal, cylindrical room with a diameter of 2.9 m, at the WIPP horizon, which differs from the previous rooms. Here, the agreement of both horizontal and vertical calculated and measured closures is within 3%, for the nearly 3 years' duration of comparison. These results, together with similar results in the other comparisons of calculation to in situ test data, have been the basis for suggesting the M-D model is technically sound and an indication of the validity of the predictive technology.

The technical basis of the model is supported by fundamental concepts where this is possible. The M-D model is based on the deformation mechanism map for steady-state creep. A deformation mechanism map for salt is given in Figure 6 (Munson, 1979). This map describes those regions of stress (plotted as the non-dimensionalized modulus reduced stress) and temperature (plotted as the homologous temperature) where a specific dislocation mechanism controls the creep process. For the conditions of the WIPP, there are potentially three distinct mechanisms involved: (1) a high temperature and low stress region based on a dislocation climb mechanism, (2) a low temperature and low stress undefined mechanism (e.g., no theoretical micromechanical mechanism is known in this region), but the region is empirically well characterized, and (3) a high stress dislocation slip mechanism. Although the WIPP conditions are expected to be isothermal at the ambient natural underground temperature, all of the stated mechanisms could still be involved because of the large range of stress states that occur around underground rooms and shafts. These mechanisms conform to the requirements for additive processes and the total steady-state creep rate is then the sum of the rates of the individual mechanisms. The boundaries between regions of the deformation map are defined as the locus where the strain rates of the adjacent mechanism regime are equal. Transient creep strain is incorporated into the model through a multiplier on the steady-state rate. Transient creep is described through a state parameter which obeys a higher order (quadratic) kinetic equation. Both stress loading and unloading changes of the long transient (single-state parameter) type can be accommodated by the model. Initial state values less than the transient strain limit will increase through workhardening until the transient strain limit is reached, while initial state values greater than the limit will decrease through recovery. At the transient strain limit, the material continues to accumulate further, unlimited strain by steady-state creep.

Table IV. Parameter Values for the M-D Model

ELASTIC PROPERTIES (DENOTED WIPP-D)
μ 12.4 GPa E 31.0 GPa υ 0.25

CREEP PROPERTIES (DENOTED WIPP-D)				
PARAMETERS	CLEAN SALT	ARGILLACEOUS SALT	UNITS	REMARKS
A_1	8.386 E22	1.407 E23	/s	FROM ERDA-9
Q_1	25,000	25,000	cal/mol	FROM ERDA-9
n_1	5.5	5.5		FROM ERDA-9
B_1	6.086 E6	8.998 E6	/s	FROM ERDA-9
A_2	9.672 E12	1.31984 E13	/s	
Q_2	10,000	10,000	cal/mol	FROM ERDA-9
n_2	5.0	5.0		FROM ERDA-9
B_2	3.034 E-2	4.289 E-2	/s	
σ_0	20.57	20.57	MPa	
q	5.335 E3	5.335 E3		FROM ERDA-9
m	3.0	3.0		THEORETICAL
K_0	6.275 E5	1.783 E6		
c	0.009198	0.009198	/T	DeVRIES [1988]
α	-17.37	-14.96		FROM ERDA-9
β	-7.738	-7.738		
δ	0.58	0.58		FROM ERDA-9

NOTE: THE ERDA-9 VALUES WERE OBTAINED FROM MUNSON AND DAWSON [1979; 1982]. HERE, M IS THE SHEAR MODULUS, E IS YOUNG'S MODULUS, AND N IS POISON'S RATION. THE A'S AND B'S ARE CREEP STRUCTURE FACTORS, THE Q'S ARE ACTIVATION ENERGIES, THE N'S ARE POWER EXPONENTS OF THE STRESS DEPENDENCIES, Q IS THE EXPONENTIAL STRESS DEPENDENCY, σ_0 IS THE CUT-OFF STRESS FOR THE SLIP MECHANISM, M IS A THEORETICAL VALUE, K_0 IS THE CONSTANT FOR THE TRANSIENT STRAIN LIMIT, C IS THE TEMPERATURE DEPENDENCE OF THE TRANSIENT STRAIN LIMIT, AND α, β, AND δ THE ARE PARAMETERS THAT GOVERN THE CURVATURE OF THE TRANSIENT CREEP RESPONSE.

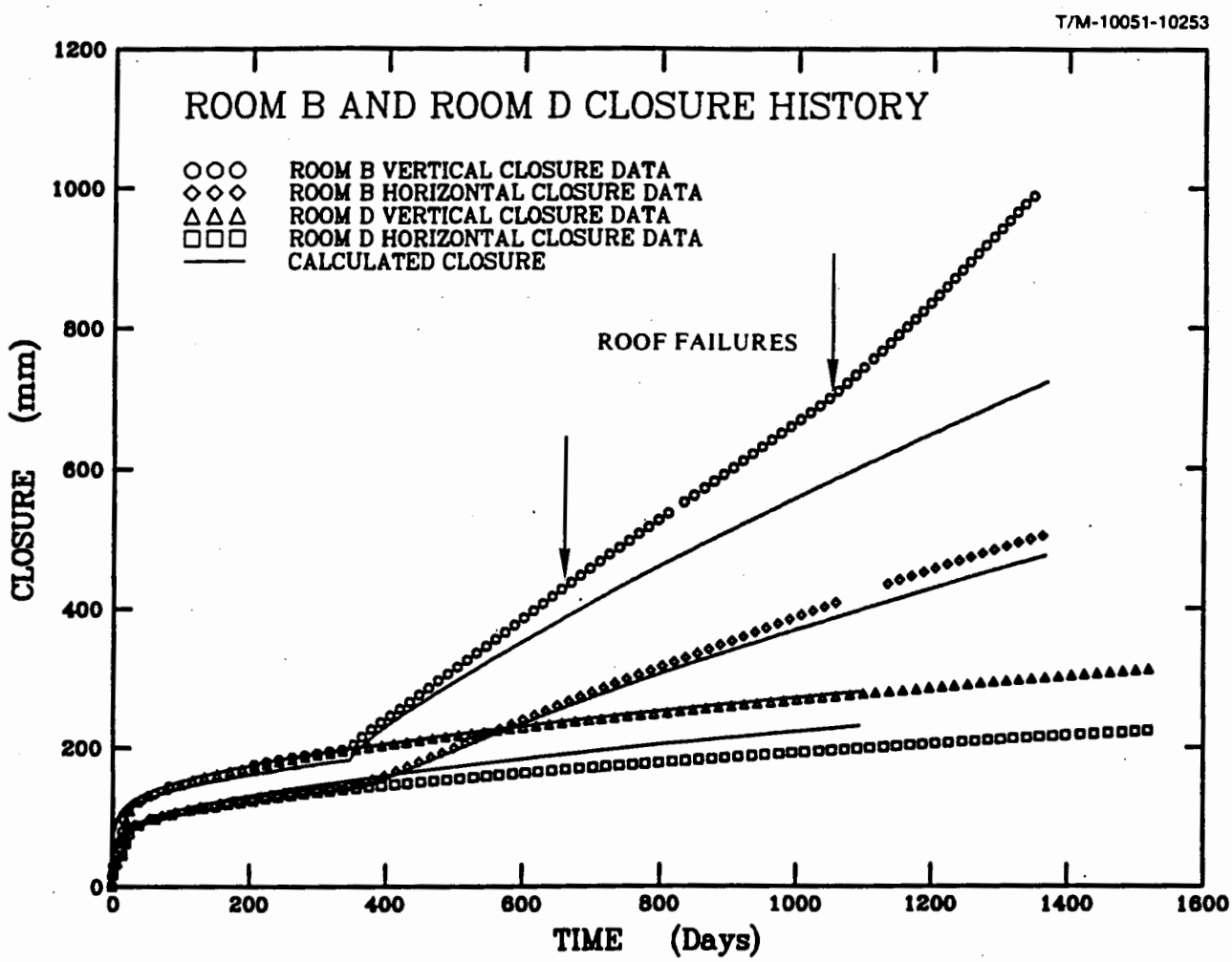

Figure 4. Calculated and measured closures of Room D and Room B.

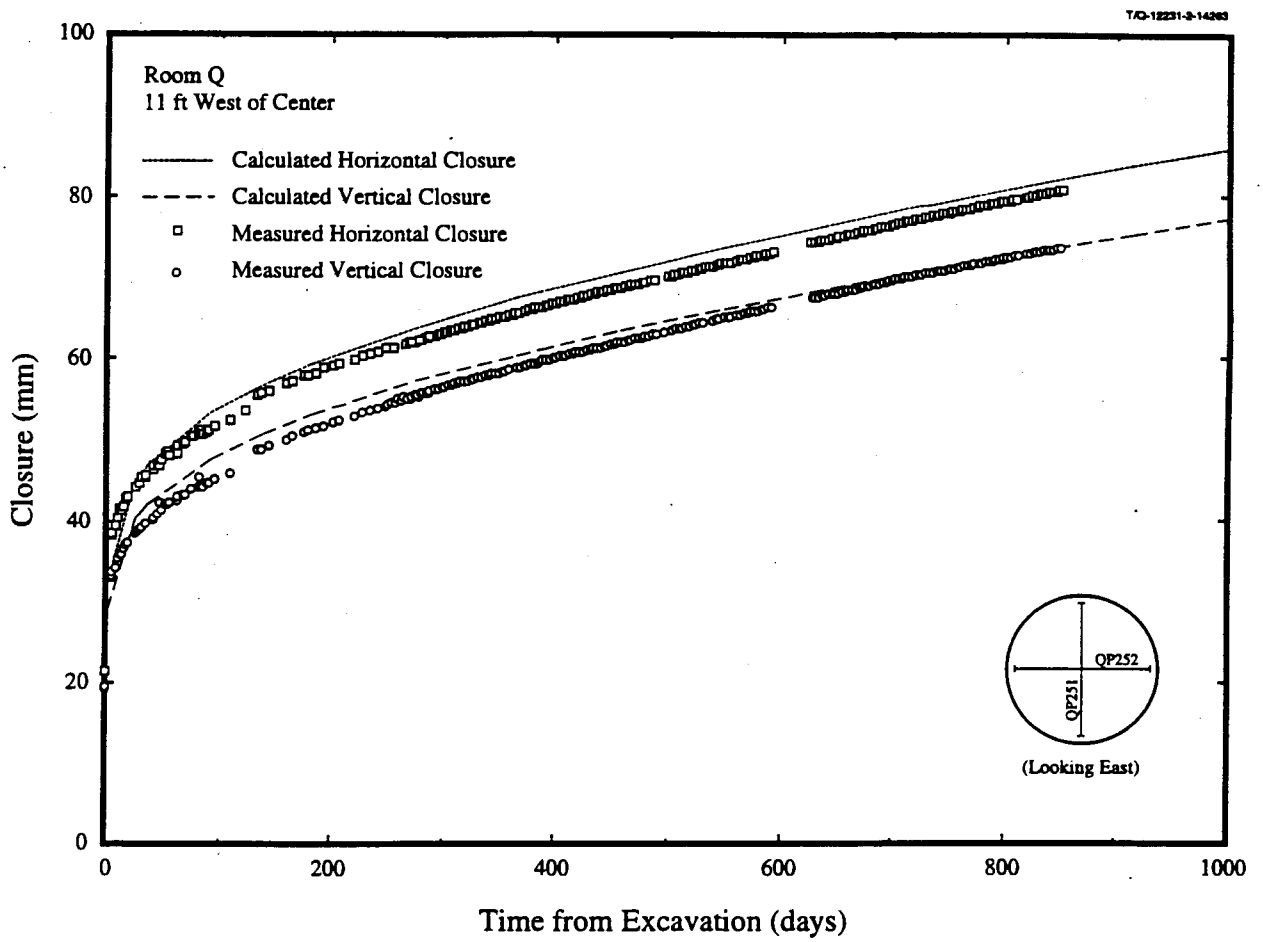

Figure 5. Comparison of calculated and measured Room Q closures.

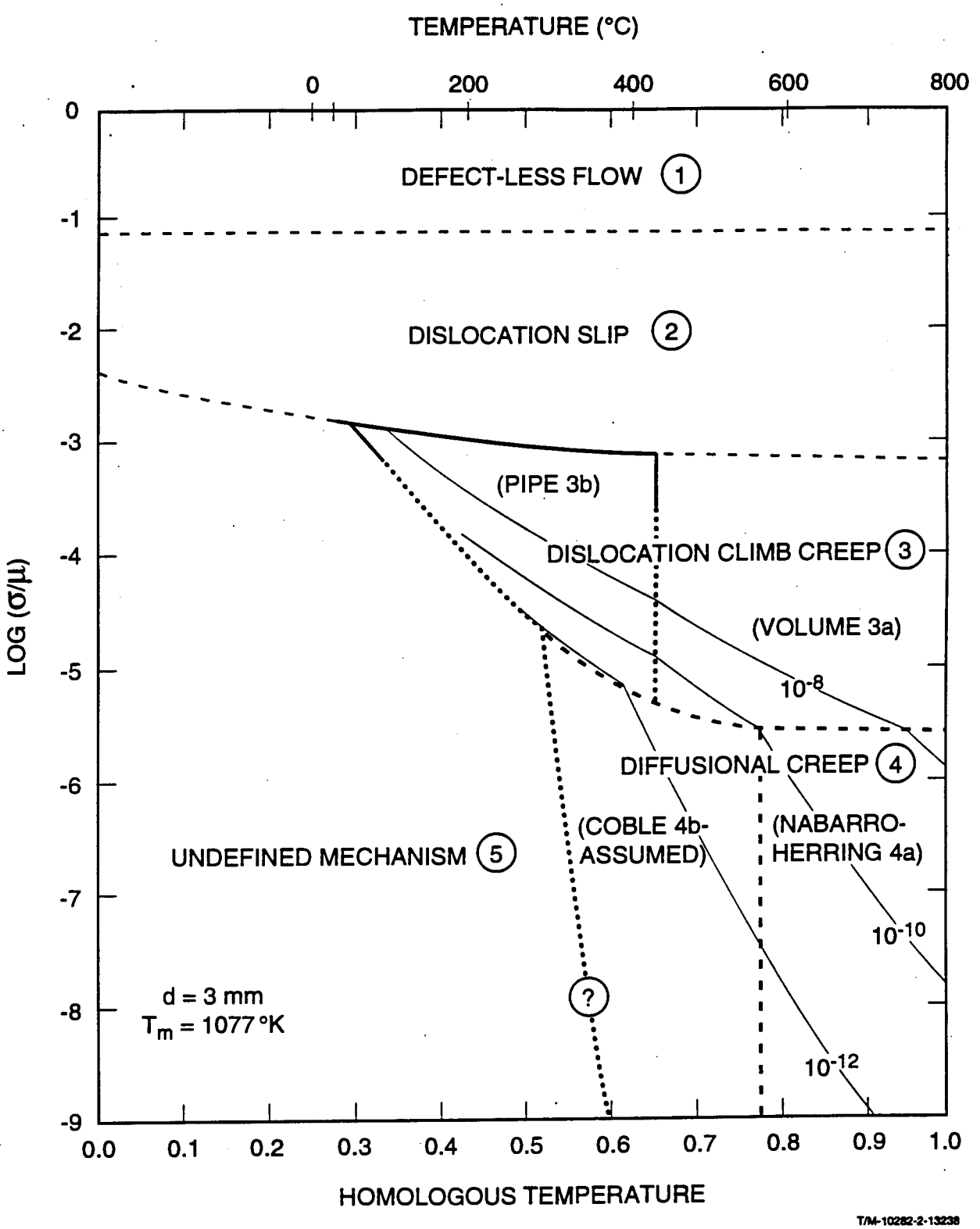

Figure 6. Deformation mechanism map for salt.

In addition, the M-D model, with the large strain SPECTROM-32 code, has been used successfully to calculate the closure of the quite complicated Engineered Alternatives Task Force (EATF) Baseline configuration, which is a repository room containing waste and crushed salt with the conditions of concurrent gas generation.

A somewhat simpler constitutive model was developed early in the project based entirely on the steady-state creep behavior in the undefined mechanism region (Morgan et al., 1986). Unlike the M-D model, this model required an arbitrary reduction of elastic moduli by a factor of 12.5 to obtain adequate agreement with the measurements in the South Drift (Morgan et al., 1985). In certain situations, this constitutive model has been used for WIPP calculations (Butcher and Mendenhall, 1993). However, the reduced modulus model is no longer used unless the M-D model has unacceptably long computation times and the simpler model has been shown to be accurate.

2.2 Flow Potential

Selection of the proper plastic flow potential is critical because this potential makes it possible to obtain the response of a material to the three-dimensional stress fields found around the underground openings. A series of thin walled, hollow salt cylinders was subjected in the laboratory to various loading paths chosen to explore the angles between the conditions of uniaxial compression and pure shear. Significantly, these experimental results can be interpreted directly, without recourse to structural calculation, to show that a Tresca plastic flow potential based on a maximum shear stress criterion describes salt creep and is therefore preferred over the von Mises criterion (Mellegard et al., 1992), which is based on the octahedral shear stress criterion. Although the difference in stress in pure shear is only 15.7%, the strong stress dependence of creep causes this to become a factor of two in creep rate in pure shear. This effect is important for closure of underground rooms in salt where significant amounts of salt can be in shear. In confirmation of the choice of the plastic flow potential, the structural calculations using the Tresca flow potential make possible the very reasonable agreements obtained.

2.3 Material Parameters

The material parameters required for the M-D model have all been determined from laboratory triaxial, compressive creep tests, except where a theoretical value exists. The reference values proposed which are the values used for all M-D model simulations of the in situ experiments (as discussed previously) are given in Table IV. As is apparent, the parameters have been determined for the two dominant types of salt layers in the stratigraphy, clean salt and

argillaceous (containing clay) salt layers. Because the wastes intended for the WIPP are not heat producing, except for limited amounts of remote-handled TRU, the thermal parameters are not important and have no influence on the typical WIPP structural problems. Other evaporite materials, such as anhydrite and polyhalite, when sufficiently close to the excavation that it is necessary to treat their explicit behavior, are treated as elastic or elastic-plastic materials. The interbeds found between the layers of salt are represented as planes of frictional slip with a coefficient of friction of 0.2, taken as a constant for all calculations and based on qualitative evaluation of in situ behavior.

At this time, the principal parameters for clean salt of the M-D model have been framed in terms of probability distribution functions (Fossum et al., 1994) and the analysis has been made to determine a distribution function for creep closure of a simulated crushed-salt-filled shaft seal configuration. Calculated creep closure was to a selected crushed salt density (Fossum and Munson, 1995). The distribution functions for argillaceous salt still have to be determined and additional evaluations of shaft closure have to be made. Comparisons must be made of the fast probability integration and Monte Carlo methods.

2.4 Stratigraphy and Initial Conditions

The stratigraphic detail for the numerical simulations is the updated version given by Munson et al. (1989a), as shown in Figure 3, which modified that given earlier by Krieg (1984). This updated stratigraphy is specialized to capture those aspects of the materials important to the mechanical behavior, and therefore differs from those reflecting more common geological aspects. Features of geological importance often are not influential in terms of mechanical behavior.

The initial stress condition of the site is essentially one of uniform rock pressure ($\sigma_1 = \sigma_2 = \sigma_3$) due to the overburden (Wawersik and Stone, 1989).

2.5 Numerical Codes

Essentially, three distinct numerical structural codes have the necessary (as noted previously in *40 CFR 268.6(b)(3)*, *40 CFR 268.6(b)(5)*, and *40 CFR 264.601*) capabilities to simulate the major aspects of the WIPP underground as follows: SANTOS, JAC-3D (Biffle, 1993), and SPECTROM-32 (Callahan et al., 1989). These codes use finite-element, numerical solution methods. Their current capabilities include a choice of flow potential, multiple material layers, slide lines to emulate interbed seams, and birth/death options simulating mining. Two codes are limited to two-dimensional simulations, while one code, JAC-3D, has the capability

for either two- or three-dimensional simulations. All of these codes can account for large (finite) strains, a feature of some importance in treating the long times and large deformations involved in some WIPP problems. All codes currently incorporate the M-D model; however, JAC-3D and SPECTROM-32 have the most experience with simulations using this model. SPECTROM-32 is rated as a Level A code according to Sandia QAP 19-1 quality assurance requirements.

2.6 Remarks

The creep models are "continuum" models and, as a result, they do not allow fracture. However, if we are addressing the long-term creep closure effects, such as that of complete repository creep closure to encapsulate the waste, the problem, in fact, is relatively simple. The creep closure involves the removal of all underground void, regardless of whether the void volume is that of the original repository room or some redistribution of this volume, such as occurs with the formation of microfractures around the room. In this case, then, the prediction involves only the general response of the entire salt body to eliminate the underground void volume; and, therefore, the use of a continuum creep model is both adequate and sufficient. Certainly, there are temporary situations, such as formation of a potentially permeable DRZ around seals, that must be considered. In fact, the calculated creep strain caused by the formation of the DRZ is quite small (3%) compared to the continuum creep stains, so that it does not affect significantly the comparison between measured and calculated continuum creep closure. However, the small strains associated with the development of microfractures can have a large effect on changes in permeability. Again, in the long-term closure, the microfractures, because of the conservation of mass (or void) do not change the encapsulation process. In the more complicated situation of concurrent gas generation, the gas will potentially act as a source within the repository to increase the required void volume and alter the encapsulation process.

The proper form of the plastic flow potential remains an issue within the technical community. Historically, most structural analysts continue to use the von Mises potential in creep structural problems. However, based on the definitive thin-walled cylinder results and the success of the calculations of *in situ* behavior, the Tresca potential should be considered the proper plastic flow criterion for creep of salt.

Currently, an issue to be resolved concerns whether the fast probability integration (FPI) methods produce the same results as the Monte Carlo or Latin Hypercube methods currently used for the WIPP program. For very complex structural calculations, Monte Carlo or Latin Hypercube methods require too many realizations or calculations to be economical. Perhaps only FPI methods are efficient enough to permit probabilistic analysis of structural responses.

However, because no mathematical proof of equivalency of the methods exist, direct comparisons of simple problems will be necessary to establish confidence in the FPI method.

2.7 Continuum Creep Data to Analysis Guide

The database and analysis history is too extensive to be included directly in this paper. As a alternative, a partial reference guide is given in Table V.

Table V. Continuum Creep Data and Analysis Guide

Conceptual Model	Model	Analysis	References (partial)
Creep closure of rooms expected to encapsulate the waste (NAS 1957) and assure sealing of shafts	M-D Multi-mechanism deformation model	Numerical finite element simulations	Model -- Munson et al. 1989a PA 1992, Vol. 3 Parameters -- Munson et al. 1989a PA 1992, Vol. 3 Flow potential -- Mellegard et al. 1992 PA 1992, Vol. 3 *In situ* data -- Matalucci et al. 1982 Munson 1991 Munson & others 1987b, 1988b, 1990b, 1991b, 1991c, 1992b, 1992c, etc. Stratigraphy -- Munson et al. 1989a PA 1992, Vol. 3 Initial conditions -- Wawersik & Stone 1985 Munson et al. 1989a PA 1992, Vol. 3 Analysis -- Munson & DeVries 1991 Munson & others 1987a, 1988a, 1989b, 1990a, 1991a, 1992a, 1993, etc.

3.0 FRACTURE

It is known that, as the continuum creep deformation of the salt immediately adjacent to the underground openings occurs, conditions for the formation of microfractures become favorable and the salt experiences a progressive increase in microfracturing. This process is evident as damage which evolves with time. These microfractures may eventually link to form discrete cracks. At late times, the discrete cracks propagate and link until the salt fails. Expression of this process *in situ* leads to the creation and accumulation of damage in the rock, which gives rise to the DRZ. The material expression of this process in the laboratory is the tertiary creep behavior, as shown in the curve which incorporates fracture in Figure 1. These details of fracture development become relevant in two specific cases: (1) At relatively small amounts of damage which is the early portion of the tertiary behavior, the formation of microfractures may cause an increase of permeability, and consequently, a potential loss of long-term seal system integrity and performance that may be reasonably expected for regulatory compliance (as given in *40 CFR 191.13*, *40 CFR 191.14*, and *40 CFR 191.24*). As a result, this effort supports the performance response of the repository rooms and drifts, especially for Disposal Room models and seal systems through Seal Design and Modeling. (2) The development of fractures and a DRZ must be recognized and appropriate steps taken to deal with the conditions encountered during operational activities, such as construction, for example. Of these two cases, the Rock Mechanics Program is primarily concerned with the first case in which only relatively small amounts of damage occur.

As previously mentioned, the relationship of the fracture model to the M-D continuum creep model and the DRZ process model is to add a crucial component to the modeling capability. The development of microfractures described by the fracture model contributes only a few percent to the closure strain, and even that strain eventually is removed by continuum creep. However, the small amount of fracture strain or damage may in fact be responsible for marked changes in permeability and deterioration of the performance of seals. This is why the fracture model is important to the compliance goal. The DRZ process model combines individual models, such as functional forms for damage healing and permeability changes with damage together with the creep and fracture models, to assess the DRZ growth evolution (growth or healing) with time.

The study to understand fracture is an important area of development of the Rock Mechanics Program and it is currently the most active. This activity includes the additional theoretical inputs to define the cleavage modes of fracture and complete the fracture model, the development of the capability to handle bed separation, the generation of the experimental

database for the argillaceous salt material, the final parameter selection for the fracture model, and the further comparisons to the underground observations of damage to demonstrate validity.

3.1 Fracture Constitutive Model

The constitutive model of fracture has been formulated to address progressive, time-dependent development of damage (Chan et al., 1992). This model, which is the multimechanism deformation (M-D) continuum creep model coupled to fracture (MDCF), is based on the Bodner-Partom (Bodner, 1985) description of tertiary creep, with the parameters determined from laboratory creep tests (Fossum et al., 1993). The Bodner-Partom description for tertiary creep is a very non-linear evolutionary equation for damage. The MDCF model defines from the damage a new strain contribution, due to deformation of the microfractures, which evolves with time. Damage enters the model directly through the damage strain and indirectly through reduction of the loaded area to increase the effective stress. From the fracture mechanism map (Gandhi and Ashby, 1979), this formulation represents two separate fracture mechanisms, one of which, stress rupture, is very relevant to the WIPP conditions. The model accounts for important effects of confining pressure in that microfracture is sensitive to confining pressure and can be completely suppressed. The model also contains a feature that permits the elimination of damage, which simulates the rehealing process, as the damaged salt is repressurized. Such repressurization is expected to occur around seals as they take up load from the overburden as the creep-closure process continues.

As in the case of the continuum creep model, the attempt during the development of the fracture model is to maintain a fundamental basis wherever possible. The fracture model is based on a fracture mechanism map which defines the regions in non-dimensionalized stress and homologous temperature that different fracture mechanisms dominate. Just as for the deformation mechanism map, the fracture mechanism map can be used as a guide to the model development. In contrast to the deformation mechanisms, fracture mechanisms are very sensitive to confining pressure. In certain instances, the confining pressure will suppress the fracture process completely. As a result, the fracture model imposes the effect of confining pressure on fracture. Of the possible fracture mechanisms, three relate directly to the conditions of the WIPP underground. These are a brittle grain boundary fracture mechanism of short-time failure which is strain-rate dependent, a stress rupture mechanism which is the long-time failure mode, and a cleavage failure mechanism. The fracture mechanism of stress rupture dominates the formation of microfractures during the development of the DRZ and is considered the most important mechanism. This mechanism appears to obey the Monkman and Grant (1956) criterion of a constant strain to long-term failure.

The MDCF model is a "ubiquitous" model in the sense that it describes the damage as though it is smoothly distributed throughout a material volume. That is, the presence of discrete fractures is not modeled or tracked in the MDCF formulation. However, this is not a significant problem in addressing the issue of the formation, growth, and healing of the DRZ for use in sealing system performance assessment and design where the damage is limited to small values. For these conditions the model is thought to be accurate. In terms of the level of validation of the fracture model, it is much less advanced than the M-D continuum creep model. As is apparent, some work remains to be done to achieve reasonable expectation of regulatory compliance. The remaining work involves further refinement of the fracture constitutive model, determination of material properties, comparison of model predictions to underground observations, and the proper incorporation of the interbed behavior. Regardless, the model is currently developed adequately to be used for seal design studies of the influence of the DRZ on seal performance.

Several "stress-based" fracture models have been used on WIPP analyses. In the analysis of the permeability changes in the DRZ, Stormont et al. (1992) used a time-independent representation of the stress strain curve and calculated changes in volumetric (dilatant) strain with increase in stress. A similar approach has been used in support of the study of design alternatives for seal systems (Van Sambeek et al., 1993). Unless specifically modified, stress-based models in general do not permit the damage to evolve independently with time as a separate material behavior, a characteristic feature that is known to occur in salt. In these models, changes in damage may occur only as the stress field changes in time. In fact, if the stress field around an opening decreases with time, accumulated damage would incorrectly appear to decrease also. In general, the stress-based fracture models need to be replaced by the time-dependent evolutionary formulation of the MDCF.

3.2 Fracture Model Parameters

The MDCF fracture material parameters have been determined for clean salt, and preliminary parameters are now becoming available for argillaceous salt. It appears based on experimental evidence that the small quantity (<4 %) of clay content in argillaceous salt has a marked effect on the microfracture behavior, increasing the rate of damage evolution and decreasing the time to failure. A comparison of creep and fracture behavior shows that, although clay increases the creep rate and the transient strain, an equivalent clay content has a much more marked influence on the fracture response. Apparently, the overall effect of clay content is quite important in that it causes argillaceous salt layers to accumulate damage at a higher rate than the clean salt layers, which appear to match the underground response. However, until the entire available database has been evaluated, the fracture model parameters will not be given.

3.3 Numerical Code MDCF Model Incorporation

The MDCF model has been incorporated into SPECTROM-32 and a number of preliminary simulations made of the WIPP underground room configurations, including the storage room configuration. It has been possible to make a preliminary comparison to the formation of the damage, as measured by ultrasonic wave speed, around the Air Intake Shaft. Although further analysis is required, the model calculation compares qualitatively with the measured results, especially in the radial extent of the damage, as shown in Figure 7. The nature of the fracture model is such that it will also predict the accumulation of large amounts of damage, essentially that equivalent to failure. In a preliminary sense, it has been used to calculate the accumulation of damage around a room of the Transuranic (TRU) Test Panel, as shown in Figure 8. While direct comparison is not yet possible because the ubiquitous model does not permit localization, the initial fracture pattern is certainly suggestive of the fracture trajectories observed in these rooms. These simulations have been encouraging because they show development of damage around the underground opening with time, which matches in a qualitative sense the general observations. The predicted behavior is thought to be more realistic than previously possible with the earlier, stress-based, time- independent fracture models which cannot evolve with time and do not have a true tertiary creep- related measure of damage.

3.4 Discrete Fracture - Fracture Mechanics Approach

For the more extreme conditions of damage accumulation, it is necessary to treat discrete crack formation and propagation; this technology is not so well developed. Work is in progress to address the problem of the localization of the damage to produce a discrete fracture. There are two distinct approaches to this problem: global and local. The classic or global approach is to convert at some point the ubiquitous results in a mesh to a discrete element with an advancing crack tip, which presents mathematical and numerical difficulties. The simplest of these global approaches (linear elastic fracture mechanics) has been applied to the WIPP problem of the response of interbeds to the pressurization of the repository by gas generation. However, with a simplistic linear elastic approximation what is often found is that the linear elastic energies misestimate severely the actual conditions of an elastic-plastic, creeping crack tip. A common assumption of a characteristic length to control the energy release has not always proven satisfactory because of difficulty in rationally specifying the length. In fact, in some cases where the "process" zone is very complicated, the mathematical representation has no

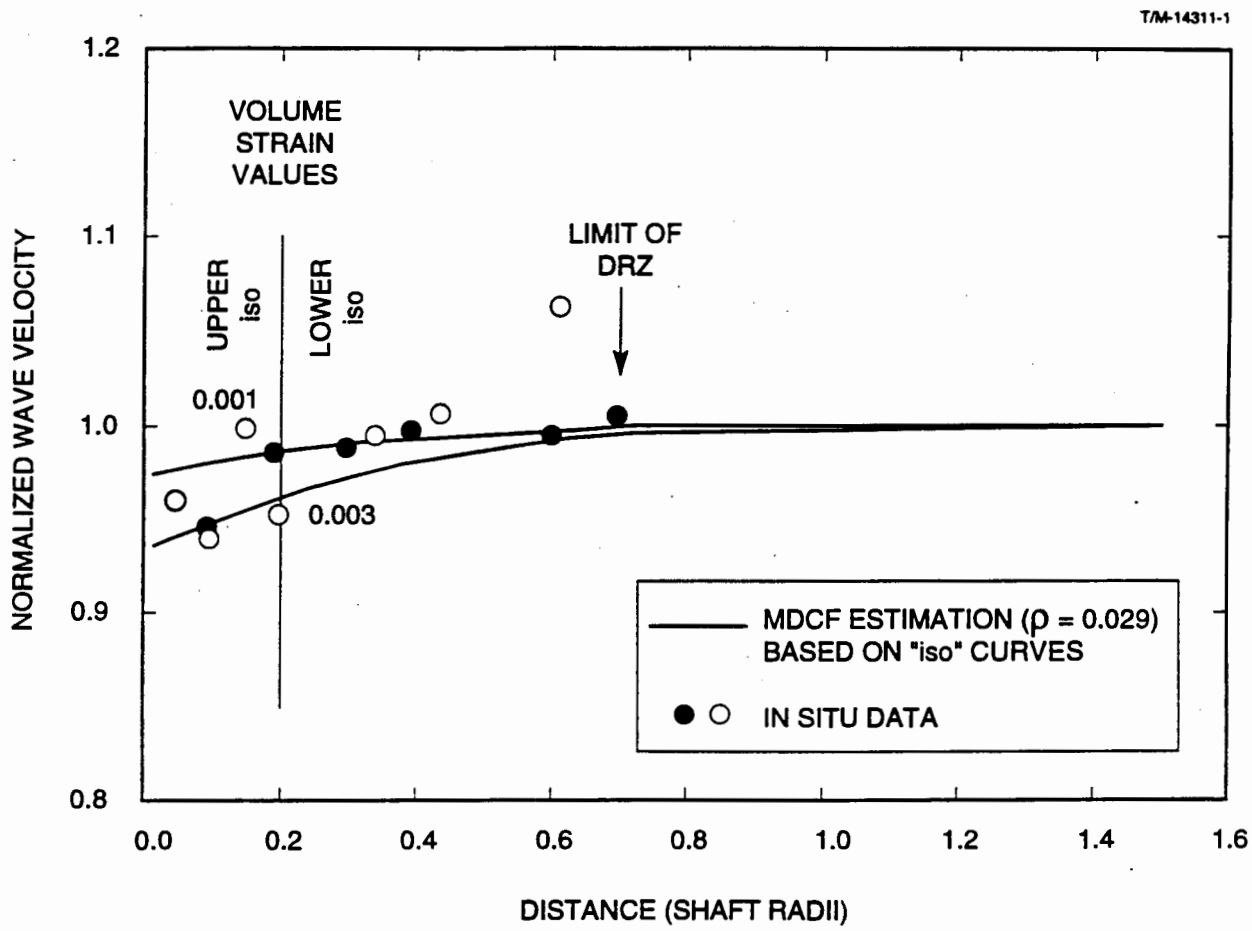

Figure 7. Comparison of in situ ultrasonic equivalent of damage against MDCF model calculation. Comparison based on isotropic ("iso") distribution of microfractures, with the upper and lower MDCF estimations obtained from the range of laboratory data of the change in ultrasonic velocity with volume dilatancy.

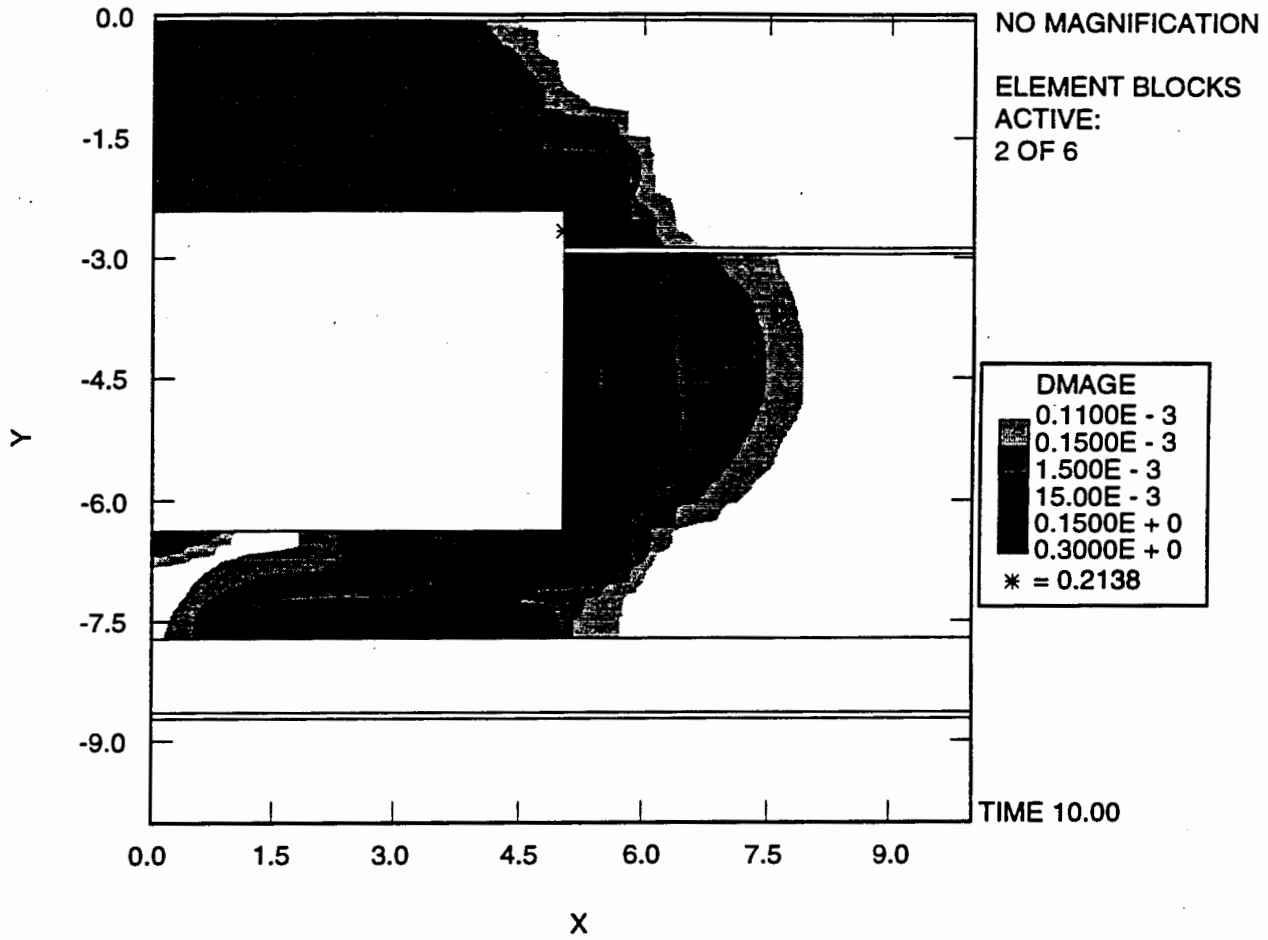

Figure 8. Predicted damage around a TRU test panel room.

independent parameter available in the solution to take the role of the fracture toughness, and the crack tip conditions no longer can be described by global parameters. In this case the stress field becomes independent of the applied stress and may become geometry dependent.

3.5 Discrete Fracture - Local Approach

A more recent development, which is an alternative to the global approach, is to use a local approach based on "adaptive meshing" where the gradients of damage or energy across a mesh serve as a measure of the need to refine the mesh. As mesh refinement occurs at regions of high damage gradients, the highly refined mesh generates a trajectory of the crack. Adaptive meshing requires only the definition of the ubiquitous model, without the need to introduce special elements to define the discrete crack. Although coding of adaptive meshing is not an easy task, this is the reason the rock mechanics program has chosen the adaptive meshing approach.

3.6 Remarks

Although the predictive technology for fracture damage and failure is not as well developed as for creep deformation, several significant advances have been made. The MDCF model already incorporates the necessary features and is capable of simulating the shaft sealing systems. The important contribution of the MDCF model is that the time-dependent accumulation of damage is strain based, in marked contrast to earlier models based on stress related quasistatic onset of dilatancy. This model is expected to replace the earlier stress-based models for use in WIPP shaft seal design calculations.

As noted, the uncertain aspects of fracture modeling appear in the manner in which the fracture damage is extended to discrete cracks. The proper, and physically correct, choice between global (fracture mechanics) and local (ubiquitous models) is not yet settled. For very complex situations, such as those around a moving crack tip in a creeping material, no global solution appears to be available so the use of fracture mechanics is not possible. Thus, for salt, at this time, a local approach appears more reasonable.

3.7 Fracture Model Data to Analysis Guide

The database and analysis history is too extensive to be included directly into this paper. As a alternative, a partial reference guide is given in Table VI.

Table VI. Fracture Model Data and Analysis Guide

Conceptual Model	Model	Analysis	References (partial)
Creep closure is accompanied by fracture evolution around shafts and rooms (PA 1992) which makes a small contribution to strain but a large potential change in permeability	MDCF Multi-mechanism deformation model coupled to	Numerical finite element simulations	Model -- Chan et al. 1992 Parameters -- (in progress) Fossum et al. 1994 Flow potential -- Mellegard et al. 1992 PA 1992, Vol. 3 *In situ* data -- (in progress) Stratigraphy -- Munson et al. 1989a PA 1992, Vol. 3 Initial conditions -- Wawersik & Stone 1985 Munson et al. 1989a PA 1992, Vol. 3 Analysis -- (in progress)

4.0 DISTURBED ROCK ZONE (DRZ)

The DRZ is the zone of rock immediately surrounding underground openings in which the mechanical and hydrologic properties have changed in response to the excavation and subsequent creep. Since the existence of the DRZ was documented (Borns and Stormont, 1988, 1989; Holcomb, 1988) and accepted at the WIPP (Lappin et al., 1990) the Project has postulated that the DRZ has an impact on (1) gas and brine storage relocation, (2) localized hydrologic response of the Salado Formation, (3) design and performance of seals, and (4) repository design. DRZ investigations address compliance issues for the Seals Program through Seal Design and Modeling and Seal Field Studies programs, since the DRZ development at the proposed seal locations determine changes in hydraulic and mechanical properties of the seal system with time. Compliance issues are addressed for Salado Hydrology by supporting Flow and Transport Modeling, Hydrologic Field Studies and Large-Scale Brine Inflow Experiment.

Except for some laboratory, numerical simulations, and minor field studies, the investigations of the DRZ were largely ended in 1991. The exceptions are the Large-Scale Brine Inflow Experiment (Room Q), where studies of hydrologic and physical behavior continue, and the Air Intake Shaft, where ultrasonic studies are still in progress. However, the current technical position would benefit from additional information, which it appears may eventually be needed. It appears especially important to monitor the time-dependent hydrologic behavior of the DRZ (e.g., water saturation, porosity, and permeability). Monitoring the time-dependent behavior of the DRZ will be of great significance from initial excavation and, when possible, during and after seal emplacement tests. Characterization is required of the DRZ in proposed seal locations. Also, the extent and propensity for fracturing in the Salado marker beds needs to be more fully investigated. Some of these concerns are being addressed by a current investigation of the DRZ developed around the small-scale seals tests.

4.1 Process Model of DRZ

As shown in Table I, the model for describing the DRZ is classified as a *process* model. This implies that the model is actually a collection of individual physical elements that describe mechanical and hydrological behavior of the DRZ behavior. Thus, the DRZ process model must, at least, incorporate the creep response through the creep model, the formation of microfractures through the MDCF fracture model for predicting damage evolution, the model for describing healing of microfractures under pressure, and a physical model relating the damage to permeability. Application of this process model to seal design, for example, permits a test of the design against performance criteria over the critical recompaction period of the crushed salt seal components.

As is evident from the results in Figures 7 and 8, some elements of the DRZ process model are currently operational, while others are well advanced and eminently available. The constitutive model of the damage evolution (MDCF) has been developed which can be applied to predict the time-dependent details of the evolution of damage. The model is able to simulate the fractional damage surrounding an excavation, either shaft or room. Because the damage measure determined by the model is not a physical quantity, a correlation function to volume dilatancy in the form of a non-associated flow rule has been established. To provide the physical link to hydrological performance, the permeability, as previously mentioned, as a function of the volume dilatancy completes the predictive capability. A functional form of the healing relationship has been established based on laboratory results. This relationship is the sum of two first-order kinetics equations and is now incorporated into the DRZ model.

Two of the elements of the DRZ process model are major models: the M-D model of continuum creep and the MDCF model of damage evolution. These models of mechanical behavior have been fully treated in the earlier discussions. The other elements will be discussed here.

4.2 Kinetics of Healing

The kinetics of the microfracture healing process have been determined through laboratory tests (Brodsky and Munson, 1994). Damaged dry salt specimens heal, as measured by the return of volume strain and ultrasonic wave speed, according to the sum of two first-order kinetic equations. The characteristic time constant of the process is on the order of days, which is short compared to that of the creep process. In seal system performance, this suggests that the damage healing depends only on the rate that the creep process repressurizes the seal. Because of the short time constants and based on void geometry, the healing process is thought to differ significantly from the compaction process of final void elimination in crushed salt.

4.3 Permeability Relationship to Damage

Although a measure of the relationship between permeability and damage can be obtained from back correlations of damage calculations to the permeabilities measured *in situ*, the most direct measure will come from laboratory experiments. In these experiments, previously damaged specimens with known volume dilatancies are used to determine permeability. Relatively few laboratory experiments are currently available from which to deduce a relationship. Consequently, additional studies will probably be necessary to improve the definition of the permeability-damage relationship.

4.4 Peripheral Inputs

There are some critical peripheral inputs to the analysis of the DRZ under the actual conditions as they pertain to seals and seal systems. It is of interest to mention the most important of these inputs here for completeness. The analysis of a seal system requires a description of the mechanical and hydrological behavior of the seal components. This especially means the behavior of the concrete and crushed salt components, because these are the principal materials being considered. In general, these peripheral inputs are being developed in WIPP Programs on Seals, external to the Rock Mechanics Program.

4.5 DRZ Characterization

The DRZ has been characterized by three approaches: visual observation, geophysical methods, and *in situ* hydrologic testing (Borns, 1985; Bechtel National, 1985; USDOE, 1988). Geophysical studies have utilized seismic refraction, seismic tomography, surface wave analysis, electromagnetic (EM) methods, and direct current (DC) methods (Borns and Stormont, 1989; Borns et al., 1990; Holcomb, 1988; Jung et al., 1991; Pfeifer et al., 1989). Taken in conjunction with the *in situ* hydrologic tests, these studies define a DRZ extending to a depth of 1 to 5 meters throughout the underground facility (Borns and Stormont, 1988; Stormont et al., 1991). The DC and EM methods indicate that fracture saturation or fracture density may vary laterally along the excavations. These *in situ* studies also demonstrate that microfracturing and desaturation of the pore space have occurred within the DRZ. The dilation that results from the microfracturing in the DRZ provides a small component of the observed room closure. The processes involved in the development of the DRZ are complex, although basically related to the strain and strain rates of the salt adjacent to the underground opening. The redistribution of stress around the excavation with the development of the DRZ drives coupled processes such as changes in permeability and porosity in response to fracture growth.

Gas flow measurements have previously been conducted in the Salado Formation immediately surrounding excavations. Measurements taken in small diameter boreholes (50 to 150 mm) show that, within 1 to 2 m of the excavation, the halite has very little resistance to fluid flow. Tracer tests (Stormont et al., 1987; Stormont, 1990) demonstrate that flow paths are consistent with the elliptical fracture pattern generally applied to describe fracture distribution around excavations. These tests have provided a qualitative description of the fluid flow properties of a DRZ adjacent to the facility rooms and drifts at the WIPP. However, such a description is difficult to accommodate from the performance assessment perspective. In fact, a conceptual model of the repository zone requires as input the quantitative distributions for the porosity, permeability, and initial saturation of the DRZ. At the present time, the fluid flow

characteristics of the DRZ have not been described by an experimentally derived conceptual model. Models of the DRZ have thus far been limited to constitutive modeling of the structural deformation processes. These observations relate to the formation of the DRZ adjacent to rooms specifically and, while the formation of the DRZ adjacent to shafts has similar characteristics, the DRZ at the shaft will differ significantly in detail.

The well instrumented Air Intake Shaft (Munson et al., 1992a) at the WIPP facility has formed the nucleus of several important studies. It has already been noted that shaft creep closure aided in the validation study of the creep model and the preliminary comparisons of the calculated MDCF damage with *in situ* ultrasonic measurements in the shaft. This shaft will undoubtedly continue to provide data for DRZ characterization. Although initially planned, permeability testing in the shaft has not been possible to date.

An *in situ* test is currently in progress to characterize the hydrological behavior of the DRZ in the vicinity of earlier small-scale concrete seal test configurations emplaced in salt. The intent of this test is to provide a linkage between the MDCF model and the needed fluid flow parameters for the DRZ. The analysis will include modeling of the excavated borehole and the seal.

4.6 Remarks

Perhaps the most relevant issue at this time regarding the DRZ concerns general agreement on a reasonable description, essentially quantitative, of the time-dependent evolution of damage, porosity, permeability, and hydrologic processes. These basic pieces of knowledge have not been completely determined, *in situ*, to provide the parameters and processes for the repository performance models or to validate current damage models. The existence of the DRZ is not in question, but the role it plays in the room response and in the shaft sealing is not currently settled. Considerable work must be done to quantify the *in situ* properties and extent to the DRZ. Certainly, a continuation of the validation effort is required to iteratively and painstakingly compare the quantitative *in situ* studies to the current and refined constitutive descriptions which predict the evolution of the damage. Other important issues that remain to be resolved are the relationships between deformation in the DRZ and the hydrologic process of the Salado and the DRZ, including evolution of porosity and permeability. The effects and significance of chemical precipitation in fractures and pores of the DRZ, which can be taken as part of the healing process, have not been investigated nor incorporated into any of the numerical models.

4.7 DRZ Process Model to Analysis Guide

As noted previously for the other rock mechanics models, the database and analysis history of the DRZ is also too extensive to be included directly into this paper. As an alternative, a partial reference guide is given in Table VII.

Table VII. DRZ Process Model Data and Analysis Guide

Conceptual Model	Model	Analysis	References (partial)
Complex fracture and deformation processes under actual conditions may alternately degrade and heal the disturbed zone with time, with changes in permeability, a potential critical performance issue for shaft seals.	Combination of several deformat-mechanical, and hydro models.	Numerical finite element simulations	Model -- (in progress) Parameters -- (in progress) *In situ* data -- Borns & Stormont 1988 Borns & Stormont 1989 Stormont 1990 Stormont et al. 1991 Healing kinetics -- Brodsky & Munson 1994 Permeability/Damage -- (in progress) Analysis -- (in progress)

5.0 SUMMARY

Although there remain small areas of incomplete development and perceived further needs, the technology produced by the Rock Mechanics Program is basically sound and reasonable. The fundamental understanding of the creep process, together with a capable predictive technology, is well developed and technically sound. This predictive technology is essential to the WIPP Program because ultimately continuum creep determines the time required for closure of the rooms and the eventual encapsulation of the waste. The creep closure response is also responsible for recompaction of the crushed salt seal components.

The level of understanding of the fracture process is not as well developed as that of continuum creep. However, significant progress has been made in that the constitutive models of fracture now are closely tied to theory and laboratory data, and moreover describe the fracture modes thought essential for the WIPP conditions. The fracture model can lead to a reasonable description of the evolution of damage in the disturbed rock zone or DRZ. Such a damage prediction capability facilitates understanding the long-term response of sealing systems, especially where the DRZ has the potential to form a detrimental high permeability path to deteriorate seal performance. Detailed examination and evaluation of the DRZ remains an issue because this will form the validation basis to decrease the level of uncertainty in our predictive capability. Evaluations and testing of the DRZ also should include the aspects of coupling the damage evolution to changes in permeability and porosity.

6.0 REFERENCES

Bechtel National. 1985. *Interim Geotechnical Field Data Report*. DOE-WIPP-221. Carlsbad, NM: U.S. Department of Energy.

Biffle, J.H. 1993. *JAC3D - A Three-Dimensional Finite Element Computer Program for the Nonlinear Quasistatic Response of Solids with the Conjugate Gradient Method*. SAND87-1305. Albuquerque, NM: Sandia National Laboratories.

Bodner, S.R. 1985. "Evolution Equations for Anisotropic Hardening and Damage of Elastic-Viscoplastic Materials," *Plasticity Today: Modelling, Methods and Applications, Udine, Italy, June 27-30, 1983*. New York, NY: Elsevier Applied Science. 471-482.

Borns, D.J. 1985. *Marker Bed 139: A Study of Drillcore From A Systematic Array*. SAND85-0023. Albuquerque, NM: Sandia National Laboratories.

Borns, D.J., and J.C. Stormont. 1988. *An Interim Report on Excavation Effect Studies at the Waste Isolation Pilot Plant: The Delineation of the Disturbed Rock Zone*. SAND87-1375. Albuquerque, NM: Sandia National Laboratories.

Borns, D.J., and J.C. Stormont. 1989. "The Delineation of the Disturbed Rock Zone Surrounding Excavations in Salt," *Rock Mechanics as a Guide for Efficient Utilization of Natural Resources, Proceedings of the 30th U.S. Symposium, West Virginia University, Morgantown, WV, June 19-22, 1989*. Ed. A.W. Khair. SAND88-2230C. Brookfield, VT: A.A. Balkema. 353-360.

Borns, D.J., M.C. Pfeifer, H.T. Andersen, and C.K. Skokan. 1990. "Electrical Methods to Delineate Fluid Flow In Situ in Bedded Salt," *Society of Exploration Geophysicists Workshop on Permeability, Fluid Pressure and Pressure Seals in the Crust, Denver, CO, August 5-8, 1990*. SAND90-1685A. Albuquerque, NM: Sandia National Laboratories.

Brodsky, N.S., and D.E. Munson. 1994. "Thermomechanical Damage Recovery Parameters for Rocksalt from the Waste Isolation Pilot Plant," *Rock Mechanics, Models and Measurements, Challenges from Industry, Proceedings of the 1st North American Rock Mechanics Symposium, University of Texas at Austin, June 1-3, 1994*. Eds. P.P. Nelson and S.E. Laubach. Brookfield, VT: A.A. Balkema. 731-740.

Butcher, B.M., and F.T. Mendenhall. 1993. *A Summary of the Models Used for the Mechanical Response of Disposal Rooms in the Waste Isolation Pilot Plant with Regard to Compliance with 40 CFR 191, Subpart B.* SAND92-0427. Albuquerque, NM: Sandia National Laboratories.

Callahan, G.D., A.F. Fossum, and D.K. Svalstad. 1989. *Documentation of SPECTROM-32: A Finite Element Thermomechanical Stress Analysis Program.* DOE/CH/10378-2, 1&2. Rapid City, SD: RE/SPEC Inc.

Chan, K.S., S.R. Bodner, A.F. Fossum, and D.E. Munson. 1992. "A Constitutive Model for Inelastic Flow and Damage Evolution in Solids Under Triaxial Compression," *Mechanics of Materials.* Vol. 14, no. 1, 1-14.

DeVries, K.L. 1988. "Simulation of Field Tests in Avery Island Dome Salt," *Key Questions in Rock Mechanics, Proceedings of the 29th U.S. Symposium, Minneapolis, MN, June 13-15, 1988.* Eds. P.A. Cundall, R.L. Sterling, and A.M. Starfield. Brookfield, VT: A.A. Balkema. 413-420.

Fossum, A.F., and D.E. Munson. 1994. "Probabilistic Creep Analysis of an Underground Structure in Salt," *International Journal of Solids and Structures.* SAND94-0588J. Albuquerque, NM: Sandia National Laboratories.

Fossum, A.F., N.S. Brodsky, K.S. Chan, and D.E. Munson. 1993. "Experimental Evaluation of a Constitutive Model for Inelastic Flow and Damage Evolution in Solids Subjected to Triaxial Compression," *International Journal of Rock Mechanics and Mining Sciences & Geomechanics Abstracts.* Vol. 30, no. 7, 1341-1344.

Fossum, A.F., T.W. Pfeifle, K.D. Mellegard, and D.E. Munson. 1994. "Probability Distributions for Parameters of the Munson-Dawson Salt Creep Model," *Rock Mechanics, Models and Measurements, Challenges from Industry, Proceedings of the 1st North American Rock Mechanics Symposium, University of Texas at Austin, June 1-3, 1994.* Eds. P.P. Nelson and S.E. Laubach. Brookfield, VT: A.A. Balkema. 715-722.

Gandhi, C., and M.F. Ashby. 1979. "Fracture Mechanism-Maps for Materials Which Cleave: F.C.C., B.C.C., and H.C.P. Metals and Ceramics," *Acta Metallurgica.* Vol. 27, 1565-1602.

Holcomb, D.J. 1988. "Cross-Hole Measurement of Velocity and Attenuation to Detect a Disturbed Zone in Salt at the Waste Isolation Pilot Plant," *Key Questions in Rock Mechanics, Proceedings of the 29th U.S. Symposium, University of Minnesota, Minneapolis, MN, June 13-15, 1988.* Eds. P.A. Cundall, R.L. Sterling, and A.M. Starfield. SAND87-3016C. Brookfield, VT: A.A. Balkema. 633-640.

Jung, Y., A. Ibrahim, and D.J. Borns. 1991. "Mapping Fracture Zones in Salt; High Resolution, Cross-Gallery Seismic Tomography," *Geophysics: The Leading Edge of Exploration.* Vol. 10, no. 4, 37-39.

Krieg, R.D. 1984. *Reference Stratigraphy and Rock Properties for the Waste Isolation Pilot Plant (WIPP) Project.* SAND83-1908. Albuquerque, NM: Sandia National Laboratories.

Krieg, R.D., C.M. Stone, and S.W. Key. 1980. *Comparisons of the Structural Behavior of Three Storage Room Designs for the WIPP Project.* SAND80-1629. Albuquerque, NM: Sandia National Laboratories.

Lappin, A.R., R.L. Hunter, P.B. Davies, D.J. Borns, M. Reeves, J. Pickens, and H.J. Iuzzolino. 1989. *Systems Analysis, Long-Term Radionuclide Transport, and Dose Assessments, Waste Isolation Pilot Plant (WIPP), Southeastern New Mexico; September 1989.* SAND89-1996. Albuquerque, NM: Sandia National Laboratories.

Matalucci, R.V., C.L. Christensen, T.O. Hunter, M.A. Molecke, and D.E. Munson. 1982. *Waste Isolation Pilot Plant (WIPP) Research and Development Program: In Situ Testing Plan, March 1982.* SAND81-2628. Albuquerque, NM: Sandia National Laboratories.

Mellegard, K.D., G.D. Callahan, and P.E. Senseny. 1992. *Multiaxial Creep of Natural Rock Salt.* SAND91-7083. Albuquerque, NM: Sandia National Laboratories.

Monkman, F.C., and N.J. Grant. 1956. "An Empirical Relationship Between Rupture Life and Minimum Creep Rate in Creep-Rupture Tests," *American Society for Testing and Materials Proceedings.* Vol. 56, 593-620.

Morgan, H.S., C.M. Stone, and R.D. Krieg. 1985. "The Use of Field Data to Evaluate and Improve Drift Response Models for the Waste Isolation Pilot Plant (WIPP)," *Research & Engineering Applications in Rock Masses, Proceedings of the 26th U.S. Symposium on Rock Mechanics, South Dakota School of Mines & Technology, Rapid City, SD, June 26-28, 1985*. Ed. E. Ashworth. Brookfield, VT: A.A. Balkema. 769-776.

Morgan, H.S., C.M. Stone, and R.D. Krieg. 1986. *An Evaluation of WIPP Structural Modeling Capabilities Based on Comparisons with South Drift Data*. SAND85-0323. Albuquerque, NM: Sandia National Laboratories.

Munson, D.E. 1979. *Preliminary Deformation Mechanism Map for Salt (with Application to WIPP)*. SAND79-0076. Albuquerque, NM: Sandia National Laboratories.

Munson, D.E. 1991. "In Situ Tests of Salt Deformation for Validation of a Radioactive Waste Repository Predictive Technology," *Preprint, 1991 SME Annual Meeting, Denver, CO, February 25-28, 1991*. Littleton, CO: Society of Mining Engineers of AIME. Vol. 20, 1914-1921.

Munson, D.E., and P.R. Dawson. 1979. *Constitutive Model for the Low Temperature Creep of Salt (With Application to WIPP)*. SAND79-1853. Albuquerque, NM: Sandia National Laboratories.

Munson, D.E., and P.R. Dawson. 1982. *A Transient Creep Model for Salt During Stress Loading and Unloading*. SAND82-0962. Albuquerque, NM: Sandia National Laboratories.

Munson, D.E., and K.L. DeVries. 1991. "Development and Validation of a Predictive Technology for Creep Closure of Underground Rooms in Salt," *Proceedings, 7th International Congress on Rock Mechanics, Aachen, Germany, September 16-20, 1991*. Ed. W. Wittke. Brookfield, VT: A.A. Balkema. Vol. 1, 127-134.

Munson, D.E., T.M. Torres, and R.L. Jones. 1987a. "Pseudostrain Representation of Multipass Excavations in Salt," *Rock Mechanics: Proceedings of the 28th U.S. Symposium, University of Arizona, Tucson, AZ, June 29-July 1, 1987*. Eds. I.W. Farmer, J.J.K. Daemen, C.S. Desai, C.E. Glass, and S.P. Neuman. Brookfield, VT: A.A. Balkema. 853-862.

Munson, D.E., R.L. Jones, D.L. Hoag, and J.R. Ball. 1987b. *Heated Axisymmetric Pillar Test (Room H): In Situ Data Report (February 1985 - April 1987)*. SAND87-2488. Albuquerque, NM: Sandia National Laboratories.

Munson, D.E., T.M. Torres, and R.L. Jones. 1988a. "Results of a Large, In Situ, Heated Axisymmetric Pillar Test at the Waste Isolation Pilot Plant (WIPP)," *Key Questions in Rock Mechanics: Proceedings of the 29th U.S. Symposium, University of Minnesota, Minneapolis, MN, June 13-15, 1988*. Eds. P.A. Cundall, R.L. Sterling, and A.M. Starfield. Brookfield, VT: A.A. Balkema. 641-651.

Munson, D.E., R.L. Jones, D.L. Hoag, and J.R. Ball. 1988b. *Mining Development Test (Room D): In Situ Data Report (March 1984 - May 1988)*. SAND88-1460. Albuquerque, NM: Sandia National Laboratories.

Munson, D.E., A.F. Fossum, and P.E. Senseny. 1989a. *Advances in Resolution of Discrepancies Between Predicted and Measured In Situ WIPP Room Closures*. SAND88-2948. Albuquerque, NM: Sandia National Laboratories.

Munson, D.E., A.F. Fossum, and P.E. Senseny. 1989b. "Approach to First Principles Model Prediction of Measured WIPP In Situ Room Closure in Salt," *Rock Mechanics as a Guide for Efficient Utilization of Natural Resources: Proceedings of the 30th U.S. Symposium, West Virginia University, Morgantown, WV, June 19-22, 1989*. Ed. A.W. Khair. Brookfield, VT: A.A. Balkema. 673-680.

Munson, D.E., K.L. DeVries, and G.D. Callahan. 1990a. "Comparison of Calculations and In Situ Results for a Large, Heated, Test Room at the Waste Isolation Pilot Plant (WIPP)," *Rock Mechanics: Contributions and Challenges, Proceedings of the 31st U.S. Symposium, Colorado School of Mines, Golden, CO, June 18-20, 1990*. Eds. W.A. Hustrulid and G.A. Johnson. Brookfield, VT: A.A. Balkema. 389-396.

Munson, D.E., R.L. Jones, J.R. Ball, R.M. Clancy, D.L. Hoag, and S.V. Petney. 1990b. *Overtest for Simulated Defense High-Level Waste (Room B): In Situ Data Report (May 1984 - February 1988)*. SAND89-2671. Albuquerque, NM: Sandia National Laboratories.

Munson, D.E., R.L. Jones, and K.L. DeVries. 1991a. "Analysis of Early Closures in Geomechanically Connected Underground Rooms in Salt," *Rock Mechanics as a Multidisciplinary Science, Proceedings of the 32nd U.S. Symposium, University of Oklahoma, Norman, OK, July 10-12, 1991*. Ed. J-C. Roegiers. Brookfield, VT: A.A. Balkema. 881-888.

Munson, D.E., S.V. Petney, R.M. Clancy, J.R. Ball, R.L. Jones, and C.L. Northrop-Salazar. 1991b. *18 W/m^2 Mockup for Defense High-Level Waste (Rooms A): In Situ Data Report: Vol. I - Mechanical Response Gages (February 1985 - June 1990)*. SAND90-2748. Albuquerque, NM: Sandia National Laboratories.

Munson, D.E., K.L. DeVries, D.M. Schiermeister, W.F. DeYonge, and R.L. Jones. 1992a. "Measured and Calculated Closures of Open and Brine Filled Shafts and Deep Vertical Boreholes in Salt," *Rock Mechanics, Proceedings of the 33rd U.S. Symposium, Santa Fe, NM, June 3-5, 1992*. Eds. J.R. Tillerson and W.R. Wawersik. Brookfield, VT: A.A. Balkema. 439-448.

Munson, D.E., S.V. Petney, T.L. Christian-Frear, J.R. Ball, R.L. Jones, and C.L. Northrop-Salazar. 1992b. *Geomechanical Evaluation (Room G): In Situ Data Report (December 1984 - November 1990)*. SAND92-0582. Albuquerque, NM: Sandia National Laboratories.

Munson, D.E., R.L. Jones, C.L. Northrop-Salazar, and S.J. Woerner. 1992c. *Multipass Mining Sequence Room Closures: In Situ Data Report*. SAND87-2687. Albuquerque, NM: Sandia National Laboratories.

Munson, D.E., S.V. Petney, T.L. Christian-Frear, J.R. Ball, R.L. Jones, and C.L. Northrop-Salazar. 1992d. *18 W/m^2 Mockup for Defense High-Level Waste (Rooms A): In Situ Data Report: Vol. II - Thermal Response Gages (February 1985 - June 1990)*. SAND90-2749. Albuquerque, NM: Sandia National Laboratories.

Munson, D.E., J.R. Weatherby, and K.L. DeVries. 1993. "Two- and Three-Dimensional Calculations of Scaled In Situ Tests Using the M-D Model of Salt Creep," *International Journal of Rock Mechanics and Mining Sciences & Geomechanics Abstracts*. Vol. 30, no. 7, 1345-1350.

NAS. 1957. *Disposal of Radioactive Waste on Land*. Publication 519. Washington, DC: National Academy of Sciences - National Research Council, Committee on Waste Disposal.

Pfeifer, M.C., D.J. Borns, C.K. Skokan, H.T. Andersen, and J.M. Starrett. 1989. "Geophysical Methods to Monitor the Development of the Disturbed Rock Zone Around Underground Excavations in Bedded Salt," *Proceedings of the Symposium on the Application of Geophysics to Engineering and Environmental Problems, Golden, CO, March 13-16, 1989*. SAND89-7055A. 400-411.

Rechard, R.P., W. Beyeler, R.D. McCurley, D.K. Rudeen, J.E. Bean, and J.D. Schrieber. 1989. *Parameter Sensitivity Studies of Selected Components of the Waste Isolation Pilot Plant Repository/Shaft System*. SAND89-2030. Albuquerque, NM: Sandia National Laboratories.

Stormont, J.C. 1990. "Discontinuous Behavior Near Excavations in a Bedded Salt Formation," *International Journal of Mining and Geological Engineering*. Vol. 8, no. 1, 35-56.

Stormont, J.C., E.W. Peterson, and P.L. Lagus. 1987. *Summary of and Observations About WIPP Facility Horizon Gas Flow Measurements Through 1986*. SAND87-0176. Albuquerque, NM: Sandia National Laboratories.

Stormont, J.C. C.L. Howard, and J.J.K. Daemen. 1991. *In Situ Measurements of Rock Salt Permeability Changes Due to Nearby Excavation*. SAND90-3134. Albuquerque, NM: Sandia National Laboratories.

Stormont, J.C., J.J.K. Daemen, and C.S. Desai. 1992. "Prediction of Dilation and Permeability Changes in Rock Salt," *International Journal for Numerical and Analytical Methods in Geomechanics*. Vol. 16, no. 8, 545-569.

Van Sambeek, L.L., D.D. Luo, M.S. Lin, W. Ostrowski, and D. Oyenuga. 1993. *Seal Design Alternatives Study*. SAND92-7340. Albuquerque, NM: Sandia National Laboratories.

Wawersik, W.R., and C.M. Stone. 1985. *Application of Hydraulic Fracturing to Determine Virgin In Situ Stress State Around Waste Isolation Pilot Plant - In Situ Measurements*. SAND85-1776. Albuquerque, NM: Sandia National Laboratories.

Wawersik, W.R., and C.M. Stone. 1989. "A Characterization of Pressure Records in Inelastic Rock Demonstrated by Hydraulic Fracturing Measurements in Salt," *International Journal of Rock Mechanics and Mining Sciences & Geomechanics Abstracts*. Vol. 26, 613-627.

WIPP PA (Performance Assessment) Department. 1992a. *Preliminary Performance Assessment for the Waste Isolation Pilot Plant, December 1992. Volume 2 - Technical Basis.* SAND92-0700/2. Albuquerque, NM: Sandia National Laboratories.

WIPP PA (Performance Assessment) Department. 1992b. *Preliminary Performance Assessment for the Waste Isolation Pilot Plant, December 1992. Volume 3 - Model Parameters.* SAND92-0700/3. Albuquerque, NM: Sandia National Laboratories.

WIPP Library

March 27, 1995

Systems Prioritization Method - Iteration 2 Baseline Position Paper:

Non-Salado Flow and Transport

C. Axness, R. Beauheim, Y. Behl, K. Brinster, T. Corbet, K. Economy,
G. Freeze, L. Meigs, H. Papenguth, D. Powers, P. Swift, M. Wallace, S. Webb

Sandia National Laboratories
Albuquerque, NM 87185

CONTENTS

ACRONYMS vi

ABBREVIATIONS vii

1.0 INTRODUCTION 1-1

2.0 FEATURES, EVENTS, AND PROCESSES INVOLVING NON-SALADO HYDROLOGY 2-1

3.0 CONCEPTUAL AND MECHANISTIC MODELS INVOLVING NON-SALADO HYDROLOGY 3-1

3.1 Hydrostratigraphy and Regional Groundwater Flow 3-1
3.1.1 Stratigraphy and Lithology in the Vicinity of the WIPP Site 3-1
3.1.2 Conceptual Models of Groundwater Flow Above the Salado Formation 3-18
3.1.3 Groundwater Geochemistry and Flow in the Culebra Dolomite Member 3-29
3.1.4 Castile Brine Reservoirs 3-31
3.1.5 Multi-Phase Flow 3-34

3.2 Culebra Flow and Transport 3-35
3.2.1 Transmissivity 3-35
3.2.2 Storativity 3-36
3.2.3 Variable-Density Flow 3-37
3.2.4 Fluid from an Intrusion Hole 3-38
3.2.5 Double Porosity 3-39
3.2.6 Channeling 3-43
3.2.7 Matrix Advection 3-43
3.2.8 Dispersion 3-45

3.3 Culebra Chemical Retardation 3-46
3.3.1 Rock-Water Interaction in the Culebra 3-47
3.3.2 Adsorption 3-52
3.3.3 Colloid-Facilitated Radionuclide Transport 3-54
3.3.4 Actinide Coprecipitation From Brine Mixing 3-60

3.4 Long Term Processes 3-61
3.4.1 Climate Change 3-62
3.4.2 Leakage in Shallow Drill Holes 3-65
3.4.3 Subsidence Over Potash Mines 3-66

4.0 CURRENTLY AVAILABLE DATA FOR ASSESSING LONG-TERM PERFORMANCE 4-1

4.1 Supra-Rustler Units 4-1
4.2 Rustler Formation 4-1
4.2.1 Unnamed Lower Member and Contact Zone with Upper Salado Formation 4-2
4.2.2 Culebra Dolomite Member 4-8
4.2.3 Tamarisk Member 4-13
4.2.4 Magenta Dolomite Member 4-17
4.2.5 Forty-niner Member 4-21
4.2.6 Discussion of Rustler Hydraulic Heads 4-26

4.3 Castile Formation 4-32
4.4 Bell Canyon Formation 4-36
4.5 Formations Below the Bell Canyon Formation 4-36
4.6 Documentation of Experimental Data and Interpretive Techniques 4-40

5.0 SUMMARY OF SPM2 BASELINE FOR NON-SALADO FLOW AND TRANSPORT 5-1

5.1 Release Paths 5-1
5.2 Culebra Flow and Physical Retardation 5-5
5.3 Chemical Retardation 5-8
5.4 Intrusion Holes and Castile Brine Reservoir 5-9
5.5 Climate Change 5-10

6.0 REFERENCES 6-1

APPENDIX A: Evolution of Patterns of Regional Groundwater Flow in Southeastern New Mexico; Response to Post-Pleistocene Changes in Climate A-1

Figures

3-1. Surface topography and drillholes near the WIPP site. 3-2
3-2. Stratigraphic column for the WIPP vicinity. 3-3
3-3. Topography of the land surface and the lateral boundary of the regional groundwater flow model. 3-26
3-4. Hydrostratigraphic units for the regional groundwater flow model. 3-28
3-5. Selected deep boreholes that penetrate the Castile Formation, northern Delaware Basin. 3-32
4-1. Distribution of Rustler halite and unnamed lower member and/or Rustler-Salado contact residuum transmissivity around the WIPP site. 4-3
4-2. Measured water levels and estimated freshwater heads of the unnamed lower member and/or Rustler-Salado contact zone. 4-6

4-3. Concentrations (meq/L) of major chemical constituents in the unnamed lower member and/or upper Salado (from Mercer, 1983). 4-10
4-4. Distribution of Rustler halite and Culebra transmissivity around the WIPP site. 4-12
4-5. Estimated freshwater heads of the Culebra. 4-16
4-6. Distribution of Rustler halite and Magenta transmissivity around the WIPP site. 4-18
4-7. Measured water levels and estimated freshwater heads of the Magenta dolomite member. 4-20
4-8. Concentrations (meq/L) of major chemical constituents in the Magenta. 4-24
4-9. Estimated freshwater heads of the Forty-Niner claystone. 4-27
4-10. Flow potentials between the Culebra dolomite and the unnamed member/upper Salado. 4-31
4-11. Flow potentials between the Magenta dolomite and the Culebra dolomite. . . . 4-34
4-12. Potentiometric surface of the hydrologic unit in the upper part of the Bell Canyon Formation (Delaware Mountain Group) at and near the proposed Waste Isolation Pilot Plant (WIPP) site. 4-38
4-13. Stratigraphic column of units below the Castile formation (from Powers et al., 1978; after Foster, 1974). 4-39

Tables

3-1. Alternative Conceptual Models for Rock-Water Interaction in the Culebra Dolomite Member of the Rustler Formation 3-51
4-1. Summary of Information on Hydraulic Testing of the Unnamed Lower Member and/or Upper Salado 4-4
4-2. Hydraulic-Head Information for the Unnamed Lower Member and/or Upper Salado 4-7
4-3. Geochemical Analyses from the Unnamed Lower Member and/or Upper Salado. 4-9
4-4. Summary of Transmissivity Data for the Culebra Dolomite Member of the Rustler Formation 4-11
4-5. Hydraulic-Head Information for the Culebra Dolomite Member of the Rustler Formation 4-14
4-6. Summary of Transmissivity Data for the Magenta Dolomite Member of the Rustler Formation 4-19
4-7. Hydraulic-Head Information for the Magenta Dolomite Member of the Rustler Formation 4-22
4-8. Geochemical Analyses from Testing in the Magenta 4-23
4-9. Summary of Transmissivity Data for the Forty-Niner Claystone 4-25
4-10. Hydraulic-Head Information for the Forty-Niner Claystone 4-28
4-11. Potential Flow Directions between the Culebra and Unnamed Member/Upper Salado 4-30
4-12. Potential Flow Directions Between the Magenta and Culebra 4-33
4-13. Potential Flow Directions between the Forty-Niner Claystone and Magenta . . . 4-35
4-14. Summary of Bell Canyon DST Results 4-37

Tables (Contined)

5-1. Modeling Parameters for a Hypothetical Brine Reservoir in the Castile Formation. 5-12

ACRONYMS

DOE	-	Department of Energy
EPA	-	Environmental Protection Agency
WIPP	-	Waste Isolation Pilot Plant
CFR	-	Code of Federal Regulations
RCRA	-	Resource Conservation and Recovery Act
SNL	-	Sandia National Laboratories
PA	-	performance assessment
SPM	-	Systems Prioritization Method
CAO	-	Carlsbad Area Office
PTB	-	Project Technical Baseline
FEPs	-	features, events, and processes
EEG	-	Environmental Evaluation Group
TDEM	-	time-domain electromagnetic
ERDA	-	Energy Research and Development Agency
GxG	-	Geostatistics Expert Group
TOC	-	total organic carbon
LLNL	-	Lawrence Livermore National Laboratory
U.S.	-	United States
COHMAP	-	
DST	-	drillstem test
USGS	-	United States Geological Survey
AEC	-	Atomic Energy Commission

ABBREVIATIONS

μ	-	micro
μg/L	-	micrograms per liter
Å	-	angstrom
amsl	-	above mean sea level
°C	-	degrees Centigrade
cm	-	centimeter
ft	-	feet
g	-	gram
gpm	-	gallons per minute
h	-	hour
in	-	inches
km	-	kilometer
m	-	meter
Ma	-	million years ago
mD	-	millidarcy
meq/L	-	milliequivalents per liter
mg/L	-	milligrams per liter
mi	-	mile
MPa	-	megapascal
nm	-	nanometer
pH	-	the base ten logarithm of hydrogen ion concentration, times negative one; a common expression for acidity
psi	-	pounds per square inch
psig	-	pounds per square inch, gauge
s	-	seconds
wt	-	weight
yr	-	year

1.0 INTRODUCTION

The U.S. Department of Energy (DOE) is preparing to request the U.S. Environmental Protection Agency (EPA) to certify compliance of the Waste Isolation Pilot Plant (WIPP) with long-term requirements of *the environmental Radiation Protection Standards for Management and Disposal of Spent Nuclear Fuel, High-Level and Transuranic Waste* (40 CFR Part 191). The DOE must also demonstrate compliance with the long-term requirements of the *Land Disposal Restrictions* of the *Resource Conservation and Recovery Act* (RCRA) (40 CFR Part 268.6). Sandia National Laboratories (SNL) has been conducting iterative performance assessments (PAs) for the WIPP to provide guidance to the project on the technical activities required to determine long-term performance of the WIPP disposal system. The most recent PA was conducted in 1992.

An effort is under way within the project to prioritize the activities needed to demonstrate with a reasonable expectation that the WIPP will satisfy the relevant quantitative long-term performance requirements. This principal tool used in this effort is referred to as Systems Prioritization Method (SPM).

SPM is a decision-analysis methodology developed for the DOE Carlsbad Area Office (DOE-CAO) by SNL that will identify relationships among schedule constraints, resource constraints, current and proposed technical programs, and the likelihood of demonstrating compliance within these constraints. In particular, the probability that specific combinations of activities will lead to a demonstration of compliance with respect to applicable long-term regulations will be estimated. These activities include experimental programs designed to reduce uncertainty in data and models used to characterize the disposal system for long-term performance assessment, and also include potential modifications to the waste acceptance criteria, waste form, and repository design. The DOE-CAO will use results of future iterations of the SPM in combination with information about time and cost of the various activities to set priorities for WIPP activities and to select a combination of activities that will form the basis for a compliance determination.

In parallel with the SPM, a Project Technical Baseline (PTB) document is being prepared that will contain the technical basis for a compliance application. Technical programs conducted in the period leading up to a final compliance determination may lead to changed or improved understanding in areas critical to defending this determination. The PTB can be updated periodically as required.

In support of both the SPM and the PTB, a series of position papers has been prepared that documents the current understanding of the main components of the disposal system and the long-term performance assessment. This paper addresses hydrology of units other than the Salado Formation, which contains the repository. Specifically, units considered here are the Castile, Bell Canyon, and other formations below the Salado Formation; and the Rustler, Dewey Lake, and other formations above the Salado. Hydrology of these units is relevant to compliance with the long-term requirements of 40 CFR 191. Because the upper and lower boundaries of the disposal unit for 40 CFR 268.6 are defined to be the top and bottom of the Salado Formation, this paper has less relevance to RCRA compliance. Hydrology of the Salado Formation is important for both regulations, and is addressed in a separate position paper.

The objectives of this paper are to:

1) Identify and describe the relationship between non-Salado hydrology and the array of scenarios that might be relevant to the long-term performance of the repository.

2) Identify and describe the array of conceptual and mechanistic models that are required to evaluate the scenarios for the purpose of compliance.

3) Identify and describe the data/information that are required to support the conceptual and mechanistic models.

4) Identify conceptual and computational models and appropriate parameter values for use in the second iteration of the SPM.

The scenarios that involve non-Salado hydrology are summarized in Section 2. The conceptual and mechanistic models are described in Section 3. Section 4 contains a summary of data and information that is presently available for use in a compliance application. Section 5 contains the portions of the SPM2 baseline that pertain to non-Salado flow and transport.

2.0 FEATURES, EVENTS, AND PROCESSES INVOLVING NON-SALADO HYDROLOGY

The features, events, and processes (FEPs) considered in this paper are those described in the Scenario Development Position Paper that involve the non-Salado units and have been retained by the Scenario Development Team for further evaluation. All FEPs relevant to Non-Salado flow and transport require man-made vertical pathways connecting the repository to Non-Salado flow units. These pathways could be features such as WIPP shafts or human intrusion boreholes. Vertical transport through these pathways is required before the flow and transport of radionuclides in the Non-Salado units must be considered. At this point in the analysis, natural processes such as climate change become relevant to performance assessment.

As shown in previous analyses (e.g., WIPP PA Department, 1992, Volume 1, Section 5), human intrusion boreholes have the greatest potential to affect disposal system performance because they provide a pathway for brine to carry radionuclides to the surface or to hydraulically conductive strata. Once introduced into the conductive strata, the radionuclides potentially could migrate laterally to the accessible environment or to another drill hole. Vertical movement of fluids in drill holes, regardless of whether the drill holes intersect the repository, could potentially modify the flow field and/or the retardation properties of the strata.

Fluids could potentially move into or out of a number of stratigraphic units above the repository (conductive zones in the Dockum Group and the Dewey Lake Formation, if these units become saturated, and the Rustler Formation) or conductive units below the repository (Castile and Bell Canyon Formations and deeper rocks). The rate at which fluids move vertically in drill holes depends mainly on the permeability, porosity, compressibility, and hydraulic head of the conductive zones connected by the drill hole, as well as the permeability of the drill hole, if plugged or closed. The permeability and hydraulic head of the conductive units are considerably different, and many flow paths are possible depending on the position, depth, and time of the drill holes. Heads at some locations in the Castile Formation and deeper rocks are high enough to drive fluid to the land surface. Consequently, fluids could move up boreholes from these units to the repository, if it were not highly pressurized, or to conductive units above the repository.

As discussed in the Scenario Development Position Paper, climate change is the principal natural process currently considered relevant to non-Salado flow and transport. A change in climate could impact the amount of moisture that infiltrates into the soil and is thereby available to recharge the groundwater system. Patterns and rates of groundwater flow are determined

partly by the amount and distribution of recharge. Vegetational changes could also impact infiltration rates, but this FEP has been screened out on the basis of low consequence.

3.0 CONCEPTUAL AND MECHANISTIC MODELS INVOLVING NON-SALADO HYDROLOGY

This section describes or refers to the conceptual and mechanistic models used to evaluate features, events, and processes (FEPs) involving flow and transport in stratigraphic units other than the Salado Formation. This paper adopts a modular approach in which we describe conceptual and mechanistic models for the individual aspects of the flow and transport system. These modules can be combined, as required, to evaluate particular FEPs.

One example, to illustrate the modular approach, is the treatment of an intrusion borehole that penetrates the repository and provides a pathway for radionuclides to move upward to the Culebra Dolomite and then migrate laterally in the Culebra toward the accessible environment. Evaluation of scenarios including this event require a conceptual model of flow above the Salado, a model for fluid flowing from an intrusion hole, models for determining distributions for transmissivity, storage, and representative head gradients for the Culebra, and a suite of conceptual and mechanistic models to describe physical and chemical retardation along the flow path. These models are discussed separately in this paper, rather than in a linked sequence as they appear in performance assessment system-level modeling.

Each model description in this chapter contains a summary statement that presents the position supported and a discussion section that details the supporting reasoning and data. Conceptual and mechanistic models are divided into four Sections. Section 3.1 contains a basic description of the hydrostratigraphy and models that describe processes or considerations that apply to multiple stratigraphic units. Section 3.2 includes models that address flow and advective transport in the Culebra Dolomite. Section 3.3 includes models that deal with chemical retardation. The final section, 3.4, addresses long-term processes that could impact performance of the repository during 10,000 years.

3.1 Hydrostratigraphy and Regional Groundwater Flow

3.1.1 Stratigraphy and Lithology in the Vicinity of the WIPP Site

This section presents the stratigraphy and lithology of the Paleozoic and younger rocks underlying the WIPP site and vicinity (Figures 3-1 and 3-2), emphasizing the units nearer the surface and excluding the Salado Formation, which is discussed in a separate document. Details and descriptions begin with the Permian (Guadalupian) Bell Canyon Formation, the upper

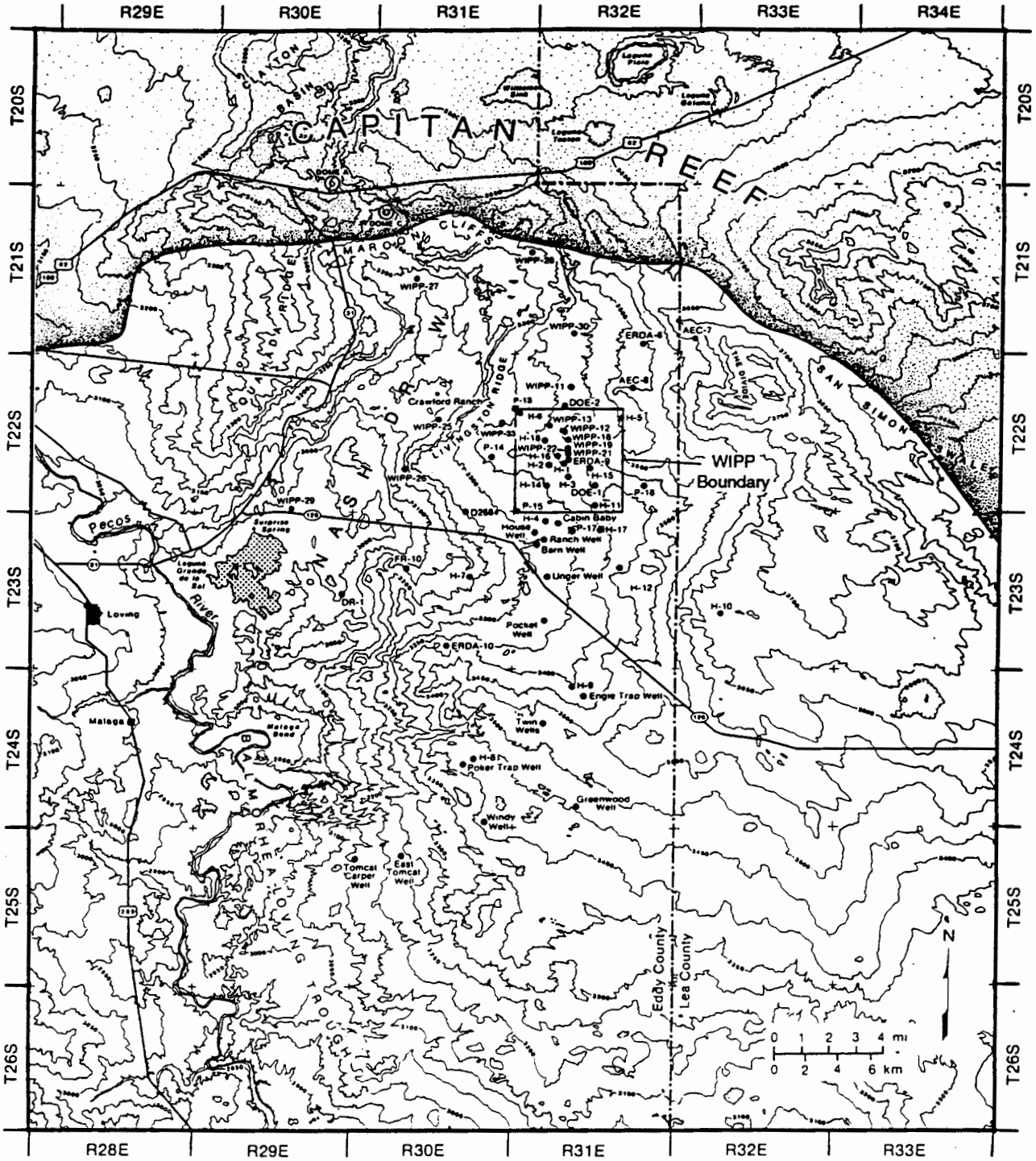

TRI-6342-612-13

Figure 3-1. Surface topography and drillholes near the WIPP site.

System	Series	Group	Formation	Member
Recent	Recent		Surficial Deposits	
Quaternary	Pleistocene		Mescalero Caliche	
			Gatuña	
Triassic		Dockum	Undivided	
Permian	Ochoan		Dewey Lake Red Beds	
			Rustler	Forty-niner
				Magenta Dolomite
				Tamarisk
				Culebra Dolomite
				Unnamed Lower
			Salado	
			Castile	
	Guadalupian	Delaware Mountain	Bell Canyon	
			Cherry Canyon	
			Brushy Canyon	

TRI-6330-89-3

Figure 3-2. Stratigraphic column for the WIPP vicinity.

unit of the Delaware Mountain Group, because this is the uppermost water-bearing formation below the evaporites that host the WIPP repository. The principal stratigraphic data are the chronologic sequence, age, and extent of rock units, including some of the nearby, relevant facies changes. Characteristics such as thickness and depth are summarized here from published sources for deeper rocks and are mainly based on WIPP data for shallower rocks (above Bell Canyon). The main lithologies for upper formations and members of some formations are described. Some of the systems (e.g., Jurassic) are not described because they do not occur at or near the WIPP Site.

3.1.1.1 GENERAL STRATIGRAPHY AND LITHOLOGY BELOW THE BELL CANYON FORMATION

The most thorough summaries of the formations and lithologies below the Bell Canyon for the site area have been prepared by Foster (1974, p. 10) and Powers et al. (1978). This section is modified from those sources; the details of these units are scattered and often exist as raw data in geophysical logs, in files of government agencies, or in private sector petroleum exploration logs. Some stratigraphic detail is given as support for later discussions of hydrocarbon resources from units below the Bell Canyon.

The known Precambrian basement near the site is projected to be 18,191 feet (5,545 meters) below the surface (Sipes, Williamson & Aycock, 1976, Vol. II, Exhibit No. 2), consistent with information presented by Foster (1974). Ages of similar metamorphic suites in the area range from about 1.14 to 1.35 billion years.

The basal units overlying Precambrian rocks are clastic rocks commonly attributed either to the Bliss Sandstone or the Ellenberger Group (Foster, 1974, p. 10), considered most likely to be Ordovician in age in this area. The Ordovician System comprises the Ellenberger, Simpson, and Montoya Groups in the northern Delaware Basin. Carbonates are predominant in these groups, with sandstones and shales common in the Simpson Group. Foster (1974, p. 12) reported 975 feet (297 meters) of Ordovician north of the site area and extrapolated a thicker section of about 1,300 feet (396 meters) at the present site (p. 17). Sipes, Williamson & Aycock, Inc. (1976, Vol. II, Exhibit No. 2) projected a thickness of 1,200 feet (366 meters) within the site boundaries.

Silurian-Devonian rocks in the Delaware Basin are not stratigraphically well-defined, and there are various notions for extending nomenclature into the basin. Common drilling practice is not to differentiate, though the Upper Devonian Woodford Shale at the top of the sequence is frequently distinguished from the underlying dolomite and limestone (Foster, 1974, p. 18).

Foster (p. 21) showed a reference thickness of 1,260 and 160 feet (384 and 49 meters) for the carbonates and the Woodford shale, respectively; he estimated thickness contours for the present WIPP site of about 1,150 (351 meters) and 170 feet (52 meters), respectively. Sipes, Williamson & Aycock, Inc. (1976) projected 1,250 feet (381 meters) of carbonate and showed 82 feet (25 meters) of Woodford.

The Mississippian System in the northern Delaware Basin is commonly attributed to "Mississippian limestone" and the overlying Barnett Shale (Foster, 1974, p. 24), but the nomenclature is not well-settled. At the reference well used by Foster (p. 25), the limestone is 540 feet (165 meters) thick and the shale is 80 feet (24 meters); isopachs at the WIPP are 480 feet (146 meters) and less than 200 feet (61 meters). Sipes, Williamson & Aycock (1976) indicate 511 feet (156 meters) and 164 feet (50 meters), respectively, within the site boundaries.

The nomenclature of the Pennsylvanian System applied within the Delaware Basin is both varied and commonly not technically consistent with accepted stratigraphic rules. Chronostratigraphic or time-stratigraphic names are applied to these lithologic units: the Morrow, Atoka, and Strawn, from base to top (Foster, 1974, p. 31). Foster (1974, p. 34) extrapolated thicknesses of about 2,200 feet (671 meters) for the Pennsylvanian at the WIPP site. Sipes, Williamson & Aycock , Inc. (1976, Vol. II, Exhibit No. 2) report 2,088 feet (636 meters) for these units. The Pennsylvanian rocks in this area are mixed clastics and carbonates, with carbonates more abundant in the upper half of the sequence.

The Permian System is the thickest system in the northern Delaware Basin, and is divided into four series from the base to top: Wolfcampian, Leonardian, Guadalupian, and Ochoan. The three lower series total 8,684 feet (2,647 meters) near the site (Sipes, Williamson & Aycock, Inc., 1976). Foster (1974) indicates a total thickness for the lower three series of about 7,665 feet (2,336 meters) from a reference well north of WIPP. Foster's isopach maps of these series indicate about 8,500 feet (2,591 meters) for the WIPP site area. The Ochoan Series at the top of the Permian is considered in more detail later because the formations host and surround the WIPP repository horizon. Its thickness at DOE-2, about 2 miles north of the site center, is 3,938 feet (1,200 meters) (Mercer et al., 1987, p. 23-24).

The Wolfcampian Series is also referred to as the Wolfcamp Formation in the Delaware Basin. In the site area, the lower part of the Wolfcamp is dominantly shale with carbonate and some sandstone (Foster, 1974, p. 38); carbonate increases to the north. Clastics increase to the east toward the margin of the Central Basin Platform. The Wolfcamp is 1,493 feet (455 meters) thick at a well near the WIPP site (Sipes, Williamson & Aycock, Inc., 1976).

The Leonardian Series is represented by the Bone Spring Limestone or Formation (erroneously called Bone Springs Limestone in many publications). The lower part of the formation is commonly interbedded carbonate, sandstone, and some shale, while the upper part is dominantly carbonate (Foster, 1974, p. 39). Near the site, the Bone Spring is 3,247 feet (990 meters) thick (Sipes, Williamson & Aycock, 1976).

The Guadalupian Series is represented in the general area of the site by a number of formations exhibiting complex facies relationships. The Guadalupian Series is known in considerable detail west of the site from outcrops in the Guadalupe Mountains, where numerous outcrops and subsurface studies have been undertaken, including King (1948), Newell et al. (1953), Dunham (1972), and many others. From the site to the north, similar facies relationships are expected, though mainly in the subsurface (Garber et al., 1989, p. 36).

Within the Delaware Basin, the Guadalupian Series comprises three formations: Brushy Canyon, Cherry Canyon, and Bell Canyon, from base to top. These formations are dominated by submarine channel sandstones with interbedded limestone and some shale. A limestone (Lamar) generally tops the series, immediately underneath the evaporative Castile Formation. Around the margin of the Delaware Basin, reefs developed during the same time the Cherry Canyon and Bell Canyon Formations were being deposited. These massive reef limestones, the Goat Seep and Capitan Limestones, are equivalent in time to these basin sandstone formations, but were developed much higher topographically around the basin margin. A complex set of limestone to sandstone and evaporite beds was deposited further away from the basin behind the reef limestones. The Capitan reef limestones are well known because the Carlsbad Caverns are partially developed in these rocks.

3.1.1.2 BELL CANYON FORMATION

The Bell Canyon is known from outcrops on the west side of the Delaware Basin (Newell et al., 1953) and from subsurface intercepts for oil and gas drilling. Mercer et al. (1987, p. 28) stated that DOE-2 penetrated the Lamar Limestone, the Ramsey sand, the Ford shale, the Olds sand, and the Hays sand. This informal nomenclature is used for the Bell Canyon in some other WIPP reports.

The Clayton Williams Badger Federal drillhole near the WIPP (Section 15, T22S, R31E) intercepted 961 feet (293 meters) of Bell Canyon, including the Lamar (Sipes, Williamson & Aycock, Inc., 1976). Reservoir sandstones of the Bell Canyon were deposited in channels that are straight to slightly sinuous. The top of the Bell Canyon is distinctive on density or acoustic

logs because of the massive and uniform lithology of the anhydrite compared to the underlying beds. In cores, the transition is sharp, as described for DOE-2 (Mercer et al., 1987, p. 312).

3.1.1.3 CASTILE FORMATION

The Castile Formation is the lowermost lithostratigraphic unit of the Late Permian Ochoan Series. It was originally named by Richardson (1904) for outcrops in Culberson County, Texas. The Castile crops out along a lengthy area along the western side of the Delaware Basin. The two distinctive lithologic sequences now known as the Castile and Salado Formations were separated into the upper and lower Castile Formation by Cartwright (1930). Lang (1935) clarified the nomenclature by restricting the Castile Formation to the lower unit and naming the upper unit the Salado Formation. By defining an anhydrite resting on the marginal Capitan Limestone as part of the Salado Formation, Lang (1939, 1942) effectively restricted the Castile to the Delaware Basin inside the ancient reef rocks.

Through detailed studies of the Castile, Anderson et al. (1972) introduced an informal system of names that are widely used and included in many WIPP reports. They named the units from the base as anhydrite 1 (A1), halite 1 (H1), anhydrite 2 (A2), etc. The informal nomenclature varies through the basin from A3 up because of complexity of the depositional system. The Castile consists almost entirely of thick beds of two lithologies: interlaminated carbonate and anhydrite, and high-purity halite. The interlaminated carbonate and anhydrite are well known as possible examples of annual layering or varves (Anderson et al., 1972).

In the eastern part of the Delaware Basin, the Castile is commonly 1,400 to 1,500 feet (430 and 460 meters) thick (derived from Borns and Shaffer, 1985, Figures 9, 11, and 16). At DOE-2, the Castile is 989 feet (301 meters) thick. The Castile is thinner in the western part of he Delaware Basin, and it lacks halite units. Anderson et al. (1978) correlated geophysical logs, interpreting thin zones equivalent to halite units as dissolution residues. Anderson (1981, 1982) further interpreted the lack of halite in the Castile and overlying units as indicating that about 50 percent of the halite in the basin has been removed by dissolution. Robinson and Powers (1987) analyzed one such unit as partly due to synsedimentary, gravity-driven, clastic deposition and suggested that the extent of dissolution may be overestimated. There is not known to be Castile dissolution in the immediate vicinity of the WIPP site.

In Culberson County, Texas, the Castile hosts major native sulfur deposits (Klemmick, 1993; Guilinger, 1993; Crawford and Wallace, 1993). The outcrops of Castile on the Gypsum Plain south of Whites City, New Mexico, have been explored for native sulfur without success

(Robinson and Powers, 1987), and there is no reported indicator of native sulfur anywhere in the vicinity of the WIPP (Siemers et al., 1978).

In part of the area around the WIPP, the Castile Formation has been significantly deformed, and pressurized brines are associated with the deformed areas (Powers et al., 1978): drillhole ERDA-6 encountered both. WIPP-12, one mile north of the site center, revealed lesser Castile structure, but it also encountered a zone of pressurized brine within the Castile.

The Castile continues to be an object of research interest unrelated to the WIPP program as an example of evaporites supposedly deposited in "deep water" (King, 1947; Anderson et al., 1972). Leslie et al. (1993) discuss alternatives and contradictory evidence. Although these discussions and a resolution might eventually affect some concepts of Castile deposition and dissolution, there is no apparent effect upon evaluation of the isolation of waste by the WIPP disposal system.

3.1.1.4 SALADO FORMATION

The Salado Formation is thick halite unit with small amounts of clay, anhydrite and other evaporite units. This formation is described in detail in the Salado SPM-2 Baseline Position Paper.

3.1.1.5 RUSTLER FORMATION

The Rustler is the youngest evaporite-bearing formation in the Delaware Basin. It was originally named by Richardson (1904) for outcrops in the Rustler Hills of Culberson County, Texas. Adams (1944, p. 1614) first used the names "Culebra member and Magenta member" to describe the two carbonates in the formation, indicating that Lang favored the names, though Lang (in Robinson and Lang, 1938) did not use these names in the most recent publication. Vine (1963) later extensively described the Rustler in Nash Draw and proposed the four formal names and one informal term for the stratigraphic subdivisions still used for the Rustler (from the base): unnamed lower member, Culebra Dolomite Member, Tamarisk Member, Magenta Dolomite Member, and Forty-niner Member. Though it has been noted (Holt and Powers, 1988; Powers and LeMone, 1990, p. 29) that the unnamed lower member might be named the Los Medaños Member, this nomenclature has not been formalized.

An additional system of informal subdivisions was contributed by Holt and Powers (1988), based on more detailed lithologic units of the non-carbonate members. These subdivisions have partially been related to hydrostratigraphic units for the Rustler (Beauheim and Holt, 1990, p. 145).

Two studies of the Rustler since Vine (1963) contribute important information about the stratigraphy, sedimentology, and regional relationships while examining more local details as well. Eager (1983) reported on relationships of the Rustler observed in the southern Delaware Basin as part of sulfur exploration in the area. Holt and Powers (1988) and Powers and Holt (1990) reported the details of sedimentologic and stratigraphic studies of WIPP shafts and cores as well as of geophysical logs from about 600 drillholes in southeastern New Mexico. Various details of the Rustler have also been reported as either a by-product of other investigations or for more limited purposes (Snyder, 1985; Lowenstein, 1988; Sewards et al., 1991).

Halite in the unnamed lower member persists *both east and west* of the WIPP site, and halite is found *only* east of the center of the WIPP in the Tamarisk and Forty-niner. Two differing depositional models have been generally used, either implicitly or explicitly, to account for the halite distribution. A long-standing and implicit model in many earlier documents (Jones, 1978) is that halite was originally deposited relatively uniformly in the non-carbonate members across southeastern New Mexico, including the WIPP site area. The modern distribution is caused by dissolution of Rustler halite to the west and progressing toward the east (Snyder, 1985). Holt and Powers (1988) and Powers and Holt (1990) described sedimentary features and textures within WIPP shafts and cores that led them to propose an explicit model of depositional facies for the mudstone-halite units; halite was dissolved syndepositionally from mudflat facies especially to the west, and was redeposited in a halite pan to the east.

In the region around WIPP, the Rustler reaches a maximum thickness of more than 500 feet (150 meters), while it is about 300 to 350 feet (90 to 110 meters) thick within most of the WIPP site. Most of the difference between the site area and the thickest areas is the thickness of the halite within Rustler members. The Tamarisk accounts for a larger part of thickness changes than do either the unnamed lower member or Forty-niner.

For the most detailed stratigraphic Rustler study around WIPP (Holt and Powers, 1988), the shafts were a crucial element, exposing features not previously reported. Cores were available from several WIPP boreholes, and their lithologies were matched to geophysical log signatures to extend the interpretation throughout a larger area in southeastern New Mexico. The procedures and results are described in some detail in Holt and Powers (1988).

3.1.1.5.1 Unnamed Lower Member

The unnamed lower member rests on the Salado with apparent conformity at the WIPP site. It consists of significant proportions of bedded and burrowed siliciclastic rocks with cross-bedding and fossil remains (Holt and Powers, 1988; Powers and Holt, 1990, p. 82-83). These beds record the transition from strongly evaporative environments of the Salado to saline lagoonal environments. The upper part of the unnamed lower member includes halitic and sulfatic beds within clastics. Holt and Powers (1988) interpret these as facies changes within a saline playa environment. The implied model from earlier descriptions (Jones, 1978) is that the non-halitic regions of the upper unnamed lower member are dissolution residues from post-depositional dissolution.

The unnamed lower member ranges from about 96 to 126 feet (29 to 38 meters) thick within the site boundaries (Holt and Powers, 1988, Figure 4.7). The maximum thickness recorded during that study was 208 feet (63 meters) southeast of the WIPP site. Halite extends west of most of the site area in this unit (Snyder, 1985; Powers, in Beauheim, 1987a). Cross sections based on geophysical log interpretations (Holt and Powers, 1988, Figure 4.4) show some apparent relationship between the thickness of the unit and the presence of halite.

Some samples from the unnamed lower member have been analyzed to determine clay mineralogy (Sewards et al., 1991, Table 2) and rubidium-strontium (Rb-Sr) systematics of clays (Brookins et al., 1990). Brookins et al. (1990, p. 4) concluded that Rb-Sr ages of clay fractions are consistent with a Late Permian age, and they also contrasted Rustler clays with Salado data. Salado clays show Rb-Sr ages and characteristics indicating more limited interaction with water and less alteration of detrital clays during Permian period than do Rustler clays.

3.1.1.5.2 Culebra Dolomite Member

The Culebra rests with apparent conformity on the unnamed lower member, though the underlying unit ranges from claystone to its lateral halitic equivalent in the site area. West of the WIPP site, in Nash Draw, the Culebra is disrupted in response to dissolution of underlying halite. Holt and Powers (1988) attribute this principally to dissolution of Salado halite, while Snyder (1985) indicates that salt was dissolved postdepositionally from the unnamed lower member. These alternative models provide the basis for differing explanations of how the existing Rustler hydrologic system developed and might continue to develop. The regulatory period of concern is short enough and boundaries close enough that these differences may not affect performance assessment.

The Culebra was described by Lang (Robinson and Lang, 1938) as a dolomite 35 feet (11 meters) in thickness; Adams (1944, p. 78) noted that oolites are present in some outcrops as well. The Culebra is generally "brown, finely crystalline, locally argillaceous and arenaceous dolomite with rare to abundant vugs with variable gypsum and anhydrite filling" (Holt and Powers, 1988, p. 3-8). Holt and Powers (1988, p. 5-11) described Culebra features in detail, noting that most of the Culebra is microlaminated to thinly laminated while some zones display no depositional fabric. Holt and Powers (1984) described an upper interval of the Culebra consisting of waxy, golden-brown carbonate, dark organic claystone, and some coarser siltstone of probable algal origin. Because of the unique organic composition of this thin layer, Holt and Powers (1988) did not include it in the Culebra for thickness computations, and this will be factored into discussions of Culebra thickness. Based on core descriptions from the WIPP project, Holt and Powers (1988, p. 5-11) concluded that "there is very little variation of depositional sedimentary features throughout the Culebra."

Vugs are an important part of Culebra porosity. They are commonly zoned parallel to bedding (Holt and Powers, 1990). In outcrop, vugs are commonly empty. In the subsurface, vugs may be filled with anhydrite, gypsum, or may have some clay lining (Holt and Powers, 1988, p. 5-11). Lowenstein 1988, (p. 20-21) noted similar features. Holt and Powers (1988, p. 8-4) attributed vugs partly to syndepositional growth as nodules and partly as later replacement textures. Lowenstein (1988) also described textures related to later replacement and alteration of sulfates. Vug or pore fillings vary across the WIPP site and contribute to the porosity structure of the Culebra (Beauheim and Holt, 1990, p. 157). Natural fractures filled with gypsum are common east of the WIPP site center and in a smaller area west of the site center.

Clay is the second most abundant mineral, averaging 3 to 5 weight percent (Sewards, 1991, p. IX-1). Clay minerals include corrensite, illite, serpentine, and chlorite. Additional discussion of these clays and their impact on transport is present in Section 3.3.1.

In a study of probable authigenic clays from the Rustler, including the Culebra, Brookins et al. (1990), found the Rb-Sr isochron of 259 $\pm$ 22 Ma consistent with the Late Permian age of the Rustler. These results indicate that there was not a significant interaction of high-Sr water with these clays since the Late Permian (Brookins et al., 1990, p. 4).

In the WIPP region, the Culebra is fairly uniform in thickness, averaging 7.7 meters, with a range from 5.5 to 11.3 meters (Cauffman et al., 1990, Appendix B). The average thickness of 7.7 meters has been used for the Culebra in performance assessment calculations.

3.1.1.5.3 Tamarisk Member

Vine (1963, p. B15) named the Tamarisk Member for outcrops near Tamarisk Flat in Nash Draw. Outcrops of the Tamarisk are distorted, and subsurface information was used to establish member characteristics. Vine reported two sulfate units separated by a siltstone, about 5 feet (1.5 meters) thick, interpreted by Jones et al. (1960) as a dissolution residue.

The Tamarisk is generally conformable with the underlying Culebra. The transition is marked by an organic-rich unit interpreted as present over most of southeastern New Mexico (Holt and Powers, 1988). The Tamarisk around the site area consists of lower and upper sulfate units separated by a unit that varies from mudstone (generally to the west) to mainly halite (to the east) (Holt and Powers, 1988, p. 5-12). Near the center of the WIPP site, the lower anhydrite was partially eroded during deposition of the middle mudstone unit, as shown in the WIPP Waste Handling and Exhaust Shafts (Holt and Powers, 1984, 1986). The lower anhydrite was completely eroded at WIPP-19 (Holt and Powers, 1988, p. 5-17). Before shaft exposures were available, the lack of the lower Tamarisk anhydrite at WIPP-19 was interpreted as the result of dissolution and the mudstone was considered a cave filling (Ferrall and Gibbons, 1980).

Halite is interpreted to be present east of the center of the WIPP site based on geophysical logs and drilling cuttings (Jones, 1978). Based mainly on cores and cuttings records from the WIPP potash drilling program, Snyder (1985) prepared a map showing the halitic areas of each of the noncarbonate Rustler members. A very similar map was prepared independently by Powers (Beauheim, 1987a) based on geophysical log characteristics.

Holt and Powers (1988, p. 5-14) described the mudstones and halitic facies in the middle of the Tamarisk, and they interpreted the unit as formed in a salt pan to mudflat system. They cited sedimentary features and the lateral relationships as evidence of syndepositional dissolution of halite in the marginal mudflat areas. In contrast, earlier authors (Jones et al., 1960; Jones, 1978; Snyder, 1985) interpreted the lateral decrease in thickness and absence of halite to the west as evidence of post-depositional dissolution. The differing concepts for halite distribution in the Rustler, and particularly the Tamarisk, have been used in explaining the large changes in hydrologic properties of the Culebra, as explained in later sections.

The Tamarisk thickness varies greatly in southeastern New Mexico, principally as a function of the thickness of halite in the middle unit (Holt and Powers, 1988, Figures 4.9 and 4.11). Within T22S, R31E, Holt and Powers (1988, Figure 4-9) show a range from 84 to 184 feet (26 to 56 meters) for the entire Tamarisk and a range from 6 to 110 feet (2 to 34 meters) (Holt and Powers, 1988, Figure 4.11) for the interval of mudstone-halite between lower and

upper anhydrites. Areas on these maps with thickness greater than about 100 feet (30 meters) and 20 feet (6 meters), respectively, correspond to halitic regions of the Tamarisk.

3.1.1.5.4 Magenta Dolomite Member

Adams (1944, p. 1614) attributes the name "Magenta member" to Lang, based on a feature north of Laguna Grande de la Sal named Magenta Point. The Magenta is a gypsiferous dolomite with abundant primary sedimentary structures and well-developed algal features (Holt and Power, 1988, p. 5-22). It does not vary greatly in sedimentary features across the site area (Holt and Powers, 1988, p. 5-22).

Around the WIPP site, Holt and Powers (1988, p. 5-22) reported that the Magenta varies from about 23 to 28 feet (7 to 8.5 meters); they did not contour the thickness because of the limited changes.

3.1.1.5.5 Forty-niner Member

Vine named the Forty-niner Member for outcrops at Forty-niner Ridge in eastern Nash Draw, but the outcrops of the Forty-niner are poorly exposed. In the subsurface around the WIPP, the member consists of basal and upper sulfates separated by a mudstone (Holt and Powers, 1984). It is conformable with the underlying Magenta. As with other members of the Rustler, geophysical log characteristics can be correlated with core and shaft descriptions to extend the geological inferences across a large area (Holt and Powers, 1988).

The Forty-niner ranges from 43 to 77 feet (13 to 23 meters) thick within T22S, R31E (Holt and Powers, 1988, Figure 4.13). East and southeast of the WIPP, the Forty-niner exceeds 80 feet (24 meters) in thickness, and some of the geophysical logs from this area indicate halite is present in the beds between the sulfates (Holt and Powers, 1988, Figure 4.3).

Within the Waste Handling Shaft, the Forty-niner mudstone displayed sedimentary features and bedding relationships indicating sedimentary transport (Holt and Powers, 1984). The mudstone has been commonly interpreted as a residue from the dissolution of halitic beds (Jones, 1978) because it is thinner where there is no halite. These beds are not known to have been described in detail prior to mapping in the Waste Handling Shaft at WIPP, and the features found there led Holt and Powers (1984, 1988) to re-examine the available evidence for, and interpretation of, dissolution of halite in Rustler units.

3.1.1.6 DEWEY LAKE (RED BEDS)

The nomenclature for rocks included in the Dewey Lake Formation (or alternatively, Dewey Lake Red Beds) was introduced during the 1960s to clarify relationships between these rocks assigned to the Upper Permian and the Cenozoic Gatuña Formation (see discussions by Schiel, 1994; Powers and LeMone, 1987). More recently, Lucas and Anderson (1993a) have suggested using the name Quartermaster Formation in place of Dewey Lake based on similar lithology and earlier usage. The Dewey Lake is retained here for WIPP project usage until the utility of using Quartermaster is clearer.

There are three main sources of data about the Dewey Lake in the area around the WIPP. Miller (1955, 1966) studied the petrology of the unit. Schiel (1988, 1994) described outcrops in the Nash Draw areas and interpreted geophysical logs of the unit in southeastern New Mexico and west Texas to infer the depositional environments and stratigraphic relationships. Holt and Powers (1990) were able to describe the Dewey Lake in detail at the Air-Intake Shaft for WIPP, confirming much of Schiel's information and adding data regarding the lower Dewey Lake.

The Dewey Lake overlies the Rustler conformably (Bachman, 1984), though local examples of the contact (e.g., Air-Intake Shaft, Holt and Powers, 1990) show minor disruption by dissolution of some of the upper Rustler sulfate. The formation is predominately reddish-brown fine sandstone to siltstone or silty claystone with greenish-gray reduction spots. Thin bedding, ripple cross-bedding, and larger channeling are common features in outcrops (Schiel, 1988), and additional soft sediment deformation features and early fracturing are described from the lower part of the formation (Holt and Powers, 1990). Schiel (1988, 1994, p. 10) attributed the Dewey Lake to deposition on "a large, arid fluvial plain subject to ephemeral flood events."

There is little direct faunal or radiometric evidence of the age of the Dewey Lake. It is assigned to the Ochoan Series of Late Permian age (Hills and Kottlowski, 1983), and it is regionally correlated with units of similar lithology and stratigraphic position. Schiel (1988, 1994) reviewed the limited radiometric data from lithologically similar rocks (Quartermaster Formation) and concluded that much of the unit could be Early Triassic in age.

Near the center of the WIPP site, Holt and Powers (1990, Figure 5) mapped 498 feet (152 meters) of Dewey Lake. The formation is thicker to the east (Schiel, 1988, 1994, p.6) of the WIPP site, in part because western areas were eroded before the overlying Triassic rocks were deposited.

The Dewey Lake is extensively fractured, and both cements and fracture fillings have been further examined to ascertain the possible contributions of surface infiltration to underlying units. Holt and Powers (1990, p. 3-8) described the Dewey Lake as cemented by carbonate above 164.5 feet (50 meters) in the Air-Intake Shaft. Some fractures in the lower part of this interval were also filled with carbonate, and the entire interval surface was commonly moist. Below this point, the cement is harder (probably anhydrite), the shaft is dry, and fractures are filled with gypsum. Holt and Powers suggested the cement change might be related to infiltration of meteoric water. They also determined that some of the gypsum-filled fractures are syndepositional (1990 p. 3-11, Figure 16). Dewey Lake fractures include horizontal to subvertical trends some of which were mapped in detail (Holt and Powers, 1986, Figures 6-8).

3.1.1.7 SANTA ROSA

There have been different approaches to the nomenclature of rocks of Triassic age in Southeastern New Mexico. Bachman (1974) generally described the units as "Triassic, undivided" or as the Dockum Group, without dividing it. Vine (1963) used "Santa Rosa Sandstone," and Santa Rosa has become common usage. Lucas and Anderson (1993b) import other formation names that are unlikely to be useful for WIPP.

The Santa Rosa has been called disconformable over the Dewey Lake (Vine, 1963, p. B25; Lucas and Anderson, 1993b, p. 232). These rocks have more variegated hues than the underlying uniformly colored Dewey Lake. Coarse-grained rocks, including conglomerates are common, and the formation includes a variety or cross-bedding and sedimentary features (Lucas and Anderson, 1993b).

Within the WIPP site boundaries, the Santa Rosa is relatively thin to absent. At the Air-Intake Shaft, Holt and Powers (1990, Figure 5) attributed about 2 feet (0.6 meters) of rock to the Santa Rosa. The Santa Rosa is a maximum of 255 feet (78 meters) thick in potash holes drilled for WIPP east of the site boundaries (Jones, 1978, Table 20B). The Santa Rosa is thicker to the east.

3.1.1.8 GATUÑA FORMATION

Lang (in Robinson and Lang, 1938) named the Gatuña for outcrops in the vicinity of Gatuña Canyon in the Claystone Basin. Rocks now attributed to the Gatuña in Pierce Canyon were once included in the "Pierce Canyon Formation" with rocks now assigned to the Dewey

Lake. The formation has been mapped from the Santa Rosa, New Mexico, area south to the vicinity of Pecos, Texas. It unconformably overlies different substrates.

Vine (1963) and Bachman (1974) provided some limited description of the Gatuña. The most comprehensive study of the Gatuña is by Powers and Holt (1993), based on WIPP investigations and landfill studies for Carlsbad and Eddy County. Much of the formation is colored light reddish brown. It is broadly similar to the Dewey Lake and Santa Rosa, though the older units have more intense hues. The formation is highly variable, ranging from coarse conglomerates to claystones with some highly gypsiferous sections. Sedimentary structures are abundant. Analysis of lithofacies indicates that the formation is dominantly fluvial in origin with areas of low-energy deposits and evaporitic minerals. It was deposited in part over areas actively subsiding in response to dissolution (Powers and Holt, 1993, p. 280).

The thickness of the Gatuña is not very consistent regionally. Powers and Holt (1993) report thicknesses up to about 300 feet (91 meters) at Pierce Canyon, with thicker areas generally subparallel to the Pecos River. To the east, the Gatuña is thin or absent. Holt and Powers (1990) reported about 9 feet (2.7 meters) of undisturbed Gatuña in the Air-Intake Shaft.

The Gatuña has been considered to be Pleistocene in age based on a volcanic glass in the upper Gatuña (Bachman, 1980) that has been identified as the Lava Creek B ash dated at 0.6 million years (Izett and Wilcox, 1982). An additional volcanic ash from Gatuña in Texas yields consistent potassium-argon (K-Ar) and geochemical data, indicating it is about 13 Ma (Powers and Holt, 1993, p. 272). Thus the Gatuña ranges in age over a period of time that may be greater than the Ogallala Formation on the High Plains east of WIPP.

3.1.1.9 MESCALERO CALICHE

The Mescalero caliche is an informal stratigraphic unit apparently first explicitly used by Bachman (1974), though Bachman (1973, p. 17) described the "caliche on the Mescalero Plain." He differentiated the Mescalero from the older, widespread Ogallala caliche or caprock on the basis of textures, noting that breccia and pisolitic textures are much more common in the Ogallala. The Mescalero has been noted over significant areas in the Pecos drainage, including the WIPP site area (Bachman, 1981), and it has been formed over a variety of substrates.

Bachman described the Mescalero as a two part unit: (1) an upper dense laminar caprock, and (2) a basal, earthy to firm, nodular calcareous deposit. Machette (1985, p.5) classified the

Mescalero as having Stage V morphologies of a calcic soil (the more mature Ogallala caprock reaches Stage VI).

Bachman (1976, p. 148) provided structure contours on the Mescalero caliche for a large area of southeastern New Mexico, including the WIPP site. From the contours and Bachman's discussion of the Mescalero as a soil, it is clear that the Mescalero is expected to be continuous over large areas. Explicit WIPP data are limited mainly to drillholes, though some drillhole reports do not mention the Mescalero. The unit may be as much as 10 feet (3 meters) thick (Bachman, 1985, p. 19).

The Mescalero was inferred on basic stratigraphic and climatic grounds as having accumulated during the early to middle Pleistocene (Bachman, 1974, 1980). Bachman (1980) reported finding a volcanic ash in the upper Gatuña along Livingston Ridge and underlying the Mescalero. This original report that this was the Pearlette "O" ash was superseded when Izett and Wilcox (1982) reported the ash as Lava Creek B, about 0.6 Ma.

The Mescalero must therefore be younger. Samples of the Mescalero from the vicinity of the WIPP were studied using uranium-trend methods (Rosholt and McKinney, 1980). Based on early written communication from Rosholt, Bachman (1985, p. 20) reports that the basal Mescalero began to form about 510,000 years ago and the upper part began to form about 410,000 years ago; these ages are commonly cited in WIPP literature. The samples are interpreted by Rosholt and McKinney (1980) in the formal report as indicating ages of 570,000 $\pm$ 110,000 years for the lower part of the Mescalero and 420,000 $\pm$ 60,000 years for the upper part.

Based on morphology of caliche along part of the souther rim of Pierce Canyon, Hawley (1993) has argued that some of the caliche within the Delaware Basin may be Ogallala instead of Mescalero. This question has not been further addressed.

The Mescalero, as a soil, indicates a stable surface on which it can develop (Bachman, 1985, p. 19). It is considered relevant to paleoclimatic considerations and as an indicator of stability or integrity of the WIPP site (Powers et al., 1978, p. 4-8). Bachman (1985, p. 27) considered the Mescalero as an impediment to erosion; the discussion by Bachman indicates the Mescalero is an indicator of surface stability over the last 500,000 years.

3.1.1.10 SURFICIAL SEDIMENTS

Above the Mescalero caliche, the Kermit and Berino soil series have been mapped across the WIPP site (Chugg et al., 1952, sheet number 113). These are sandy soils developed on eolian material (Chugg et al., 1952, pp. 16, 25). The Kermit-Berino soils include active dune areas. The Berino has a sandy A horizon; the B horizons include more argillaceous material and weak to moderate soil structures. A and B horizons are described as non-calcareous, and the underlying C horizon is commonly caliche. Bachman (1980) interpreted the Berino soil as a paleosol that is a remnant B horizon of the underlying Mescalero.

Rosholt and McKinney (1980) applied uranium-trend methods to samples of the Berino from the WIPP site area. They interpreted the age of formation of the Berino as 330,000 ± 75,000 years. Though this is generally consistent with the age of the underlying Mescalero, it is not understood why the ages are not closer if the Berino formed at the same time as the Mescalero.

3.1.2 Conceptual Models of Groundwater Flow Above the Salado Formation

Summary Statement: There are two conceptual models of groundwater flow in strata above the Salado Formation, the confined model and the groundwater basin model. The confined model considers only flow in individual stratigraphic units with relatively high hydraulic conductivity. The groundwater basin model considers flow in all units, including those with extremely low hydraulic conductivity, as part of a single hydrologic system. In a practical sense, these models are complementary. The groundwater basin model better represents the real groundwater flow system, but the confined model is a justified, and perhaps necessary, simplification for use in some PA flow and transport calculations.

Discussion: There are two conceptual models of groundwater flow in strata above the Salado Formation, the confined model and the groundwater basin model. The first, the confined model, focuses on lateral flow in the relatively more permeable units. It is an empirical model in that it is based primarily on hydrologic and geochemical data collected as part of the site characterization process. For example, the present-day north-to-south flow in the Culebra can be established by hydraulic head data without knowing the locations of discharge and recharge areas. This model recognizes that there appears to be a potential for vertical flow across confining layers but assumes that this flow can be neglected except in regions where the confining units have been disturbed and are more permeable. This conceptual model is the basis for the 1992 PA calculations of flow and transport in the Culebra Dolomite. The domain of this

conceptual model is thought to be a subdomain of the hydrologic system that controls its behavior and, therefore, calculations based on this model require boundary conditions that represent hydrologic processes outside of the model domain. For example, heads along a portion of the boundary were raised or lowered to simulate the effects of climate change on recharge to the flow system in the 1992 PA (Swift et al., 1994).

The second model is based on the concept of the groundwater basin. This conceptual model has a strong theoretical basis (Hubbert, 1940; Tóth, 1963; Freeze and Witherspoon, 1967) and is widely accepted and applied by hydrogeologists. A groundwater basin is a three-dimensional, closed hydrologic unit bounded on the bottom by an "impermeable" rock unit (actually a stratigraphic layer with much smaller permeability than the layers above), on the top by the ground surface, and on the sides by groundwater divides. The upper boundary of the flow domain is the water table, which may or may not coincide with the land surface. All rocks in the basin have finite permeability, i.e., hydraulic continuity exists throughout the basin. Implicit in this description of the groundwater basin is that the entire length of each flow path is contained within the basin. All recharge to the basin (if it occurs) is by infiltration of precipitation to the water table, and all discharge from the basin (if it occurs) is by flow across the water table to the land surface.

Differences in elevation of the water table across the basin are assumed to generate the hydraulic gradients to drive groundwater flow. Water flows along gradients of hydraulic head from regions of high head to regions of low head. The highest and lowest heads in the basin occur at the water table at its highest and lowest points, respectively. Therefore groundwater generally flows from the elevated regions of the water table, downward across confining layers (layers with relatively low permeability), laterally along conductive layers (layers with relatively high permeability), and finally upward to exit the basin in regions where the water table (and by association, the land surface) is at low elevations. Infiltration is necessary to maintain relief on the water table. If infiltration were to stop for a sufficient period of time, flow from regions of high to low head would "level" the water table, and groundwater would become stagnant. However, a lack of infiltration rarely, if ever, actually results in stagnant conditions because long periods of time are required for groundwater to "drain" from the regions of higher head. The time required for a system to drain is controlled by the thickness, permeability, and compressibility of confining layers in the basin, as well as the initial relief of the water table. The adjustment time could be tens of thousands of years or longer.

The pattern of groundwater flow depends on the lateral extent and depth of the basin, the shape of the water table, and the heterogeneity of the permeability of the rocks in the basin. Field observations and numerical studies have demonstrated that flow in a conductive layer is

parallel to the upper and lower surfaces of the layer and flow in a confining layer is approximately vertical. Even extremely slow vertical flow in confining layers is significant on a regional scale because it is summed over very large horizontal surfaces.

3.1.2.1 VERTICAL FLOW THROUGH RUSTLER CONFINING LAYERS

The issue of whether or not vertical flow occurs through confining layers in the Rustler Formation is pertinent to the evaluation of the two conceptual models. Evidence of zero vertical flow would invalidate the groundwater basin model because it based on the concept of hydraulic continuity. Both models are compatible with the existence of extremely slow vertical flow. Pumping tests and geochemical data have been interpreted to show that vertical flow through Rustler confining units is "insignificant." Hydrologic modeling studies support the existence of extremely slow vertical flow through confining layers. These positions are not necessarily contradictory. The fact that vertical flow is too slow to leave a geochemical signature or to be observed during pumping tests does not mean that it is zero. To date, an argument for zero vertical flow has not been presented. The arguments concerning vertical flow are summarized below.

3.1.2.1.1 Possible Role of Karst Dissolution in Vertical Flow in the Rustler

The term karst is usually applied to regions where dissolution of dolomite and/or limestone has resulted in collapse of the surface, forming a distinctive topography. In the vicinity of the WIPP, however, the term is applied to features formed by dissolution of evaporites such as halite and anhydrite as well as some carbonates (Bachman, 1987). As discussed in the following paragraphs, evidence suggests that some karst features have developed east of Nash Draw in the past, and may be continuing to form in the Los Medaños area between the WIPP and Nash Draw.

As is typical of both arid to semi-arid regions with surficial deposits of eolian sand and karst regions where dissolution has created subsurface channels for runoff, there is no well-developed surface-water drainage system in the area to the northwest, west, and southwest of the WIPP site. Small intermittent streams lead into depressions that are in some cases eolian blowouts and, in at least one location, a dissolution sinkhole. Northwest of the WIPP and outside the land-withdrawal boundary, the WIPP-33 borehole was drilled in a small depression to test the hypothesis that this was the location of a sinkhole that extended downward through the Salado Formation. When the well showed no abnormalities in the upper Salado, drilling was

stopped. However, the borehole showed that almost all the anhydrite in the upper Rustler had been altered to gypsum and that no halite was present. The Magenta appeared to have been almost completely dissolved, the Culebra was highly fractured, and anhydrites below the Culebra were altered to gypsum (Sandia National Laboratories and United States Geological Survey, 1981). Circulation was lost intermittently throughout drilling and tool drops of several feet were noted. About 1500 m to the northeast at borehole P-13, driller's records report the Rustler to be completely intact with halite present and the anhydrites mostly unaltered (Jones, 1978).

Sinkholes are also present south of Los Medaños, in the vicinity of the H-7 and H-9 boreholes (see Figure 3.1.1-1). San Simon Swale and San Simon Sink east of the WIPP may also be karst features.

Models of groundwater flow to date have not considered vertical flow through sinkholes, and have instead examined effects of halite dissolution of the upper Salado over large areas (Corbet and Wallace, 1993; Appendix A of this report), or the effects of selectively varying the location of vertical flow (Haug et al., 1987; Davies, 1989). Sinkholes could affect regional flow by providing point sources for inflow to deeper units or by providing interconnections between conductive layers separated by less conductive units. In both processes, effects would be similar to those discussed in Section 3.4.2 regarding open boreholes through the Rustler Formation.

3.1.2.1.2 Geochemical Evidence Related to Vertical Flow

Siegel et al. (1991a) summarize an effort to interpret the chemical, mineralogical, isotopic, and hydrological data available as of 1989. Siegel et al. concluded that the bulk of the data argues against significant vertical flow. The following paragraph is from the executive summary (page ES-3) of that report:

> Mineralogical and isotopic studies of sulfates in overlying layers also show that no significant amounts of either solutes or water have permeated vertically downward from the surface to recharge the Culebra. Specifically, much of the anhydrite in the Tamarisk member between the Magenta and Culebra members has not been hydrated to gypsum by recrystallization in the presence of fresh water, D/H ratios in gypsum throughout the Rustler are not consistent with a pervasively large water/rock ratio accompanying such hydration, and comparison of $^{87}Sr/^{86}Sr$ ratios of gypsums and carbonates in Rustler, Dewey Lake, and surface rocks shows that secondary sulfates and carbonates in the Rustler did not form in a hydrological regime that was uniformly interconnected with overlying rocks and the surface. Thus, the available mineralogical, hydrological, and

isotope data indicate no significant vertical connection between the Culebra and overlying strata.

The results of another geochemical investigation performed by Bodine et al. (1991) suggest instead that groundwater in the Culebra and other conductive layers has been in contact with anhydrites and halites in the intervening confining layers. They presented the distribution of dissolved constituents in groundwater from the Rustler Formation in terms of salt norms. A salt norm (Bodine and Jones, 1986) can be envisioned as the hypothetical assemblage of mineral salts that would have precipitated from an evaporated water sample and would be in equilibrium with the last vestige of the remaining water. The salt norms yield a diagnostic characterization of the water that aids in the interpretation of possible origins of the solutes and past water-rock interactions. Their analysis of the distribution of salt norms of Rustler groundwater suggests that meteoric water has moved into the Magenta, Culebra, and Rustler-Salado contact zone. The salt norms of these waters indicate that they have interacted chemically with the anhydrites and halites in the intervening confining layers. This implies that at least a portion of the water in the conductive units has migrated through the confining units.

3.1.2.1.3 Hydrologic Observations Related to Vertical Flow

Hydrologic observations have also been presented to argue both for and against vertical flow across the Tamarisk Member, a unit of extremely low hydraulic conductivity separating the Culebra and Magenta dolomites. LaVenue et al. (1990, p. 2-15), for example, note that heads in the Magenta do not respond to pumping in the Culebra. They used this observation to support a decision to not consider vertical flow when modeling flow in the Culebra. The lack of drawdown in the Magenta as the Culebra is pumped does confirm that the confining layer is laterally extensive and has low hydraulic conductivity. However, as discussed in the following paragraph, the fact that we do not observe drawdowns in the Magenta during pumping tests in the Culebra should not be used to infer that flow through the layers does not occur in the undisturbed flow field.

Neuman and Witherspoon (1969a, 1969b) described mathematically the change in hydraulic head with time that would occur in an aquifer as water is pumped from that aquifer, as well as the change in hydraulic head that would occur in a second aquifer and a confining unit separating the two aquifers. Application of this analysis to the Culebra, Magenta, and Tamarisk shows that the decrease in hydraulic head with time (i.e., the drawdown) in the Culebra would be less if vertical leakage from the Tamarisk occurred than if the no leakage occurred. The leakage would initially come from storage in the Tamarisk. At later times, water could be drawn

from the Magenta if the pumping continued long enough that the drawdown of heads in the Tamarisk propagated across its entire thickness. Therefore the effects of leakage would be recognized first in the drawdown response of the Culebra and only much later, if ever, in the Magenta.

3.1.2.1.4 Numerical Modeling of Vertical Flow

Haug et al. (1987) and Davies (1989) used numerical models to investigate the possible importance of vertical flow in the undisturbed flow field. They applied constant-head conditions along the lateral boundaries of a horizontal domain and used source terms to represent vertical flow at specified rates in selected portions of the domain. Results from these studies show that vertical flux can be accommodated, and perhaps is necessary, when calibrating this type of model. For example, Haug et al. (1987) found that it was impossible to calibrate their steady-state confined model with respect to fluid density without adding small but realistic vertical fluxes in selected regions. Haug et al. (1987, p. 8-2) concluded that "... future modeling studies should not attempt to simulate the Culebra dolomite as a completely confined hydraulic system but rather as a leaky-confined aquifer." Davies (1989), also using this approach, performed simulations in which vertical flow accounted for as much as 25 percent of the total flux through the Culebra.

Following a different approach to evaluate the possible importance of vertical flow, Davies (1989), Corbet and Wallace (1993), and Corbet (Appendix A of this report) performed simulations that explicitly include strata that overlie and underlie the Culebra. Davies simulated flow in a vertical, two-dimensional domain, while Corbet and Wallace performed three-dimensional simulations. The relief of the water table over the model domain drives flow in both the two- and three-dimensional simulations. No-flow conditions along the lateral boundaries represent flow divides. These boundary conditions assure that all flow into or out of the Culebra must be by vertical leakage through adjacent confining layers. Just as a model that assumes perfectly confined conditions cannot demonstrate that vertical leakage does not occur, results from these simulations cannot demonstrate that it does occur. These results do, however, demonstrate that simulations based on a conceptual model in which vertical leakage is an important component can reproduce basic features of the regional flow system. For example, modern-day flow within the WIPP-site boundary is toward the south in the Culebra Dolomite, but is to the west in the overlying Magenta Dolomite. The three-dimensional simulations show that this counter-intuitive condition can be explained as a natural consequence of the regional heterogeneity of the hydrologic system and of slow vertical leakage through the Tamarisk Member.

Given the lack of evidence for zero vertical flow through confining layers and the support for slow vertical flow provided by hydrologic models, the current position is that flow through unfractured confining units in the Rustler Formation is finite but extremely slow. Flow through confining layers can justifiably be neglected in calculations of flow and transport in single conductive units at the scale of the land withdrawal area. However, hydraulic continuity through confining units must be retained in regional three-dimensional flow models.

3.1.2.2 IMPLEMENTATION OF THE CONCEPTUAL MODELS

3.1.2.2.1 Confined Model

Implementation of the confined model for use in the 1992 PA is described in Chapter 7 of Volume 2 and Chapter 6 of Volume 4 of the Preliminary Performance Assessment for the Waste Isolation Pilot Plant, December 1992 (WIPP PA Department, 1992-1993).

3.1.2.2.2 Groundwater Basin Model

The groundwater basin model was first implemented in two dimensions along a vertical east-west trending cross-section extending from the axis of Nash Draw to a topographically high region east of the WIPP site (Davies, 1989). A three-dimensional numerical representation of the groundwater basin model (SECOFL3D) is currently being developed and used to investigate long-term regional flow of groundwater in strata above the Salado Formation. The numerical model solves transient or steady-state equations of groundwater flow. This model differs from other three-dimensional models used to simulate regional groundwater flow in that it treats the water table as a free surface that rises and falls in response to groundwater flow and the amount of moisture available for recharge to the saturated zone. Seepage faces (areas where groundwater can discharge from the flow system) form in regions where the water table is maintained at the land surface. Unsaturated flow above the water table is not considered in this numerical representation.

For transient simulations, the model solves

$$\nabla \bullet K \nabla h = S_s \frac{\partial h}{\partial t} \qquad (3\text{-}1)$$

on the interior of the domain to assure conservation of mass. In this equation, hydraulic head h is the dependent variable, K is a spatially-dependent hydraulic-conductivity tensor, and S_s is specific storage. No-flow boundary conditions are imposed on the bottom and vertical sides of the domain. The following pair of equations define a kinematic condition that is imposed on the top boundary to represent the free surface (Bear and Verruijt, 1987):

$$h(x,y,z_{wt}) = z_{wt}(x,y) \tag{3-2}$$

$$(K \bullet \nabla h + N) \bullet \nabla (h - z) = S_y \frac{\partial zwt}{\partial t} \tag{3-3}$$

In these equations, z_{wt} is the elevation of the water table, N is the normal flux due to recharge and/or evapotranspiration, and S_y is the specific yield. The kinematic condition is applied if the elevation of the water table is below the land surface. If the water table is at the land surface, the kinematic condition may need to be converted to a seepage face. The seepage boundary condition is

$$h(x,y,z_{wt},t) = z_{ls}(x,y) \tag{3-4}$$

where z_{ls} is the local land surface elevation and t_{wt} is the time at which the water table encounters the land surface. To determine whether the kinematic or the seepage boundary condition should be applied, the vertical speed of the water table, $\partial z_{wt} / \partial t$ is computed. The algebraic sign of the quantity shows whether the water table is falling or rising. The seepage condition is applied at a particular location if the water table there is rising. The kinematic condition is applied if the water table is falling.

The lateral boundary of the numerical model follows groundwater divides that enclose a region that is believed to be sufficiently large to control regional groundwater flow in the supra-Rustler strata (Figure 3-3). Groundwater divides are assumed to coincide with major topographic highs and depressions (Hubbert, 1940; Tóth, 1963; Freeze and Witherspoon, 1967). The boundary follows Nash Draw and the Pecos River valley along the west and south and the axis of San Simon Swale to the east. The boundary continues up the San Simon Swale and dissects topographic highs in the northern part of the model region.

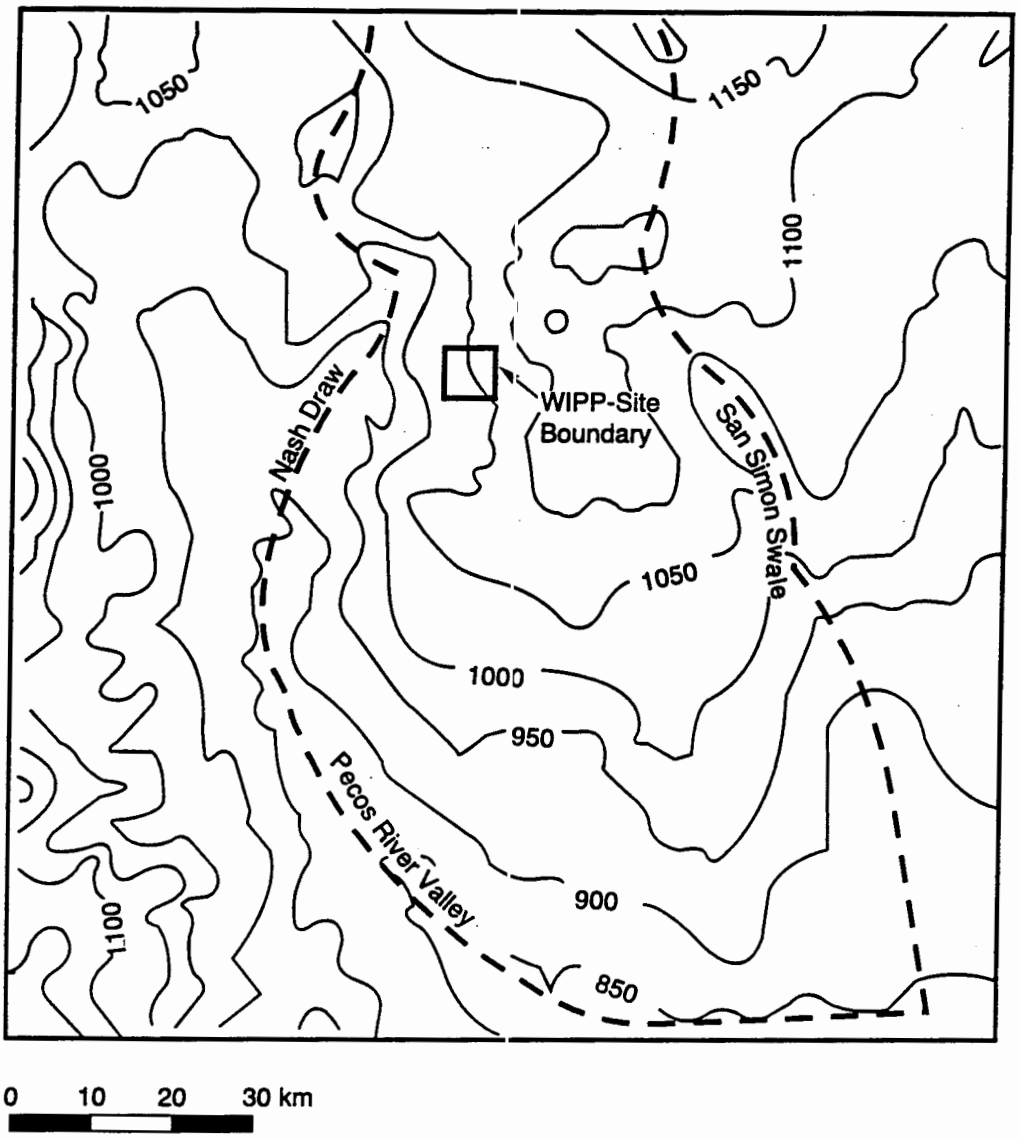

TRI-6115-67-0

Figure 3-3. Topography of the land surface and the lateral boundary of the regional groundwater flow model. Contour interval is 50 m. Model boundary follows groundwater divides along topographic depressions to the west, south, and east, and dissects topographic highs to the north. No-flow boundary conditions are used along the entire lateral boundary.

The base of the numerical model is positioned along the top of the Salado Formation. The hydraulic conductivity of the Salado is sufficiently small that its upper surface can be represented in this model as a no-flow boundary. The rocks above the Salado are represented as ten hydrostratigraphic units (Figure 3-4). Each hydrostratigraphic unit is heterogenous with respect to hydraulic conductivity. Values of hydraulic conductivity are assigned to portions of the model domain to represent the rock type (i.e., whether the rock is a dolomite, anhydrite, halite, mudstone, or siltstone) and the extent to which geologic processes have modified the hydraulic properties of the rocks. Geologic processes considered include dissolution of the upper portion of the Salado Formation and the resulting fracturing and disruption of overlying rocks, dissolution of minerals that previously filled fractures, and plugging of rock pores by halite cements. As discussed in Section 3.1.2, karst features extending tens to hundreds of meters might disrupt confining layers and thereby facilitate increased localized recharge. Features of this scale are not currently represented in the hydraulic conductivity distribution used for the groundwater basin model.

Simulations performed using three-dimensional numerical models have enhanced the conceptual understanding of groundwater flow above the Salado in the vicinity of the WIPP (Corbet and Wallace, 1993; Appendix A of this report). This understanding, in turn, has been applied to evaluate several scenarios discussed in this paper, including the change in groundwater flow due to future changes in climate, the impact of subsidence over potash mines, and the effect of shallow boreholes.

Corbet and Wallace (1993) reported on early results of the three-dimensional modeling study. These simulations were performed using a modified version of a computer code, MODFLOW, developed by the United States Geological Survey (McDonald and Harbaugh, 1988; McDonald et al., 1991). Sandia National Laboratories modified this code to represent seepage faces in an approximate way. These simulations did not accurately represent groundwater flow near the WIPP because each hydrostratigraphic unit was assumed to be homogenous with respect to hydraulic conductivity. Nonetheless, these simulations did demonstrate several important aspects of the natural hydrogeologic system. The simulations suggested that groundwater flow in the Culebra Dolomite is strongly influenced by the relief of the water table. A substantial portion of the water flowing in the Culebra is from slow vertical leakage from overlying confining layers. Also flow rates and directions in the Culebra are sensitive to the amount of moisture that infiltrates to the water table.

Results from more recent simulations performed using the SECOFL3D code confirmed the results of the earlier simulations and provided additional information about the effects of climate change (Appendix A of this report). These simulations incorporate the rigorous

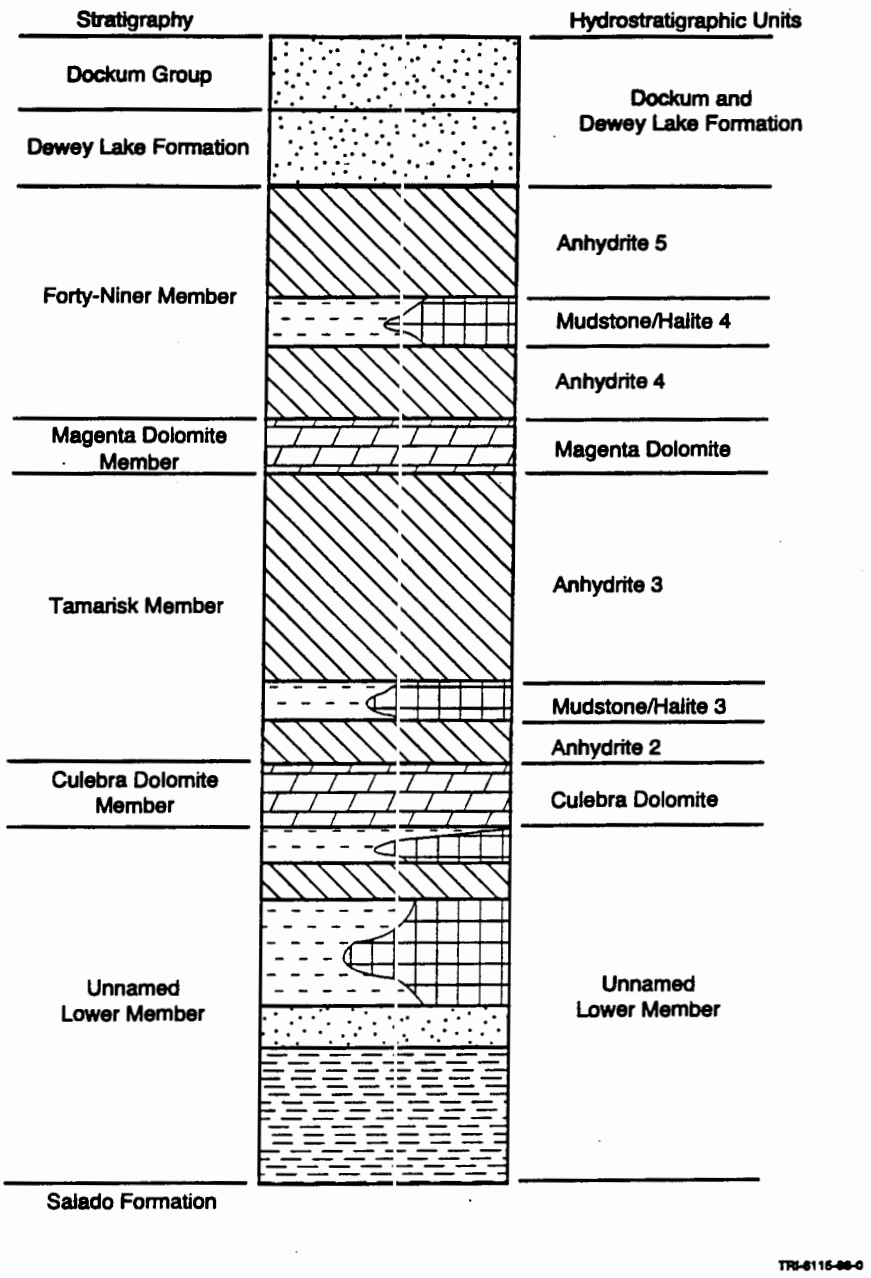

Figure 3-4. Hydrostratigraphic units for the regional groundwater flow model. See Appendix A for additional discussion.

treatment of the free surface and seepage face boundary conditions described above, as well as a distribution of hydraulic properties that reflects the effect of geologic processes.

3.1.3 Groundwater Geochemistry and Flow in the Culebra Dolomite Member

Summary Statement: A complete understanding of the geohydrology of the Culebra Dolomite would include a conceptual model of the relationship between water chemistry and the Culebra flow field that is consistent with both geochemical and hydrologic observations. The distribution of hydraulic head and modeling studies indicate that present-day flow in the Culebra is toward the south. The water chemistry along some calculated flow paths changes from a saline (about 3 molal) NaCl-type water to more dilute (less than 0.1 molal) $CaSO_4$-type water. This condition is counter-intuitive in that rock-water interactions that could cause this change in chemistry along a flow path have not been identified. Several conceptual models have been proposed to explain the relationship between groundwater flow and water chemistry. The proposed models still contain important inconsistencies and have yet not been reconciled with more recent hydrologic modeling studies. Therefore, the issue of understanding the relationship between water chemistry and groundwater flow in the Culebra remains unresolved at this time.

Discussion: The major solute composition of groundwater in the Culebra Dolomite Member varies spatially in the vicinity of the WIPP site and can be described in terms of hydrochemical facies. Siegel et al. (1991a) present the most recent delineation of these facies. Potentiometric data indicate that present-day flow lines cross facies boundaries and that, in places, flow appears to occur from saline (about 3 molal) NaCl waters to more dilute (less than 0.1 molal) $CaSO_4$ type waters. The Environmental Evaluation Group (EEG) pointed out that a satisfactory explanation for this change in water chemistry along proposed flow lines had not been presented as of 1985 (Neil et al., 1983; Ramey, 1985). In response to this observation, several studies have been performed to address this issue. A detailed review of that work is beyond the scope of this position paper, and would not add to existing published reviews (refer to Lappin, 1988; Lappin et al., 1989, Sections 3.3.2 and 3.3.3; WIPP Performance Assessment Division, 1992, Volume 2, Section 2.2.3.6; U.S. Department of Energy, 1994a, Section 2.2.2). The most recently completed and published body or work on this topic used results from interpretations based on an extensive compilation of lateral changes in isotopic (stable and radiogenic) ratios of Culebra rock, mineral, and groundwater; solute (major and minor ions) concentrations in Culebra groundwater; and the mineralogy of the Culebra (Lambert, 1987; Lambert and Carter, 1987; Lambert and Harvey, 1987; Bodine et al., 1991; Siegel and Lambert, 1991; Siegel et al., 1991b; Lambert, 1991, 1992; Siegel and Anderholm, 1994). A concise summary of that work can be found in Siegel et al. (1991a, pages ES-1 to ES-5). The objective of the following

discussion is only to provide a brief review of the results of some of the more extensive regional geochemistry investigations and the interpretations made by the authors.

One possible model for the relationship between the geochemical facies distribution and the present-day flow paths has been proposed by Chapman (1986, 1988). She coupled an extensive compilation of stable and radiogenic isotope ratios of Rustler Formation groundwaters with isotopic data from regional groundwaters and surficial waters. Chapman cited evidence for short residence times of Culebra groundwaters and postulated that recharge from the surface could account for the less concentrated groundwaters south of the WIPP Site. That explanation, however, is not supported by interpretations of isotopic and solute data presented by Lambert, Siegel, and others. Specifically, radiogenic isotopic signatures suggest that the age of the groundwater in the Culebra is on the order of tens of thousands of years (Lambert, 1987; Lambert and Carter, 1987; Lambert and Harvey, 1987). Those authors contend that there has been a change in the location and amount of recharge since the last glacial maximum and that the present distribution of solutes and isotopes in the Culebra is a relict of a flow regime of a wetter climate, in which the recharge area was in the vicinity of Nash Draw resulting in an eastward paleo-flow direction. The current distribution of hydrogeochemical facies according to this interpretation, therefore, represents a rock-water system that is still slowly reaching a new chemical and physical equilibrium. However, a conceptual or calculational model of how paleo-flow could have been to the east has not been presented.

At present, the issue of the relationship between water chemistry and groundwater flow in the Culebra remains unresolved. It is possible that the lack of resolution reflects the way the problem has been posed and the relatively simple conceptual models that have been used to represent the hydrology of the system. Previous discussions, for example, have focused on flow directions but not flow rates. Numerical simulations of flow in the Culebra suggest that flow rates are orders of magnitude slower in the region of the NaCl facies than in the region of the $CaSO_4$ facies (see for example, LaVenue et al., 1990). It is possible that the geochemical signature of flow from the NaCl facies to the $CaSO_4$ facies is not observed because only minute amounts of water flow along this path. In addition, some of the previous studies have not considered, or have ruled out, transport of solutes from units above and below the Culebra. For example, the region of the NaCl facies correlates well with the extent of halite in strata above and below the Culebra. The possibility that the NaCl facies results from vertical advective or diffusive transport into a region of extremely slow flow in the Culebra has not been adequately investigated. Preliminary results of three-dimensional calculations using the groundwater basin approach suggest that it will be helpful in addressing these issues to treat the hydrology as three-dimensional, transient system. On the basis of these preliminary results, resolution of the apparent inconsistency between geochemical facies and present-day Culebra flow directions

appears to be possible through further flow analyses coupled with a re-examination of the geochemical data.

3.1.4 Castile Brine Reservoirs

Summary Statement: Pressurized brine reservoirs are found at some locations in the uppermost anhydrite layer of the Castile Formation. Time-domain electromagnetic (TDEM) surveys indicate the possible presence of three or four of these reservoirs beneath portions of the WIPP disposal rooms. Flow from a brine reservoir through an intrusion borehole into the Culebra dolomite can be modeled by treating the brine reservoir as an exponentially decaying source characterized by the parameters pressure, volume, and storativity. Future calculations of possible flows from brine reservoirs should use values for volume and storativity based on the available data, and should limit the number of independent reservoirs that might be encountered to four.

Discussion: Pressurized brine reservoirs have been encountered within the uppermost anhydrite layer of the Castile Formation in at least 13 boreholes in the Delaware Basin (Figure 3-5) (Popielak et al., 1983). Two of these boreholes, WIPP-12 and Belco-Hudson, are on or within a mile of the WIPP site. Many more boreholes penetrating the Castile near the WIPP site have not encountered brine reservoirs (e.g., AEC-8, Badger Unit Federal #1, Cabin Baby-1, Cotton Baby, DOE-1, DOE-2, James Ranch #1, WIPP-11, and WIPP-13). TDEM surveys (Earth Technology Corporation, 1988, p. 8) conducted at the WIPP site can be interpreted to suggest the presence of one to four Castile brine reservoirs that may extend beneath portions of the WIPP disposal rooms. A conservative implementation of this interpretation for assessment calculations is to specify four discrete reservoirs rather than a single reservoir, because a subsequent hit of a different reservoir would encounter a pressurized, rather than unpressurized, reservoir.

Based on the TDEM survey, PA has assumed that Castile brine reservoirs underlie 25 to 57% of the WIPP disposal area. Therefore, 25 to 57% of the exploratory boreholes penetrating the WIPP repository in PA human-intrusion scenarios connect the Culebra and the repository to a Castile brine reservoir. The 1992 PA model of the brine reservoir followed the approximation developed by Reeves et al. (1991), summarized below.

Reeves et al. (1991) examined ways to implement a borehole connection between a brine reservoir, the repository, and the Culebra in a numerical model. Based on interpretation of hydraulic tests of the brine reservoir encountered in WIPP-12, they conceptualized the brine

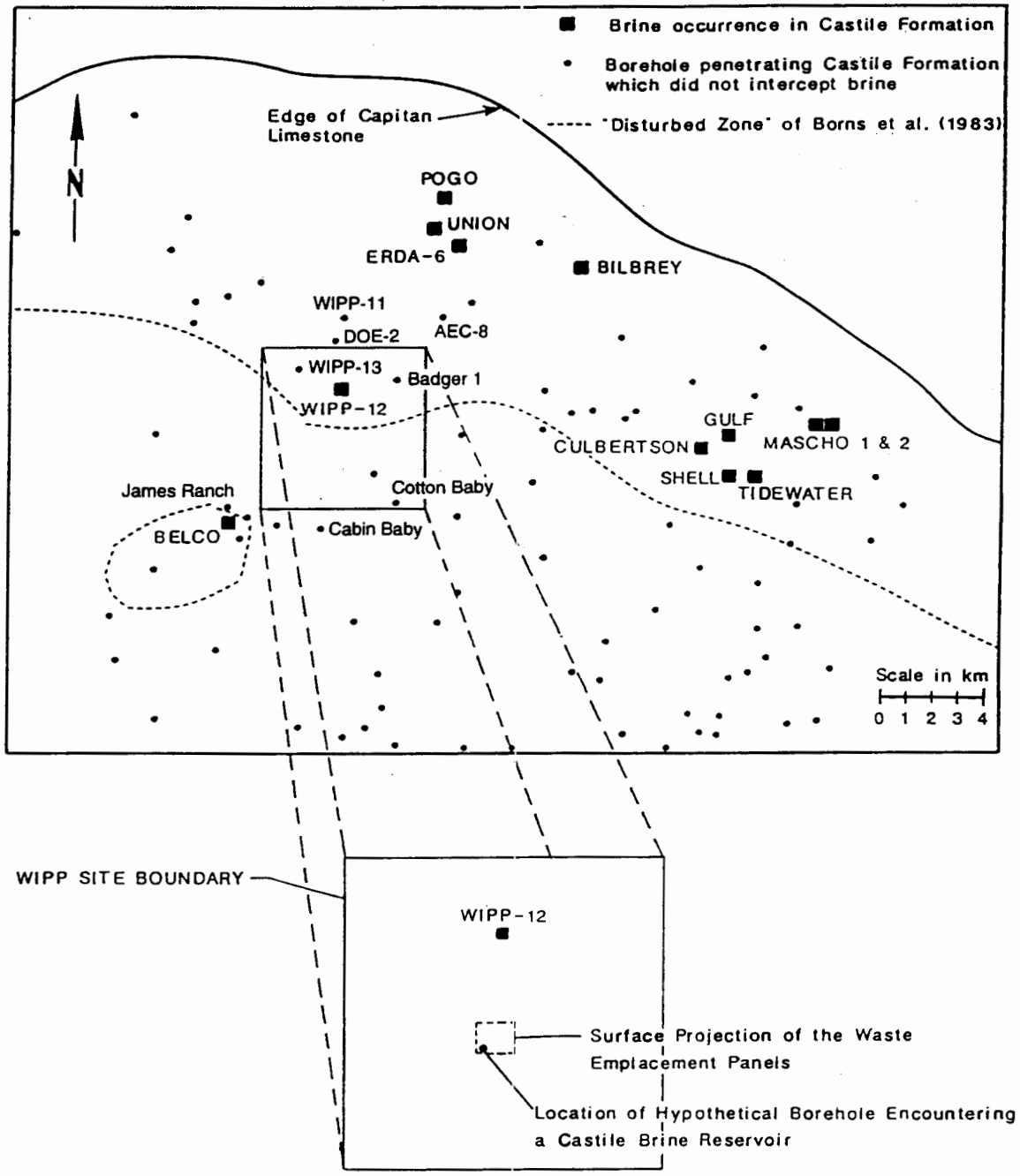

Figure 3-5. Selected deep boreholes that penetrate the Castile Formation, northern Delaware Basin.

reservoir as a three-component system: an inner highly fractured ring having a transmissivity between 7×10^{-6} and 7×10^{-2} m^2/s, an outer less fractured ring having a transmissivity between 7×10^{-8} and 7×10^{-4} m^2/s, and an infinite surrounding region of intact anhydrite having a transmissivity between 1×10^{-13} and 1×10^{-9} m^2/s (p. 2-6). They found (p. 5-12) that so long as borehole permeability was in the range from 10^{-14} to 10^{-10} m^2, the only properties of a Castile brine reservoir that were important in calculating flow into the Culebra dolomite were the reservoir pressure, storativity, and outer-ring radius (or reservoir volume); the different transmissivities and the radius of the inner ring were found to be unimportant over the ranges considered. This finding allows a brine reservoir to be treated as an exponentially decaying source term in numerical models.

The combination of brine reservoir volume and storativity used in the 1992 PA calculations was such that the initial pressure of the brine reservoir did not appreciably deplete over 10,000 years. In effect, the brine reservoir behaved as a constant-pressure source and the release of brine and radionuclides to the Culebra was overestimated. The 1992 PA calculations assumed a brine reservoir volume of 2×10^8 m^3. Popielak et al. (1983, p. H-54) estimated the WIPP-12 reservoir volume to be about 3×10^6 m^3, with a range of uncertainty from 3×10^5 to 1×10^7 m^3. The ERDA-6 reservoir volume is estimated at 1×10^5 m^3, with a range of uncertainty from 1×10^4 to 5×10^5 m^3 (Popielak et al., 1983, p. H-48). Future calculations should not use reservoir volumes larger than the 1×10^7 m^3 upper limit on the WIPP-12 reservoir volume.

The storativity range used in the 1992 PA calculations was developed from erroneous values presented in Reeves et al. (1991, Table A-1, p. A-2,3) for the volumes of brine produced from the WIPP-12 reservoir during different testing activities. The total volume indicated by Table A-1 of Reeves et al. (1991) is 37,924 m^3, whereas the correct value is only 13,469 m^3 (D'Appolonia, 1982, Figure 4; 1983, p. 3-1). Thus, the storativity range of 2×10^{-2} to 2 m^3/Pa used in the 1992 PA (Sandia WIPP Project, 1992, p. 4-15) should be reduced to 7×10^{-3} to 7×10^{-1} m^3/Pa in future calculations.

The 1992 PA also considered each borehole hitting a Castile brine reservoir to be an independent event, with each hit encountering a fully pressurized and separate brine reservoir. Based on the results of the TDEM survey (Earth Technology Corporation, 1988, p. 8), specifying four discrete reservoirs is a conservative implementation for assessment calculations.

3.1.5 Multi-Phase Flow

Summary Statement: Numerical evaluations of flow and transport in the Culebra to date have treated the unit as being fully saturated (single-phase liquid only) . No numerical studies have been performed to make a determination of the effect of unsaturated conditions which could occur as a result of gas entering the unit through a borehole either from the Castile brine reservoir or the repository.

Discussion: Two-phase flow conditions in the Culebra and other non-Salado units may occur as a result of gas flow up a human intrusion borehole. Two-phase flow conditions may alter the flow field, which in turn may impact transport. Unsaturated flow conditions are present above the water table in the Dewey Lake Formation and Dockum Group.

Unsaturated flow occurs naturally in formations above the water table. Due to capillary pressure differences between the units, the various layers above the water table can act as capillary barriers to inflow or infiltration. The natural dip of the layers can divert the flow laterally from its infiltration location, and the storage capacity of the unsaturated units could alter the flow rate at the water table compared to the inflow at land surface.

Human intrusion scenarios may introduce gas into the boreholes either from such sources as the Castile brine reservoirs or from gas in the repository due to gas generation in the waste. Depending on the borehole details including the plugs, some of this gas may be introduced into non-Salado formations or flow to the surface. Because of the lower pressures in the units above the Salado, the gas volume will expand over the volume occupied in the reservoir. Gas bubbles could alter the natural flow patterns and velocities of the brine due to flow blockage and density differences, and the gas bubbles could migrate differently than the brine. Fracture-matrix flow could be significantly changed with the introduction of gas due to the capillary pressure difference between the phases, possibly resulting in gas flow primarily in fractures and brine flow restricted to the matrix. Chemistry could also be changed by the introduction of gas into the non-Salado units.

At the present time, the non-Salado formations are analyzed using single-phase or fully saturated approaches, assuming that two-phase conditions associated with gas release and/or unsaturated zone flow above the water table do not significantly impact transport calculations. An evaluation of the possible effects of unsaturated and two-phase conditions, including scoping studies as necessary, could be conducted to assess the potential impact on system performance. For example, it is possible that permeability of the borehole plugs is high enough that any gas released up a borehole would escape to the surface and not enter the Culebra.

3.2 Culebra Flow and Transport

This section contains conceptual and mechanistic models concerning fluid flow and transport in the Culebra. Calculations of radionuclide transport in the Culebra are performed in two steps. First, calculations are performed to determine a flow field and its respective specific discharge. Specific discharge is the rate at which groundwater flows through a unit cross-sectional area of rock. Although specific discharge has the units of velocity, it does not represent the actual velocity of flow. The real velocity (interstitial velocity) is faster because the fluid can only flow through the area provided by pores and fractures in the rock, rather than the entire cross-sectional area. A second step is required to transform the specific-discharge field into the interstitial velocity and to account for physical and chemical retardation of the radionuclides. This second step is more complex because it must take into consideration the fact that the Culebra is fractured and both the fractures and adjacent porous matrix participate in solute transport. This type of transport is commonly referred to as double-porosity transport.

A critical piece of information required to calculate the specific-discharge field is the distribution of the rock's transmissivity. The transmissivity of the Culebra has been measured at a relatively large number of locations (see Section 4.2.2). The models used to transform these discrete data into a continuous distribution of transmissivity are described in Section 3.2.1. Knowledge of a second parameter, the rock storativity, is required to perform calculations of a flow field that changes with time. As discussed in Section 3.2.2, fewer measurements of rock storativity have been made. Section 3.2.3 considers the effects of the spatial distribution of fluid density in the Culebra on the flow field. Artificial change to the density distribution can be introduced by leakage from boreholes (Section 3.2.4). Leakage from boreholes could also introduce multi-phase (gas in addition to liquid) flow into the Culebra and, through, rock/water interactions modify the hydraulic and retardation properties of the Culebra. Models that incorporate the effects of fractures, the double-porosity model and the channeling model, are described in Sections 3.2.5 and 3.2.6. Finally, Section 3.2.8 discusses the role of dispersion in radionuclide solute transport.

3.2.1 Transmissivity

Summary Statement: Measured transmissivity values (see Section 4.2.2) vary spatially over several orders of magnitude, trending from lower values east of WIPP to higher values west of WIPP. The spatial variations in transmissivity are implemented by numerically generating realizations conditioned on observed head and transmissivity values using the pilot point technique (LaVenue and RamaRao, 1992). Multiple realizations are generated and sampled on

to address the uncertainty associated with the transmissivity field. Transmissivity is assumed to be constant over time.

3.2.2 Storativity

Summary Statement: Interpreted storativity values vary spatially in the vicinity of the WIPP over a few orders of magnitude. Performance assessments to date have assumed a spatially invariant value for storativity. This assumption results in incorrect Darcy velocities in transient flow simulations, although the magnitude of this uncertainty cannot be quantified at this time.

Discussion: Storativity is an important hydraulic parameter during transient events, such as pumping or injection, because it affects the head gradients that are created, which in turn affect the groundwater velocities. Therefore, precise calculations of solute transport under transient conditions rely on accurate definition of the storativity (and transmissivity) field. Storativity values interpreted from hydropad-scale pumping tests of the Culebra at the WIPP site range from 3×10^{-6} (Gonzalez, 1983) to 3×10^{-4} (Saulnier, 1987; Beauheim, 1989). Storativity data are sparse, however, and no attempt at defining a storativity field over the WIPP site has been performed.

In the GRASP-INV modeling used to define the transmissivity fields for the 1992 PA calculations (LaVenue and RamaRao, 1992), a constant storativity value of 2×10^{-5} was assigned throughout the modeling domain. Because the transmissivity fields are calibrated to transient events, the assumption of a spatially constant storativity leads to imprecise definition of transmissivity fields and, hence, imprecise estimates of the Darcy velocities in calculations based on those transmissivity fields. The magnitude and direction of the flow uncertainties resulting from the approach employed cannot be determined without numerical simulations.

Future GRASP-INV modeling should solve for both the transmissivity and storativity fields that are consistent with the observed transient head data. The resultant storativity and transmissivity fields should be used for any calculations of transient flow and transport conducted for PA. An alternative approach to assesses the degree of flow uncertainty associated with assuming a constant storativity value may be to conduct sensitivity calculations examining the impact on integrated release of a range of storativity values that corresponds with the observed range from field tests. WIPP PA may wish to consider alternative inverse techniques that simultaneously estimate transmissivity and storativity from transient data.

3.2.3 Variable-Density Flow

Summary Statement: To be strictly correct, calculations of flow in the Culebra Dolomite would account for the fact that fluid density and the elevation of the Culebra vary spatially. However, variable-density flow analyses have indicated that ignoring differences in density and elevation in flow calculations does not introduce an unacceptable level of error when calculating long-term flow in the Culebra within the accessible environment boundary at the WIPP.

Discussion: Groundwater flows from regions of higher to lower mechanical energy. For practical purposes, the mechanical energy of groundwater has two components, energy imparted by compressing the water (i.e., pressure-related driving forces) and the energy imparted by lifting the water from one elevation to another (i.e., gravity-related driving forces). If the density of the fluid does not vary spatially, or the flow is strictly horizontal, then the net effects of these two components can be represented in terms of a single quantity, hydraulic head. Flow will then occur parallel to gradients of hydraulic head. Otherwise the components of the driving force for flow must be calculated separately and the flow will occur along the resultant of the flow vectors computed for each component of the driving force.

Neither of these conditions for using the concept of hydraulic head is met in the Culebra. The density of groundwater ranges from about 1.0 to 1.1 gram per cubic centimeter within the WIPP-site boundary due to differences in concentrations of total dissolved solids. The elevation of the Culebra ranges from 775 to 875 meters above mean sea level in the same region. Therefore when calculating flow in the Culebra, the two components of mechanical energy must be treated separately in order to avoid introducing some error. There is no correction that can be made (for example, converting to equivalent fresh-water head) that allows combining the two components into a hydraulic head without introducing error. The driving force component due to compressing the water is represented as the gradient of fluid pressure. The component due to lifting water is represented as the unit weight of water multiplied by the gradient of elevation.

Davies (1989) investigated the amount of error that is introduced by using equivalent freshwater heads rather than the two components of driving force to calculate regional groundwater flow in the Culebra. He found that, within the WIPP-site boundary, the use of freshwater heads resulted in errors of calculated flow directions of less than ten degrees. However in an area located about five to ten kilometers south of the WIPP-site, flow directions calculated using fresh-water heads were in error by as much as 70 degrees.

The analysis by Davies shows that not accounting for the spatial variation of density and elevation could introduce errors in the calculated flow field in a region that is south of the

WIPP-site and beyond the accessible environment boundary. Given that the region where errors are large is beyond the boundary at which regulatory releases are calculated and that other aspects of the calculation introduce comparable or larger uncertainty (e.g., transmissivity distribution), it is believed that ignoring the variation in fluid density is a valid approximation when calculating long-term groundwater flow and transport in the Culebra Dolomite for WIPP performance assessment.

3.2.4 Fluid from an Intrusion Hole

Summary Statement: Connection of the Culebra with the Salado and a Castile brine reservoir through an intrusion borehole could allow brine to flow into the Culebra. This could cause the head in the Culebra to increase, locally inducing radial flow from the borehole. The area affected will depend on the local transmissivity and storativity of the Culebra, as well as on the flow rate into the Culebra. The Reeves et al. (1991) study of the impact of human intrusion boreholes that penetrate indicated that for expected conditions and much of the range of brine reservoir and breach borehole parameters, the fluid disturbance created in the Culebra by the breach borehole had minimal impact on the flow field and that under these conditions, transport calculations need not included the transient impact of locally increased hydraulic head near the breach borehole. This study also found that for extreme conditions at the head end of the brine-reservoir volume and pressure range and the high end of borehole permeabilities, travel time for a conservative solute can be reduced by as much as 7.4 percent due to increased heads in the Culebra in the vicinity of the borehole. This effect can be implemented in an undisturbed flow field by increasing hydraulic heads in the vicinity of the borehole. Potential density, chemical, and multiphase effects from the intrusion fluid are discussed in other sections.

Discussion: The fluid from an intrusion borehole could have the following four effects on flow and transport in the Culebra:

1) Increase hydraulic gradients and flow velocities in the vicinity of the borehole.

2) Change the density of the Culebra fluid.

3) Result in rock/water interactions that locally alter flow and transport properties in the Culebra.

4) Result in local multiphase flow conditions in the Culebra.

Reeves et al. (1991, p. 3-12 to 3-18) quantify the impact of an intrusion borehole on the Culebra flow field. At 10,000 years, the disturbed flow field is predicted to be only 12.5 m wide downstream from the well. Conditional on the assumptions of their model, for a borehole permeability of 10^{-10} m^2, the travel time to the site boundary is predicted to be 7.4% faster than the undisturbed case. For lower borehole permeabilities, the impact on travel time is less.

The other effects listed above are discussed in Sections 3.2.3, 3.3.1, and 3.1.5.

3.2.5 Double Porosity

Summary Statement: At some locations on and around the WIPP site, the Culebra Dolomite is a double-porosity medium. In this usage, double porosity simply means that the Culebra has two porosities, matrix and fracture. Observations from core samples and the results of hydraulic and tracer tests provide evidence for areas where the Culebra responds as a double-porosity medium and other regions where it responds as a single-porosity, matrix-only medium.

The double-porosity conceptualization used by WIPP PA Department (1992) assumes that advective transport occurs only in fractures, with diffusion of radionuclides and contaminants occurring between the fractures and matrix. Sensitivity studies (Helton et al., 1992; WIPP PA Department, 1993, v. 4; Reeves et al., 1991) have shown that cumulative release can be reduced if radionuclides that are transported in the fractures can diffuse into the matrix. In the double-porosity conceptualization as implemented by PA, one of the most important parameters for transport is the effective surface area for diffusion which is represented by the fracture spacing (matrix block size).

It is acceptable to model the entire Culebra as a double-porosity medium. This may cause calculated transport velocities to be slightly too high in the lower transmissivity zones where the Culebra actually behaves as a single-porosity medium, leading to overestimates of radionuclide transport. Because of limitations in the number and spatial distribution of Culebra boreholes in the immediate vicinity of the area above the waste-storage panels, PA is not, at present, able to take credit for potentially reduced transport in this area due to the potential presence of single-porosity, matrix-only transport conditions in this area.

Discussion: At some locations on and around the WIPP site, the Culebra is a double-porosity medium. By double porosity we simply mean the Culebra has two porosities. The primary porosity or original porosity is the porosity within the rock matrix. Analysis of core samples suggests that the matrix porosity (or volume of void space between grains divided by total

volume) is in the range of .03 to .30, with an average value of 0.16 (Kelley and Saulnier, 1990; Reeves et al. 1991). The secondary porosity is the void space of the fractures divided by total volume. A critical issue for transport in a fractured medium is the degree to which fractures and matrix interact.

In a double-porosity, fractured medium, flow is generally conceptualized as occurring primarily in the fractures because flow velocities are usually orders of magnitude higher in the fractures than the matrix. However, diffusive (or advective) transport of radionuclides or contaminants from fractures into the matrix can act as an important physical retardation process.

The double-porosity conceptualization used by WIPP PA Department (1992) assumes that advective transport occurs only in fractures, with diffusion of radionuclides and contaminants occurring between the fractures and matrix. Sensitivity studies (Helton et al., 1992; WIPP PA Department, 1993, v.4; Reeves et al., 1991) have shown that cumulative release can be reduced if radionuclides that are transported in the fractures can diffuse into the matrix. Matrix diffusion causes physical retardation because the matrix provides a reservoir for 'storage' of radionuclides. In addition, matrix diffusion can enhance chemical retardation by greatly increasing the surface area onto which the radionuclides can potentially sorb.

Field tests near the WIPP site have provided evidence for areas where the Culebra appears to respond as a double-porosity medium and other areas where it appears to respond as a single-porosity (matrix-only) medium. Conservative tracer tests have been conducted within the Culebra at several locations for transport scales ranging from approximately 20 to 40 m. Convergent-flow and two-well recirculating tracer tests provide data that can be used to characterize the flow and transport process. The observed long time period required for initial (detectable) tracer breakthrough (74 to 316 days) for the H-2 and H-4 tracer tests suggests the prevalence of single-porosity, matrix-only transport at these locations. Hydraulic-test responses at these two hydropads also indicate single-porosity, matrix-only conditions. Interpretations of pumping tests and tracer tests at the H-3, H-6 and H-11 hydropads suggest that the Culebra behaves as a double-porosity (fracture plus matrix) medium at these locations. Significant fracture participation in transport is evidenced by rapid initial tracer breakthrough (1 to 21 hrs) on one travel path at each of the H-3, H-6, and H-11 hydropads (Jones et al., 1992).

All areas where the Culebra is interpreted as a single-porosity, matrix-only medium are locations where the tested rock has a low transmissivity. Based on hydraulic tests alone, the argument could be made that, at these locations, the Culebra is actually a single-porosity, fracture-only medium. (A single-porosity, fracture-only medium is one where the matrix is impermeable and transport takes place only in the fractures.) If the Culebra is a fracture-only

medium at these locations, treating the entire Culebra as a double-porosity medium with some matrix diffusion in transport calculations could overestimate the time required for solutes to travel across the areas of low transmissivity. However, all core samples of the Culebra from wells across the WIPP site show some matrix porosity. For almost all of the samples tested, porosities were measured to be greater than 5% (Kelley and Saulnier, 1990). Therefore, the position taken for the SPM baseline is that the Culebra has some matrix porosity at all locations and that the double-porosity model implemented in the baseline will not underestimate radionuclide transport.

In the double-porosity conceptualization as implemented by PA, one of the most important parameters for transport is the effective surface area for diffusion per unit volume of fluid, which is represented by the fracture spacing (matrix block size). This parameter has been characterized by convergent flow tracer tests at three hydropads at the WIPP site (Jones et al., 1992). Two of these hydropads are located along the primary offsite travel paths southeast of the waste storage panels. Subsequent reviews of these tracer tests through the international INTRAVAL program raised a number of questions about the test conditions that may have impacted interpretation of the fracture-spacing parameter. In response to these questions, a new tracer is currently being fielded to address the questions raised through the INTRAVAL review.

Values of two double-porosity parameters have been interpreted from the convergent-flow tracer tests conducted at the H-3, H-6, and H-11 hydropads (Jones et al., 1992): fracture porosity and fracture spacing (matrix-block length). The values presented by Jones et al. (1992), however, are specific to the numerical model used for test interpretation and do not represent intrinsic or exact properties of the Culebra. The fracture porosity values, for example, were calculated assuming that tracer traveled in a straight line from the tracer-injection well to the tracer-recovery well under radial flow conditions. Within the numerical model used for the test interpretations (SWIFT II), this fracture porosity was assumed to exist within three orthogonal fracture sets with equal and uniform apertures. In actuality, the fracture porosities presented by Jones et al. (1992) represent the effective flow porosity for any fracture geometry, but always under the assumptions of continuous, isotropic radial flow.

The fracture spacings presented by Jones et al. (1992) are also specific to the assumed cubic fracture geometry, as well as to assumptions made about the flow rate along the various flow paths. The fracture spacings cannot be considered separately from other parameters used in the tracer-test analyses. That is, fracture spacing is directly correlated with matrix tortuosity and free water diffusion coefficient through the characteristic matrix diffusion time (τ) given by (Reeves et al., 1987):

$$\tau = L^2/\theta D \tag{3-5}$$

where: L = one-half the fracture spacing
Θ = matrix tortuosity
D = free water diffusion coefficient.

In the interpretations presented in Jones et al. (1992), values of Θ and D were specified based on laboratory data and values for L were determined for each tracer test through curve matching. In effect, the uncertainty in all three parameters was lumped into the estimate of fracture spacing.

The parameter defined through tracer-test interpretations, however, is not fracture spacing but the ratio of fracture surface area to matrix volume. The tracer-breakthrough behavior in a tracer test would be the same for any fracture geometry having the same surface to volume ratio, so long as the tracer does not diffuse all the way to the center of the matrix block. That is, the breakthrough curve produced by a test of a system with cubic matrix blocks would be identical to the curve produced by a test of a system with slab blocks with one-third the thickness of the cubic blocks, until the tracer reached the center of the slabs. The time at which this occurs is given by the characteristic matrix diffusion time defined above. Tracer tests provide no information on fracture geometry until the characteristic matrix diffusion time is exceeded and matrix saturation effects begin to be observed. Jones et al. (1992) assumed cubic (or spherical) matrix blocks in their tracer-test interpretations. If their results are to be used to simulate transport through a system having a different assumed geometry, their calculated fracture spacings should be adjusted to create the correct surface to volume ratio in the new geometry.

For any fracture geometry, the characteristic matrix diffusion times for radionuclides would be different than those determined for the benzoate tracers used in the tracer tests at WIPP because of different free water diffusion coefficients. The other two parameters contributing to the diffusion time, fracture spacing and matrix tortuosity, can be used to simulate radionuclide transport so long as the ratio of the specific values used, as given in the above equation, does not change. That is, fracture spacing and matrix tortuosity are correlated parameters and should not be sampled independently of one another.

It is appropriately conservative to model the entire Culebra as a double-porosity medium even though portions of it appear to be single porosity. This may cause calculated velocities to be too high in the lower transmissivity (single-porosity) zones, leading to overestimates of radionuclide transport.

3.2.6 Channeling

Summary Statement: Fracture channelling can theoretically result in up to approximately a factor of 10 increase in radionuclide release relative to models that assume uniform flow over entire fracture planes due to higher velocities and reduced surface area for matrix diffusion. The degree of fracture channeling and its impact on transport in the Culebra are not well known at present. The ongoing tracer test program at the H-19 test pad has been designed to address this type of transport issue.

Discussion: Fracture channeling occurs through discontinuous networks of relatively high-conductivity channels within individual fracture planes. Typically these channels represent areas where fracture apertures and fracture connectivity are greatest. Areas where fracture apertures are smaller, or where flow paths run into dead ends, represent relatively stagnant areas that may provide temporary storage of solutes. Observations by Holt and Powers (1990, p. 3-19) of the Culebra in the Air Intake Shaft indicate that flow is concentrated within a 1.7-m-thick horizon that is more extensively fractured than the rest of the Culebra. However, all fractures are not equally productive and individual fractures do not produce water uniformly over their entire lengths. Rasmuson and Neretnieks (1986, p. 1247) report that 90% of the water flowing through a fracture typically passes along only 5 to 20% of the fracture plane.

Relative to the case of uniform flow over the entire fracture plane, channeling increases the fluid velocity and reduces the fracture surface area available for matrix diffusion. Increasing fluid velocity decreases both travel time and matrix diffusion. Reducing the surface area available for diffusion likely would not be significant for regional-scale transport because the travel time would be larger than the time required for fracture and matrix solute concentrations to reach equilibrium (Dykhuizen, 1992, p. 2450), provided that the fractures and channels were no more than approximately a meter apart. Fracture channelling can theoretically result in up to approximately a factor of 10 increase in radionuclide release relative to models that assume uniform flow over entire fracture planes due to higher velocities and reduced surface area for matrix diffusion. The degree of fracture channeling and its impact on transport in the Culebra are not well known at present. The ongoing tracer test program at the H-19 test pad has been designed to address this type of transport issue.

3.2.7 Matrix Advection

Summary Statement: The 1992 PA double-porosity transport model assumes that all flow takes place in the fractures and that there is diffusion of radionuclides into the matrix. Sensitivity

studies have shown that cumulative releases can be reduced if radionuclides that are transported in fractures can diffuse into the matrix (Reeves et. al, 1987; Reeves et al., 1991; Helton et al., 1992; WIPP PA Department, 1993, v. 4). Matrix advection is an additional process that may increase transport into the matrix, thereby causing an additional reduction in releases. The past approach of not incorporating matrix advection, because it is less significant than advection through the fractures, is clearly conservative.

Discussion: In regions where the Culebra Dolomite is fractured, it is a double-porosity medium. In addition, in fractured regions, the Culebra is a double-permeability medium. In this usage, double permeability simply means that both the fractures and the matrix are permeable and have the potential for water to flow through them. Analysis of core samples indicates that the Culebra matrix is permeable. Permeability estimates based on gas permeability core tests are in the range of 8×10^{-18} to 5×10^{-14} m^2 (Kelley and Saulnier, 1990). These core tests provide evidence that there is significant matrix permeability in the samples tested.

The 1992 PA double-porosity transport model assumes that all flow takes place in the fractures and that there is diffusion of radionuclides into the matrix. Sensitivity studies have shown that cumulative releases can be reduced if radionuclides that are transported in fractures can diffuse into the matrix (WIPP PA Department, 1993). Matrix diffusion causes physical retardation because the matrix provides a reservoir for 'storage' of radionuclides. In addition, matrix diffusion can enhance chemical retardation by greatly increasing the surface area onto which radionuclides can potentially sorb. Advective transport (i.e., flow) of radionuclides into the matrix can potentially increase the speed at which radionuclides are transported into and within the matrix. If gradients are sufficient, matrix advection is a much more rapid process than matrix diffusion. Matrix advection may also increase the total quantity of radionuclides that are transported into the matrix, thereby increasing both the potential storage capacity of the matrix and enhancing the surface area for potential sorption.

Advective flow into and within the matrix has not been included in past PA models. Matrix advection has not been incorporated into past models because it is much less significant than advection through the fractures. Incorporation of matrix advection would also require modification of existing codes. The past approach of including matrix diffusion, but not matrix advection, is clearly conservative because incorporation of matrix advection would lead to a decrease in the cumulative release of radionuclides. If at some point is was judged to be useful to the project to take credit for matrix advection, this would be technically feasible with additional modification of existing codes and perhaps additional laboratory characterization of matrix permeabilities.

3.2.8 Dispersion

Summary Statement: Dispersion causes contaminants released into a porous medium to spread out beyond the volume where advection alone would take it. Hydrodynamic dispersion represents the total measure of this spreading, and is made up of two components: mechanical dispersion and diffusion. In a double-porosity system, diffusion has a much larger influence on cumulative release of contaminants across a boundary than mechanical dispersion. The PA double-porosity transport model includes adequate and defensible representations of both diffusion from fractures into matrix and mechanical dispersion in the fractures. Additional complexity is not warranted.

Discussion: Dispersion causes contaminants released into a porous medium to spread out beyond the volume where advection alone would take it. Hydrodynamic dispersion represents the total measure of this spreading, and is made up of two components: mechanical dispersion and diffusion. Mechanical dispersion is caused by local variations in velocity, while diffusion is caused by chemical gradients. Mechanical dispersion of contaminants released in a plume in double-porosity media is controlled to various degrees by:

1) Velocity variations within individual fractures caused by variations in fracture aperture;

2) Partitioning of contaminants between fractures at fracture intersections;

3) Preferential fracture (or fracture zone) orientations;

4) Different fracture characteristics within different layers of the medium (i.e., vertical heterogeneity);

5) Lateral changes in fracture characteristics (density, connectivity, aperture, orientation, etc.); and

6) Advective flow from fracture to matrix, after which the dispersive properties of the matrix become important.

In single-porosity systems, diffusion is rarely an important dispersive process compared to the mechanical dispersion resulting from advection-related phenomena. Advection, however, tends to concentrate contaminants along the most conductive flowpaths, creating concentration gradients between the highly and less conductive regions. Diffusion driven by these concentration gradients acts to move contaminants from regions of high advection to regions of

low advection, thus retarding the overall transport of the contaminants. In a double-porosity medium, diffusion can move contaminants from the highly conductive fractures to the much less conductive matrix, as discussed in Section 3.2.5. The contrast in advection rates between fractures and matrix in a double-porosity medium is typically much greater than the small-scale contrasts found in a single-porosity medium. Thus, diffusion can represent a much greater proportion of the total hydrodynamic dispersion in a double-porosity medium than it typically does in a single-porosity medium.

The 1992 WIPP PA calculations employed a double-porosity model in which mechanical dispersion and diffusion were treated as discrete phenomena. Mechanical dispersion was accounted for in the fractures by the inclusion of longitudinal and transverse dispersivities (coefficient of mechanical dispersion divided by velocity) defined for each grid block based on the size of the block and the variance of the transmissivity field (WIPP PA Dept., 1992, Vol. 2, p. 7-18 to 7-20). Additional dispersion was created by the variation in transmissivities among grid blocks. Advection in the matrix was not considered in the model. Diffusion was considered in only one dimension, and only between fractures and matrix and within the matrix (WIPP PA Dept., 1992, Vol. 2, p. 7-18); diffusion within the fractures was ignored because it is insignificant compared to mechanical dispersive processes.

Dispersion affects the first-arrival time of contaminants at a down-gradient location as well as the peak concentration of contaminants. Dispersion has little effect, however, on the cumulative release of contaminants across a boundary. Reeves et al. (1991) found that dispersion was less important than matrix porosity, fracture spacing (specific surface for diffusion), Darcy flux, free-water diffusivity, and matrix tortuosity in calculating the cumulative release of radionuclides through the Culebra. WIPP compliance with 40 CFR 191B is based on the cumulative release, not concentration, of radionuclides crossing the WIPP boundary. Thus, dispersion is not an important parameter in evaluations of WIPP's compliance, and the PA treatment of dispersion is adequate.

3.3 Culebra Chemical Retardation

PA calculations and sensitivity analyses (Helton et al., 1991; WIPP PA Department, 1992; Bertram-Howery et al., 1990) have identified the radionuclide retardation factor (relative transport rate of radionuclides with respect to the ambient fluid flow velocity) in the Culebra as a key parameter for the WIPP facility compliance with regulations. Radionuclide retardation could result from both physical and chemical factors. Physical retardation due to matrix diffusion has been demonstrated through double-porosity models (Reeves et al., 1987; 1991).

However, no experimental data for actinides exist on physical retardation due to matrix diffusion under conditions expected to be present in the Culebra Dolomite. Chemical retardation is caused by various chemical reactions that may occur between the chemical species in the solution and at the solid/solution interface. The chemical retardation phenomenon has been observed both in laboratory and field tests associated with groundwater pollution studies involving organic pollutants (Mackay et al., 1986) and inorganic pollutants (Weber et al., 1991, and references therein). This phenomenon also forms the basis for chromatographic methods for chemical separation (Heftmann, 1961).

3.3.1 Rock-Water Interaction in the Culebra

Summary Statement: The conceptual model of chemically retarded transport in the Culebra is dependent on several flow and transport related parameters, which are affected by the nature of fluid flow within the Culebra and the distribution of minerals in the Culebra. Evidence available to date indicates that chemically retarded transport in the Culebra will occur and will attenuate the cumulative radionuclide release. Some of the numerical models used to simulate retarded transport may incorrectly predict the cumulative releases, however, due to incorrect assumptions about the distribution of minerals and the nature of fluid flow within the Culebra. Currently, the potentially large amount of sorption on the proposed "clay mineral linings" on fracture surfaces is not included in performance assessment models. The baseline conceptual model for chemically retarded transport is advective flow through high-angle fracture sets that do not have a concentration of clay minerals adjacent to them (and are not clay "lined"), coupled with diffusive transport of solutes into a matrix with a mineralogy equivalent to the bulk mineralogy of the Culebra (i.e., about 95 wt. % dolomite and 5 wt. % clay minerals).

Discussion: In constructing a conceptual model for chemical and physical retardation of actinide elements in the Culebra, two critical factors must be considered: (1) the nature of the substrates that are present in the flow path; and (2) the amount of surface area available for mineral-solute interaction. In implementing the conceptual model using experimentally determined parameters with a numerical code, consideration must be given to geometric scaling issues and chemical equilibrium (e.g., adsorption kinetics). Obviously, numerical codes to evaluate solute transport must adequately represent the system and produce accurate predictions. However, because of the potentially very large number of variables that would be required in an exact solution of the conceptual model, simplifying assumptions based on experimental results and observations must be made.

Foremost in developing a conceptual model for chemically retarded transport is consideration of the rock fabric and the nature of the fluid flow through that rock fabric. An accurate and concise description of geologic aspects of the Culebra that are pertinent to chemical and physical retardation can be found in the 1992 WIPP preliminary performance assessment documentation (WIPP PA Department, 1992, Volume 2, p. 2-16 through 2-23, and references cited therein) and in other parts of this position paper. Some specific points warrant discussion here.

The two major minerals that are considered to be important for adsorption in the Culebra are dolomite, which is a potentially important adsorbent because of the vast amount present in the Culebra, and clay minerals, which are not nearly as abundant as dolomite, but are typically quite powerful adsorbents. Most of the clay minerals in the Culebra are detrital in origin, deposited along bedding planes while the evaporite minerals, such as dolomite, were forming. The clay minerals are concentrated in discontinuous lenses or are present as anastomosing networks, but are generally concentrated along sub-horizontal planes. The mineralogy of some of the clay minerals (e.g., what is now present as corrensite) were diagenetically altered, but their spatial distribution did not change since deposition. Bioturbation apparently was not substantial enough to homogenize the distribution of minerals as is observed in some carbonate rock types. In many carbonate rocks, pressure-solution produces stylolites, which usually appear as jagged surfaces where insoluble residue is concentrated. Stylolites are not observed in the Culebra. Petrographic and visual observation of the Culebra demonstrates that the distribution of clay minerals has not changed appreciably since deposition. Further, authigenic clay minerals are not present in appreciable quantities: the clay minerals are detrital, and were present before fracturing. Because clay minerals are so important to chemically retarded transport, substantial effort has been made on evaluating them.

Fractures in the Culebra can be divided into two categories based on their orientation. One category are those caused by parting along the sub-horizontally oriented planes of relative weakness in the rock resulting from the concentrations of clay minerals at bedding planes. Sub-horizontal fractures, therefore, have a relatively greater concentration of clay minerals adjacent to them. There is typically not a discrete clay mineral layer (i.e., "clay lining") that uniformly coats the surfaces of the fractures, and conceptual models involving discrete clay mineral "linings" cannot currently be supported.

Concentrations of clay minerals *adjacent* to sub-horizontal fracture surfaces can be supported, however. Unfortunately, the incomplete core coverage coupled with the mineralogic heterogeneity of the Culebra makes it difficult to defend the concept of advective fluid flow solely through sub-horizontal fractures with concentrations of clay minerals adjacent to them.

Further, documenting the concentrations and lateral distributions of clay minerals adjacent to fractures, as well as physico-chemical parameters necessary to calculate transport (e.g., porosity, diffusion constants, thickness), would be a difficult task.

The second set of fractures observed in the Culebra are high-angle fractures (greater than 45 degrees from horizontal) and are not distinctly controlled by distribution of clay or other minerals. Detailed examination of core samples of the Culebra has shown that many of the high-angle fractures are filled to various extents with gypsum. Beauheim and Holt (1990, Figure 2-13) demonstrated that the percentage of high-angle fractures that are filled with gypsum crystals increases eastward across the site. The presence of post-depositional gypsum fill indicates that groundwater has flowed through those high-angle fracture sets in the past, but the age of these fillings is not known.

Lines of evidence that have been used to deduce which fracture set is currently the active flow path include visual observations in the air intake and waste handling shafts, examination of post-depositional gypsum fill, and examination of a rust-colored coating (possibly iron oxyhydroxide) on fracture surfaces. Those observations support fluid flow in both the sub-horizontal fractures as well as the high-angle fractures (refer to Section 3.2.5), and it is not clear which fracture set is currently the preferred groundwater flow path. It is not likely that the fluid flow path can be elucidated without substantial work. It may also be difficult to defend flow through a particular fracture set across the entire WIPP site, because of the heterogeneity in Culebra rock fabric.

Results of field tracer tests conducted within the WIPP land-withdrawal boundary suggest that, on at least local scales (approximately 1 to 100 m), fluid flow in the Culebra is controlled by the double-porosity nature of the rock, in that groundwater flows through fracture porosity by advection and dissolved solutes move into the intercrystalline pores in the matrix by aqueous diffusion (refer to Section 3.2.5). Transport in this region may occur, however, by matrix advection or matrix advection coupled with fracture advection. For purposes of evaluating the conceptual model of rock-water interaction in the Culebra, a critical issue is the mineral surface area available for retardation; whether a solute is transported to a mineral surface in the rock matrix by diffusion or advection is of secondary importance. Regardless of the mechanism of transport, movement of solutes through the matrix will increase chemical retardation. However, in the absence of the matrix diffusion component, significant levels of chemical retardation may occur on minerals in close proximity to fracture surfaces. This may be particularly true if advective fluid flow is primarily through the sub-horizontal fractures, which have a greater concentration of clay minerals adjacent to them.

On the basis of the properties of the Culebra described above, thirteen alternative conceptual models for flow and transport are possible (Table 3-1). The thirteen cases are constructs that result from possible combinations of advective and diffusive flow, matrix or fracture transport, flow through high-angle or sub-horizontal fractures, and differences in distributions of clay minerals within the rock. It is recognized that many of the conceptual models are not very probable, and may be eliminated from serious consideration for reasons described. Implicit in this discussion is an assumption that K_d values suitable for use in a compliance application will be available.

The link between the nature of fluid flow in the Culebra and chemical retardation is a fundamental part of constructing a conceptual model for retarded transport. In other words, chemical retardation is conditional on the mechanism(s) of fluid transport. Conceptual models numbers 1-6 in Table 3-1 represent cases in which fracture advection-matrix diffusion is the operative solute transport mechanism, and is by far the most likely mechanism according to results to date. Conceptual models numbers 7-12 represent cases in which no matrix diffusion occurs and that flow occurs solely by fracture advection. Conceptual model number 13, included for completeness, is a case in which the dominant flow mechanism is by matrix advection. This case will not be considered further at this time because it is not consistent with currently supported conceptual models.

For each of the two main groups of conceptual models (1-6 and 7-12), the fracture advection component of fluid flow may be *dominated* by flow through sub-horizontal fractures, high-angle fractures, or both. The conceptual models within those two groups reflect the possible alternatives. Conceptual models numbers 1 and 7 represent the "fall-back" positions for cases involving fracture advection-matrix diffusion and fracture advection, respectively, in which no retardation occurs (i.e., K_ds are defined as 0). Available information on actinide sorption in the Culebra demonstrate that sorption will occur, but those early scoping data do not provide sufficient quantification of K_ds (refer to 3.2.4).

Because we do not know whether the dominant advective flow path in the Culebra is through high-angle or sub-horizontal fractures, and because we do not know the connectivity of those fracture sets, the current baseline assumption is that advective flow occurs through the high-angle fracture set only, which do not have detrital clay minerals in close proximity to them (conceptual model number 2). To simulate retardation for this conceptual model, a weighted distribution coefficient calculated from the expert panel estimates of K_ds. The apparent bulk rock K_d for each actinide is estimated by combining a 95% weighting of the matrix (i.e., dolomite) K_ds with a 5% weighting of the clay mineral K_ds. The 5 weight % clay mineral figure was estimated based on the bulk concentration of clay in the Culebra as described in work by

Table 3-1. Alternative Conceptual Models for Rock-Water Interaction in the Culebra Dolomite Member of the Rustler Formation

Conceptual Model Number (Arbitrary)	Localized Solute Transport	Potential Solute/Rock Interactions			Closest 1992 PA Sensitivity Analysis Section[2]	Estimated Chemical Retardation Potential
	Mechanism	Surfaces Exposed	Mineral Distribution[1]	Distribution Coefficient(s)		
1	fracture advection; matrix diffusion	fractures + matrix	not important ($K_d = 0$)	$K_d = 0$ (no retardation)		none
2[3]	fracture advection; matrix diffusion	high-angle fractures + matrix	homogenous	weighted clay + dolomite K_d		moderate to high
3	fracture advection; matrix diffusion	sub-horizontal fractures + matrix	concentrations of clay-minerals in matrix adjacent to fractures	clay K_d; dolomite K_d	see text	high to very high
4	fracture advection; matrix diffusion	sub-horizontal fractures + matrix	clay-mineral "lined" fractures	clay K_d; dolomite K_d	section 8.4.4; Figures 8.4-12 to 8.4-13	very high
5	fracture advection; matrix diffusion	high-angle fractures + matrix	concentrations of clay-minerals in matrix adjacent to fractures	weighted clay + dolomite K_d		high
6	fracture advection; matrix diffusion	sub-horizontal + high-angle fractures + matrix	concentrations of clay-minerals in matrix adjacent to fractures	alternate between [weighted clay + dolomite K_d] and [clay K_d; dolomite K_d]	section 8.4.3; Figures 8.4-7 to 8.4-11	high
7	fracture advection; no matrix diffusion	fractures	not important ($K_d = 0$)	$K_d = 0$ (no retardation)		none
8	fracture advection; no matrix diffusion	high-angle fractures	homogenous	weighted clay + dolomite K_d		low
9	fracture advection; no matrix diffusion	sub-horizontal fractures	concentrations of clay-minerals in matrix adjacent to fractures	clay K_d	see text	low to moderate
10	fracture advection; no matrix diffusion	sub-horizontal fractures	clay-mineral "lined" fractures	clay K_d	section 8.4.2; Figures 8.4-2 to 8.4-6	moderate
11	fracture advection; no matrix diffusion	high-angle fractures	homogenous	weighted clay + dolomite K_d		low
12	fracture advection; no matrix diffusion	sub-horizontal + high-angle fractures	homogenous	alternate between [weighted clay + dolomite K_d] and [clay K_d; dolomite K_d]		low
13	matrix advection	matrix	homogenous	weighted clay + dolomite K_d		extremely high

[1] The possibility of Fe-oxyhydroxide coatings on fractures has not been considered in these scenarios.
[2] See Volume 4 of WIPP PA (1992-1993).
[3] Baseline conceptual model, with $K_d = 0$.

Sewards (1991) and Powers and Holt (1990). For this conceptual model, concentrations of clay minerals adjacent to fractures are not recognized.

3.3.2 Adsorption

Summary Statement: The 1992 preliminary performance assessment assumed that adsorption of solutes on solid phases obeys a linear isotherm with local chemical equilibrium between solute and solid phases. Conclusive data in support of these assumptions are not currently available. The impact of these assumptions on radionuclide release cannot be estimated at this time due to the lack of relevant information. Therefore, a bounding position at this time with regard to adsorption is to take no credit for adsorption.

In addition, the 1992 performance assessment assumed that K_d values based on batch experiments are applicable to advective and/or diffusive transport and they are not sensitive to model cell size chosen in the numerical implementation of the transport model.

Discussion: Currently, chemical retardation factors (R) in PA analyses are calculated using the following equation (Freeze and Cherry, 1979):

$$R = 1 + (\rho_b/\phi)K_d \tag{3-6}$$

where K_d is the distribution coefficient for each radionuclide and ϕ and ρ_b are the porosity and bulk density of the rock, respectively. This equation can be derived from the advection-dispersion equation assuming local equilibrium for adsorption and a linear relationship between the amount of a solute adsorbed on the unit amount of the solid, S, and the concentration of the solute, C.

$$S = K_d\ C \tag{3-7}$$

This is the linear isotherm model called the K_d-model. However, other forms of isotherms are quite common (Fetter, 1993). These other forms of isotherms show saturation effects at higher solute concentrations, i.e., isotherms level off at higher concentrations. In some cases, as the solute concentration is further increased, adsorption increases rapidly due to additional processes such as surface precipitation (as monolayers on surfaces) coming into play, and the isotherm takes on the S-shape. Note that currently the linear isotherms for some of the actinides are based on single measurement (Dosch, 1980, 1981; Dosch and Lynch, 1978; Lynch and Dosch, 1980; Nowak, 1980; Serne et al., 1977; Tien et al., 1983). These single-point isotherms are obviously not absolutely correct because one could connect the zero-point and the

measured non-zero point of an isotherm using an infinite number of possible curves, including a straight line (i.e., the linear isotherm). Not knowing what the actual isotherms for various actinides look like, it is difficult to assess if the PA calculations based on linear isotherms are conservative.

Another assumption made by PA is that local chemical equilibrium always exists between solutes and solid phases. However, chemical nonequilibrium is quite common for many organic solutes (see Brusseau et al., 1989 and references therein), and some of the actinides may also exhibit nonequilibrium. Since the equilibration times for relevant actinides are not known, it is not possible to assess the impact of the assumption of local chemical equilibrium on radionuclide release.

Because the assumptions of isotherm linearity and local chemical equilibrium are not fully supported and the impact of these assumptions on radionuclide release cannot be estimated at this time due to the lack of relevant information, the bounding position at this time with regard to adsorption is to take no credit for adsorption, i.e., K_d is assumed to be zero. It should be noted that this is an overly conservative position because Dosch and other workers (see references cited earlier) have clearly established that the Culebra rock significantly adsorbs various actinides, although actual K_ds are not quantifiable at this time.

When additional measured-retardation factors and/or K_d values are available, will they be valid for any conceptual model and are they sensitive to the scale of the experiments? The K_d values are applicable to advective and/or diffusive flow because K_d is inherently a property of a solution-solid interface for an adsorbate-adsorbent pair and, therefore, does not depend on the conceptual model being employed for chemical transport. Adsorption of an actinide, and consequently its chemical retardation, is not affected by whether the water flow is advective, diffusive, or both, but rather by what minerals the actinides encounter during their transport. Similarly, in a homogeneous medium, K_d is a function of the chemical composition of the medium, but not the size of the medium (e.g., core sample size). This is implicit in the definition of K_d based on Eq. (3-7); the scale independence of K_d is valid even when the adsorption isotherm is nonlinear. The same conclusions are applicable to the distribution coefficient Ka on a per-unit-surface-area basis because Ka is defined in the same way as K_d (Freeze and Cherry, 1979) in the case of chemical transport through fractures. Therefore, K_d values for a given actinide based on laboratory mechanistic adsorption experiments (core size: 20 - 100 micrometer), or laboratory column experiments (core size: up to 100 cm), or field tracer tests (sample size in tens of meters) should be approximately the same if the physical-chemical conditions are comparable and can be used for any model cell size. K_d values obtained from these different experiments may vary to some degree from sample to sample and their size.

Since K_d is expected to be scale-independent, as explained above, these variations could be due to several factors:

1) The Culebra is highly heterogeneous at both micro and macro scales. One approach to incorporate these variabilities is through a cumulative distribution function (CDF) for K_d as in the (Sandia WIPP Project, 1992).

2) Chemical equilibration time for some or all reactions is comparable or greater than liquid transit time through a model cell. In these cases, chemicals move from one location to the next before local chemical equilibrium is established, as implied in Eqs. (3-6) and (3-7).

3) K_d variations observed in different samples could be due to different processes (adsorption, ion exchange, and/or precipitation) being responsible for sorption in different samples.

3.3.3 Colloid-Facilitated Radionuclide Transport

Summary Statement: The presence of actinide-bearing colloidal particles in the WIPP system has the potential to accelerate or retard the transport of actinides relative to transport of dissolved species. For long-term performance assessment calculations conducted to date, the impact of colloidal particles on actinide transport was not quantified. Because there is a possibility that colloidal particles can increase transport rates relative to dissolved species, not including colloids in transport calculations for assessment is not necessarily conservative. For example, some colloidal particles are sufficiently large to be excluded from participating in matrix diffusion. Actinides sorbed on the surfaces of those colloidal particles will not be physically retarded, and actinide transport by colloids therefore must be considered. Preliminary results from a recently initiated experimental program suggest a reduction in the potential impact of colloid particles on actinide transport. Specifically, "hard-sphere" carrier colloids are not mobile, regardless of whether they have sorbed radionuclides on their surfaces, and so are eliminated from participation in actinide transport. Actinide intrinsic colloids and "soft-sphere" carrier colloids (e.g., humic materials) may be mobile, but are sufficiently small to undergo matrix diffusion in the Culebra and so will be physically retarded. Actinides that are bioaccumulated by or sorbed on microbes, however, will be transported primarily by fracture advection because the relatively large sizes of microbes precludes them from entering the intercrystalline pores of the Culebra matrix.

Discussion: Quantification of actinide transport by colloidal particles requires coupling of various aspects of hydrogeology, geochemistry, and colloid chemistry (see, e.g., McDowell-

Boyer et al., 1986; Hwang et al., 1990; Nuttall et al., 1991; Bennett et al., 1993; van der Lee et al., 1993). Those aspects may be grouped into the following categories: (1) the physico-chemical behavior of colloidal particles in the dispersent, including the formation of the particles and their kinetic and chemical stabilities; (2) interaction of the colloidal particles with actinides; and (3) the hydrologic behavior of colloidal particles in the subsurface environment. The potential importance of colloid-facilitated radionuclide transport has only been recognized for about a decade (see, e.g., Avogadro and de Marsily, 1983) and rigorous transport models and computer codes suitable for long-term performance assessment of the WIPP Site are not yet available. However, by focusing on concepts included in the three categories above with specific consideration to the WIPP environment, quantifying the impact of colloidal particles on actinide transport has been simplified to the point where it is a tractable problem.

The following text includes a brief review of different types of actinide-bearing colloids and their behavior in WIPP environments.

3.3.3.1 PHYSICO-CHEMICAL BEHAVIORS OF COLLOIDAL PARTICLES

Carrier colloids, which are ordinarily non-radioactive, are colloidal-sized particles that may act as substrates for sorption of actinides as well as other metals (carrier colloids with sorbed actinides are referred to in the published literature as pseudocolloids, Type II colloids, and Fremdkolloide) (Lieser et al., 1986a, 1986b, 1990; Buddemeier and Hunt, 1988; Kim, 1991). The carrier colloid category is further subdivided on the basis of known physico-chemical behaviors of those colloidal particles.

"Hard-sphere" carrier colloids, traditionally referred to as hydrophobic colloids in colloid chemistry, have discrete well-defined particle-fluid boundaries and are stabilized in very low ionic strength solutions by electrostatic effects caused by the electric double layer surrounding the particles (Hiemenz, 1986). At high ionic strengths (which are actually quite low relative to brines associated with the WIPP), however, the electric double layer surrounding the "hard-sphere" colloids collapses, and virtually eliminates electrostatic repulsion between particles (Gregory, 1978; van Olphen, 1991, p. 24; see also Derjaguin and Landau, 1941; Verwey and Overbeek, 1948; Matijević, 1973). Forces of attraction between the particles (i.e., van der Waals forces) causes agglomeration of particles to form clusters large enough to settle by gravity. This phenomenon has been known empirically for well over a century (see, e.g., Hardy, 1900) and was theoretically explained in the middle of this century (Derjaguin and Landau, 1941; Verwey and Overbeek, 1948).

The WIPP Site is unique among proposed nuclear waste repositories in that groundwaters in both the near-field (i.e., the disposal room) and the far-field (i.e., the Culebra) environments consist of high ionic strength brines (refer to Brush, 1990; Siegel et al., 1991b). Experiments at Sandia National Laboratories (SNL) have confirmed that dispersions of "hard-sphere" carrier colloids are not kinetically stable in Culebra brine simulants (hydrogeochemical facies "A" and "C;" Siegel et al., 1991b), Salado Formation-like brine simulants (Brine A; Molecke, 1983; Brush, 1990), and Castile Formation brine simulants (ERDA-6; Brush, 1990). Therefore, "hard-sphere" carrier colloids have been eliminated from further consideration in quantifying transport of actinides. This group of colloids includes many of the colloidal particles identified at other sites (see McCarthy and Degueldre, 1993, Table 6). Colloidal particles that can be eliminated from consideration in transport of actinides at the WIPP Site include iron(III)-(hydr)oxides, clay minerals, and mineral constituents of the host rock. Further, colloidal particles produced from drilling (i.e., cuttings) and mineral precipitates formed from brine mixing will not be kinetically stable.

Sterically stabilized "hard-sphere" carrier colloids are coated with compounds capable of modifying the colloids' surface behavior so that electrostatic attraction and repulsion forces are overcome, rendering them kinetically stable. An example of this colloid type are colloidal particles stabilized by organic compounds in sea water (Honeyman, 1991; Honeyman and Santschi, 1992). Microbes are probably best placed in this category, although their cell walls are not rigid. At the WIPP Site, concentrations of naturally occurring microbes are on the order of 10^9 to 10^{10} cells per liter (Francis and Gillow, 1994, Table 1). In the presence of nutrients provided by WIPP waste constituents, those concentrations are likely to increase. Microbes are important for actinide transport because they may act as substrates for sorption of actinides, but also may bioaccumulate actinides. In addition to microbes, it is well known from industrial research that colloidal dispersions can be sterically stabilized in electrolytes by the addition of some types of polymers (see, e.g., Theng, 1979; Sato and Ruch, 1980). It is unlikely, however, that potential steric compounds such as alcohols and carboxylic acids produced as by-products of microbial degradation of WIPP waste could be present in large enough concentrations to have an impact on stability of "hard-sphere" carrier colloids in the extremely high ionic strength brines associated with the WIPP. Until results from the ongoing colloid experimental program are available, sterically stabilized "hard-sphere" carrier colloids (i.e., microbes) should be included in transport calculations.

"Soft-sphere" carrier colloids are flexible particles with rather indistinct particle-fluid boundaries, and are essentially dissolved macromolecules. They are not affected by ionic strength in the same way as "hard-sphere" carrier colloids. "Soft-sphere" carrier colloids are closest in form and behavior to particles referred to as hydrophilic colloids in the traditional

colloid chemistry literature (Lyklema, 1978; Hiemenz, 1986); examples include humic and fulvic acids (Choppin, 1988; Tiller and O'Melia, 1993). Because this type of colloid is not destabilized by high ionic strengths, "soft-sphere" carrier colloids may be important in transport of actinides at the WIPP. Humic and fulvic materials (high-molecular weight organic macromolecules) are of particular concern because of their well-known capability of complexing with metal cations, including actinides (Choppin, 1988, Dearlove et al., 1990; Vlassopoulos et al., 1990; Tipping, 1993; van der Lee et al., 1993). The concentrations of humic materials in deep subsurface groundwaters is typically quite small, because of the long periods of time available for oxidation of those materials. Existing information on total organic carbon (TOC) concentrations in Culebra groundwaters, for example, shows that TOC is on the order of 1 mg/L (Myers et al., 1991) which is quite low. An additional potential source of humic materials is from soil constituents of WIPP waste (U.S. Department of Energy, 1994b, Table 4-1, Waste Matrix Code Group 4200), or perhaps from long-term microbial degradation of cellulosic constituents in the waste. Experiments are in progress at SNL to investigate this type of colloid.

Actinide intrinsic colloids (also known as true colloids, Type I colloids, and Eigenkolloide) are thought to form by condensation reactions of hydrolyzed actinide ions (Maiti et al., 1989), to form macromolecules, or "polymers," of colloidal size. It is believed that the actinide ions are bridged by hydroxyl groups or oxygen ions (Kim, 1991). Following the oxidation state analogy described earlier in this paper, the tendency of actinides to hydrolyze and to form intrinsic colloids follows the order: $M^{4+} > M(VI)O_2^{2+} > M^{3+} > M(V)O_2^{+}$ (Choppin, 1983; Kim, 1991). The tendency for formation of one particular actinide intrinsic colloid, the Pu(IV)-polymer, is enhanced by increased concentrations of Pu(IV), temperature, and basic conditions (Toth et al., 1981). Examples can be found the literature of polymeric species of most of the actinides of importance to WIPP (see e.g., Baes and Mesmer, 1976; Kim, 1991). It is important, however, to note the sizes of polymers described in the literature. It is well known that as polyvalent metals, the actinides can form lower polymers such as dimers, trimers, tetramers, and hexamers. However, in terms of physical transport behavior, the lower polymers will behave no differently than dissolved monomeric species. In contrast, the higher polymers, such as the Pu(IV)-polymer, may reach colloidal sizes (1 nm to 1 μm) and will have different hydrodynamic properties than the sub-colloidal-sized dissolved species.

The most well-known and well-studied actinide intrinsic colloid is the Pu(IV)-polymer. Most of the knowledge about the Pu(IV)-polymer comes from research at relatively high Pu concentrations in highly acidic solutions (e.g., Kraus, 1956; Costanzo et al., 1973; Bell et al., 1973a, b; Lloyd and Haire, 1978; Toth et al., 1981), which was conducted to help improve processing techniques. Investigations focusing on chemical conditions relevant to environmental

concerns have been conducted more recently (Cleveland, 1979; Rai and Swanson, 1981; Kim, 1991; Nitsche et al., 1992). A conclusive demonstration of the mechanisms of formation of the Pu(IV)-polymer has not yet been made, but there is a preponderance of evidence that shows that polymerization is strongly linked to hydrolysis (see e.g., Kim, 1991), and that the initial polymerization produces an amorphous macromolecule that becomes crystalline with time (see Cleveland, 1979, and references therein). Lloyd and Haire (1978) showed that the aged polymer actually consists of nanometer-sized mineral crystallites. Rundberg et al. (1988) and Triay et al. (1991) used different analytical methods to confirm the particulate nature of the Pu(IV)-polymer, and also estimated that the size was on the order of nanometers. In terms of implications for transport at the WIPP, if the Pu(IV)-polymer is indeed a crystalline colloidal particle, rather than a "soft-sphere"-like (hydrophilic) colloid, it would behave like a "hard-sphere" (hydrophobic) colloid. As such, it would be destabilized by high ionic strength solutions, such as WIPP brines. Critics may point out that they are familiar with Pu(IV)-polymer solutions that have remained stable for years. That observation is not necessarily inconsistent with the notion that the Pu(IV)-polymer is a "hard-sphere" type colloid. For example, Overbeek (1982) reported that some of the gold sols (dispersions of 3 nm diameter metallic gold, a "hard-sphere" type colloid) used in historically important experiments by Michael Faraday in the mid-1800s were still in existence at the time of Overbeek's publication. Experiments are in progress to evaluate the formation and behavior of actinide intrinsic colloids, including the Pu(IV)-polymer, at Lawrence Livermore National Laboratory (LLNL). Until such results are available, however, actinide-intrinsic colloids should be considered to be dissolved macromolecules which are not destabilized by high ionic strength WIPP brines.

In summary, "hard-sphere" carrier colloids can be eliminated from further consideration because of the destabilizing effects of the high ionic strength brines associated with the WIPP. The remaining subtypes, sterically stabilized "hard-sphere" carrier colloids (microbes), "soft-sphere" (humic materials) carrier colloids, and actinide-intrinsic colloids cannot be eliminated. The remaining portion of this discussion focuses on the sources and transport behaviors of those colloids.

3.3.3.2 SOURCES OF COLLOIDAL PARTICLES

In an intrusion scenario, there are two potential sources of actinide-bearing colloids: the disposal room environment (which also includes colloids introduced to the disposal room from Castile Formation groundwaters), and colloids formed in situ within the Culebra. In an undisturbed situation, the types of colloids that could be present in Culebra and Castile Formation brines are "hard-sphere" carrier colloids, microbes, and "soft-sphere" carrier colloids

(humic materials). As described above, the high ionic strengths of the brines will destabilize the "hard-sphere" carrier colloids; actinides may sorb onto those colloids, but they will be immobilized. Because of the presence of soils in WIPP waste (U.S. Department of Energy, 1994b, Table 4-1, Waste Matrix Code Group 4200), the concentration of humic materials in disposal room brines is likely to exceed the concentration of humic materials in Castile or Culebra brines. Likewise, because of the nutrients provided by organic components of the waste, the concentrations of microbes in the disposal room environment will exceed the concentration of microbes in Castile or Culebra brines. Actinide-intrinsic colloids are more likely to form in environments of greater actinide concentrations such as the disposal room environment, rather than the Culebra. The source of colloidal particles that may participate in transport of actinides is clearly dominated by those introduced from the disposal room environment. It follows that investigation of colloid-facilitated actinide transport in the Culebra has close ties to the characterization and quantification of mobile colloidal actinides for the Actinide Source Term Program (refer to the Source Term position paper for details).

3.3.3.3 TRANSPORT BEHAVIORS

Because the sizes of colloidal particles are significantly greater than the sizes of dissolved species, colloidal particles behave differently in terms of transport. In quantifying colloid-facilitated actinide transport in the Culebra, the primary distinction in colloid subtypes is whether the sizes of colloidal particles are larger or smaller than the mean pore throat diameters (0.63 μm; Kelley and Saulnier, 1990, p. 4-10) of the intercrystalline pores in the Culebra matrix. Colloidal particles that are smaller than the pore throats will be transported into the rock matrix by physical diffusion, and, therefore, transport will be retarded physically. In contrast, colloidal particles that are larger than pore throats will be excluded from the matrix and will be transported by advection and diffusion in fractures (see, e.g., Vilks, 1994). The subtypes of colloidal particles considered here fall into two categories in terms of hydraulic properties: (1) actinide intrinsic colloids and "soft-sphere" carrier colloids (humic materials) behave as dissolved macromolecules that are small enough to enter the pore throats in the Culebra, but are sufficiently larger than other dissolved species to have reduced physical diffusion rates; and (2) microbes, which are larger than the mean pore throat diameter in the Culebra, and will not undergo matrix diffusion. Conservative estimates of the effective diffusion constants for the macromolecular-type colloidal particles have been made on the basis of their sizes (the free water diffusion constant for a solute in a liquid is inversely proportional to the radius of the diffusing particle; see Bird et al., 1960; Hiemenz, 1986, p. 81).

The WIPP Project recognizes that there are other phenomena, such as surface (physical) filtration, chemical filtration by sorption of colloids themselves onto fixed substrates, and equilibrium sorption and desorption of actinides on surfaces of carrier colloids, that will affect the transport of actinides by colloidal particles (see Bennett et al., 1993). Rigorous quantification of the effects of those phenomena, however, is not tractable at the current time for long-term performance assessment calculations for a system as complex as the WIPP. Disregarding those phenomena, however, will not result in greater releases. Furthermore, those phenomena which are being disregarded are expected to be of secondary importance on reducing releases compared to other phenomena, such as the kinetic and chemical stability behavior of colloids in WIPP brines.

3.3.4 Actinide Coprecipitation From Brine Mixing

Summary Statement: In an intrusion scenario, mixing of disposal room brines with Culebra brines are likely to result in a non-equilibrium condition resulting in precipitation of actinide-bearing minerals (coprecipitation) or in dissolution of Culebra minerals. The 1992 preliminary performance assessment did not evaluate effects due to brine mixing. Coprecipitation will decrease radionuclide release and reduce transmissivity in proximity of the borehole, whereas rock dissolution will increase transmissivity by opening clogged fractures or widening existing fractures. Coprecipitation may result in the formation of relatively large crystals in the rock matrix, or it may result in the formation of "hard-sphere" type colloids (see Section 3.3.3). In the latter case, those colloidal particles will be destabilized by the high ionic strengths of the Culebra brines, rendering them and any coprecipitated actinides immobile. Adequate experimental results or models are not currently available to quantify a reduction in actinide transport by coprecipitation. However, it is reasonable to assume that disregarding the effects of coprecipitation or dissolution is a conservative assumption.

Discussion: In most natural environments, mixing of groundwaters in equilibrium with different subsurface environments produces non-equilibrium conditions resulting in precipitation of solids or dissolution of minerals in the host rock.

Scoping calculations using chemical equilibrium modeling have demonstrated that at the WIPP site, mixing of disposal room brines (which may be dominated by Castile or Salado brines) with Culebra brines may result in precipitation of sulfate or carbonate minerals. On the basis of published literature, actinide elements are often readily incorporated into the crystal lattices of carbonate minerals (see e.g., the review by Stout and Carroll, 1993). Precipitation of actinide-bearing minerals or immobile colloidal particles is an appealing prospect in terms of

performance of the WIPP, because this retardation mechanism is not reversible like adsorption. Once the mineral forms, it is not likely to dissolve unless new non-equilibrium conditions are introduced. In addition to providing a potentially immobile sink for actinides, precipitation of minerals due to brine mixing may also reduce the transmissivity of the Culebra in proximity of the intrusion borehole.

Alternatively, brine mixing could result in dissolution of the host rock until equilibrium is reached. If the pH of the disposal room brine is outside the stability range of dolomite (about pH6 to pH9), dissolution of dolomite in the Culebra is likely to occur. However, equilibrium would be reached in a very short time because of the reactivity of dolomite. Any dissolution required for the brine to reach a new equilibrium would, therefore, occur near the borehole, and increases in transmissivity due to dissolution would be localized. Because of the relatively high ionic strengths of possible disposal room brines, dissolution of the host rock may also occur due to ionic strength effects (see, e.g., Freeze and Cherry, 1979, p. 107-108). However, that effect is expected to be secondary compared to dissolution due to exceeding the pH stability range of dolomite.

In summary, mixing of disposal room brines with Culebra brines is likely to produce a non-equilibrium condition. Localized dissolution of the host rock may occur to neutralize the pH of the brine mixture, but because of the rapid dissolution kinetics of dolomite, dissolution is expected to be limited to the proximity of the intrusion borehole. If precipitation occurs, actinides are likely to be included in mineral precipitates, and will be immobile, regardless of whether they are colloidal particles or relatively large crystals. Unfortunately, quantifying retardation of actinides due to coprecipitation is complicated by the need to consider precipitation kinetics, the effects of complexes on actinide coprecipitation, and coupling solute flow rates with coprecipitation. Consequently, whereas benefit could be gained if actinide coprecipitation were quantified, it is conservative to disregard the effects of brine mixing.

3.4 Long Term Processes

This section contains conceptual and mechanistic models concerning processes that potentially could act over thousands of years to alter patterns of groundwater flow in strata above the Salado Formation.

3.4.1 Climate Change

Summary Statement: Climate in southeastern New Mexico may be wetter and cooler at some times during the next 10,000 years than it is at present. A wetter and cooler climate may result in an increase in the amount of water infiltrating to the saturated zone, thereby raising the water table. Conceptually, a rise in the elevation of the water table could increase the hydraulic gradient or change its direction in the Culebra or other members of the Rustler Formation. Three-dimensional modeling work to date, however, suggests that the hydrologic system may respond too slowly for significant changes in the hydraulic gradient in the Culebra to occur within 10,000 years. A rise in the water table could also affect performance by increasing the extent of the saturated zone in the rocks above the Rustler Formation.

Discussion

Paleoclimates and Climatic Variability

Geologic data from southeastern New Mexico and the surrounding region show repeated alternations of wetter and drier climates throughout the last 1.5 million years, corresponding to global cycles of glaciation and deglaciation. Data from plant and animal remains and paleo-lake levels permit quantitative climate reconstructions for the region only for the last glacial cycle, and confirm the interpretation that conditions were coolest and wettest during glacial maxima (Swift, 1993). The hottest and driest conditions since the last glaciation have been similar to those of the present. Modeling of global circulation patterns suggests that these changes resulted from the disruption and southward displacement of the winter jet stream by the ice sheet, causing an increase in the frequency and intensity of winter storms throughout the American Southwest (COHMAP Members, 1988). Mean annual precipitation 22,000 to 18,000 years ago, when the last North American ice sheet reached its southern limit roughly 1500 km north of the WIPP, was approximately twice that of the present. Mean annual temperatures may have been as much as 5°C colder than at present.

Glacial periodicities have been stable for the last 800,000 years (Hays et al., 1976; Imbrie et al., 1984; Imbrie, 1985). Barring anthropogenic changes in the Earth's climate, relatively simple modeling of climatic response to orbital changes in insolation suggests that the next glacial maximum will occur in approximately 60,000 years (Imbrie and Imbrie, 1980). The extent to which unprecedented anthropogenic climate changes may alter this conclusion is uncertain, but presently available models of climatic response to an enhanced greenhouse effect (e.g., Mitchell, 1989; Houghton et al., 1990) do not predict changes of a larger magnitude than those of the last 1.5 million years. Furthermore, published models do not suggest significant

increases in precipitation in southeastern New Mexico following global warming (Washington and Meehl, 1984; Wilson and Mitchell, 1987; Schlesinger and Mitchell, 1987; Houghton et al., 1990). Even allowing for anthropogenic change, climate variability at the WIPP can be bounded by extremes of the last 1.5 million years (Swift, 1993).

Relatively shorter-term climatic fluctuations have occurred throughout the last 1.5 million years with periodicities on the scale of hundreds to thousands of years. The causes of these nonglacial fluctuations are, in general, unknown, but paleoclimatic data indicate that precipitation may have approached glacial highs at some times during the last 10,000 years (Swift, 1993). Based on the past record, fluctuations of this sort are probable during the next 10,000 years, and must be included in long-term assessments.

Hydrologic Modeling of Climate Change

In regions with dry climates, such as present-day southeastern New Mexico, the water table (i.e., the top of the saturated zone) is at some depth below the land surface. Only a small portion of the total precipitation infiltrates and percolates downward through the unsaturated zone. If the climate were to become cooler and wetter, the amount of moisture that infiltrated to the water table could be somewhat greater, and consequently the water table could rise. According to the groundwater basin conceptual model (Section 3.1.2), the elevation and shape of the water table determine to a large extent the patterns of groundwater flow in the basin. Consequently, a climate change could alter groundwater flow in the Dewey Lake Formation and Dockum Group, as well as in the more conductive units of the Rustler Formation.

The present-day position of the water table in the vicinity of the WIPP is not well-known because the Dewey Lake Formation and Dockum Group produce very little water to most test holes. The observation that only a small amount of water can be produced from a given drill hole indicates either that the penetrated rock is unsaturated or that its conductivity is small. Brine from an intrusion hole could flow into both saturated and unsaturated portions of the Dewey Lake and the overlying Dockum Group, but could only be transported laterally for long distances toward the accessible environment in the saturated portion. Therefore a wetter climate could impact transport in the Dewey Lake and Dockum Group in two ways. First, it could increase the thickness or lateral extent of the saturated region. Second, the wetter climate could change flow directions and rates in the previously saturated portion.

Within the WIPP-site boundary, the Rustler Formation is fully saturated. Maximum gradients of hydraulic head in the Rustler are expected to occur when the infiltration rate is

sufficient to raise the water table to the ground surface at all locations. This is because the energy available to move groundwater in a basin depends on the difference in elevation between the highest and lowest positions of the water table. In regions with wet climates, the water table tends to be close to the ground surface everywhere. In regions with drier climates, the water table tends to remain near the land surface in topographically low areas but its elevation fluctuates under topographically high areas in response to changes in infiltration. The difference between the high and low parts of the water table, and consequently the gradient driving groundwater flow, is therefore maximized if the water table is everywhere near the land surface. On a regional scale these gradients will be similar to the slope of the land surface. At a local scale, however, hydraulic gradients can be greater or less than the slope of the overlying land surface.

The SECOFL3D code was used to perform a preliminary investigation of the possible impact of climate change on groundwater flow above the Salado Formation (Appendix A of this report). The results of this investigation must be considered to be tentative because it is based on a single set of model parameters. Simulations using a wide range of model parameters are in progress.

First a steady-state flow field calculated using a value of maximum potential recharge of 0.1 cm/yr was compared to a flow field calculated using a value of 0.01 cm/yr. The maximum potential recharge rate is the fastest rate that moisture is allowed to infiltrate through the unsaturated zone to the water table. Both rates used are a small fraction the present-day annual precipitation, approximately 30 cm/yr, at WIPP. However, the larger rate is sufficient to maintain the water table near the land surface. The simulation results suggest that even this difference in potential recharge of less than a tenth of a centimeter per year could have an impact on flow patterns given a sufficiently long period of time for flow patterns to adjust. Simulated flow in the Culebra near the WIPP site, for example, is toward the south given the lower rate of recharge, but is toward the west if the higher rate of recharge is assumed. The flow pattern for the lower recharge rate (0.01 cm/yr) is similar to the pattern observed today. The hydraulic gradient is approximately twice as steep in the calculation with higher recharge. Whether or not flow driven to the west by a steeper gradient would actually result in shorter travel times to the accessible environment depends on details of the transmissivity distribution which could not be included in these simulations.

These steady-state results show *how much* a climate change could impact flow in the Culebra *if* the change persisted long enough for flow patterns to adjust completely to the new climate. The steady-state calculations, therefore, show the maximum, or bounding, impact of a given climate change. As the second part of this study, a transient simulation was performed

to evaluate *how fast* a climate change could impact groundwater flow patterns. The simulated period of time was the past 14,000 years. Using the estimated precipitation record for this period (Swift, 1993) as a basis for the temporal pattern of recharge, the recharge rate was decreased from 0.1 to 0.01 cm/yr over the period from 14,000 until 8,000 years before the present. The rate remained at 0.01 cm/yr for the rest of the simulation. Flow in the Culebra adjusted slowly enough that the simulated flow pattern for the present-day is more representative of the 0.1 cm/yr recharge rate assumed for 14,000 years ago than the current 0.01 cm/yr rate. This result implies that the undisturbed pattern of groundwater flow in the Rustler Formation would not change much over the next 10,000 years even if the climate became wetter in the near future.

These simulations also provide information on how much a change in climate could affect the thickness of saturated zone in the Dewey Lake Red Beds and the Dockum Group. The saturated thickness of these units is an important factor in determining whether or not they could act as lateral pathways for radionuclide migration. The simulations suggest that if groundwater flow adjusted to the higher, 0.1 cm/yr, recharge rate, the water table in the vicinity of WIPP would be near the land surface and consequently nearly the entire thickness of these units would be saturated. At the lower recharge rate, the simulated thickness of the saturated zone is 45 to 80 meters less. This result suggests that perhaps the most important impact of climate change would be to increase the thickness of saturated sediments above the Rustler Formation.

3.4.2 Leakage in Shallow Drill Holes

Summary Statement: The drill holes considered in this section are those that reach the Salado Formation or overlying units but do not penetrate the repository. These holes could provide pathways for vertical flow between conductive units if their plugs degrade. Application of the groundwater basin conceptual model suggests that the most likely impact of leaking holes would be to rotate the direction of groundwater flow in the Culebra Dolomite toward the west.

Discussion: We applied the groundwater basin conceptual model (Section 3.1.2) and current knowledge about the shallow flow regime to evaluate the possible impact of leaking shallow holes on groundwater flow in strata above the Salado. Pertinent knowledge about the shallow flow regime includes:

- Sufficient head data exist to determine horizontal flow directions in the vicinity of WIPP for the Culebra and Magenta dolomites. Flow in the Culebra is generally directed to the south, and flow in the Magenta is toward the west and southwest.

- Within the controlled area, hydraulic heads in the Magenta are higher than those in the Culebra. The few head measurements are available for the Dewey Lake are also higher than the head of the Culebra at those locations. Therefore flow in a leaking borehole would be downward into the Culebra from overlying conductive units.

Given the concepts of groundwater basin flow described in Section 3.1.2, the differing directions of flows within the Culebra and the Magenta make hydrologic sense. Because of the low conductivity of the Tamarisk Member, there is a significant head loss between the Magenta and the Culebra. Flow in the Magenta more closely reflects the imprint of the local topography, which slopes from east to west in the vicinity of the WIPP site. Flow in the Culebra more closely reflects the imprint of the regional land slope, which is generally north to south, paralleling the overall topography of the northern Delaware Basin.

The effect of a leaky borehole in this system will be to increase the vertical conductivity of all units. In those units that already have a relatively high conductivity, this increase may be nominal, but in tighter units (such as the Tamarisk) this increase can be important. An increase in vertical conductivity leads to a decrease in head loss across the thickness of the unit. Given a sufficient number of boreholes connecting the Magenta and the Culebra, differences in head across the Tamarisk would be reduced. Heads and gradients in the Culebra could become more like those in the Magenta. If this were the case, flow in the Culebra would pivot from a southerly direction to a west-southwest direction.

3.4.3 Subsidence Over Potash Mines

Summary Statement: Potash ore occurs in the middle portion of the Salado Formation (above the repository horizon) under nearly 2070 km^2 of the Delaware Basin, including some portions of the WIPP controlled area. Subsidence has occurred over potash mines in the past and will continue to occur over the regions that are already mined. An unknown amount of additional mining may occur in the future. Subsidence is expected to lower the absolute elevation of the land surface by up to a few meters and may therefore create depressions that would collect surface runoff. Subsidence might also alter the hydraulic conductivities of Rustler units. The effect on flow would be similar to that described for shallow boreholes (Section 3.4.2) for the same fundamental reasons.

Discussion: The WIPP land withdrawal area occupies a portion of the southeastern quadrant of the federally managed Potash Area. This Potash Area covers approximately 2070 km^2 and overlaps the boundaries of the region thought to control regional groundwater flow (Corbet and

Wallace, 1993). The potash zones occupy a portion of the middle member of the Salado Formation. Subsidence has occurred over mined areas in the past and continues to occur.

Although the land surface in subsiding areas is lowered and there may be local changes in drainage patterns, the overall topographic features that affect regional groundwater flow will remain similar to those of the present. However, subsidence may have impacts other than lowering of the land surface, including possible fracturing of units that overlie the potash zone. This fracturing could lead to an increase in conductivity for those units. The degree of increase and the relative change in conductivity from unit to unit could have an effect on the long-term groundwater flow behavior for Rustler units.

Because the Tamarisk and Forty-niner members presently have very low conductivities, fracturing may cause larger increases in conductivity in those units than in the Culebra and Magenta. The effect on flow would be similar to that described for shallow boreholes that do not intrude the repository (see Section 3.4.2), for the same fundamental reasons. That effect would be a change in the direction of the hydraulic gradients in the land withdrawal area. Currently they direct flow in the Culebra from north to south. If the scenario were to occur, they could rotate flow in the Culebra towards the west.

4.0 CURRENTLY AVAILABLE DATA FOR ASSESSING LONG-TERM PERFORMANCE

Data and information relevant to non-Salado containment include flow and transport parameters and their distributions in the non-Salado hydrostratigraphic units. Sections 4.1 through 4.5 briefly summarize the interpreted hydraulic head, transmissivity, storativity, fluid density, porosity, and retardation parameters for the non-Salado units. The raw data used to calculate these parameter values are referenced in Section 4.6. References to documentation in previous performance assessments (WIPP PA Division, 1991; Sandia WIPP Project, 1992) are made where possible.

4.1 Supra-Rustler Units

The Santa Rosa (or Dockum Group) constitutes a productive aquifer east of the WIPP site in Lea County, New Mexico (Nicholson and Clebsch, 1961). The only evidence of water in the Santa Rosa at the WIPP site was found in well H-5, where a water table was found immediately above the contact with the underlying Dewey Lake Redbeds (Mercer, 1983, p. 71).

The Dewey Lake Red Beds contain a productive zone of saturation, probably under water-table conditions, in the southwestern to south-central portion of the WIPP site and south of the site. This zone is typically found in the middle of the Dewey Lake, 180 to 265 ft (55 to 81 m) below ground surface, and appears to derive much of its transmissivity from open fractures. Short-term production rates of 25 to 30 gpm 5.7 to 6.8 m^3/hr) were observed in boreholes P-9 (Jones, 1978, v. 1, p. 168), WQSP-6, and WQSP-6A. Open fractures and/or moist (but not fully saturated) conditions have also been observed at similar depths north of the zone of saturation, at locations such as H-1, H-2, and H-3 (Mercer, 1983, p. 70). Where present, the saturated zone may be perched or simply underlain by less transmissive rock. Fractures below the productive zone tend to be completely filled with gypsum. No hydraulic tests have been conducted in the productive portion of the Dewey Lake. Tests of the lower portion of the Dewey Lake were attempted in DOE-2 (Beauheim, 1986) and H-14 (Beauheim, 1987a) but transmissivities were too low to be measured in both cases.

4.2 Rustler Formation

As discussed in Section 3.1.1, the Rustler Formation contains five members. Extensive well testing has only been performed on the most transmissive Rustler unit, the Culebra Dolomite Member. Few tests have been performed in units other than the Culebra.

4.2.1 Unnamed Lower Member and Contact Zone with Upper Salado Formation

Mercer (1983) reports values of transmissivity for the unnamed lower member or the "Rustler-Salado contact residuum" from 20 locations in the vicinity of the WIPP site. The Rustler-Salado contact residuum is a clay-rich bed with broken gypsum crystals and some fine-grained sandstone. Jones (1973) interpreted it to have been formed by dissolution of clay-bearing evaporites of the upper part of the Salado Formation. It occurs west of the margin of upper Salado dissolution shown in Figure 4-1. These transmissivity values and an additional value (from well H-16) reported by Beauheim (1987a) are shown, along with the locations of the wells at which the measurements were made, in Figure 4-1. A summary of test information from these locations is presented in Table 4-1. This summary was compiled from data contained in Mercer and Orr (1979), Mercer et al. (1981), Dennehy (1982), Dennehy and Mercer (1982), Mercer (1983), Richey (1986; 1987a), and Beauheim (1987a). Table 4-1 indicates that the tests at wells H-8c, WIPP-25, WIPP-27, WIPP-28, and WIPP-29 were conducted over intervals contained entirely within the residuum of the upper Salado. This indication is somewhat misleading, because at these locations, the contact between the Rustler and Salado is not a discrete horizon. At all of these locations, blocks of the unnamed lower member have been translated downward and mixed with Salado residue/breccia, and the contact has been arbitrarily defined as the uppermost occurrence of clasts of the red-tinted gypsum found at the top of the Salado in undisturbed sequences. Thus, the transmissivity values reported for these locations apply to a mixture of disrupted upper Salado and lower Rustler components.

The test intervals at the other wells varied in length between 22 and 143 ft (6.7 and 44 m) with different stratigraphic coverages, but all included at least the lower 8 ft (2.4 m) of the Rustler and the upper 4 ft (1.2 m) of the Salado. Most of the transmissivity values for the Rustler-Salado contact zone range from 3×10^{-5} to 6×10^{-4} ft^2/day (3×10^{-11} to 6×10^{-10} m^2/s). No correlation is evident between test-interval thicknesses and transmissivities, indicating varying hydraulic conductivity. If the measured transmissivities are considered to be derived entirely from whatever portions of the lower siltstone of the unnamed member were included in the test intervals, the average hydraulic conductivity of the siltstone ranges from about 2×10^{-6} to 4×10^{-5} ft/day (7×10^{-12} to 1×10^{-10} m/s). Transmissivities higher than 6×10^{-4} ft^2/day (6×10^{-10} m^2/s) were measured at five locations. Dissolution of the upper Salado has occurred at four of these locations (wells H-6c, H-7c, P-14, and WIPP-26; see Figure 4-2), and the test intervals included 13 to 40 ft (4 to 12 m) of the upper Salado and residuum which probably contributed the increased transmissivity. Only the value from WIPP-30 (0.2 ft^2/day [2×10^{-7} m^2/s]) where no dissolution of the upper Salado is believed to have occurred, cannot be explained by dissolution/collapse-related transmissivity enhancement.

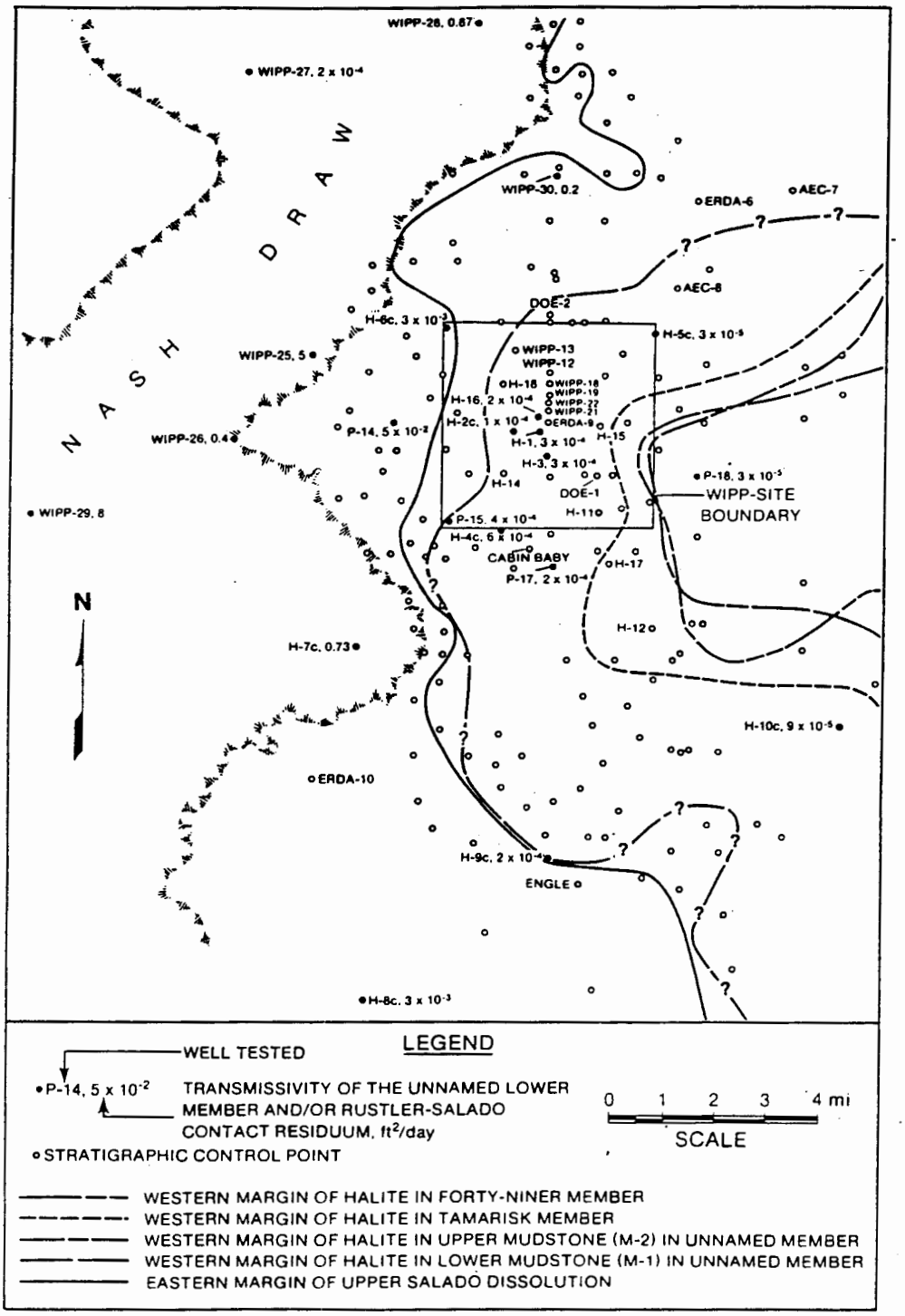

Figure 4-1. Distribution of Rustler halite and unnamed lower member and/or Rustler-Salado contact residuum transmissivity around the WIPP site.

Table 4-1. Summary of Information on Hydraulic Testing of the Unnamed Lower Member and/or Upper Salado

Well	Unnamed Lower Member Depth Interval (ft)[a]	Depth Interval Tested (ft)	Completion Interval (ft)	Transmissivity (ft^2/day)[a]	Comments[a]
H-1	699-818[b]	699-842[c]	803-827[c]	3×10^{-4}	
H-2c	645-764	743-795[c]	743-795[c]	1×10^{-4}	
H-3 (b1)	694-821	800-868[c]	813-837[c]	3×10^{-4}	
H-4c	516-626	610-661[d]	610-661[d]	6×10^{-4}	
H-5c	924-1041	1025-1076[e]	1025-1076[e]	3×10^{-5}	
H-6c	627-721	699-741[f]	699-741[f]	3×10^{-3}	top of Salado salt at 723 ft
H-7c	274-380[b]	356-420[g]	356-420[g]	7.3×10^{-1}	top of Salado salt at 405 ft
H-8c	614-733	734-808[g,h]	734-808[g]	3×10^{-3}	top of Salado salt at 798 ft
H-9c	677-791	783-816[g]	783-816[g]	2×10^{-4}	
H-10c	1391-1501	1483-1538[g]	1483-1538[g]	9×10^{-5}	
H-16	724-842[i]	739-851[i]	738-851[i]	2×10^{-4} [i]	
P-14	595-687	676-700[c]	676-700[c]	5×10^{-2}	top of Salado salt at 695 ft
P-15	435-542	532-560[c]	532-560[c]	4×10^{-4}	
P-17	583-715	702-726[c]	702-726[c]	2×10^{-4}	
P-18	938-1088	1076-1100[c]	1076-1100[c]	3×10^{-5}	
WIPP-25	472-565	579-608[h,j]	579-608[j]	5×10^{0}	top of Salado salt at 600 ft
WIPP-26	209-309	228-329[j]	228-329[j]	4×10^{-1}	top of Salado salt at 320 ft
WIPP-27	318-416	426-460[h,j]	426-460[j]	2×10^{-4}	top of Salado salt at 508 ft
WIPP-28	446-531	549-589[h,j]	549-589[j]	8.7×10^{-1}	top of Salado salt at 589 ft
WIPP-29	42-143	216-250[h,j]	216-250[j]	8×10^{0}	top of Salado salt at 521 ft
WIPP-30	654-749	731-753[j]	731-753[j]	2×10^{-1}	

[a] Data from Mercer (1983) except as noted
[b] Revision of published depth by R.P. Snyder, USGS, personal communication
[c] Data from Mercer and Orr (1979)
[d] Data from Mercer et al. (1981)
[e] Data from Dennehy and Mercer (1982)
[f] Data from Dennehy (1982)
[g] Data from Richey (1986)
[h] No Rustler tested
[i] Data from Beauheim (1987a)
[j] Data from Richey (1987a; OFR 87-37)

Water levels take months to years to stabilize in wells completed in low-transmissivity zones such as the unnamed member. Most of the wells in which the lower Rustler and/or upper Salado were tested did not remain completed to those zones long enough for water levels to stabilize, but were instead recompleted to allow testing/monitoring of overlying units. As a result, reliable water-level data are available only from those wells where unnamed member or Rustler-Salado transmissivities greater than 6 x 10^{-4} ft^2/day (6 x 10^{-10} m^2/s) were measured.

Richey (1987b) presents the water-level data collected from the Rustler-Salado contact zone by the USGS between 1977 and 1985. Stabilized water levels were attained only in wells H-6c, H-7c, H-8c, P-14, WIPP-29, and WIPP-30. Water levels rose slowly in WIPP-25, WIPP-26, and WIPP-28 during their monitoring periods; the last measurements made can be used as minimum water-level elevations at those locations. Of the other wells where Rustler-Salado water levels were measured, only the data from H-2c and P-17 are adequate to place lower bounds on the stabilized water-level elevations that are useful in understanding flow directions. A similarly useful lower bound can be placed on the stabilized water-level elevation at H-16 using fluid-pressure data presented by Beauheim (1987a).

Figure 4-2 presents the water-level elevations measured in the 12 wells listed above. The water-level elevations measured at the wells completed entirely in the residuum of the upper Salado (H-8c, WIPP-25, WIPP-28, and WIPP-29) do not appear to be significantly different from the water-level elevations at the wells completed across the Rustler-Salado contact, indicating probable good hydraulic communication between the brine aquifer in the upper Salado residuum and the lower Rustler siltstone. Drawing conclusions about flow directions from the water-level data is difficult, however, because the density of the Rustler-Salado water varies between the wells. One basis for evaluating general directions of groundwater flow is provided when the water-level elevations are converted to freshwater-head elevations (the elevation to which a column of freshwater would stand while exerting the same pressure at the midpoint of the well-completion interval as the actual water in the well). Because of the dip of the Rustler, however, freshwater-head elevations calculated from the midpoints of the well-completion intervals do not share a common elevation datum and, therefore, interpretation of potential flow directions may be misleading (Davies, 1987). Moreover, any calculation of freshwater head is only as good as the measurement or estimate of the density (or specific gravity) of the water in the well at the time of the water-level measurement.

The freshwater-head elevations shown on Figure 4-2 were estimated using fluid-density or specific-gravity data presented by Mercer (1983), Richey (1986; 1987a), and Beauheim (1987a) (see Table 4-2). Most of the density/specific-gravity measurements were made in connection with exercises that involved purging the wellbores, and the water-level

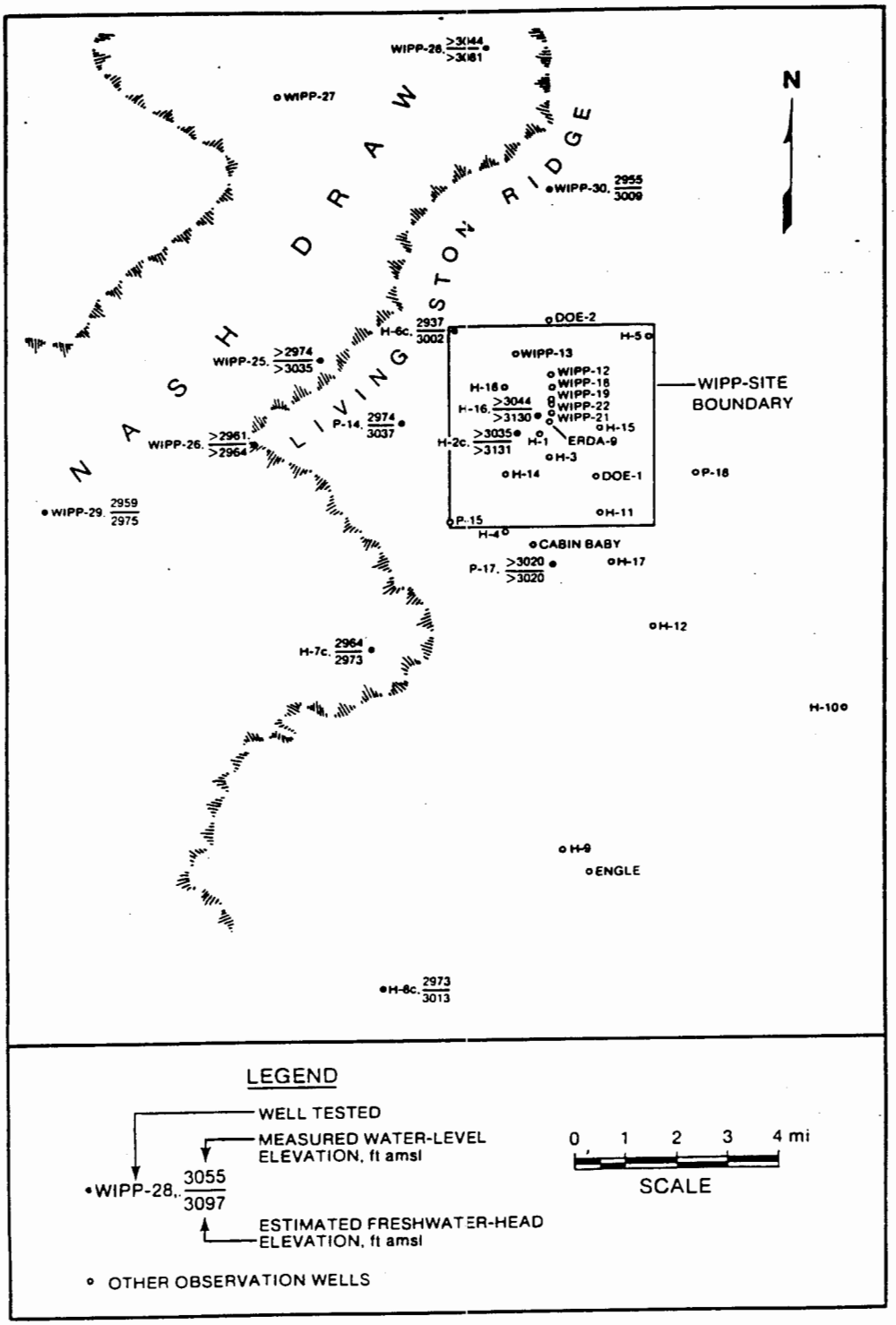

Figure 4-2. Measured water levels and estimated freshwater heads of the unnamed lower member and/or Rustler-Salado contact zone.

Table 4-2. Hydraulic-Head Information for the Unnamed Lower Member and/or Upper Salado

Well	Ground-Surface Elevation (ft amsl)[a]	Stabilized Depth to Water (ft)[b]	Date of Water-Level Measurement	Depth to Middle of Completion Interval (ft)[c]	Borehole-Fluid Density Pressure (g/cm^3) (± 0.02)	Freshwater-Head Elevation (ft amsl)	Middle of Completion Interval Pressure (psi)
H-2c	3378	<343	2/79	769	1.225[c]	>3131±9	226.1±3.7
H-6c	3348	411	7-12/80	720	1.21[c]	3002±6	162.0±2.7
H-7c	3163	199	'79-'80	388	1.048[c]	2973±4	85.8±1.6
H-8c	3433	460	11-12/80	771	1.13[d]	3013±6	152.3±2.7
H-16	3410	<366[e]	12/87	795[f]	1.2[f]	>3130±2	>223.3±1.0
P-14	3360	386	'79-'80	688	1.21[g]	3037±6	158.3±2.6
P-17	3336	<316	5/82	714	unknown	>3020	>172.5
WIPP-25	3212	<238	6/80	593	1.173[c]	>3035±7	>180.4+3.1
WIPP-26	3152	<191	6/80	278	1.04[h,i]	>2964+4	>37.7+1.9
WIPP-28	3347	<303	6/80	569	1.140[c]	>3081±5	>131.4±2.3
WIPP-29	2977	18	3-6/80	233	1.075[h]	2975±4	99.9±1.9
WIPP-30	3428	473	6/80	742	1.202[h]	3009±5	140.1±2.3

[a] Data from Gonzales (1989)
[b] Data from Richey (1987b; OFR 87-120) except as noted
[c] Data from Mercer (1983) except as noted
[d] Data from Richey (1986)
[e] Converted from pressure data presented in Beauheim (1987a)
[f] Data from Beauheim (1987a)
[g] Calculated from water analysis presented in Mercer (1983) and Figure E.1 of Haug et al. (1987)
[h] Data from Richey (1987a; OFR 87-37)
[i] Uncertainty = +0.05

measurements were made following recovery from those exercises. Because these wells were in general poorly developed, the waters entering the wellbores following the sampling exercises may have had slightly different densities from the waters removed. Thus, the density measurements were assumed to have an uncertainty of ± 0.02 g/cm^3 when used to calculate freshwater heads. The uncertainty in density is higher at WIPP-26, but only in the direction of higher density, because of apparent density stratification in the wellbore (Richey, 1987a). No fluid-density measurements were made on Rustler-Salado water from P-17 during the period from 1981 to 1982 when the only reliable water-level measurements were made. The only conclusion that can be drawn from the P-17 data is that the freshwater head cannot be lower than the measured water level. Table 4-2 summarizes the hydraulic-head data available for the unnamed lower member and/or upper Salado. Geochemical analyses from testing in the unnamed lower member are tabulated in Table 4-3. Concentrations of major chemical constituents in the unnamed lower member are shown in Figure 4-3.

4.2.2 Culebra Dolomite Member

Mercer (1983) reported values for Culebra transmissivity at 20 locations. Beauheim (1987a) provided values for Culebra transmissivity at 15 new locations, and new estimates at seven locations for which values had previously been reported. Combined with testing performed for Project Gnome (Cooper and Glanzman, 1971) and other recent work performed at DOE-2 (Beauheim, 1986), H-3 (Beauheim, 1987c), H-11 (Saulnier, 1987), WIPP-13 (Beauheim, 1987b), AEC-7 (Beauheim et al., 1991), and D-268 (Beauheim et al., 1991), the Culebra has been tested at 41 locations in the vicinity of the WIPP (Table 4-4). Figure 4-4 shows these 41 locations and the most-recent transmissivity values at each provided by the reports referenced above, as well as the distribution of halite within the Rustler over the same area. In general, the highest Culebra transmissivities (tens to thousands of ft^2/day) are found in areas where no halite is present in the Rustler, and the lowest transmissivity ($\leq$ 0.004 ft^2/day [$\leq 4 \times 10^{-9}$ m^2/s]) is found at P-18 where halite is present in all three non-dolomite Rustler members. At the two wells (H-12 and H-17) where halite is absent from the Forty-niner but present in the Tamarisk and unnamed member, the transmissivity of the Culebra is about 0.2 ft^2/day (2×10^{-7} m^2/s). Where halite is present only in the unnamed lower member, Culebra transmissivity ranges from 0.07 to 89 ft^2/day (7×10^{-8} to 9×10^{-4} m^2/s).

Culebra transmissivities of about 1 ft^2/day (10^{-6} m^2/s) or greater appear to be related to fracturing. Where the transmissivity of the Culebra is less than 1 ft^2/day (10^{-6} m^2/s), few or no open fractures have been observed in core and the Culebra's hydraulic behavior during

Table 4-3. Geochemical Analyses from the Unnamed Lower Member and/or Upper Salado

Well	Date of Sample	Geologic Unit	Density (gm/ml at 20°C)	Ph Units	Alkalinity Field (mg/L as $CaCO^3$)	Bicarbonate FET-FLD (mg/L as CO^3)	Carbonate FET-FLD (mg/L as HCO^3)	Nitrogen NO^2+NO^2 Dissolved (mg/L as N)	Sulfide Total (mg/L as S)	Hardness (mg/L as $CaCO^3$)
H-1	77-02-23	312RSLRL	--	7.9	554	675	0	.29	--	160000
H-2C	77-02-23	312RSLRL	--	5.9	163	199	0	1.1	--	130000
H-3	77-02-23	312RSLRL	--	7.6	383	467	0	.77	--	150000
H-4C	79-03-16	312RSLRL	--	--	1	1	0	.27	--	130000
H-5C	79-05-16	312RSLRL	--	--	180	300	--	--	--	340000
H-6C	79-04-09	312RSLRL	--	--	1	--	--	--	--	97000
H-7C	80-03-20	312RSLRL	1.048	6.8	35	--	--	.03	--	10000
H-8C	80-09-06	312RSLRL	--	7.6	21	--	--	.00	.6	4800
H-9C	80-05-20	312RSLRL	1.202	7.0	24	--	--	1.1	--	6800
H-10C	80-05-19	312RSLRL	1.198	6.3	53	--	--	.84	--	49000
P-14	77-02-24	312RSLRL	--	7.2	182	222	0	.34	--	6400
P-15	79-04-03	312RSLRL	--	--	45	--	--	--	--	3400
P-17	79-05-11	312RSLRL	--	--	650	--	--	.04	--	200000
P-18	79-05-11	312RSLRL	1.266	5.35	400	--	--	.06	.0	--
WIPP-25	80-03-19	312RSLRL	1.173	7.2	80	--	--	.04	--	15000
WIPP-26	80-03-18	312RSLRL	1.078	8.5	160	--	--	.05	--	12000
WIPP-27	80-05-21	312RSLRL	1.205	7.8	--	--	--	--	--	--
WIPP-28	80-03-20	312RSLRL	1.140	7.0	--	--	--	--	--	--
WIPP-29	80-03-18	312RSLRL	1.068	7.3	130	--	--	.23	--	10000
WIPP-30	80-03-19	312RSLRL	1.201	7.0	320	--	--	.04	--	12000

Well	Hardness, Noncarbonate (mg/L $CaCO^3$)	Calcium Dissolved (mg/L as Ca)	Magnesium, Dissolved (mg/L as Mg)	Sodium, Dissolved (mg/L as Na)	Potassium, Dissolved (mg/L as K)	Chloride, Dissolved (mg/L as Cl)	Sulfate Dissolved (mg/L as SO^4)	Fluoride, Dissolved (mg/L as F)	Silica, Dissolved (mg/L as SiO^2)	Boron, Dissolved (μg/L as B)	Solids, Residue at 105°C (mg/L)
H-1	160000	13000	30000	56000	17000	210000	520	--	<1	110000	480000
H-2C	130000	9200	25000	66000	9100	200000	1300	--	2.0	150000	450000
H-3	150000	18000	25000	59000	14000	210000	37	--	1.0	1900	327000
H-4C	130000	8300	27000	66000	8600	210000	1400	1.7	1.3	360000	322000
H-5C	340000	2100	82000	14000	21000	290000	2000	<.1	1.6	67000	412000
H-6C	97000	4200	21000	80000	8000	200000	2000	1.0	1.4	200000	316000
H-7C	10000	2600	910	22000	210	41000	2900	.8	7.2	3100	79800
H-8C	4700	1200	430	46000	660	70000	5300	.4	.8	1300	130000
H-9C	6800	1300	870	130000	1200	190000	2600	.1	3.8	19000	326000
H-10C	49000	1500	11000	100000	4000	190000	3300	.7	3.2	120000	323000
P-14	6200	570	1200	120000	1300	180000	10000	--	2.0	1700	350000
P-15	3300	770	350	24000	1400	38000	2800	1.3	1.3	3700	--
P-17	20000	15000	40000	23000	8800	180000	1200	3.8	15	880	--
P-18	--	10000	37000	48000	12000	220000	480	2.3	.4	160000	--
WIPP-25	15000	650	3200	90000	2400	130000	12000	.0	2.6	35000	252000
WIPP-26	12000	2700	1300	52000	1000	88000	7600	.0	2.5	30000	153000
WIPP-27	4700	1160	1040	102000	2570	154000	5190	.2	.1	1300	363000
WIPP-28	13000	615	2070	65000	2070	102000	11000	.2	6.0	54000	--
WIPP-29	10000	850	2000	32000	1000	49000	12000	.9	3.5	21000	129000
WIPP-30	11000	850	2300	120000	15000	170000	7000	.0	3.5	77000	302000

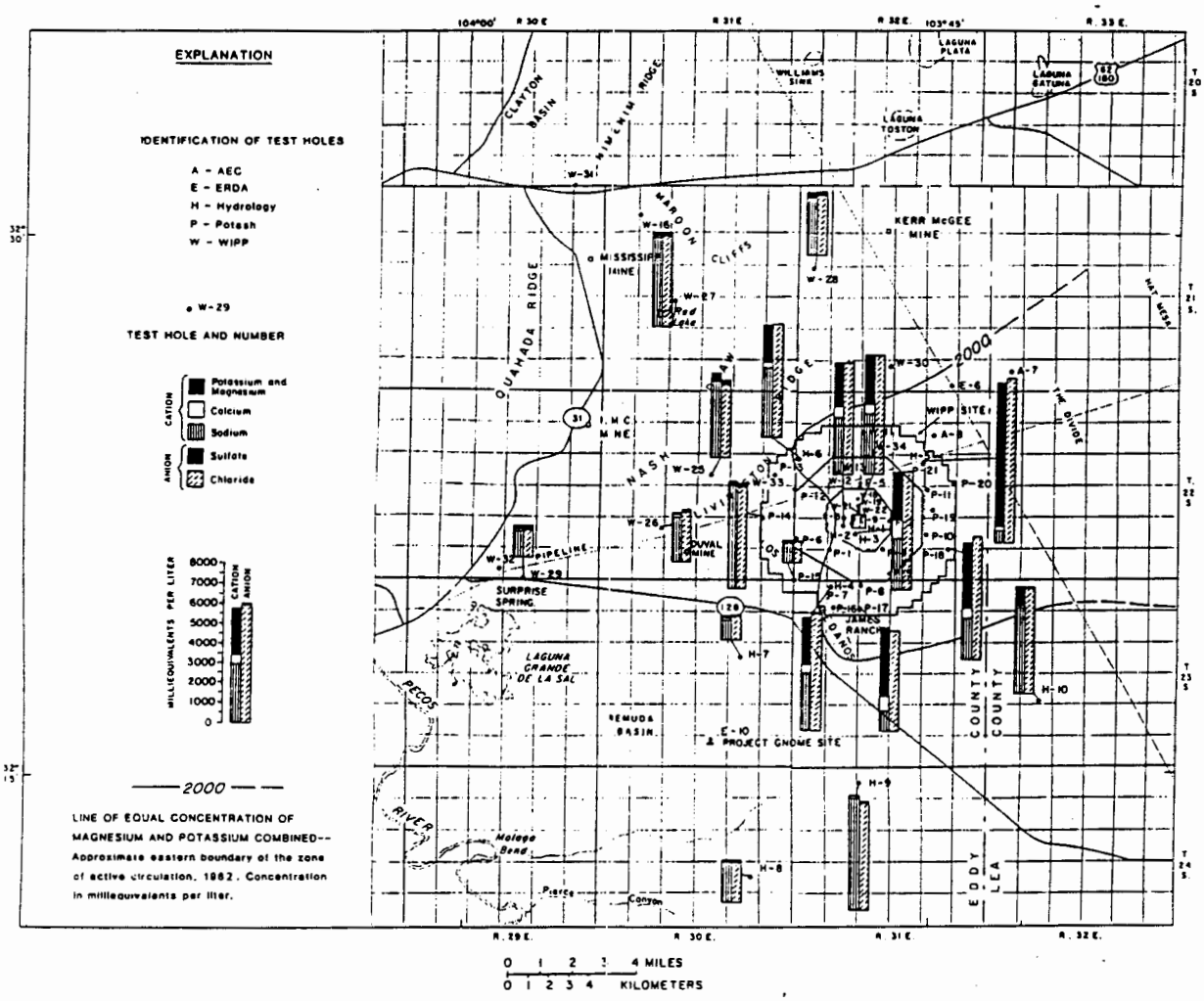

Figure 4-3. Concentrations (meq/L) of major chemical constituents in the unnamed lower member and/or upper Salado (from Mercer, 1983).

Table 4-4. Summary of Transmissivity Data for the Culebra Dolomite Member of the Rustler Formation

Well	Culebra Depth Interval (ft)	Transmissivity (ft^2/day)	Reference
AEC-7	870-896	1.8×10^{-1}	Beauheim et al. (1991)
Cabin Baby-1	503-529	2.8×10^{-1}	Beauheim (1987a)
D-268	370-392	2.2×10^{0}	Beauheim et al. (1991)
DOE-1	821-843	1.1×10^{1}	Beauheim (1987a)
DOE-2	824-846	8.9×10^{1}	Beauheim (1986)
Engle	659-681	4.3×10^{1}	Beauheim (1987a)
ERDA-9	704-727	4.6×10^{-1}	Beauheim (1987a)
H-1	676-699	8.7×10^{-1}	Beauheim (1987a)
H-2	623-645	7×10^{-1}	Beauheim and Upton (in preparation)
H-3	672-694	2.3×10^{0}	Beauheim (1987b)
H-4c	490-516	6.5×10^{-1}	Beauheim (1987a)
H-5	897-920	2×10^{-1}	Mercer (1983)
H-6	492-511	3.3×10^{1}	Beauheim and Upton (in preparation)
H-7	237-283	$>1 \times 10^{3}$	Mercer (1983)
H-8b	588-614	8.2×10^{0}	Beauheim (1987a)
H-9	647-677	1.15×10^{2}	Beauheim and Upton (in preparation)
H-10b	1360-1391	7×10^{-2}	Mercer (1983)
H-11	730-756	2.7×10^{1}	Saulnier (1987)
H-12	823-850	1.8×10^{-1}	Beauheim (1987a)
H-14	545-571	3.0×10^{-1}	Beauheim (1987a)
H-15	861-883	1.3×10^{-1}	Beauheim (1987a)
H-16	702-724	8.0×10^{-1}	Beauheim (1987a)
H-17	706-731	2.2×10^{-1}	Beauheim (1987a)
H-18	689-713	2.0×10^{0}	Beauheim (1987a)
P-14	573-595	1.4×10^{2}	Mercer (1983)
P-15	413-435	9.1×10^{-2}	Beauheim (1987a)
P-17	558-583	1.0×10^{0}	Beauheim (1987a)
P-18	909-938	$<4 \times 10^{-3}$	Beauheim (1987a)
USGS-1	517-549	4.7×10^{2}	Cooper and Glanzman (1971)
WIPP-12	810-835	1×10^{-1}	Beauheim (1987a)
WIPP-13	703-726	6.9×10^{1}	Beauheim (1987c)
WIPP-18	787-808	3.0×10^{-1}	Beauheim (1987a)
WIPP-19	756-779	6.0×10^{-1}	Beauheim (1987a)
WIPP-21	729-753	2.5×10^{-1}	Beauheim (1987a)
WIPP-22	742-764	3.7×10^{-1}	Beauheim (1987a)
WIPP-25	447-472	2.7×10^{2}	Mercer (1983)
WIPP-26	186-209	1.25×10^{3}	Mercer (1983)
WIPP-27	292-318	6.5×10^{2}	Mercer (1983)
WIPP-28	420-446	1.8×10^{1}	Mercer (1983)
WIPP-29	12-42	1×10^{3}	Mercer (1983)
WIPP-30	631-653	1.8×10^{-1}	Beauheim (1987a)

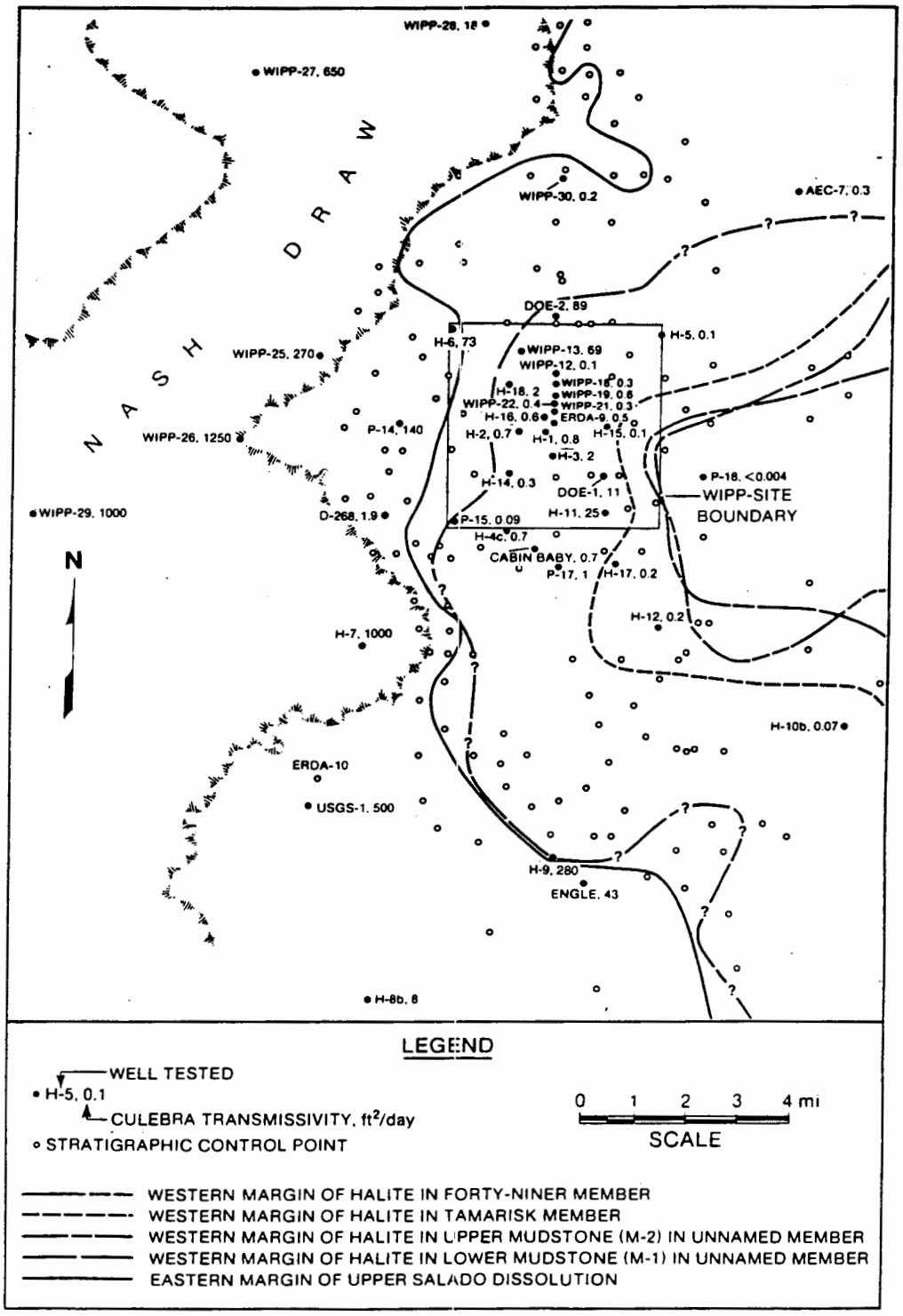

Figure 4-4. Distribution of Rustler halite and Culebra transmissivity around the WIPP site.

pumping or slug tests is that of a single-porosity medium. Where transmissivities are between 1 and at least 100 ft^2/day (10^{-6} and 10^{-4} m^2/s), numerous open fractures are observed in core and the hydraulic behavior of the Culebra during pumping tests is that of a double-porosity medium. Where the transmissivity of the Culebra is greater than approximately 100 ft^2/day (10^{-4} m^2/s), Culebra core is heavily fractured to the point of brecciation. Double-porosity hydraulic behavior is less apparent in these highly transmissive areas, perhaps because matrix-block size decreases as fracture frequency increases, decreasing the time lag observed between the hydraulic response of the fractures and that of the matrix.

In most of the wells completed to the Culebra, water levels have been measured on a regular basis since the wells were constructed. Thus, with about 60 wells at 41 drilling-pad locations currently or once completed to the Culebra, abundant water-level data are available. Culebra water levels at and around the WIPP site have been affected, however, by continuous drainage into one or more WIPP shafts since the construction of the Exploratory Shaft (now the Salt Handling Shaft) in late 1981, as well as by numerous pumping tests and water-quality sampling exercises conducted since 1980. Thus, definition of the potentiometric surface of the Culebra undisturbed by WIPP activities is non-trivial.

Cauffman et al. (1990) performed a thorough review of Culebra water-level data, borehole- and formation-fluid-density data, and WIPP-related hydraulic stresses, and derived estimates of the undisturbed freshwater heads at 35 wells. These estimates are presented in Table 4-5, and are shown contoured (freehand) on Figure 4-5. The freshwater-head contours indicate a southwesterly flow direction down Nash Draw, a southerly flow direction across the WIPP site, and an area of low gradients with apparent westerly flow south of the WIPP site. Davies (1989) reports that flow directions in this southern area of low hydraulic gradients are difficult to define reliably because density-related flow-driving forces may be larger than pressure-related flow-driving forces within this part of the Culebra, suggesting that flow in this area may have a larger easterly, down-dip component than is predicted considering only equivalent freshwater heads.

4.2.3 Tamarisk Member

Less is known about the hydraulic properties of the Tamarisk than about those of the other Rustler members. No hydraulic tests of the Tamarisk anhydrites (A-2 and A-3) have ever been performed because of apparent low transmissivity. Hydraulic tests of the Tamarisk claystone have been attempted at only four locations: H-3b3 (1984 unpublished field notes), DOE-2 (Beauheim, 1986), H-14 (Beauheim, 1987a), and H-16 (Beauheim, 1987a). Drillstem

Table 4-5. Hydraulic-Head Information for the Culebra Dolomite Member of the Rustler Formation

Well	Ground-Surface Elevation (ft amsl)[a]	Freshwater-Head Elevation (ft amsl)[b]	Depth to Middle of Culebra (ft)[c]	Middle of Culebra Pressure (psi)	Culebra Fluid Density (g/cm^3)[b]
AEC-7	3657	3058±3	883	123.1±1.3	?
Cabin Baby-1	3327	2989±2	516	77.1±0.9	?
D-268	3279	3002±1	381[d]	45.1±0.4	?
DOE-1	3465	2998+9,-7	832[e]	158.2+3.9,-3.0	1.088
DOE-2	3418	3069±5	835[f]	210.6±2.2	1.041
H-1	3398	3029±7	688	138.2±3.0	1.022
H-2c	3378	3029+6	634	123.5+2.6	1.006
H-3b1	3389	3009+6	683	131.3+2.6	1.035
H-4b	3333	2995±4	510	74.5±1.7	1.014
H-5b	3505	3064±5	909	202.8±2.2	1.102
H-6b	3348	3060±3	616	142.1±1.3	1.038
H-7b	3164	2994±2	260	39.0±0.9	0.999
H-8b	3434	2992+2	601	68.9+0.9	1.000
H-9b	3406	2978+4	662	101.4+1.7	1.000
H-10b	3687	3023±7	1376	308.5±3.0	1.047
H-11b2	3412	2994+5,-3	743[g]	140.8+2.2,-1.3	1.078
H-12	3426	2998±4	837[h]	177.2±1.7	1.095
H-14	3345	3003+2	558[h]	93.6+0.9	1.010
H-15	3480	2999+9	872[h]	169.4+3.9	1.154
H-16	3410	>3006±1[i]	713[h]	>134.0±0.6	1.037[j]
H-17	3384	2989±3	719[h]	140.4±1.3	1.100
H-18	3413	3057+5,-4	701[h]	149.5+2.2,-1.7	1.017
P-14	3360	3041±3	584	114.8±1.3	1.018
P-15	3310	3008±3	424	52.9±1.3	1.015
P-17	3336	2991±2	571	97.9±0.9	1.061
USGS-1	3426	2985+1	533[k]	39.9+0.4	1.000
USGS-4	3413	2985	489[k]	26.4	1.000
USGS-8	3410	2989	477[k]	24.3	1.000

Table 4-5. Hydraulic-Head Information for the Culebra Dolomite Member of the Rustler Formation (Continued)

Well	Ground-Surface Elevation (ft amsl)[a]	Freshwater-Head Elevation (ft amsl)[b]	Depth to Middle of Culebra (ft)[c]	Middle of Culebra Pressure (psi)	Culebra Fluid Density (g/cm^3)[b]
WIPP-12	3471	3059±4	823	178.1±1.7	?
WIPP-13	3405	3064±4	713	161.2±1.7	1.046
WIPP-18	3456	3051±4	798	170.3±1.7	?
WIPP-25	3212	3047±3	460	127.8±1.3	1.009
WIPP-26	3152	3016±1	198	26.9±0.4	1.009
WIPP-27	3177	3078±2	305	89.3±0.9	1.093
WIPP-28	3347	3075+3,-4	433	69.8+1.3,-1.7	1.032
WIPP-29	2977	2970±1	27	8.7±0.4	?
WIPP-30	3427	3069+6,-7	642	123.1+2.6,-3.0	1.018

[a] Data from Gonzales (1989)
[b] Data from Cauffman et al. (1990) except as noted
[c] Data from Mercer (1983) except as noted
[d] Data from Beauheim et al. (1991)
[e] Data from Freeland (1982)
[f] Data from Mercer et al. (1987)
[g] Data from Mercer (1990)
[h] Data from Beauheim (1987a)
[i] Lowered by drainage into WIPP shafts; converted from pressure data presented in Stensrud et al. (1988a)
[j] Specific-gravity value from Culebra in Air-Intake Shaft (Lyon, 1989)
[k] Data from Cooper and Glanzman (1971)

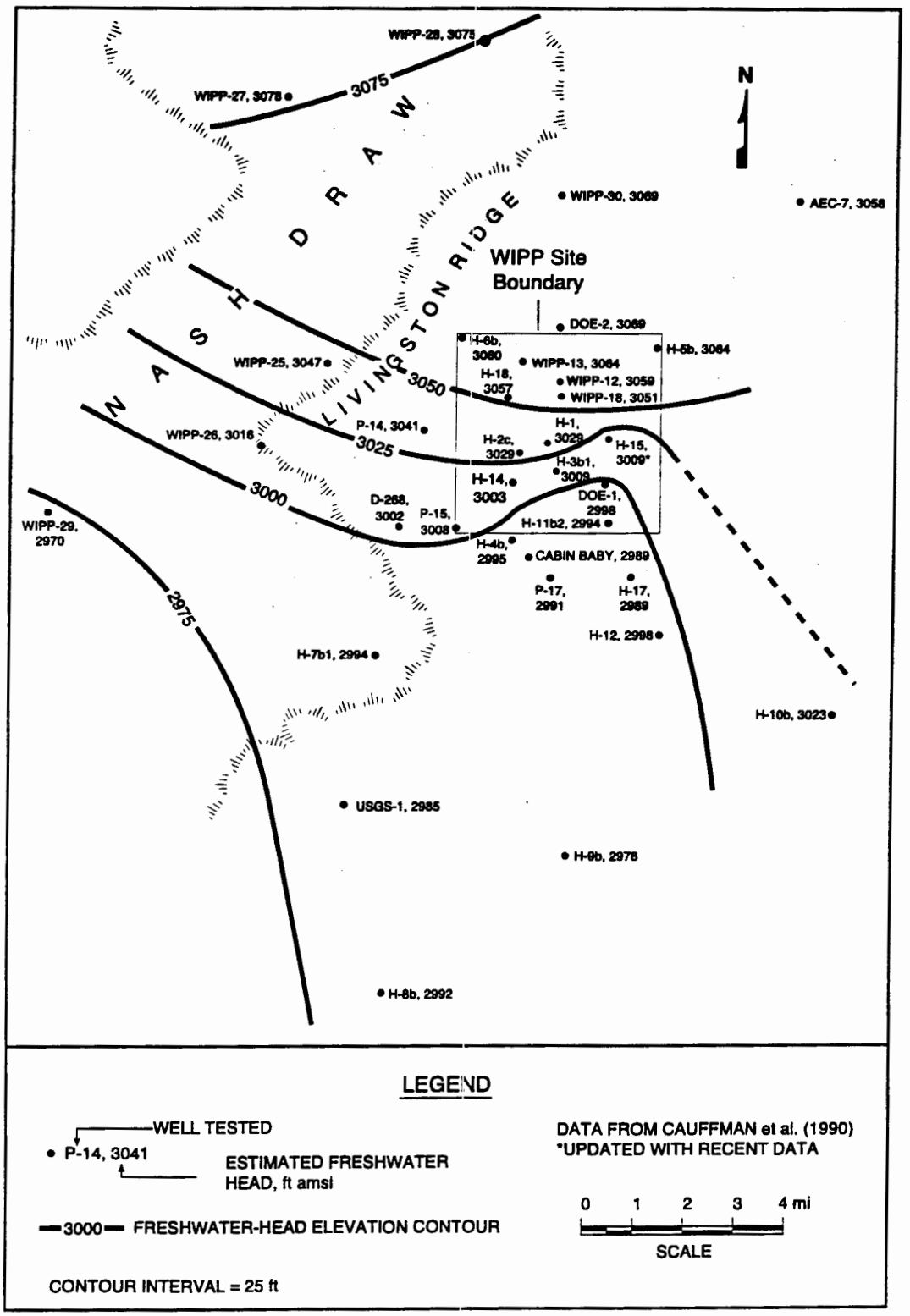

Figure 4-5. Estimated freshwater heads of the Culebra.

measure over a period of several days. Based on the interpretation of similar tests performed and/or pulse tests failed at all four locations, as the transmissivities were apparently too low to successfully on the unnamed lower member at H-16, Beauheim (1987a) concluded that the transmissivity of the Tamarisk claystone is likely 10^{-5} ft^2/day or less. The transmissivity of the Tamarisk claystone might be expected to be greater west of the WIPP site in Nash Draw where dissolution of the upper Salado and Rustler has occurred, but no direct measurements have been made in this area. The transmissivities of the Tamarisk anhydrites in Nash Draw may also have been increased by dissolution and subsidence-induced fracturing.

No measurements of the undisturbed hydraulic head within the Tamarisk claystone have ever been made. The same low transmissivity that prevented successful hydraulic testing of the Tamarisk at H-3b3, DOE-2, H-14, and H-16 also prevented measurements of hydraulic heads at those locations.

4.2.4 Magenta Dolomite Member

Hydraulic tests have been performed on the Magenta dolomite at 16 locations (Mercer, 1983; Beauheim, 1986, 1987a; Beauheim et al., 1991). The transmissivity values obtained from these tests are shown on Figure 4-6 and in Table 4-6. Most of the transmissivity values are less than or equal to 0.1 ft^2/day (10^{-7} m^2/s). Higher values of transmissivity, 0.3 and 1.0 ft^2/day (3×10^{-7} and 10^{-6} m^2/s), are found at H-6a and H-9a, respectively. No halite is present in the Rustler at either of these two locations. The two highest values of Magenta transmissivity, 375 and 53 ft^2/day (4×10^{-4} and 5×10^{-5} m^2/s), are found in Nash Draw at WIPP-25 and WIPP-27, respectively, where dissolution of the upper Salado has caused collapse and fracturing of the overlying Rustler. Mercer (1983) noted that the transmissivity of the Magenta at WIPP-25 may have been overestimated because of possible leakage from the Culebra along fractures during hydraulic testing. Dissolution of the upper Salado has apparently not affected the Magenta at all locations where it has occurred, however, as the transmissivity of the Magenta is very low at H-8, and could not be measured at WIPP-28.

Between 1979 and 1981, stabilized water levels were measured in 13 wells completed to the Magenta (Richey, 1987b). Figure 4-7 shows the elevations of these stabilized water levels, along with estimated freshwater-head elevations calculated using borehole-fluid-density (or specific-gravity) data presented in Mercer et al. (1981), Dennehy and Mercer (1982), Mercer (1983), Lambert and Robinson (1984), Richey (1986), and Richey (1987a). The contours of the freshwater heads indicate a southwesterly flow direction within the Magenta in the northern

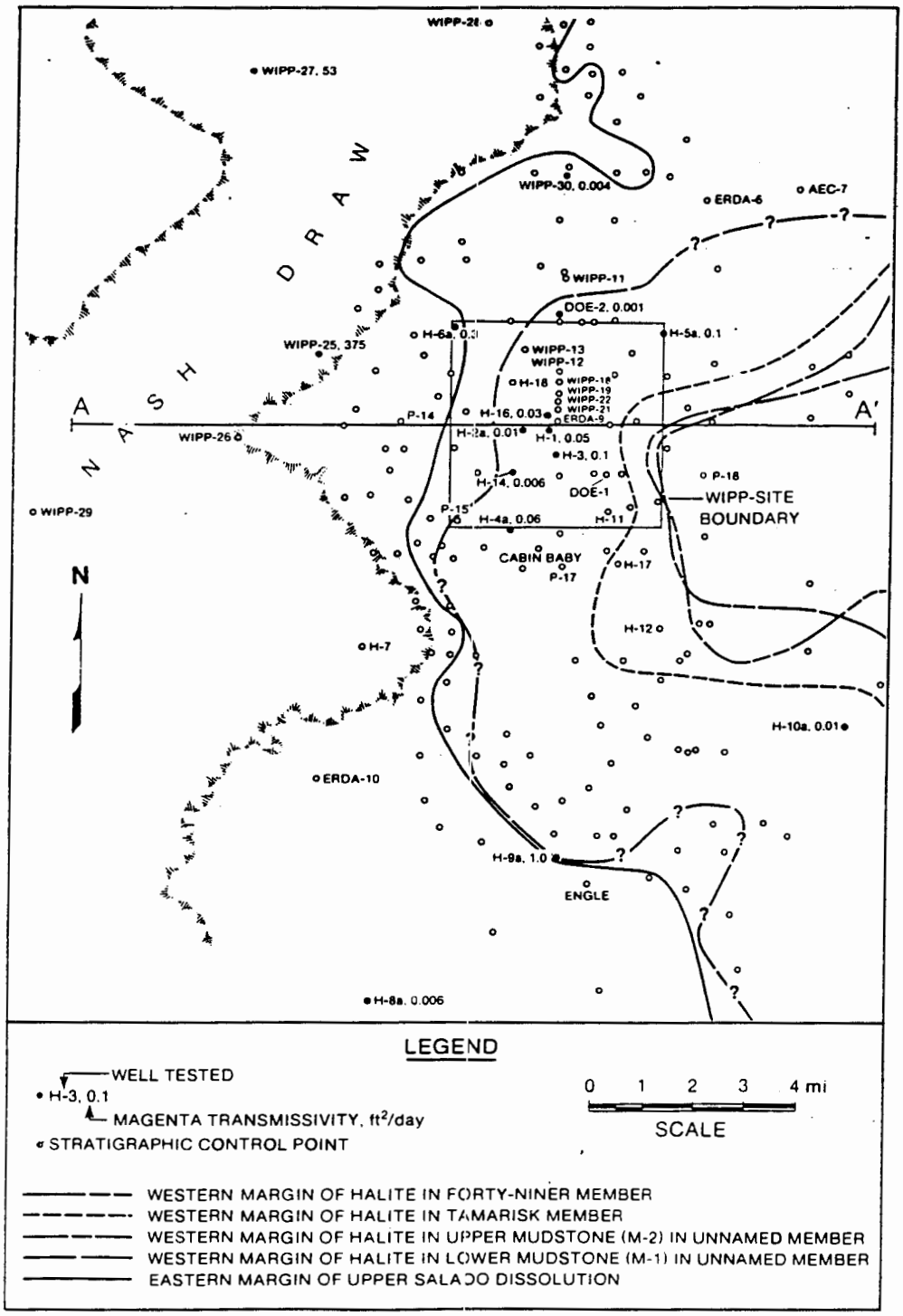

Figure 4-6. Distribution of Rustler halite and Magenta transmissivity around the WIPP site.

Table 4-6. Summary of Transmissivity Data for the Magenta Dolomite Member of the Rustler Formation

Well	Magenta Depth Interval (ft)[a]	Transmissivity (ft^2/day)[a]	Comments
DOE-2	699-722[b]	1×10^{-3} [c]	
H-1	563-589	5×10^{-2}	
H-2a	515-543	1×10^{-2}	
H-2b1	515-540[d]	2.4×10^{-3} [d]	
H-3b1	559-584	1×10^{-1}	
		1.6×10^{-1} [d]	
H-4a	375-400	6×10^{-2}	
H-5a	783-810	1×10^{-1}	
H-6a	492-511	3×10^{-1}	
H-8a	466-488	6×10^{-3}	
H-9a	523-554	1×10^{0}	
H-10a	1256-1280	1×10^{-2}	
H-14	424-448[e]	6×10^{-3} [e]	
H-16	590-616[e]	3×10^{-2} [e]	
WIPP-25	302-328	3.75×10^{2}	
WIPP-27	176-194	5.3×10^{1}	
WIPP-28	285-310	low	testing unsuccessful
WIPP-30	513-537	4×10^{-3}	

[a] Data from Mercer (1983) except as noted
[b] Data from Mercer et al. (1987)
[c] Data from Beauheim (1986)
[d] Data from Beauheim et al. (1991)
[e] Data from Beauheim (1987a)

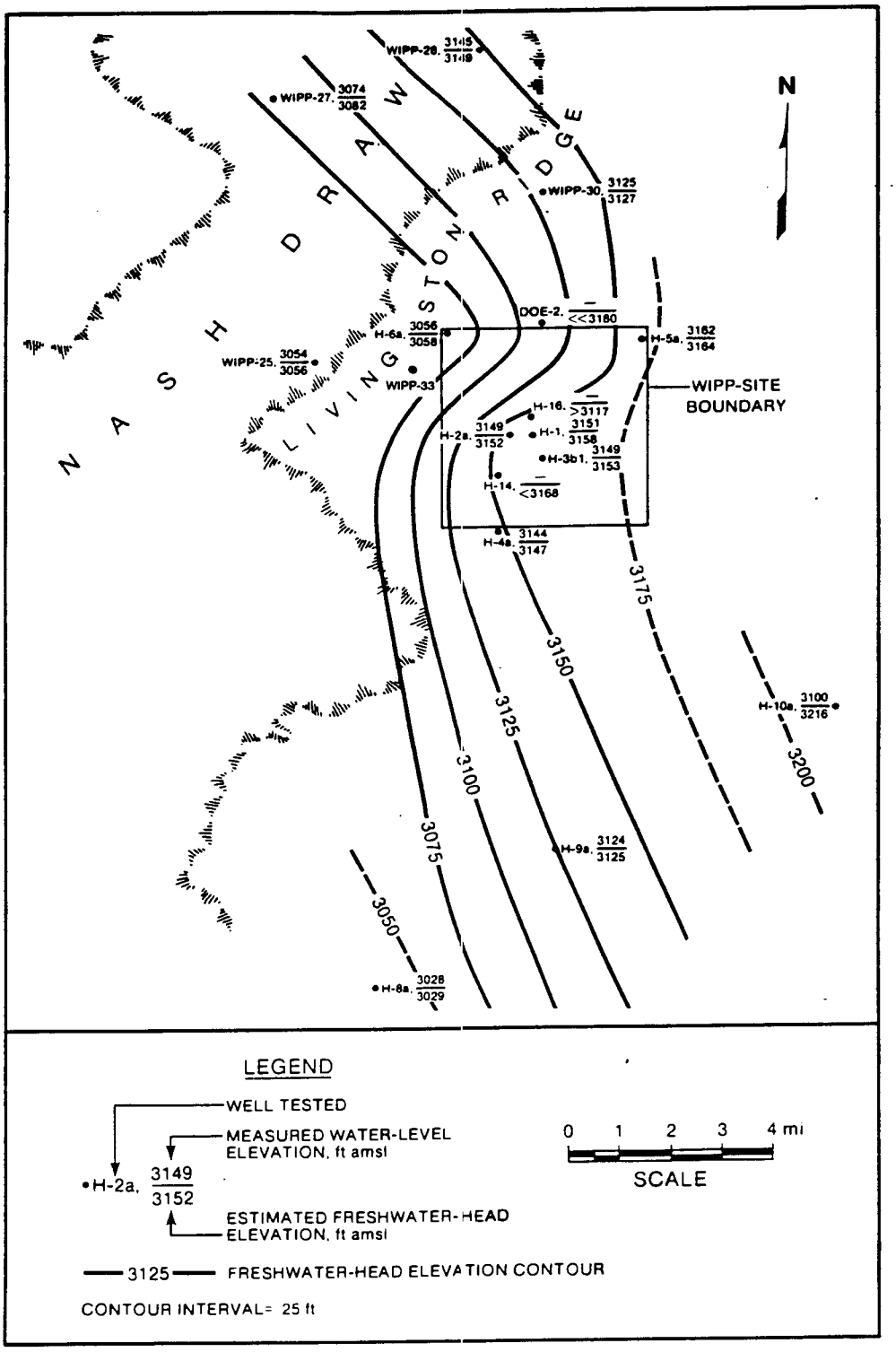

TRI-6330-97-2

Figure 4-7. Measured water levels and estimated freshwater heads of the Magenta dolomite member.

portion of Nash Draw, and a generally westward flow direction toward Nash Draw over the rest of the region.

The hydraulic head at H-6a shown on Figure 4-7 seems anomalously low compared to that at surrounding wells, and causes a flexure in the contour lines across the northern portion of the WIPP site. The low head at H-6a may be related to drainage into dissolution cavities in the upper Rustler such as those encountered at WIPP-33 (Sandia and USGS, 1981). If so, it may be a relatively localized perturbation in the Magenta potentiometric surface, and not affect heads as far to the east as is indicated on Figure 4-7.

Also shown on Figure 4-7 are freshwater heads estimated from pressure measurements made at DOE-2, H-14, and H-16. The pressure measurements at DOE-2 and H-14 were reported by Beauheim (1986 and 1987a) to represent upper bounds on the stabilized formation pressures, while the pressure measurement at H-16 reflects drainage from the Magenta into the nearby WIPP shafts since 1981 (Beauheim, 1987a). With these caveats, the estimated freshwater heads at DOE-2, H-14, and H-16 are in qualitative agreement with the pattern of freshwater heads derived from the water-level data. Table 4-7 summarizes the hydraulic-head data available for the Magenta dolomite. Geochemical analyses from testing in the Magenta are tabulated in Table 4-8. Concentrations of major chemical constituents in the Magenta are shown in Figure 4-8.

4.2.5 Forty-niner Member

The claystone water-producing unit (M-4) of the Forty-niner has been hydraulically tested at only four locations: DOE-2 (Beauheim, 1986), H-3d (Beauheim et al., 1991), H-14 (Beauheim, 1987a), and H-16 (Beauheim, 1987a). At these locations, the interbed thickness ranges from 10 to 15 ft (3 to 4.6 m). Transmissivities reported for the claystone interbed are summarized in Table 4-9. As is the case with the other Rustler members, the transmissivity of the Forty-niner claystone might be assumed to be higher west of the WIPP site in Nash Draw as a result of subsidence and fracturing, but no direct measurements have been made in that area. Where the H-4 halite unit is found with the M-4 claystone east of the WIPP site, the transmissivity of the claystone is probably less than where the halite is absent.

Testing of a Forty-niner anhydrite/gypsum alone has been attempted only in H-14 (Beauheim, 1987a). At H-14, a drillstem test was performed in the upper 25 ft of the upper Forty-niner anhydrite (A-5). This test was qualitative in nature, and showed only that the transmissivity of the anhydrite must be several orders of magnitude lower than that of the

Table 4-7. Hydraulic-Head Information for the Magenta Dolomite Member of the Rustler Formation

Well	Ground-Surface Elevation (ft amsl)[a]	Stabilized Depth to Water (ft)[b]	Date of Water-Level Measurement	Depth to Middle of Magenta (ft)[c]	Borehole-Fluid Density (g/cm^3) (± 0.01)[c]	Freshwater-Head Elevation (ft amsl)	Middle of Magenta Pressure (psi)
DOE-2	3418	>>310[d]	10/84	711[e]	1.18[e,f]	<<3180±8	<<305.0±3.5
H-1	3398	247	2-3/79	576	1.021	3158±3	145.6±1.4
H-2a	3378	229	7-9/81	529	1.012	3152±3	131.6±1.3
H-3b1	3389	240	'78-'79	572	1.010	3153±3	145.3±1.4
H-4a	3333	189	'79-'80	388	1.017	3147±2	87.7±0.9
H-5a	3506	344	'78-'80	797	1.008	3164±5	197.9±2.0
H-6a	3347	291	'78-'80	502	1.007	3058±2	92.1±0.9
H-8a	3433	405	'80-'84	477	1.008[g]	3029±1	31.4±0.3
H-9a	3406	282	'80-'83	539	1.006[g]	3125±3	112.0±1.1
H-10a	3687	587	'80-'82	1268	1.171[f,g]	3216±14	345.6±5.9
H-14	3346	>221[h]	10/86	436[i]	1.2[f,i]	<3168±4	<111.8±1.9
G-16	3410	<344[j,k]	11/87	603[i]	1.2[f,i]	>3117±1[j]	>134.5±0.6
WIPP-25	3212	158	'80-'84	315	1.010	3056±2	68.7±0.7
WIPP-27	3177	103	'81-'82	185	1.095[f]	3082±2	38.9±0.7
WIPP-28	3347	202	'81-'82	298	1.048[f]	3149±2	43.6±0.8
WIPP-30	3428	303	'82-'83	525	1.01[l]	3127±2	97.2±1.0

[a] Data from Gonzales (1989)
[b] Data from Richey (1987b; OFR 87-120) except as noted
[c] Data from Mercer (1983) except as noted
[d] Converted from pressure data presented in Beauheim (1986)
[e] Data from Beauheim (1986)
[f] Uncertainty = ± 0.02
[g] Data from Richey (1986)
[h] Converted from pressure data presented in Beauheim (1987a)
[i] Data from Beauheim (1987a)
[j] Lowered by drainage into WIPP shafts
[k] Converted from pressure data presented in Stensrud et al. (1988b)
[l] Data from Lambert and Robinson (1984)

Table 4-8. Geochemical Analyses from Testing in the Magenta

Well	Date of Sample	Geologic Unit	Density (gm/ml at 20°C)	Ph Units	Alkalinity Field (mg/L as $CaCO^3$)	Bicarbonate FET-FLD (mg/L as CO^3)	Carbonate FET-FLD (mg/L as HCO^3)	Nitrogen NO^2+NO^2 Dissolved (mg/L as N)	Sulfide Total (mg/L as S)	Hardness (mg/L as $CaCO^3$)
H-1	76-06-04	310MGNT	--	7.4	75	92	0	--	.0	3300
H-2A	77-02-22	310MGNT	--	8.6	61	74	0	.04	--	2700
H-3	77-05-10	310MGNT	--	8:0	42	51	0	.08	--	5000
H-4A	78-12-14	310MGNT	--	8.0	52	63	--	.01	--	2200
H-5A	78-12-14	310MGNT	--	7.8	41	50	--	.01	--	1300
H-6A	78-12-20	310MGNT	--	7.3	42	51	--	.03	--	2000
H-8A	80-02-12	310MGNT	1.006	9.3	26	--	--	.06	--	2200
H-9A	80-02-05	310MGNT	1.003	8.5	35	--	--	.02	--	2100
H-10A	80-03-21	310MGNT	1.175	7.1	0	--	--	.03	--	17000
WIPP-25	80-09-04	310MGNT	1.010	7.5	150	--	--	.64	1.2	3300
WIPP-27	80-07-24	310MGNT	1.080	6.8	57	--	--	.32	--	11000
	80-02-20	310MGNT	--	6.5	180	--	--	.40	1.8	17000
WIPP-30	80-09-24	310MGNT	--	8.8	62	--	--	00	.0	2400

Well	Hardness, Noncarbonate (mg/L $CaCO^3$)	Calcium Dissolved (mg/L as Ca)	Magnesium, Dissolved (mg/L as Mg)	Sodium, Dissolved (mg/L as Na)	Potassium, Dissolved (mg/L as K)	Chloride, Dissolved (mg/L as Cl)	Sulfate Dissolved (mg/L as SO^4)	Fluoride, Dissolved (mg/L as F)	Silica, Dissolved (mg/L as SiO^2)	Boron, Dissolved (μg/L as B)	Solids, Residue at 105°C (mg/L)
H-1	3300	890	270	5700	70	8000	3900	2.8	1.3	2200	18900
H-2A	2700	820	170	2700	81	4100	2400	--	6.0	220	12000
H-3	4900	1200	480	9300	250	15000	3400	1.8	6.4	13000	32000
H-4A	2100	210	410	7000	130	7500	7000	2.5	6.4	13000	22300
H-5A	1300	240	170	1500	53	880	3200	2.8	9.0	11000	--
H-6A	2000	520	160	1100	46	1200	2700	1.4	7.7	2500	--
H-8A	2200	870	17	2400	84	3500	2100	.7	.9	3100	9410
H-9A	2000	550	170	800	28	750	2700	1.8	3.3	2600	5460
H-10A	17000	2500	2600	93000	510	160000	2700	1.3	1.9	3900	270000
WIPP-25	3100	910	240	3100	.8	5600	1900	1.5	25	1900	18700
WIPP-27	11000	1100	1900	34000	1800	61000	9400	.0	1.7	26000	106000
	17000	3600	2000	43000	10000	85000	2900	.4	13	230	173000
WIPP-30	2400	690	170	5500	190	8700	3200	1.9	.7	12000	19000

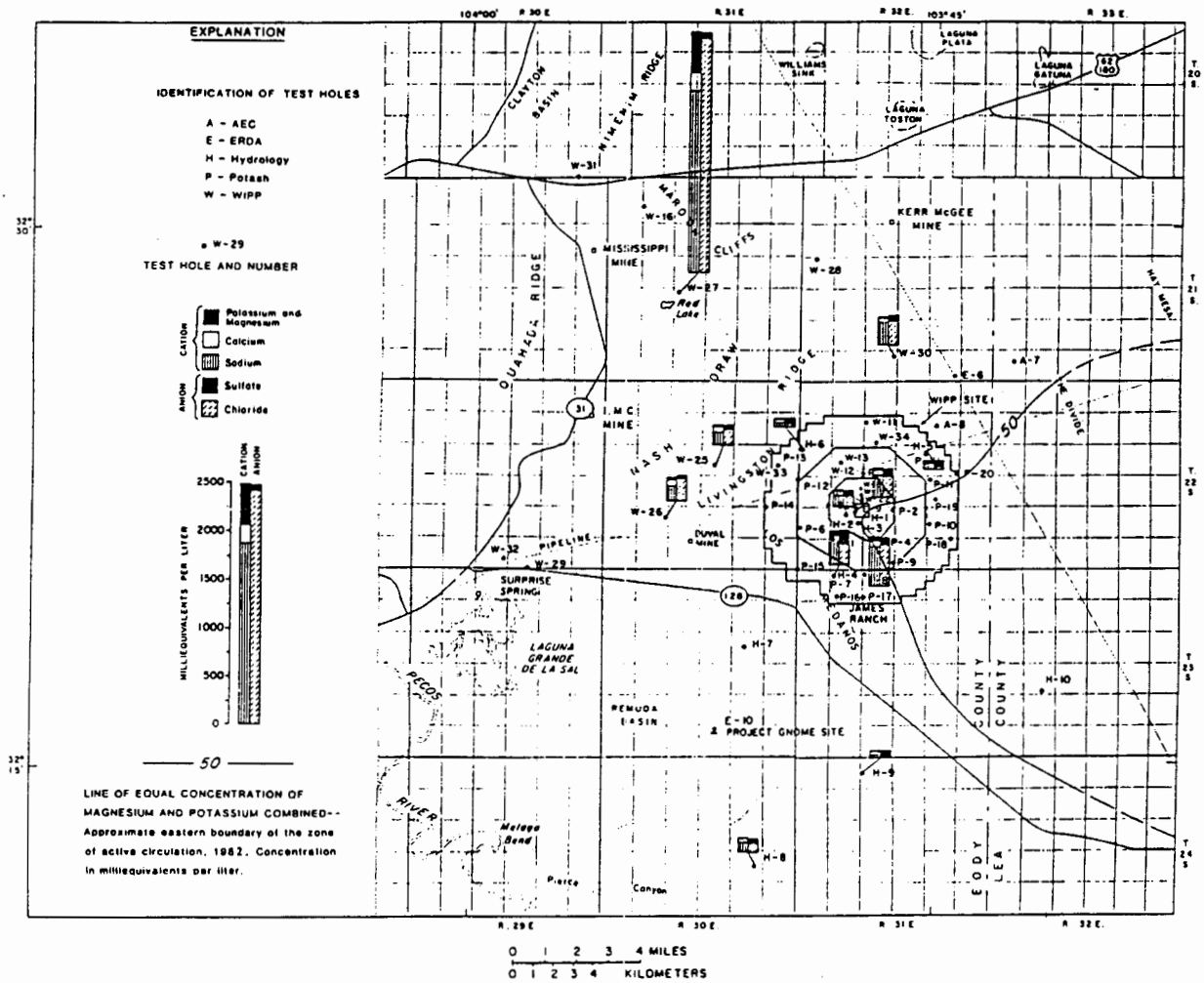

Figure 4-8. Concentrations (meq/L) of major chemical constituents in the Magenta.

Table 4-9. Summary of Transmissivity Data for the Forty-Niner Claystone

Well	Forty-niner Claystone Depth Interval (ft)	Transmissivity (ft^2/day)	Reference
DOE-2	670-681	2.5×10^{-3} to 1.1×10^{-2}	Beauheim (1986)
H-3d	536-546	3.5×10^{-3} to 4.5×10^{-3}	Beauheim et al. (1991)
H-14	390-405	3.0×10^{-2} to 7.1×10^{-2}	Beauheim (1987a)
H-16	563-574	5.0×10^{-3} to 5.6×10^{-3}	Beauheim (1987a)

Forty-niner claystone. Where still present in Nash Draw, the Forty-niner anhydrites/gypsums may have very high transmissivities as a result of dissolution and subsidence-induced fracturing.

Measurements of the hydraulic head of the Forty-niner claystone have been made at wells H-3d, H-14, H-16, and DOE-2. Beauheim (1987a) summarizes these observations, and presents estimates of static fluid pressures at the midpoint of the claystone. The greatest uncertainty in these estimates was attached to the measurement from DOE-2. Re-examination of the original data from DOE-2 (Beauheim, 1986) indicates that a "static" pressure 12 psi (.083 MPa) lower than that reported by Beauheim (1987a) probably provides a more accurate upper bound on the Forty-niner head at that location. The Forty-niner hydraulic-head data are summarized in Figure 4-9 and Table 4-10.

Figure 4-9 shows the static fluid-pressure estimates for the Forty-niner claystone at H-3d, H-14, H-16, and DOE-2 converted to freshwater heads. Firm conclusions cannot be drawn from so few data, but the data are not inconsistent with an assumption of southwesterly to westerly flow towards Nash Draw. The relatively low head at H-16 may, as suggested by Beauheim (1987a), be related more to localized drainage into the WIPP shafts than to the undisturbed regional head distribution.

4.2.6 Discussion of Rustler Hydraulic Heads

Comparisons of hydraulic heads between different water-producing units within the Rustler are useful, as they allow evaluation of the potential directions of vertical fluid flow between the water-producing units and the effectiveness of intervening confining beds, and illustrate areal variations in the hydraulic properties of the different Rustler members. A rigorous quantitative evaluation of hydraulic-head differences between units generally requires that the heads share a common elevation datum. No meaningful elevation datum can be defined, however, when the specific gravities (densities) of the fluids in the units to be compared are different.

A qualitative evaluation of the potential directions of fluid flow can be performed, however, using a procedure here described as the "equilibrium-fluid-density" approach. Static pressures at the mid-formation depth are calculated for the units of interest. By subtracting the pressure in the unit at the higher elevation from the pressure in the unit at the lower elevation, and dividing by the vertical distance separating the two units, a pressure-depth gradient can be calculated. In a system at equilibrium (i.e., no vertical hydraulic gradient), this pressure-depth gradient corresponds to the density of the fluid in the system. Thus, the calculated

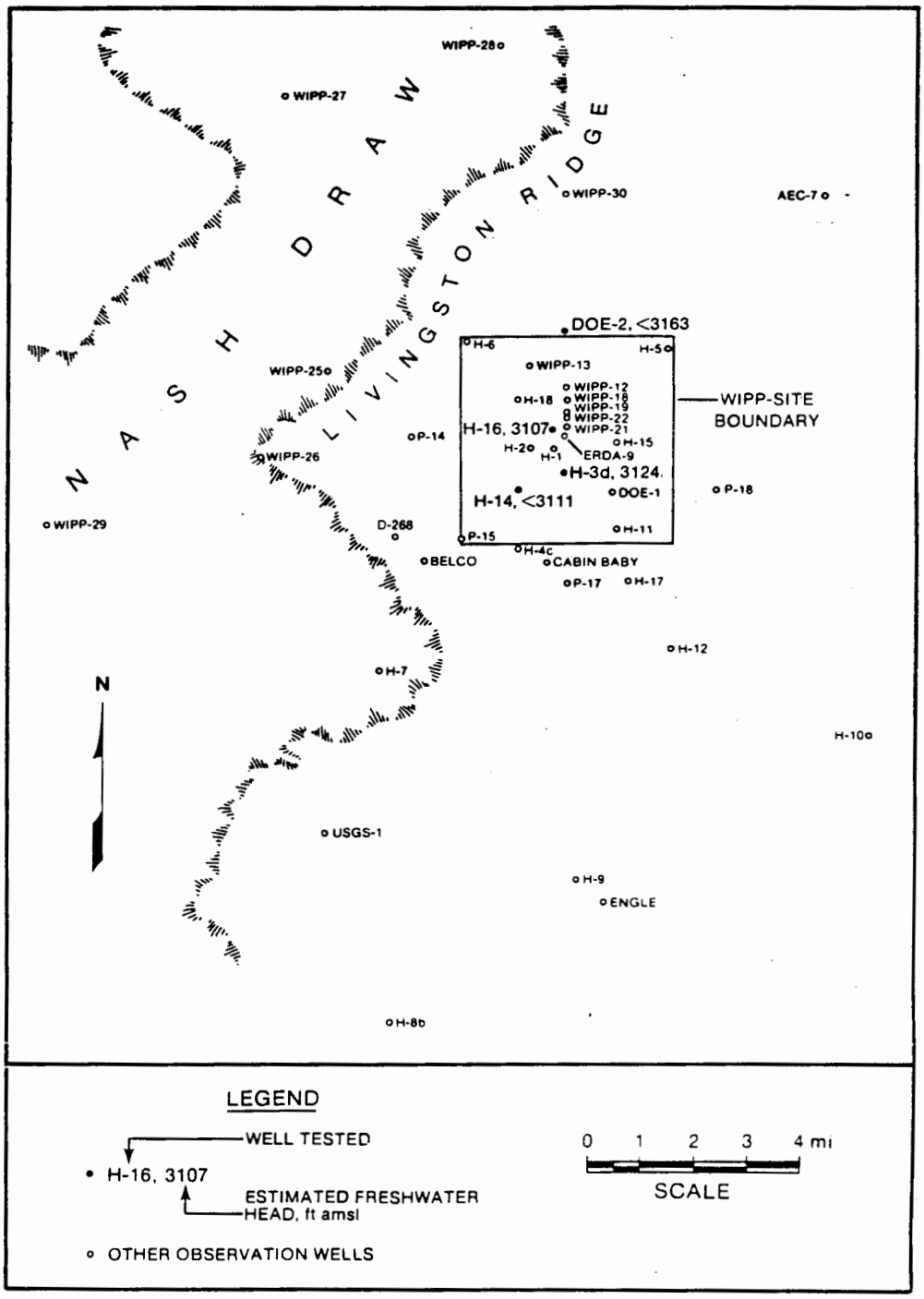

Figure 4-9. Estimated freshwater heads of the Forty-Niner claystone.

Table 4-10. Hydraulic-Head Information for the Forty-Niner Claystone

Well	Ground-Surface Elevation (ft amsl)[a]	Depth to Middle of Forty-niner Claystone (ft)[b]	Fluid Pressure at Middle of Claystone (psig)[b]	Freshwater-Head Elevation (ft amsl)
DOE-2	3418	675	<182[c]	<3163
H-3d	3389	541	120	3124
H-14	3345	398	<71	<3111
H-16	3410	568	115	3107

[a] Data from Gonzales (1989)
[b] Data from Beauheim (1987a) except as noted
[c] Data recalculated from Beauheim (1986)

pressure-depth gradient can be converted to the equivalent density of the fluid that would be required to be present for the heads in the two units to be at equilibrium. If the density of this hypothetical fluid is lower than the densities of both actual fluids, the head in the upper unit is higher than the equilibrium condition and the potential flow direction is downward. If the hypothetical density is greater than that of both actual fluids, the head in the upper unit is lower than the equilibrium condition and the potential flow direction is upward. If the hypothetical density is equal to or intermediate between the densities of the actual fluids, then the hydraulic heads in the two units are very nearly at equilibrium and no qualitative conclusions about potential flow directions can be drawn. The greater the difference between the hypothetical equilibrium fluid density and the actual fluid densities, the greater the hydraulic gradient between units.

4.2.6.1 HYDRAULIC-HEAD DIFFERENTIALS BETWEEN THE UNNAMED LOWER MEMBER/UPPER SALADO AND THE CULEBRA

Adequate data for comparisons of the hydraulic heads in the unnamed lower member and/or Rustler-Salado contact residuum water-producing unit with those in the Culebra are available for 12 well locations. Table 4-11 presents calculations of potential flow directions between the unnamed member/upper Salado and the Culebra using the method outlined above. Regions around the WIPP site having different potential flow directions are shown aerially in Figure 4-10. At wells H-2, H-16, and P-17, the hydraulic gradient between the unnamed lower member and the Culebra is upward.

At H-6, H-7, WIPP-26, and WIPP-30, the hydraulic gradient is downward from the Culebra to the unnamed member.

This pattern of vertical hydraulic gradients is generally explainable by the presence or absence of upper Salado dissolution. The three locations mentioned above where vertical gradients are upward, H-2, H-16, and P-17, are also locations where dissolution of the upper Salado has not occurred. Whereas, at the locations where gradients are downward, Salado dissolution has occurred.

Table 4-11. Potential Flow Directions between the Culebra and Unnamed Member/Upper Salado

Well	Difference in Depth (R/S-CUL) (ft)	Difference in Formation Pressure (RS-CUL) (psi)	Pressure-Depth Gradient (psi/ft)	Equilibrium Fluid Density (g/cm^3)	Rustler/ Salado Fluid Density (g/cm^3)[a]	Culebra Fluid Density (g/cm^3)[b]	Potential Flow Direction
H-2	135	>102.6+3.7 -6.3	>0.760+0.027 -0.047	>1.754+0.063 -0.108	1.225	1.006	upward
H-6	104	19.9±4.0	0.191±0.038	0.442±0.089	1.21	1.038	downward
H-7	128	46.8±2.5	0.366±0.020	0.844±0.045	1.048	0.999	downward
H-8	170	83.4+2.7 -3.6	0.491+0.016 -0.021	1.132+0.037 -0.047	1.13[c]	1.000	indeterminate
H-16	82	89.3±1.6	1.089±0.020	2.513±0.045	?	1.037[d]	upward
P-14	104	43.5±3.9	0.418±0.038	0.965±0.087	1.21[e]	1.018	indeterminate
P-17	143	>74.6[f]+? -0.9	>0.522[f]+? -0.006	>1.204[f]+? -0.015	?	1.061	upward
WIPP-25	133	>52.6±4.4	>0.395±0.033	>0.913±0.076	1.173	1.009	downward?
WIPP-26	80	>10.8+2.3 -0.4	>0.135+0.029 -0.005	>0.312+0.066 -0.012	1.04[g]	1.009	downward
WIPP-28	136	>61.6+4.0 -3.6	>0.453+0.029 -0.026	>1.045+0.068 -0.061	1.140	1.032	indeterminate
WIPP-29	206	91.2±2.3	0.443±0.011	1.022±0.026	1.072[g]	1.187[h]	indeterminate
WIPP-30	100	17.0+5.3 -4.9	0.170+0.053 -0.049	0.392+0.122 -0.113	1.202[g]	1.018	downward

[a] Data from Mercer (1983) except as noted
[b] Data from Cauffman et al. (1990) except as noted
[c] Data from Richey (1986)
[d] Specific-gravity value from Culebra in Air-Intake Shaft (Lyon, 1989)
[e] Calculated from water analysis presented in Mercer (1983) and Figure E.1 of Haug et al. (1987)
[f] Based on assumed R/S fluid density of 1.000 g/cm^3; values would increase if density were higher
[g] Data from Richey (1987a)
[h] Specific-gravity value from Randall et al. (1988)

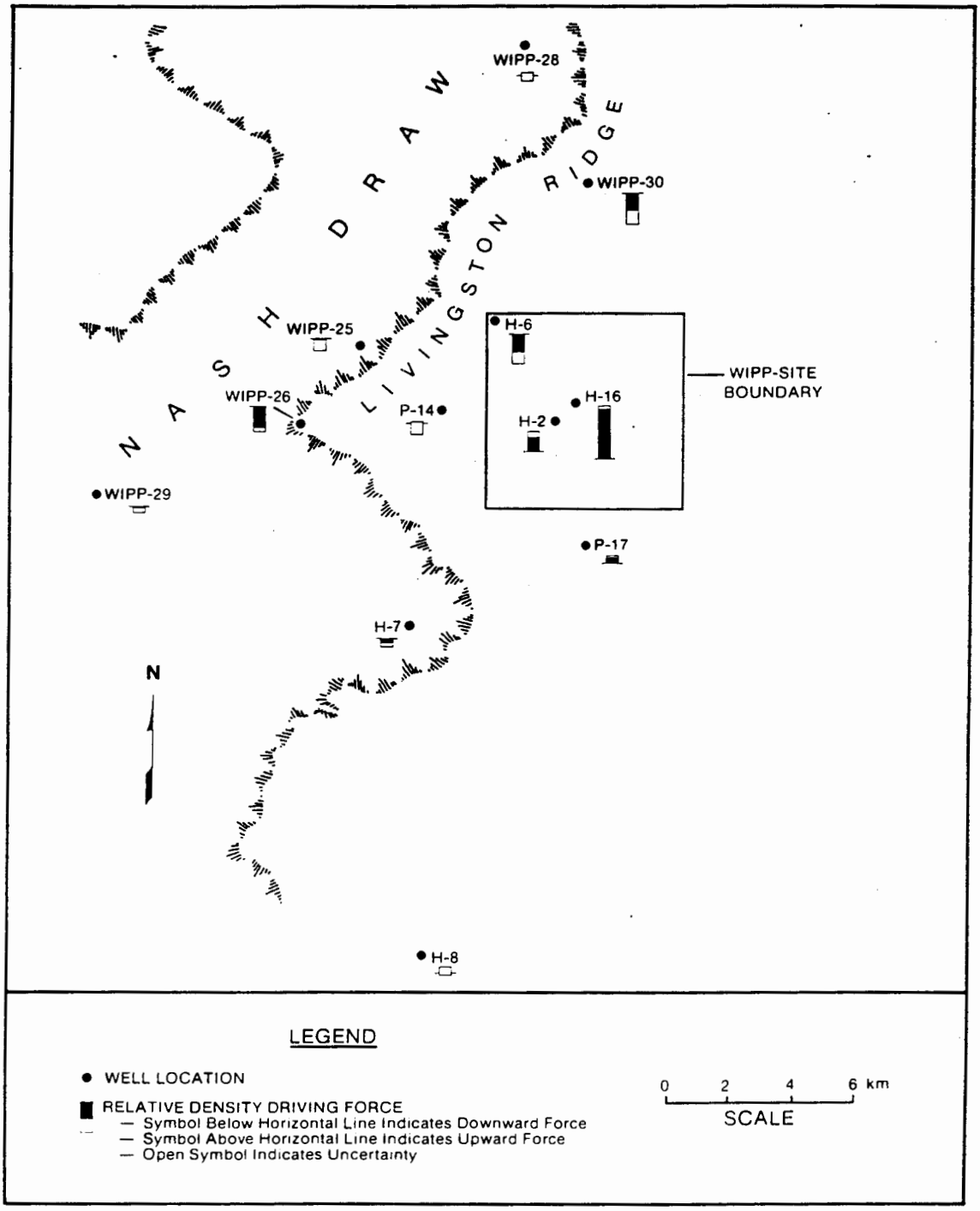

TRI-6344-55-0

Figure 4-10. Flow potentials between the Culebra dolomite and the unnamed member/upper Salado.

4.2.6.2 HYDRAULIC-HEAD DIFFERENTIALS BETWEEN THE CULEBRA AND THE MAGENTA

Because no hydraulic-head data are available for the Tamarisk, potential directions of vertical fluid flow through the central members of the Rustler can only be inferred by comparing hydraulic heads in the Culebra and Magenta. Table 4-12 shows the results of calculations of potential flow directions between the Culebra and the Magenta using the equilibrium-fluid-density approach outlined in Section 4.2.6. The areal distribution of vertical flow potentials is shown in Figure 4-11. The potential direction of fluid flow between the Magenta and Culebra appears to be downward at all 16 well locations for which hydraulic-head comparisons are possible except at H-6. At H-1, H-2, H-3, H-4, H-9, H-10, H-14, and H-16, the pressure/depth gradients between the Culebra and Magenta are negative, reflecting the fact that higher pressures are observed at the middle of the Magenta than are observed at the middle of the Culebra even though the Magenta overlies the Culebra. Strong potentials for downward flow also exist at DOE-2 and H-5, and lesser downward potentials exist at H-8, WIPP-28, and WIPP-30. Slight potentials for downward flow from the Magenta to the Culebra also appear to exist at WIPP-25 and WIPP-27, although differences between Magenta and Culebra fluid densities and the hypothetical equilibrium fluid density are small. Within the resolution of the calculations, Magenta and Culebra heads at H-6 appear to be in equilibrium. Where the Magenta is unsaturated at H-7 and WIPP-26, the Culebra head is below the base of the Magenta.

4.2.6.3 HYDRAULIC-HEAD DIFFERENTIALS BETWEEN THE MAGENTA AND THE FORTY-NINER

Magenta and Forty-niner claystone hydraulic heads can be compared at only four locations: DOE-2, H-3, H-14, and H-16. Table 4-13 shows calculations of potential flow directions performed using the equilibrium-fluid-density approach presented in Section 4.2.6. Despite uncertainties in actual fluid densities, the potential flow direction can be concluded to be upward from the Magenta to the Forty-niner claystone at all four locations considered. Hypothetical equilibrium fluid densities are 1.25 g/cm^3 or greater at all four wells.

4.3 Castile Formation

Pressurized brine reservoirs have been encountered in the Castile Formation. For the purposes of non-Salado flow and transport, parameterization of a representative Castile brine reservoir is necessary. Data for these Castile parameters are discussed in detail in Reeves et al. (1991, p. 2-1 to 2-16), Popielak et al. (1983), and Mercer (1987). A summary of parameters

Table 4-12. Potential Flow Directions Between the Magenta and Culebra

Well	Difference in Depth (CUL-MAG) (ft)	Difference in Formation Pressure (CUL-MAG) (psi)	Pressure-Depth Gradient (psi/ft)	Equilibrium Fluid Density (g/cm^3)	Culebra Fluid Density (g/cm^3)[a]	Magenta Fluid Density (g/cm^3)[b]	Potential Flow Direction
DOE-2	124	>5.6±5.7	>0.045±0.046	>0.104±0.113	1.041	1.005[c]	downward
H-1	112	-7.4±4.4	-0.066±0.039	--[d]	1.022	1.021	downward
H-2	105	-8.1+3.9 -1.3	-0.077+0.037 -0.012	--[d]	1.006	1.012	downward
H-3	111	-14.0+4.0 -1.4	-0.126+0.036 -0.013	--[d]	1.035	1.006[e]	downward
H-4	122	-13.2±2.6	-0.108±0.021	--[d]	1.014	1.020[f]	downward
H-5	112	4.9±4.2	0.044±0.038	0.101±0.087	1.102	1.008[f]	downward
H-6	114	50.0±2.2	0.439±0.019	1.012±0.045	1.038	1.003[f]	indeterminate
H-8	124	37.5+1.2 -0.3	0.302+0.010 0.002	0.698+0.022 -0.006	1.000	1.008[g]	downward
H-9	123	-10.6+2.8 -1.1	-0.086+0.023 -0.009	--[d]	1.000	1.006[g]	downward
H-10	108	-37.1±8.9	-0.344±0.082	--[d]	1.047	1.171[g]	downward
H-14	122	-18.2+2.8 -1.9	-0.149+0.023 -0.016	--[d]	1.010	?	downward
H-16	110	-0.5±1.2	-0.005±0.011	--[d]	1.037[h]	?	downward
WIPP-25	145	59.1±2.0	0.408±0.014	0.941±0.032	1.009	1.004[i]	downward?
WIPP-27	120	50.4±1.6	0.420±0.013	0.969±0.031	1.093	1.09[i]	downward?
WIPP-28	135	26.2+2.1 -2.5	0.194+0.016 -0.019	0.448+0.036 -0.043	1.032	1.048	downward
WIPP-30	117	25.9+3.6 -4.0	0.221+0.031 -0.034	0.511+0.071 -0.079	1.018	1.01[i]	downward

[a] Data from Cauffman et al. (1990) except as noted
[b] Data from Mercer (1983) except as noted
[c] Average of Magenta fluid specific gravities at H-5c and H-6c (Lyon, 1989)
[d] Negative densities not possible; flow potential is clearly downward
[e] Specific-gravity data from Randall et al. (1988)
[f] Specific-gravity data from Lyon (1989)
[g] Data from Richey (1986)
[h] Specific-gravity value from Culebra in Air-Intake Shaft (Lyon, 1989)
[i] Data from Lambert and Robinson (1984)

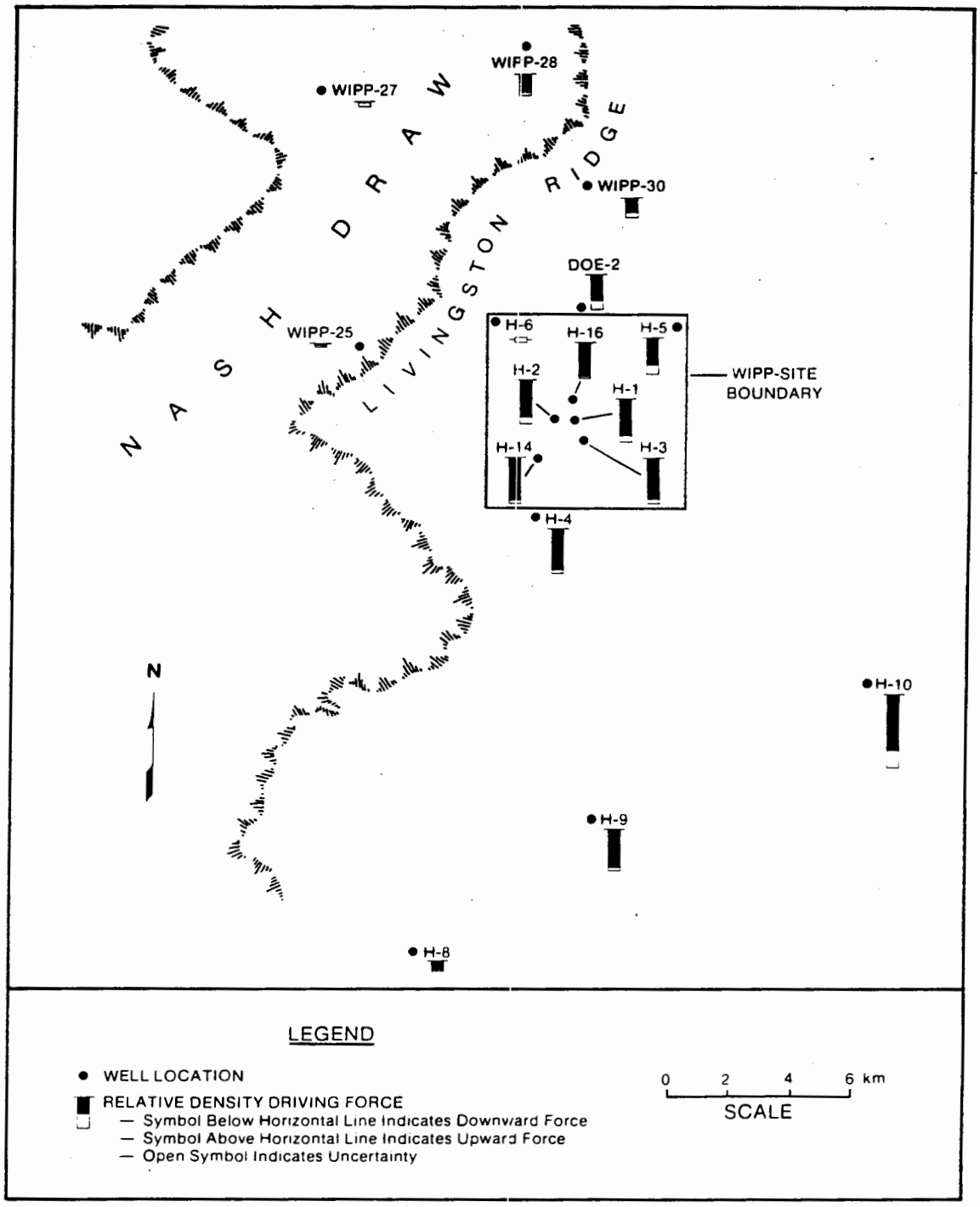

TRI-6344-56-0

Figure 4-11. Flow potentials between the Magenta dolomite and the Culebra dolomite.

Table 4-13. Potential Flow Directions between the Forty-Niner Claystone and Magenta

Well	Difference in Depth (MAG-49) (ft)	Difference in Formation Pressure (MAG-49) (psi)	Pressure-Depth Gradient (psi/ft)	Equilibrium Fluid Density (g/cm^3)	Magenta Fluid Density (g/cm^3)[a]	Forty-niner Fluid Density (g/cm^3)	Potential Flow Direction
DOE-2	36	23	0.64	1.47	?	?	upward
H-3	31	25	0.81	1.86	1.006[b]	?	upward
H-14	38	41	1.08	2.49	?	?	upward
H-16	35	19	0.54	1.25	?	?	upward

[a] Specific gravities of Magenta fluids from H-3, H-4, H-5, and H-6 range from only 1.003 to 1.018 (Randall et al., 1988)

[b] Specific-gravity value from Randall et al. (1988)

determined to be representative by Reeves et al., 1991 has been used in the specification of the Non-Salado baseline model for SPM-2 and is presented in Section 5 (Table 5-1).

4.4 Bell Canyon Formation

Data on the Bell Canyon Formation are available from five WIPP test holes as well as from studies reported in the petroleum literature. Drillstem tests (DSTs) of the Bell Canyon were performed in boreholes AEC-7 (Mercer, 1983), AEC-8 (SNL and D'Appolonia, 1983), ERDA-10 (SNL and D'Appolonia, 1983b), DOE-2 (Mercer et al., 1987), and Cabin Baby-1 (Beauheim et al., 1983). The interpreted results of the DSTs are summarized in Table 4-14. Hiss (1976) and McNeal (1965) constructed potentiometric surface maps for the upper Bell Canyon, and their data were combined with the WIPP data by Mercer (1983) to produce the potentiometric surface map shown in Figure 4-12. Mercer (1983, p. 29) reports that the Bell Canyon channel sandstones typically have porosities ranging from 20 to 28 percent and permeabilities (citing Berg, 1979) ranging from 14 to 90 mD ($\sim 1 \times 10^{-7}$ to $\sim 9 \times 10^{-7}$ m/s). The siltstones separating the sandstone channels have porosities ranging from 10 to 20 percent and permeabilities less than 0.1 mD ($\sim 1 \times 10^{-9}$ m/s).

4.5 Formations Below the Bell Canyon Formation

Data on units below the Bell Canyon Formation in the vicinity of the WIPP site are sparse. The data available come from drilling and DST records compiled in the late 1970s and early 1980s. Figure 4-13 shows a stratigraphic column for the WIPP site starting at the Precambrian basement and extending to the Castile. A number of the formations shown are targets for petroleum exploration, including the Ellenburger, Silurian, Morrow, Atoka, Strawn, Bone Spring, Brushy Canyon, and Bell Canyon. According to Lambert (in Lambert and Mercer, 1978, p. III-2), these zones, with the possible exception of the Bone Spring, "have sufficient pressure to stand fluid above the storage horizon plus porosity and permeability sufficiently large enough to allow flow rates of several hundred barrels per day." The Atoka and Strawn Formations appear to have the highest hydraulic heads and water productions of these units. Heads in the Atoka are reported between 3375 and 6552 ft (1029 and 1891 m) above sea level (for a fluid density of 1.08 g/cm^3), and water production rates of 0.6 to 6 gpm (0.13 and 13 m^3/h) at ground surface have been sustained for several years. Heads in the Strawn are reported between 3350 and 6203 ft above sea level, with sustained productions of 3 to 8 gpm

Table 4-14. Summary of Bell Canyon DST Results

Hole	Tested Interval (ft below ground surface)	Unit Name	Hydraulic Conductivity (ft/day)	Reference
AEC-7	4481-4702	Ramsey, Trap, and Olds	4×10^{-2}	Mercer (1983)
	4597-4702	Lower 37 ft. of Castile Anhydrite I down through Olds	4×10^{-2}	
AEC-8	4292-4393	Lamar and upper	2×10^{-6}	Mercer (1983)
	4809-4815	Ramsey	7×10^{-3}	
	4832-4848	Lower Hays? Lower Hays?	2×10^{-2}	
ERDA-10	3847-3913	Lamar and Ramsey	4×10^{-4}	Mercer (1983)
	4114-4417	Lower Hays	5×10^{-2}	
Cabin Baby-1	4036-4089	Lamar	1×10^{-6}	Beauheim et al. (1983)
	4093-4125	Ramsey	5×10^{-5} to 2×10^{-4}	
	4131-4163	Olds	5×10^{-5} to 2×10^{-4}	
	4170-4291	Hays	1×10^{-3} to 4×10^{-3}	
DOE-2	4138-4180[1]	Ramsey	2×10^{-4}	Beauheim (1986)
	4177-4218[2]	Olds	2×10^{-4}	
	4220-4325[3]	Hays	5×10^{-3}	

[1]Effective thickness 4144-4172
[2]Effective thickness 4187-4217
[3]Effective thickness 4255-4325

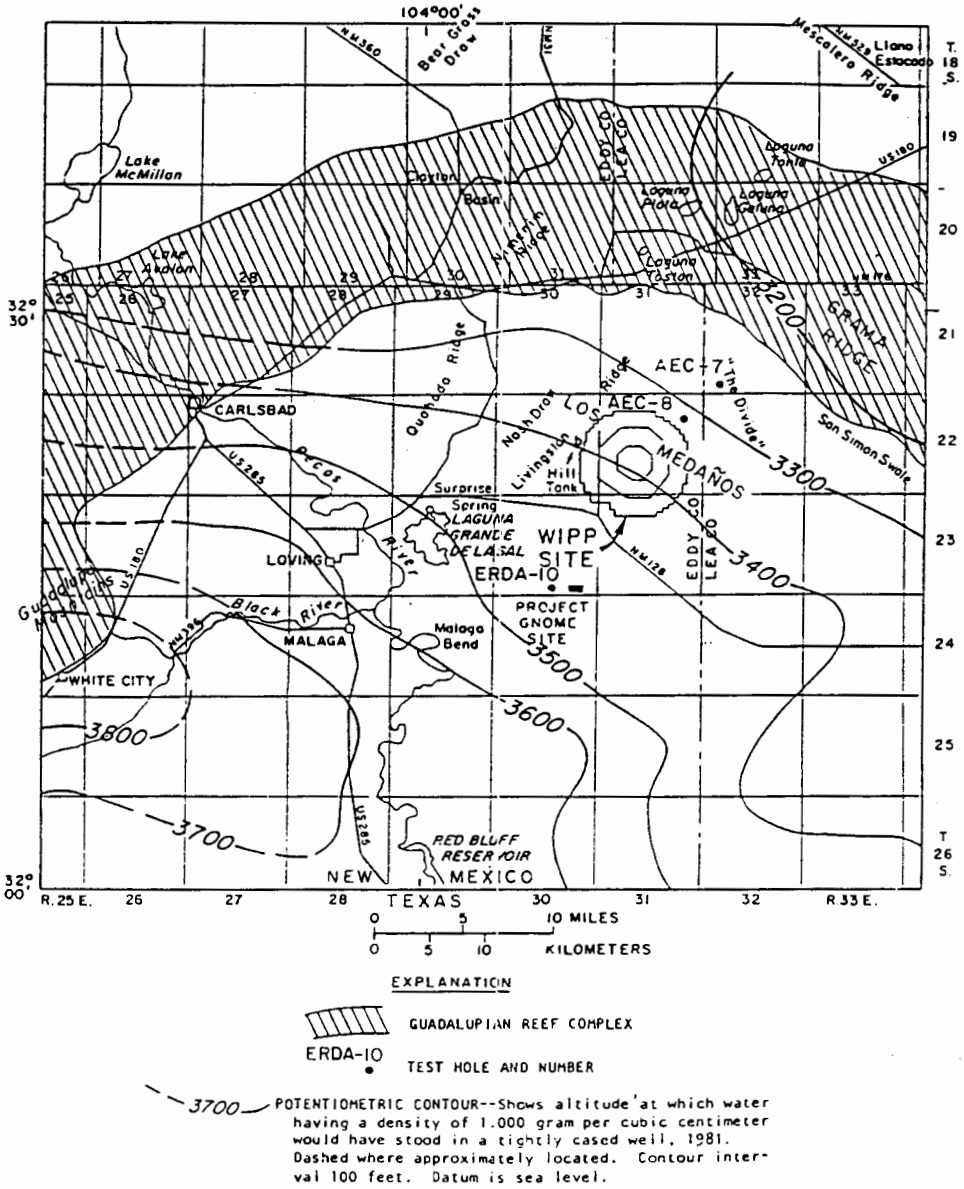

Figure 4-12. Potentiometric surface of the hydrologic unit in the upper part of the Bell Canyon Formation (Delaware Mountain Group) at and near the proposed Waste Isolation Pilot Plant (WIPP) site.

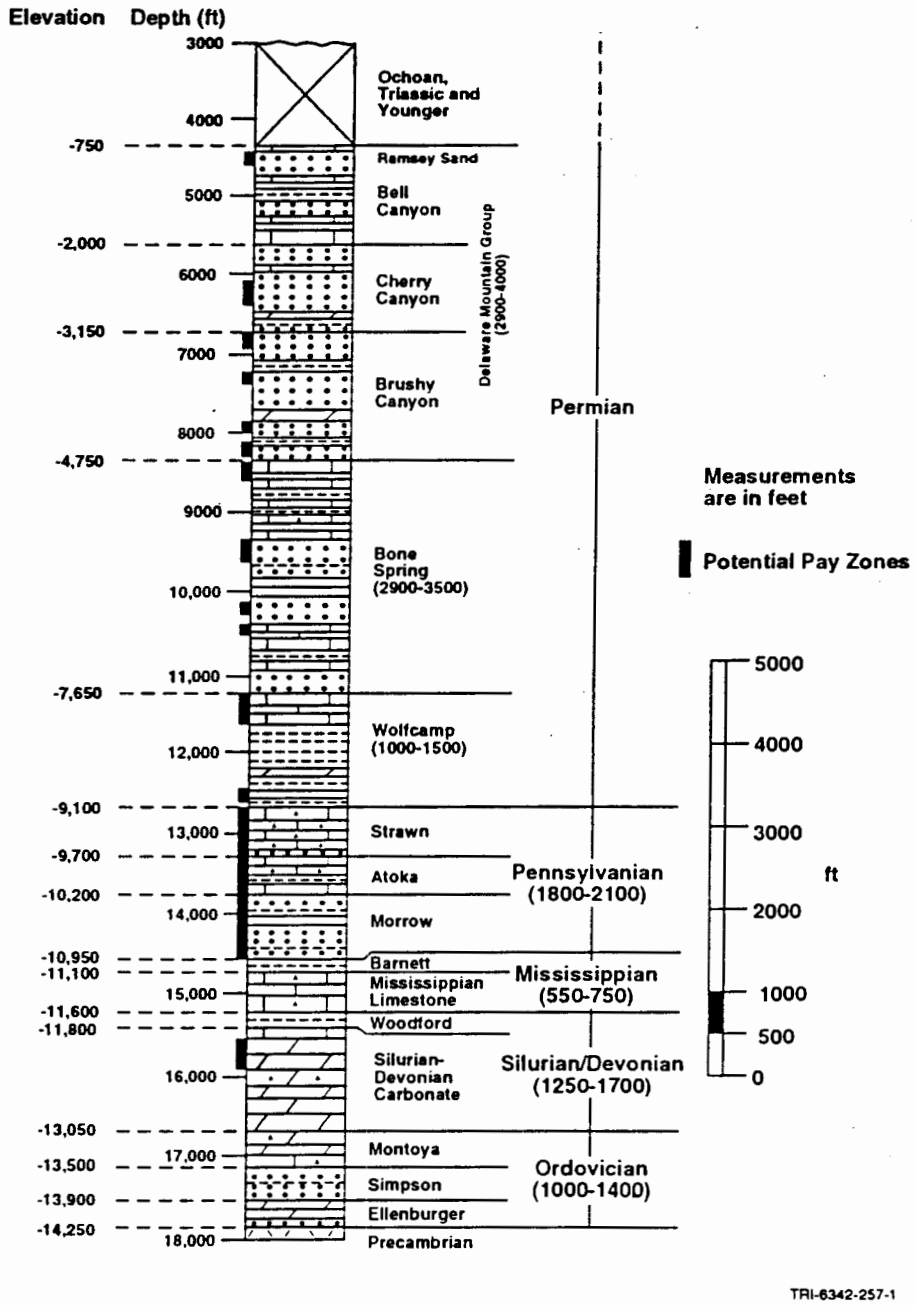

Figure 4-13. Stratigraphic column of units below the Castile formation (from Powers et al., 1978; after Foster, 1974).

(.7 and 1.8 m^3/h) of water. Measured permeabilities in the Pennsylvanian formations range from 0.1 mD ($\sim 1 \times 10^{-9}$ m/s) to about 50 mD ($\sim 5 \times 10^{-7}$ m/s) and porosities range from 6 to 20 percent (Roswell Geological Society, 1977). With regard to the Bone Spring, Lambert (in Lambert and Mercer, 1978, p. III-3) states that "bottom-hole pressure data indicate the majority of the seven wells tested had insufficient heads to prevent downward movement of shallower water and, therefore, contamination of this zone with radionuclides could possibly occur." Thus, in the event that a borehole breach of the reached units below the Castile Formation, the deep could serve either as pressure sources to drive fluids upward to strata such as the Culebra or as sinks receiving fluids from higher units.

4.6 Documentation of Experimental Data and Interpretive Techniques

Experimental data were collected from field hydraulic tests and field tracer tests. These test results are documented in a series of Hydrologic Data Reports (#1 through #8) (Hydro Geo Chem, 1985; Intera and Hydro Geo Chem, 1985; Intera, 1986; Saulnier et al., 1987; Stensrud et al., 1987; 1988a; 1988b; 1990), Basic Data Reports (e.g., Mercer et al., 1987), and U.S. Geological Survey (USGS) reports (e.g., Richey, 1986). Interpretation of the raw data is described in interpretive reports referenced throughout this section.

5.0 SUMMARY OF SPM2 BASELINE FOR NON-SALADO FLOW AND TRANSPORT

The following baseline model describing the non-Salado component of the WIPP system that was developed in November and December of 1994 as input for the second phase of the Systems Prioritization Methodology (SPM2). This baseline was developed by a working group composed of staff from the Geohydrology Department, the WIPP Performance Assessment Computational Support Department, and the WIPP Compliance Support Department. An important driving objective of the baseline model development was that the model assumptions be based on information available as of December 1994 and defensible with respect to technical peers from the regulatory arena. In mid December, a project decision was made to change the baseline guidance from production of a "defensible" baseline to a "realistically conservative" baseline. Given the short period of time available to implement this change, this guidance was implemented by incorporating the anticipated outcomes of previously defined Activity 1 into the baseline, under the assumption that the project will complete this activity to confirm that the results are as anticipated and that the baseline assumptions are justified.

In the specification of parameters to be sampled for the baseline SPM2 analysis, a conscious effort has been made to focus on parameters for which radionuclide release at the accessible environment boundary is known to be sensitive from calculations made in previous performance assessments and other sensitivity studies (WIPP Performance Assessment Department, 1993; Reeves et al., 1987; 1991). The general format for the following description of the non-Salado baseline model is to first describe what has been specified and/or assumed for a particular model component, followed by comments on the rationale for that particular specification and/or assumption.

5.1 Release Paths

The PA code BRAGFLO is being used to partition flow in an intrusion borehole to three locations: The Culebra, The Magenta, the top surface of the Rustler, and the full thickness of the Dewey Lake, assuming that the entire unit is saturated. Other members of the Rustler Formation are relatively tight rock lithologies with low hydraulic conductivities and very little transport of radionuclides is expected to occur within these units. Because of the large accessible porosity, expected large radionuclide retention capacity, and (perhaps) unsaturated conditions, it is assumed that no radionuclide releases will occur through the Dewey Lake. This assumption is being evaluated through limited additional studies. Radionuclides that enter the Magenta are assumed not to reach the accessible environment during 10,000 years. Releases from the Culebra will be calculated using SECO-TRANSPORT.

For the BRAGFLO calculation that partitions flow to different hydrologic units, the value of transmissivity chosen for the Culebra will be the highest value in the portion of the calibrated transmissivity fields that overlies the panels. In order to streamline the calculation process, this transmissivity will be taken as the highest value sampled from the Culebra region directly overlying the waste-disposal panels in any of the 70 realizations of the Culebra transmissivity field (LaVenue and RamaRao, 1992).

The value of transmissivity for the Magenta will be the lowest measured value for that unit over or near the panels, 1 x 10^{-8} m^2/s (from borehole H-2a, Mercer, 1983). The specified thickness of the Magenta will be 8.5 meters (from borehole H-2, Mercer, 1983, Table 1). The specified Magenta freshwater head will be 961 meters (Figure 3-7, Lappin et al., 1989). The specified porosity for the Magenta will be 0.09, estimated based on the measured porosity values of Culebra Dolomite (0.066 and 0.115, Lappin et al., 1989 Tables E-8 and E-9) at a location (H-10) with roughly comparable measured transmissivity (7.5 x 10^{-8} m^2/s, Lappin et al., 1989, Table 3-7). Storativity in the Magenta Dolomite is assumed to be comparable to that in the Culebra Dolomite.

For purposes of partitioning fluid flow into the Dewey Lake, a combination of local-scale and regional-scale properties has been assumed. The value of hydraulic conductivity in the Dewey Lake is assumed to be 10^{-8} m/s, which is the same as the value being used for Dewey Lake in the current three-dimensional regional model (Corbet, 12/23/94, personal communication), and the same as was used in the U.S. Geological Survey regional flow model (Davies, 1989). This value is typical for a fine-grained sandstone. Implementation within BRAGFLO assigns a transmissivity of 2 x 10^{-5} m^2/s for the entire unit, which correlates to a conductivity of approximately 1 x 10^{-7} m/s. The value of freshwater head to be used for the Dewey Lake is 980 meters. The value of porosity is 0.15, based on an analogue of the Wilcox Sandstone, a silty/shaley sandstone (Table 10.1 in Davis and Deweist, 1966). The value of compressibility to be used is 10^{-10} Pa^{-1}, which is the middle of the range for intact rock (Table 2.5 in Freeze and Cherry, 1979).

Because other members of the Rustler Formation are relatively tight rock lithologies with low hydraulic conductivities and very little transport of radionuclides is expected to occur within these units, these units are assumed to have zero transmissivity. This assumption is "realistically conservative" because these units generally have very low transmissivities and this assumption partitions the flow that would have gone into these units into higher transmissivity units.

Discussion: Based on extensive geologic characterization and hydraulic testing during the site characterization, the Culebra Dolomite has been identified as the most transmissive, laterally

continuous, water-bearing unit overlying the WIPP repository. Recent work on three-dimensional flow modeling of the entire stratigraphic section overlying the Salado has highlighted the fact that it is unrealistic to assume that all contaminated brine leaving the WIPP repository through a human intrusion borehole will flow only into the Culebra Dolomite. The specification of parameters for BRAGFLO partitioning of flow described above allows flow into three transmissive horizons, the Culebra and Magenta Dolomites, and fine-grained sandstones of the Dewey Lake. Because the Culebra is expected to be the most important, laterally continuous release pathway, the hydraulic assumptions underlying the flow partitioning described above maximize the amount of contaminated brine entering the Culebra by specifying the transmissivity to be the highest value sampled from the Culebra region directly overlying the waste-disposal panels in any of the 70 realizations of the Culebra transmissivity field.

The early conceptual model for flow in the Dewey Lake and overlying units (i.e. the Dockum Group) was that flow in these units is limited to matrix-only flow through a high-porosity matrix, with little to no extensively connected higher-transmissivity zones (Mercer, 1983). However, field studies proposed to confirm this conceptual model were never completed. In addition, limited information, such as the lost circulation zone in H-3d and the recent encounter of a saturated fracture zone in WQSP-6 that produced relatively large quantities of water, highlight the still-open question of the conceptual model for flow through the Dewey Lake.

Based on the limited information available, the present conceptual model for the Dewey Lake is that, for purposes of considering hydrology and/or contaminant transport, the unit can be thought of as containing two distinct parts. The lower portion of the unit (approximately 100 m) can be thought of as tightly cemented in both the matrix and fractures, with the cement being gypsum/anhydrite. This portion of the unit would be expected to behave as an equivalent porous medium for purposes of contaminant transport. The upper portion of the unit (approximately 50 m) can be thought of as being less well-cemented, with calcite cement. The limited information available indicates that the relatively transmissive features that have been identified (such as at H-3d and WQSP-6) occur just above the change in cement, and are fracture-controlled. Therefore, the conceptual model is that contaminant transport in this portion of the unit, if it needed to be modeled numerically, would need to be modeled as a dual-porosity phenomenon.

No specific hydrologic information is available concerning the lower portion of the Dewey Lake. The preliminary information available recently from well WQSP-6 indicates a hydraulic conductivity of approximately 3.5×10^{-6} m/s, from production over a thickness of approximately 10 m. At some locations, however, the Dewey Lake is apparently not saturated.

In addition, the time-dependent position of the water table in the Dewey Lake over 10,000 years is not certain. However, if the upper portion of the Dewey Lake is assumed to be 50 m thick, it is assumed to be completely saturated, and the hydraulic conductivity of the 50-meter thickness is assumed to be constant at the values estimated from well WQSP, this equates to a transmissivity for the upper portion of the Dewey Lake of approximately 2×10^{-4} m^2/s, one order of magnitude greater than assigned earlier to the entire thickness of the Dewey Lake.

As noted above, calculation of the quantity of flow entering the Dewey Lake is controlled by the assumed values for head (980 meters) and hydraulic conductivity. The input head value is based on the approximate elevation of fractures in borehole H-3d, in which circulation was lost, followed by drainage of drilling fluids back into the hole, indicating that this zone lies above the current water table, and is capable of accepting fluid from other sources. The original input conductivity (1×10^{-8} m/s) is a moderately low conductivity, typical of fined-grained sandstone, and is thought to be appropriate for the Dewey Lake as a whole on a regional scale. It is approximately two orders of magnitude lower than the local-scale conductivity interpreted more recently for a portion of the unit, based on preliminary results from hole WQSP-6A. The net impact of this difference, however, is to concentrate more fluid flow into the Culebra than might actually be the case locally. However, as explained below, we believe that this difference is "conservative," since the non-Salado working group believes that there will be no release from the Dewey Lake, even at the higher potential input.

At this time, detailed studies of the 10,000-year time dependence of fluid flow in the Dewey Lake have not been completed. The saturated thickness that might pertain at a specific human-intrusion borehole is not known. However, it is expected that the Dewey Lake, with its abundant clay minerals and sulfides, will have a large radionuclide-retardation capacity under saturated conditions. In addition, under locally unsaturated conditions, fluids injected into the formation from an intrusion borehole would be expected to remain static after saturating some volume around the borehole.

Obviously, open questions about the conceptual model for flow and transport in the Dewey Lake remain, and not enough is known about the flow and transport properties of the Dewey Lake Formation to perform detailed flow and transport calculations. The non-Salado working group, however, believes that a reasonable baseline position is that there will be *no* radionuclide releases from the Dewey Lake Formation. The long-term viability of this position, however, is contingent upon completion of a "side effort" containing several elements. Hydrologic aspects of this side effort include: a) compilation of existing hydrologic and geologic data on the Dewey Lake (from core and investigations at both the H-3 and H-19 pads); b) completion of a limited pumping test at well WQSP-6A, to provide quantitative site-specific

data; c) compilation of a revised conceptual model for fluid flow in the Dewey Lake; d) use of a regional three-dimensional model to calculate the effect of climate change on water-table position and hence flow and transport within the Dewey Lake; and e) performing one-dimensional calculations of infiltration through the unsaturated zone. Geochemical/transport aspects of this side effort include: a) definition of a "defensible" sorption distribution coefficient for the Dewey Lake, from existing literature data; b) investigation of the colloid-transport behavior of red-bed rock types in the literature; c) combination these results into a revised conceptual model for contaminant transport in the Dewey Lake; d) completion of one-dimensional transport calculations in the Dewey Lake, to estimate a K_d *below which* there might be release across the site boundary; and e) comparison of the results of the one-dimensional transport calculations with the literature-based estimate of the range of distribution coefficients which should be expected. Assuming that these activities are completed, and that the results are roughly as anticipated, the "realistically conservative" baseline model assumes that the results will indicate that there is no significant chance of radionuclide transport from any shaft or potential human-intrusion borehole to the WIPP site boundary over 10,000 years. This expectation is based on the beliefs that: a) the revised conceptual models for both hydrology and contaminant transport in the Dewey Lake will be similar to those described here, and will indicate a large radionuclide-retardation capacity; and b) the one-dimensional contaminant-transport calculations will indicate that the K_d required before releases would be realistic will be "orders of magnitude" smaller than that which is concluded to be realistic, on the basis of a literature survey.

The assumption that no releases will occur from the Magenta is based on the hydraulic test results from wells on the WIPP site (Beauheim, 1987a) that all indicate that flow in the Magenta occurs only in the matrix and that the conductivity is lower than that of the Culebra. Early numerical simulations of flow and transport in the Magenta suggested much slower transport than in the Culebra (Barr et al., 1983). Therefore, it is expected that no radionuclides entering the Magenta will reach the accessible environment boundary within the 10,000-year regulatory time frame.

5.2 Culebra Flow and Physical Retardation

In the baseline calculations, flow and transport within the Culebra is to be treated assuming two-dimensional, perfectly-confined, double-porosity conditions. Following the treatment in the 1992 Performance Assessment calculations, advection of radionuclides is assumed to occur only in fractures but radionuclides may diffuse into the matrix. In order to not overestimate the amount of diffusion in the baseline, model properties are to be assumed that

limit the fracture surface area. This is to be implemented by assigning a value of one to the number of fractures present in the numerical transport model. Other transport parameters to be used in the baseline include a fixed value for fracture porosity of 0.001 and for tortuosity of 0.08. Longitudinal dispersion is to use a single value (100 meters) equal to the median used in the 1992 Performance Assessment calculations. The spatial distribution of transmissivity of the Culebra should be explicitly implemented in the baseline model by sampling from the currently available transmissivity fields (LaVenue and RamaRao, 1992).

Discussion: The assumption that the Culebra is a fractured medium across the entire model domain would result in large releases in the absence of physical (i.e., matrix diffusion) and/or chemical retardation. Based on hydraulic test results, the non-Salado Working Group believes that it is likely that some parts of the model domain may be more realistically treated as a single-porosity matrix-flow-only medium. Given the limited distribution of subsurface data, the concept that some flow along the release path would occur in a single-porosity (matrix only) medium cannot be defended with even a moderate level of confidence. While hydraulic tests at H-1, H-2, and ERDA-9 showed single-porosity, porous medium behavior, hydraulic tests at H-3 and other locations indicate double-porosity conditions and pumping tests have demonstrated apparently continuous fracture zones over distances of as long as 6 kilometers, for example from WIPP-13 to WIPP-30.

Diffusion into the matrix has the potential to greatly reduce releases (Reeves et al, 1987; Reeves et al., 1991). Direct evidence indicating matrix diffusion comes from interpretations of tracer tests (Jones et al., 1992). Indirect evidence includes double-porosity hydraulic test responses and the physical characteristics of the Culebra (high porosity and moderate tortuosity). However, alternative interpretations that do not indicate matrix diffusion have been proposed by external review groups. In response to these reviews by external technical groups, improved tests are planned to address alternative interpretations. Therefore, the baseline transport model for the Culebra should include matrix diffusion, but in a realistically conservative way. The amount of diffusion depends mainly on the amount of surface area at the rock-water interface. The judgment of the working group was that the appropriate defensible implementation of matrix diffusion is to specify a numerical model input of a single fracture, which will limit surface area.

Three other processes that could impact releases given the double-porosity model are channeling, matrix advection, and multiphase (gas from the intrusion hole) flow. In the baseline model, the impacts of reduced surface area for matrix diffusion due to channeling are incorporated into the assumption of a single fracture. Matrix advection is a potentially beneficial process because it provides a second mechanism in addition to diffusion for moving contaminants into the less mobile matrix environment. Under multiphase flow conditions, the presence of gas

could enhance contaminant movement into the matrix even further by occupying the fractures and forcing brines into the matrix. Because neither of these potentially beneficial processes has yet been quantified, neither are included in the baseline model and both are included as activities.

A single value of fracture porosity is specified for the baseline because the baseline model already assumes relatively fast advective flow through the assumption of a single fracture. Therefore, it makes no sense to apply a "realistic range" to the fracture porosity parameter when the model already assumes an artificial single-fracture geometry. The low end of the fracture porosity range is considered unrealistically conservative given the single-fracture assumption. Therefore, the value selected is the mid-range value rounded to one significant digit (0.001). A "medium low" value of tortuosity was selected in order to limit matrix diffusion in the baseline model without being unrealistically conservative.

The baseline model value of 100 meters for dispersivity is the median value from the 1992 PA calculations. This value may be somewhat conservative, given the implementation of heterogeneous transmissivity distribution for the Culebra flow field. Given the relatively low sensitivity of the integrated release performance measure to dispersion (Reeves et al., 1991), this parameter selection is not anticipated to have a large impact. However, the dispersivity parameter is important for concentration-based performance measures (such as dose). Therefore if at some point the performance measure for WIPP change, serious consideration must be given to the specifying dispersivity at a local scale (e.g., tracer test scale), allowing heterogeneity in the transmissivity distribution to account for larger scale dispersion.

Because assuming transport in a single fracture limits matrix diffusion in the baseline model and radionuclide transport is rapid relative to assuming that a larger number of fractures are present, which is not defensible given the open questions about existing tracer tests, uncertainty in the Culebra transmissivity field is not anticipated to have a significant effect on the baseline model results. Three options for incorporation of the transmissivity field were considered: 1) the single field (from the suite of available fields from LaVenue and RamaRao (1992) with the fastest release time; 2) a single mean field from the available suite; 3) random sampling on the full suite of available fields. The argument for a single field option (1 or 2) is that given the baseline transport model, the transmissivity field is not likely to have a significant impact on releases and the calculational burden can be reduced by using a single field. However, the first approach is questionable because this approach assumes a particular release point and the fastest release might be a non-representative outlier. The second approach is questionable because a the mean field is not conservative. Therefore, the third approach was judged to be most appropriate.

5.3 Chemical Retardation

Conceptual model for water-rock interaction in the Culebra

The baseline model assumes that advective transport occurs in the fractures with diffusion into the matrix. In terms of the accessibility of mineral assemblages for chemical interactions, it is assumed that no clay "linings" are present and that minerals present in the bulk rock are available for chemical interactions.

Discussion: Two sets of fractures have been observed in core samples from the Culebra. It is currently not possible to differentiate whether the dominant groundwater flow path is through the high-angle set or through the sub-horizontal set. A conclusion that the dominant flow path is through the latter would be preferable with respect to compliance, but is not currently technically defensible. Consequently, the technical baseline position is that the dominant flow path is through the high-angle fractures, and that the mineral assemblage that is contacted by a solute in that flow path is represented by the bulk rock composition of the Culebra (i.e., there are no clay "linings").

Distribution Coefficients for Chemical Retardation of Actinides in the Culebra

Distribution coefficients (K_d) in the baseline model are assumed to be zero.

Discussion: In accordance with the Consultation and Cooperation agreement (1988, as modified), laboratory experimental programs are well underway to determine K_d values. On the basis of scoping work published by Dosch and others in the late 1970s and early 1980s, and our current (preliminary) laboratory results, we have strong indications that we will be able to demonstrate significant levels of retardation for the five actinides of particular concern to transport in the Culebra (uranium, plutonium, thorium, americium, neptunium). Because of stipulations in the C and C Agreement, however, we are required to use K_d values of zero for the technical baseline until non-zero K_d values are experimentally justified.

Chemical Retardation of Actinides due to Mixing of Disposal Room Brines with Culebra Brines

In the baseline model, mixing effects are assumed to be negligible.

Discussion: Preliminary results from numerical calculations based on chemical equilibrium (thermodynamic) principles suggest that mixing of brines may result in precipitation of sulfate minerals, and perhaps carbonate minerals. However, we do not have sufficient evidence, such

as laboratory results, to quantify the amount of actinides that might co-precipitate with those mineral precipitates. Disregarding the effects of mixing, however, is technically defensible and conservative.

Colloid-Facilitated Radionuclide Transport in the Culebra

In the Culebra, three sub-types of colloids are considered in the baseline. "Soft-sphere" carrier colloids (chiefly humic materials) and actinide intrinsic colloids are small enough to undergo matrix diffusion. Microbes (sterically stabilized carrier colloids) are too large to undergo matrix diffusion and will be transported by fracture advection. Based on preliminary results of ongoing experimental activities, it is likely that actinide intrinsic colloids will not be important in actinide transport, but they cannot currently be eliminated from the baseline. Free water diffusion constants for the actinide intrinsic colloids and humic materials have been estimated on the basis of sizes of those particles relative to sizes of dissolved solutes. The largest colloidal particle that could undergo matrix diffusion is limited to about 0.5 μm, which is the approximate mean size of pore throats in the Culebra (0.63 μm, see Section 3.3.3). Assuming that the sizes of dissolved species is on the order of 1 Å, the free water diffusion constants for macromolecular colloidal particles with mean diameters of about 0.5 μm have been estimated by reducing the free water diffusion constant of the dissolved species by a factor of 5000 (i.e., 0.5×10^{-6} meter $\div$ 1×10^{-10} meter). A macromolecular particle size of 0.5 μm is large for a macromolecular colloidal particle, but not unusual for actinide intrinsic colloids (see Section 3.3.3. Again, on the basis of preliminary results of current experimental work, it is anticipated that the reduction factor value of 5000 will be decreased substantially.

Discussion: The source of actinide-bearing colloidal particles is the disposal room environment; only a small population of colloidal particles could form in situ in the Culebra, and that amount is negligible compared to the population of colloidal particles that could be introduced from the disposal room. Concentrations of colloidal actinides introduced to the Culebra, therefore, are defined by the Actinide Source Term. "Hard-sphere" carrier colloids may sorb actinides in the disposal room environment, but will be destabilized by the high ionic strengths of the disposal room brine, and will not be mobile.

5.4 Intrusion Holes and Castile Brine Reservoir

The baseline model will use a depleting reservoir model similar to that developed by Reeves et al. (1991). Each reservoir will have a size and storativity representative of the reservoir hit by WIPP-12 (as discussed in Section 3.1.4). There will be four reservoirs that

conceptually cover an equal portion of the fraction of the footprint of repository that is assumed to overlie brine reservoirs. This fraction the "brine reservoir area fraction" will be as sampled in the 1992 Performance Assessment. No credit is taken for reservoir depletion by drill holes that could theoretically hit reservoirs beyond the boundaries of the repository.

The properties of a Castile brine reservoir potentially present beneath the WIPP repository will be assumed to be those given for the Base Case in Table 2-1 of Reeves et al. (1991). This table is attached here as Table 5-1. Reeves et al. (1991, p. 5-12) found that as long as borehole permeability was in the range from 10^{-14} to 10^{-10} m^2, the only properties of a Castile brine reservoir that are important to calculating flow into the Culebra dolomite are the reservoir pressure, storativity (compressibility), and out-ring radius (or reservoir volume); the different transmissivities and radius of the inner zone were found to be unimportant over the ranges considered. Based on this finding, the Castile brine reservoir model for baseline calculations is specified to be a single-zone, with the outer-zone radius and transmissivity given in Table 5-1. Also, the intact Castile is assumed to have no hydraulic impact on the reservoir and, therefore, the reservoir can be assumed to be an isolated hydrologic unit.

Discussion: The expected impact of this implementation is that the reservoir is expected to deplete in the event of human intrusion, i.e. to show decreasing rates of fluid flow at decreasing pressures. We believe that this approach is not "overly conservative," in that it allows for recognition of the fact that the reservoir is not infinite in extent. Realistically, drill holes that miss the repository but hit of a brine reservoir that extends beneath the repository (i.e. a "near miss") could deplete reservoir pressures and thus decrease the impact of a later hole that hit both the repository and that same reservoir. This process has not been analyzed in detail and has not been incorporated into current Performance Assessment models. Therefore, a conservative approach is taken that assumed that depressurization due to "near misses" does not occur.

5.5 Climate Change

For the baseline model, climate change will be treated in a manner similar to that used in the 1992 Performance Assessment (Swift et al., 1994). A simple conservative steady-state calculation will be made with heads raised to the land surface along the northern boundary while the head remains fixed at its present steady-state value along its southern boundary.

Discussion: Over the 10,000 year period that WIPP is to operate, long-term changes in climatic conditions will induce changes to recharge and boundary conditions in the Culebra. A precise prediction of these changes is difficult because precipitation over these time periods can only by

estimated by assuming that past climate patterns will continue and these patterns are estimated based on floral and faunal evidence. The time lag for response in the Culebra to changes in land-surface climatic changes is still being investigated.

In view of these uncertainties, a bounding approach to climate change has been taken that both maximizes gradients and keeps flow to the south, which maintains the significant effect of the high-transmissivity zone in the southeast portion of the site area. This is a reasonably defensible position until three-dimensional model studies of the regional system are available and provide involved information on the magnitude and time lag for transient climatic impacts.

Table 5-1. Modeling Parameters for a Hypothetical Brine Reservoir in the Castile Formation. Table 2.1 of Reeves et al. (1991)

Parameter	Symbol	High End	Base Case	Low End	Range	Units
Initial pressure	P_{bo}	17.4	12.7	10.0 [a]	7.0 - 17.4	MPa
Effective thickness	Δz_b	(b)	7.0	(b)	7.0 - 24.0	m
Transmissivity of inner ring	T_{bi}	7×10^{-2}	7×10^{-4}	7×10^{-6}	7×10^{-6} to 7×10^{-2}	m^2/s
Distance to inner/outer zone contact	r_{bi}	900	300	100	100 - 900	m
Transmissivity of outer ring	T_{bo}	7×10^{-4}	7×10^{-6}	7×10^{-6}	7×10^{-8} to 7×10^{-4}	m^2/s
Distance to outer ring/intact Castile contact	r_{bo}	8,600	2,000	100 (c)	30 - 8,600	m
Transmissivity of intact Castile	T_c	1×10^{-9}	1×10^{-11}	1×10^{-13}	1×10^{-13} to 1×10^{-9}	m^2/s
Porosity						
- brine reservoir	ϕ_b	0.01	0.005	0.001	0.001 - 0.01	
- intact Castile	ϕ_c	n.a.	0.005	n.a.	constant	
Bulk compressibility of medium						
- brine reservoir	C_{bR}	1×10^{-8}	1×10^{-9}	1×10^{-10}	1×10^{-10} to 1×10^{-8}	1/Pa
- intact Castile	C_{bc}	4.8×10^{-10}	4.8×10^{-11}	4.8×10^{-12}	4.8×10^{-12} to 4.8×10^{-10}	1/PA
Fluid density	ρ	n.a.	1,240	n.a.	constant	kg/m^3
Fluid viscosity	μ	n.a.	1.6×10^{-3}	n.a.	constant	Pa•s
Fluid compresibility	c_w	n.a.	3×10^{-10}	n.a.	constant	1/Pa

(a) A minimum pressure of 9.7 MPa is required to provide a driving force to cause flow from the brine reservoir depth to the Culebra. Therefore, the lower-end value of the range was not selected.

(b) Sensitivity to effective thickness is included in the transmissivity values.

(c) The minimum radial distance r_{bo} to the contact between the more permeable reservoir and the surrounding intact rock cannot be less than r_{bi}.

n.a. means not applicable.

6.0 REFERENCES

Adams, J.E. 1944. "Upper Permian Ochoa Series of the Delaware Basin, West Texas and Southeastern New Mexico," *American Association of Petroleum Geologists Bulletin.* Vol. 28, no. 11, 1596-1625.

Anderson, R.Y. 1981. "Deep-Seated Salt Dissolution in the Delaware Basin, Texas and New Mexico," *Environmental Geology and Hydrology in New Mexico.* Eds. S.G. Wells, W. Lambert, and J.F. Callender. New Mexico Geological Society Special Publication no. 10. [Roswell, NM]: New Mexico Geological Society. 133-145.

Anderson, R.Y. 1982. "Deformation-Dissolution Potential of Bedded Salt, Waste Isolation Pilot Plant Site, Delaware Basin, New Mexico," *Scientific Basis for Nuclear Waste Management V, Materials Research Society Proceedings, Berlin, Germany, June 7-10, 1982.* Ed. W. Lutze. New York, NY: North-Holland. Vol. 11, 449-458.

Anderson, R.Y., W.E. Dean, Jr., D.W. Kirkland, and H.I. Snider. 1972. "Permian Castile Varved Evaporite Sequence, West Texas and New Mexico," *Geological Society of America Bulletin.* Vol. 83, no. 1, 59-85.

Anderson, R.Y., K.K. Kietzke, and D.J. Rhodes. 1978. "Development of Dissolution Breccias, Northern Delaware Basin, New Mexico and Texas," *Geology and Mineral Deposits of Ochoan Rocks in Delaware Basin and Adjacent Areas, A Symposium on Ochoan Rocks of Southeast New Mexico and West Texas, Carlsbad, NM, May 4, 1977.* Ed. G.S. Austin. New Mexico Bureau of Mines & Mineral Resources Circular 159. Socorro, NM: New Mexico Bureau of Mines and Mineral Resources. 47-52.

Avis, J.D., and G.J. Saulnier, Jr. 1990. *Analysis of the Fluid-Pressure Responses of the Rustler Formation at H-16 to the Construction of the Air-Intake Shaft at the Waste Isolation Pilot Plant (WIPP) Site.* SAND89-7067. Albuquerque, NM: Sandia National Laboratories.

Avogadro, A., and G. de Marsily. 1984. "The Role of Colloids in Nuclear Waste Disposal," *Scientific Basis for Nuclear Waste Management VII, Materials Research Society Symposia Proceedings, Boston, MA, November 14-17, 1983.* Ed. G.L. McVay. New York, NY: North-Holland. Vol. 26, 495-505.

Bachman, G.O. 1973. *Surficial Features and Late Cenozoic History in Southeastern New Mexico.* Open-file Report 4339-8. Reston, VA: U.S. Geological Survey.

Bachman, G.O. 1974. *Geologic Processes and Cenozoic History Related to Salt Dissolution in Southeastern New Mexico.* Open-file Report 74-194. Denver, CO: U.S. Geological Survey.

Bachman, G.O. 1976. "Cenozoic Deposits of Southeastern New Mexico and an Outline of the History of Evaporite Dissolution," Journal of Research, *U.S. Geological Survey.* Vol. 4, no. 2, 135-149.

Bachman, G.O. 1980. *Regional Geology and Cenozoic History of Pecos Region, Southeastern New Mexico*. Open-file Report 80-1099. Denver, CO: U.S. Geological Survey.

Bachman, G.O. 1981. *Geology of Nash Draw, Eddy County, New Mexico*. Open-file Report 81-31. Denver, CO: U.S. Geological Survey.

Bachman, G.O. 1984. *Regional Geology of Ochoan Evaporites, Northern Part of Delaware Basin*. Circular 184. Socorro, NM: New Mexico Bureau of Mines and Mineral Resources.

Bachman, G.O. 1985. *Assessment of Near-Surface Dissolution At and Near the Waste Isolation Pilot Plant (WIPP), Southeastern New Mexico*. SAND84-7178. Albuquerque, NM: Sandia National Laboratories.

Bachman, G.O. 1987. *Karst in Evaporites in Southeastern New Mexico*. SAND86-7078. Albuquerque, NM: Sandia National Laboratories.

Baes, C.F., Jr., and R.E. Mesmer. 1976. *The Hydrolysis of Cations*. New York, NY: John Wiley & Sons.

Barr, G.E., W.B. Miller, and D.D. Gonzalez. 1983. *Interim Report on the Modeling of the Regional Hydraulics of the Rustler Formation*. SAND83-0391. Albuquerque, NM: Sandia National Laboratories.

Bear, J., and A. Verruijt. 1987. *Modeling Groundwater Flow and Pollution*. Boston, MA: D. Reidel Publishing Company.

Beauheim, R.L. 1986. *Hydraulic-Test Interpretations for Well DOE-2 at the Waste Isolation Pilot Plant (WIPP) Site*. SAND86-1364. Albuquerque, NM: Sandia National Laboratories.

Beauheim, R.L. 1987a. *Interpretations of Single-Well Hydraulic Tests Conducted At and Near the Waste Isolation Pilot Plant (WIPP) Site, 1983-1987*. SAND87-0039. Albuquerque, NM: Sandia National Laboratories.

Beauheim, R.L. 1987b. *Interpretation of the WIPP-13 Multipad Pumping Test of the Culebra Dolomite at the Waste Isolation Pilot Plant (WIPP) Site*. SAND87-2456. Albuquerque, NM: Sandia National Laboratories.

Beauheim, R.L. 1987c. *Analysis of Pumping Tests of the Culebra Dolomite Conducted at the H-3 Hydropad at the Waste Isolation Pilot Plant (WIPP) Site*. SAND86-2311. Albuquerque, NM: Sandia National Laboratories.

Beauheim, R.L. 1989. *Interpretation of H-11b4 Hydraulic Tests and the H-11 Multipad Pumping Test of the Culebra Dolomite at the Waste Isolation Pilot Plant (WIPP) Site*. SAND89-0536. Albuquerque, NM: Sandia National Laboratories.

Beauheim, R.L., and R.M. Holt. 1990. "Hydrogeology of the WIPP Site," *Geological and Hydrological Studies of Evaporites in the Northern Delaware Basin for the Waste Isolation Pilot Plant (WIPP), New Mexico, Field Trip #14 Guidebook, Geological Society of America 1990 Annual Meeting, Dallas, TX, October 29-November 1, 1990.* Leaders: D.W. Powers, R.M. Holt, R.L. Beauheim, and N. Rempe. SAND90-2035J. Dallas, TX: Dallas Geological Society. 131-179.

Beauheim, R.L., B.W. Hassinger, and J.A. Klaiber. 1983. *Basic Data Report for Borehole Cabin Baby-1 Deepening and Hydrologic Testing.* WTSD-TME-020. Albuquerque, NM: D'Appolonia Consulting Engineers, Inc. for U.S. Department of Energy.

Beauheim, R.L., T.F. Dale, and J.F. Pickens. 1991. *Interpretations of Single-Well Hydraulic Tests of the Rustler Formation Conducted in the Vicinity of the Waste Isolation Pilot Plant Site, 1988-1989.* SAND89-0869. Albuquerque, NM: Sandia National Laboratories.

Bell, J.T., C.F. Coleman, D.A. Costanzo, and R.E. Biggers. 1973a. "Plutonium Polymerization—III. The Nitrate Precipitation of Pu(IV) Polymer," *Journal of Inorganic and Nuclear Chemistry.* Vol. 35, no. 2, 629-632.

Bell, J.T., D.A. Costanzo, and R.E. Biggers. 1973b. "Plutonium Polymerization—II. Kinetics of the Plutonium Polymerization," *Journal of Inorganic and Nuclear Chemistry.* Vol. 35, no. 2, 623-628.

Bellin, A., P. Salandin, and A. Rinaldo. 1992. "Simulation of Dispersion in Heterogeneous Porous Formations: Statistics, First-Order Theories, Convergence of Computations," *Water Resources Research.* Vol. 28, no. 9, 2211-2228.

Bennett, D.G., S.K. Liew, L. Nanu, D. Read, and J.B. Thomas. 1993. "Modelling Colloidal Transport of Radionuclides Through Porous Media," *High Level Radioactive Waste Management, Proceedings of the Fourth Annual International Conference, Las Vegas, NV, April 26-30, 1993.* New York, NY: American Society of Civil Engineers. Vol. 4, 638-645.

Berg, R.R. 1979. "Reservoir Sandstones of the Delaware Mountain Group, Southeast New Mexico," *Guadalupian Delaware Mountain Group of West Texas and Southeast New Mexico.* Ed. N.M. Sullivan. Permian Basin Publication 79/18. Midland, TX: Permian Basin Section, Society of Economic Paleontologists and Mineralogists. 75-95.

Bertram-Howery, S.G., M.G. Marietta, R.P. Rechard, P.N. Swift, D.R. Anderson, B.L. Baker, J.E. Bean, Jr., W. Beyeler, K.F. Brinster, R.V. Guzowski, J.C. Helton, R.D. McCurley, D.K. Rudeen, J.D. Schreiber, and P. Vaughn. 1990. *Preliminary Comparison with 40 CFR Part 191, Subpart B for the Waste Isolation Pilot Plant, December 1990.* SAND90-2347. Albuquerque, NM: Sandia National Laboratories.

Bird, R.B., W.E. Stewart, and E.N. Lightfoot. 1960. *Transport Phenomena.* New York, NY: John Wiley & Sons.

Bodine, M.W., Jr., and B.F. Jones. 1986. *The Salt Norm: A Quantitative Chemical-Mineralogical Characterization of Natural Waters.* United States Geological Survey Water Resources Report 86-4086. Reston, VA: United States Geological Survey.

Bodine, M.W., Jr., B.F. Jones, and S.J. Lambert. 1991. "Chapter 4: Normative Analysis of Groundwaters from the Rustler Formation Associated with the Waste Isolation Pilot Plant, Southeastern New Mexico," *Hydrogeochemical Studies of the Rustler Formation and Related Rocks in the Waste Isolation Pilot Plant Area, Southeastern New Mexico.* Eds. M.D. Siegel, S.J. Lambert, and K.L. Robinson. SAND88-0196. Albuquerque, NM: Sandia National Laboratories. 4-1 through 4-140.

Borns, D.J., and S-E. Shaffer. 1985. *Regional Well-Log Correlation in the New Mexico Portion of the Delaware Basin.* SAND83-1798. Albuquerque NM: Sandia National Laboratories.

Borns, D.J. 1983. *Petrographic Study of Evaporite Deformation Near the Waste Isolation Pilot Plant (WIPP).* SAND83-0166. Albuquerque, NM: Sandia National Laboratories.

Brinster, K.F. 1991. *Preliminary Geohydrologic Conceptual Model of the Los Medaños Region Near the Waste Isolation Pilot Plant for the Purpose of Performance Assessment.* SAND89-7147. Albuquerque, NM: Sandia National Laboratories.

Brookins, D.G., S.J. Lambert, and D.B. Ward. 1990. *Authigenic Clay Minerals in the Rustler Formation, WIPP Site Area, New Mexico.* SAND89-1405. Albuquerque, NM: Sandia National Laboratories.

Brush, L.H. 1990. *Test Plan for Laboratory and Modeling Studies of Repository and Radionuclide Chemistry for the Waste Isolation Pilot Plant.* SAND90-0266. Albuquerque, NM: Sandia National Laboratories.

Brusseau, M.L., R.E. Jessup, and P.S.C. Rao. 1989. "Modeling the Transport of Solutes Influenced by Multiprocess Nonequilibrium," *Water Resources Research.* Vol. 25, no. 9, 1971-1988.

Buddemeier, R.W., and J.R. Hunt. 1988. "Transport of Colloidal Contaminants in Groundwater: Radionuclide Migration at the Nevada Test Site," *Applied Geochemistry.* Vol. 3, no. 5, 535-548.

Cartwright, L.D., Jr. 1930. "Transverse Section of the Permian Basin, West Texas and Southeast New Mexico," *American Association of Petroleum Geologists Bulletin.* Vol. 14, no. 8, 969-981.

Cauffman, T.L., A.M. LaVenue, and J.P. McCord. 1990. *Ground-Water Flow Modeling of the Culebra Dolomite. Volume II: Data Base.* SAND89-7068/2. Albuquerque, NM: Sandia National Laboratories.

Chapman, J.B. 1986. *Stable Isotopes in Southeastern New Mexico Groundwater: Implications for Dating Recharge in the WIPP Area.* EEG-35. Santa Fe, NM: Environmental Evaluation Group.

Chapman, J.B. 1988. *Chemical and Radiochemical Characteristics of Groundwater in the Culebra Dolomite, Southeastern New Mexico.* EEG-39. Santa Fe, NM: Environmental Evaluation Group.

Choppin, G.R. 1983. "Solution Chemistry of the Actinides," *Radiochimica Acta.* Vol. 32, no. 1-3, 43-53.

Choppin, G.R. 1988. "Humics and Radionuclide Migration," *Radiochimica Acta.* Vol. 44/45, pt. 1, 23-28.

Chugg, J.C., G.W. Anderson, D.L. Kink, and L.H. Jones. 1952. *Soil Survey of Eddy Area, New Mexico.* U.S. Department of Agriculture.

Cleveland, J.M. 1979. "Critical Review of Plutonium Equilibria of Environmental Concern," *Chemical Modeling in Aqueous Systems Speciation: Sorption, Solubility, and Kinetics, 176th Meeting of the American Chemical Society, Miami Beach, FL, September 11-13, 1978.* Ed. E.A. Jenne. ACS Symposium Series 93. Washington, DC: American Chemical Society. 321-338.

COHMAP (Cooperative Holocene Mapping Project) Members. 1988. "Climatic Changes of the Last 18,000 Years: Observations and Model Simulations," *Science.* Vol. 241, no. 4869, 1043-1052.

Cooper, J.B., and V.M. Glanzman. 1971. *Geohydrology of Project Gnome Site, Eddy County, New Mexico.* United States Geological Survey Professional Paper 712-A. Washington, DC: US Government Printing Office.

Corbet, T.F., and M.G. Wallace. 1993. "Post-Pleistocene Patterns of Shallow Groundwater Flow in the Delaware Basin, Southeastern New Mexico and West Texas," *Carlsbad Region, New Mexico and West Texas, New Mexico Geological Society Forty-fourth Annual Field Conference, October 6-9, 1993.* Eds. D.W. Love, J.W. Hawley, B.S. Kues, J.W. Adams, G.W. Austin, and J.M. Barker. SAND93-1318J. Roswell, NM: New Mexico Geological Society. 321-325.

Costanzo, D.A., R.E. Biggers, and J.T. Bell. 1973. "Plutonium Polymerization—I. A Spectrophotometric Study of the Polymerization of Plutonium(IV)," *Journal of Inorganic and Nuclear Chemistry.* Vol. 35, no. 2, 609-622.

Crawford, J.E., and C.S. Wallace. 1993. "Geology and Mineralization of the Culberson Sulfur Deposit," *Carlsbad Region, New Mexico and West Texas, New Mexico Geological Society Forty-fourth Annual Field Conference, October 6-9, 1993.* Eds. D.W. Love, J.W. Hawley, B.S. Kues, J.W. Adams, G.S. Austin, and J.M. Barker. Roswell, NM: New Mexico Geological Society. 301-316.

Cvetkovic, V.D., and A.M. Shapiro. 1990. "Mass Arrival of Sorptive Solute in Heterogeneous Porous Media," *Water Resources Research*. Vol. 26, no. 9, 2057-2067.

Dagan, G. 1989. *Theory of Flow and Transport in Porous Formations*. New York, NY: Springer-Verlag.

Dagan, G., and V. Cvetkovic. 1993. "Spatial Moments of a Kinetically Sorbing Solute Plume in a Heterogeneous Aquifer," *Water Resources Research*. Vol. 29, no. 12, 4053-4061.

D'Appolonia. 1982. *Data File Report, ERDA-6 & WIPP-12 Testing, Volume I - Text*. Report to Westinghouse Electric Corporation and US DOE WIPP Office. Pittsburgh, PA: D'Appolonia Consulting Engineers, Inc. (Copy on file at the Nuclear Waste Management Library, Sandia National Laboratories, Albuquerque, NM.)

D'Appolonia. 1983. *Data File Report, ERDA-6 & WIPP-12 Testing, Part B, Revisions, Addenda, and Errata, Volumes IVA through V, Revised September, 1983*. Report to Westinghouse Electric Corporation and US DOE WIPP Office. Pittsburgh, PA: D'Appolonia Consulting Engineers, Inc. (Copy on file at the Nuclear Waste Management Library, Sandia National Laboratories, Albuquerque, NM.)

Davies, P.B. 1987. "Modeling Areal, Variable-Density, Ground-Water Flow Using Equivalent Freshwater Head -- Analysis of Potentially Significant Errors," *Proceedings of the Solving Ground Water Problems with Models Conference and Exposition, Denver, CO, February 10-12, 1987*. Dublin, OH: National Water Well Association. Vol. 2, 888-903.

Davies, P.B. 1989. *Variable-Density Ground-Water Flow and Paleohydrology in the Waste Isolation Pilot Plant (WIPP) Region, Southeastern New Mexico*. Open-File Report 88-490. Albuquerque, NM: U.S. Geological Survey.

Davis, S.N., and R.J.M. Dewiest. 1966. *Hydrogeology*. New York, NY: John Wiley and Sons.

Dearlove, J.P.L., G. Longworth, M. Ivanovich, J.I. Kim, B. Delakowitz, and P. Zeh. 1990. "Organic Colloid Transport of Radionuclides at Gorleben, West Germany," *Waste Management '90, Proceedings of the Symposium, Tucson, AZ, February 25-March 1, 1990*. Ed. R.G. Post. Tucson, AZ: University of Arizona. Vol. 2, 565-569.

Dennehy, K.F. 1982. *Results of Hydrologic Tests and Water-Chemistry Analyses, Wells H-6A, H-6B, and H-6C, at the Proposed Waste Isolation Pilot Plant Site, Southeastern New Mexico*. United States Geological Survey Water-Resources Investigations 82-8. Albuquerque, NM: U.S. Geological Survey.

Dennehy, K.F., and J.W. Mercer. 1982. *Results of Hydrologic Tests and Water-Chemistry Analyses, Wells H-5A, H-5B, and H-5C, at the Proposed Waste Isolation Pilot Plant Site, Southeastern New Mexico*. United States Geological Survey Water-Resources Investigations 82-19. Albuquerque, NM: U.S. Geological Survey.

Derjaguin, B.V., and L. Landau. 1941. "A Theory of the Stability of Strongly Charged Lyophobic Sols and the Coalescence of Strongly Charge Particles in Electrolytic Solutions," *Acta Phys.-Chim. USSR*. Vol. 14: 633.

Destouni, G., and V.D. Cvetkovic. 1991. "Field Scale Mass Arrival of Sorptive Solute into the Groundwater," *Water Resources Research*. Vol. 27, no. 6, 1315-1325.

Dosch, R.G. 1980. *Assessment of Potential Radionuclide Transport in Site-Specific Geologic Formations*. SAND79-2468. Albuquerque, NM: Sandia National Laboratories.

Dosch, R.G. 1981. *Solubility and Sorption Characteristics of Uranium (VI) Associated with Rock Samples and Brines/Groundwaters from WIPP and NTS*. SAND80-1595. Albuquerque, NM: Sandia National Laboratories.

Dosch, R.G., and A.W. Lynch. 1978. *Interaction of Radionuclides with Geomedia Associated with the Waste Isolation Pilot Plant (WIPP) Site in New Mexico*. SAND78-0297. Albuquerque, NM: Sandia National Laboratories.

Dunham, R.J. 1972. *Capitan Reef, New Mexico and Texas: Facts and Questions to Aid Interpretation and Group Discussion*. Publication No. 72-14. Tulsa, OK: Society of Economic Paleontologists and Mineralogists.

Dykhuizen, R.C. 1992. "Diffusive Matrix Fracture Coupling Including the Effects of Flow Channeling," *Water Resources Research*. Vol. 28, no. 9, 2447-2450.

Eager, G.P. 1983. "Cores from the Lower Dewey Lake, Rustler, and Upper Salado Formations, Culberson County, Texas," *Permian Basin Cores*. Eds. R.L. Shaw and B.J. Pollan. P.B.S.-S.E.P.M. Core Workshop Vol. 2. Tulsa, OK: Society of Economic Paleontologists and Mineralogists, Permian Basin Section. Vol. 2, 273-283.

Earth Technology Corporation. 1988. *Final Report for Time Domain Electromagnetic (TDEM) Surveys at the WIPP Site*. SAND87-7144. Albuquerque, NM: Sandia National Laboratories.

Enfield, C.G., and G. Bengtsson. 1988. "Macromolecular Transport of Hydrophobic Contaminants in Aqueous Environments," *Ground Water*. Vol. 26, no. 1, 64-70.

Ferrall, C.C., and J.F. Gibbons. 1980. *Core Study of Rustler Formation Over the WIPP Site*. SAND79-7110. Albuquerque, NM: Sandia National Laboratories.

Fetter, C.W. 1993. *Contaminant Hydrogeology*. New York, NY: Macmillan Publishing Company.

Foster, R.W. 1974. *Oil and Gas Potential of a Proposed Site for the Disposal of High-Level Radioactive Waste*. ORNL/SUB-4423/1. Socorro, NM: New Mexico Bureau of Mines and Mineral Resources, New Mexico Institute of Mining and Technology; Oak Ridge, TN: Oak Ridge National Laboratory.

Francis, A.J., and J.B. Gillow. 1994. *Effects of Microbial Processes on Gas Generation Under Expected Waste Isolation Pilot Plant Repository Conditions. Progress Report Through 1992.* SAND93-7036. Albuquerque, NM: Sandia National Laboratories.

Freeland, M.H. 1982. *Basic Data Report for Borehole DOE-1, Waste Isolation Pilot Plant (WIPP) Project, Southeastern New Mexico.* TME 3159. Albuquerque, NM: U.S. Department of Energy, Waste Isolation Pilot Plant.

Freeze, R.A., and J.A. Cherry. 1979. *Groundwater.* Englewood Cliffs, NJ: Prentice-Hall.

Freeze, R.A., and P.A. Witherspoon. 1967. "Theoretical Analysis of Regional Groundwater Flow: 2. Effect of Water-Table Configuration and Subsurface Permeability Variation," *Water Resources Research.* Vol. 3, no. 2, 623-634.

Garber, R.A., G.A. Grover, and P.M. Harris. 1989. "Geology of the Capitan Shelf Margin-Subsurface Data from the Northern Delaware Basin," *Subsurface and Outcrop Examination of the Capitan Shelf Margin, Northern Delaware Basin, San Antonio, TX, April 23, 1989.* Eds. P.M. Harris and G.A. Grover. SEPM Core Workshop Vol. 13. Tulsa, OK: Society of Economic Paleontologists and Mineralogists. 3-269.

Gelhar, L.W. 1993. *Stochastic Subsurface Hydrology.* Englewood Cliffs, NJ: Prentice-Hall.

Gelhar, L.W., and C.L. Axness. 1983. "Three-Dimensional Stochastic Analysis of Macrodispersion in Aquifers," *Water Resources Research.* Vol. 19, no. 1, 161-180.

Gonzales, M.M. 1989. *Compilation and Comparison of Test-Hole Location Surveys in the Vicinity of the Waste Isolation Pilot Plant Site.* SAND88-1065. Albuquerque, NM: Sandia National Laboratories.

Gonzalez, D.D. 1983. *Hydrogeochemical Parameters of Fluid-Bearing Zones in the Rustler and Bell Canyon Formations: Waste Isolation Pilot Plant (WIPP), Southeast New Mexico (SENM).* SAND83-0210. Albuquerque, NM: Sandia National Laboratories.

Gregory, J. 1978. "Flocculation by Inorganic Salts," *The Scientific Basis of Flocculation.* Ed. K.J. Ives. Alphen aan den Rijn: Sijthoff & Noordhoff. 89-99.

Guilinger, J.R. 1993. "The Geology and Development of the Phillips Ranch Sulfur Deposit," *Carlsbad Region, New Mexico and West Texas, New Mexico Geological Society, Forty-fourth Annual Field Conference, October 6-9, 1993.* Eds. D.W. Love, J.W. Hawley, B.S. Kues, J.W. Adams, G.S. Austin, and J.M. Barker. Roswell, NM: New Mexico Geological Society. 21-23.

Hardy, W.B. 1900. "A Preliminary Investigation of the Conditions Which Determine the Stability of Irreversible Hydrosols," *Proceedings of the Royal Society of London.* Vol. 66, 110-125.

Harms, J.C., and C.R. Williamson. 1988. "Deep-Water Density Current Deposits of Delaware Mountain Group (Permian), Delaware Basin, Texas and New Mexico," *American Association of Petroleum Geologists Bulletin*. Vol. 72, no. 3, 299-317.

Haug, A., V.A. Kelley, A.M. LaVenue, and J.F. Pickens. 1987. *Modeling of Ground-Water Flow in the Culebra Dolomite at the Waste Isolation Pilot Plant (WIPP) Site: Interim Report*. SAND86-7167. Albuquerque, NM: Sandia National Laboratories.

Hawley, J.W. 1993. "The Ogallala and Gatuna Formations in the Southeastern New Mexico Region, a Progress Report," *Carlsbad Region, New Mexico and West Texas, New Mexico Geological Society, Forty-fourth Annual Field Conference, October 6-9, 1993*. Eds. D.W. Love, J.W. Hawley, B.S. Kues, J.W. Adams, G.S. Austin, and J.M. Barker. Roswell, NM: New Mexico Geological Society. 261-269.

Hays, J.D., J. Imbrie, and N.J. Shackleton. 1976. "Variations in the Earth's Orbit: Pacemaker of the Ice Ages," *Science*. Vol. 194, no. 4270, 1121-1132.

Heftmann, E., ed. 1961. *Chromatography: Adsorption, Partition, Ion Exchange, Electrochromatography, Column, Slab, Paper, Gas*. New York, NY: Reinhold Pub. Corp.

Helton, J.C., J.W. Garner, R.D. McCurley, and D.K. Rudeen. 1991. *Sensitivity Analysis Techniques and Results for Performance Assessment at the Waste Isolation Pilot Plant*. SAND90-7103. Albuquerque, NM: Sandia National Laboratories.

Helton, J.C., J.W. Garner, R.P. Rechard, D.K. Rudeen, and P.N. Swift. 1992. *Preliminary Comparison with 40 CFR Part 191, Subpart B for the Waste Isolation Pilot Plant, December 1991. Volume 4: Uncertainty and Sensitivity Analysis Results*. SAND91-0893/4. Albuquerque, NM: Sandia National Laboratories.

Hiemenz, P.C. 1986. *Principles of Colloid and Surface Chemistry*. 2nd ed. New York, NY: Marcel Dekker, Inc.

Hills, J.M., and F.E. Kottlowski. 1983. *Southwest/Southwest Mid-Continent Region, Correlation of Stratigraphic Units of North America (COSUNA) Project*. Correlation Chart Series 1983. Tulsa, OK: The AAPG Bookstore.

Hiss, W.L. 1976. "Stratigraphy and Ground-Water Hydrology of the Capitan Aquifer, Southeastern New Mexico and Western Texas." PhD dissertation. Boulder, CO: University of Colorado at Boulder.

Holt, R.M., and D.W. Powers. 1984. *Geotechnical Activities in the Waste Handling Shaft Waste Isolation Pilot Plant (WIPP) Project Southeastern New Mexico*. WTSD-TME-038. Carlsbad, NM: U.S, Department of Energy, Waste Isolation Pilot Plant.

Holt, R.M., and D.W. Powers. 1986. *Geotechnical Activities in the Exhaust Shaft*. DOE-WIPP-86-008. Carlsbad, NM: U.S. Department of Energy.

Holt, R.M., and D.W. Powers. 1988. *Facies Variability and Post-Depositional Alteration Within the Rustler Formation in the Vicinity of the Waste Isolation Pilot Plant, Southeastern New Mexico*. DOE/WIPP 88-004. Carlsbad, NM: Westinghouse Electric Corporation.

Holt, R.M., and D.W. Powers. 1990. *Geologic Mapping of the Air Intake Shaft at the Waste Isolation Pilot Plant*. DOE-WIPP 90-051. Carlsbad, NM: Westinghouse Electric Corporation.

Honeyman, B.D. 1991. "Surface Chemistry, Colloids and Trace-Element Scavenging," *Marine Particles: Analysis and Characterization*. Eds. D.C. Hurd and D.W. Spencer. Geophysics Monograph 63. Washington, DC: American Geophysical Union. 437-451.

Honeyman, B.D., and P.H. Santschi. 1992. "The Role of Particles and Colloids in the Transport of Radionuclides and Trace Metals in the Oceans," *Environmental Particles*. Eds. J. Buffle and H.P. van Leeuwen. Chelsea, MI: Lewis Publishers, Inc. Vol. 1, 379-423.

Houghton, J.T., G.J. Jenkins, and J.J. Ephraums. 1990. *Climate Change: The IPCC Scientific Assessment*. New York, NY: Cambridge University Press.

Hubbert, M.K. 1940. "The Theory of Ground-Water Motion," *The Journal of Geology*. Vol. 48, no. 8, pt. 1, 785-944.

Hwang, Y., P.L. Chambré, W.W.-L. Lee, and T.H. Pigford. 1990. "Analytic Studies of Colloid Transport in Fractured Porous Media," *Scientific Basis for Nuclear Waste Management XIII, Materials Research Society Symposia Proceedings, Boston, MA, November 27-30, 1989*. Eds. V.M. Oversby and P.W. Brown. Pittsburgh, PA: Materials Research Society. Vol. 176, 599-605.

Hydro Geo Chem, Inc. 1985. *WIPP Hydrology Program, Waste Isolation Pilot Plant, SENM Hydrologic Data Report #1*. SAND85-7206. Albuquerque, NM: Sandia National Laboratories.

Imbrie, J. 1985. "A Theoretical Framework for the Pleistocene Ice Ages," *Journal of the Geological Society*. Vol. 142, pt. 3, 417-432.

Imbrie, J., and J.Z. Imbrie. 1980. "Modeling the Climatic Response to Orbital Variations," *Science*. Vol. 207, no. 4434, 943-953.

Imbrie, J., J.D. Hays, D.G. Martinson, A. McIntyre, A.C. Mix, J.J. Morley, N.G. Pisias, W.L. Prell, and J.J. Shackleton. 1984. "The Orbital Theory of Pleistocene Climate: Support from a Revised Chronology of the Marine $\delta^{18}O$ Record," *Milankovitch and Climate, Understanding the Response to Astronomical Forcing, Proceedings of the Advanced Research Workshop on Milankovitch and Climate, Palisades, NY, November 30-December 4, 1982*. Eds. A. Berger, J. Imbrie, J. Hays, G. Kukla, and B. Satzman. Boston, MA: D. Reidel Publishing Company. Pt. 1, 269-305.

Intera Technologies, Inc. 1986. *WIPP Hydrology Program, Waste Isolation Pilot Plant, Southeastern New Mexico, Hydrologic Data Report #3*. SAND86-7109. Albuquerque, NM: Sandia National Laboratories.

Intera Technologies, Inc., and Hydro Geo Chem, Inc. 1985. *WIPP Hydrology Program, Waste Isolation Pilot Plant, Southeastern New Mexico, Hydrologic Data Report #2*. SAND85-7263. Albuquerque, NM: Sandia National Laboratories.

Izett, G.A., and R.E. Wilcox. 1982. *Map Showing Localities and Inferred Distributions of the Huckleberry Ridge, Mesa Falls, and Lava Creek Ash Beds (Pearlette Family Ash Beds) in the Western United States and Southern Canada*, Denver, CO: U.S. Geological Survey. Miscellaneous Investigations Map I-1325, Scale 1:400,000.

Johnson, K.S. 1978. "Stratigraphy and Mineral Resources of Guadalupian and Ochoan Rocks in the Texas Panhandle and Western Oklahoma," *Geology and Mineral Deposits of Ochoan Rocks in Delaware Basin and Adjacent Areas*. Comp. G.S. Austin. Circular 159. Socorro, NM: New Mexico Bureau of Mines and Mineral Resources. p. 57-62.

Jones, C.L., M.E. Cooley, and G.O. Bachman. 1973. *Salt Deposits of Los Medaños Area, Eddy and Lea Counties, New Mexico*. Open-File Report 4339-7. Albuquerque, NM: U.S. Geological Survey.

Jones, C.L. 1978. *Test Drilling for Potash Resources: Waste Isolation Pilot Plant Site, Eddy County, New Mexico*. Open-File Report 78-592. Denver, CO: U.S. Geological Survey. Vols. 1-2.

Jones, C.L., C.G. Bowles, and K.G. Bell. 1960. *Experimental Drill Hole Logging in Potash Deposits of the Carlsbad District, New Mexico*. Open-file Report 60-84. U.S. Geological Survey.

Jones, T.L., V.A. Kelley, J.F. Pickens, D.T. Upton, R.L. Beauheim, and P.B. Davies. 1992. *Integration of Interpretation Results of Tracer Tests Performed in the Culebra Dolomite at the Waste Isolation Pilot Plant Site*. SAND92-1579. Albuquerque, NM: Sandia National Laboratories.

Kelley, V.A., and G.J. Saulnier, Jr. 1990. *Core Analyses for Selected Samples from the Culebra Dolomite at the Waste Isolation Pilot Plant Site*. SAND90-7011. Albuquerque, NM: Sandia National Laboratories.

Kim, J.I. 1991. "Actinide Colloid Generation in Groundwater," *Radiochimica Acta*. Vol. 52/53, pt. 1, 71-81.

King, P.B. 1948. *Geology of the Southern Guadalupe Mountains, Texas*. Professional Paper 215. Washington, DC: U.S. Geological Survey.

King, R.E. 1947. "Sedimentation in Permian Castile Sea," *American Association of Petroleum Geologists Bulletin*. Vol. 31, no. 3, 470-477.

Klemmick, G.F. 1993. "Geology of the Pokorny Sulfur Deposit, Culberson County, Texas," *Carlsbad Region, New Mexico and West Texas, New Mexico Geological Society, Forty-fourth Annual Field Conference, October 6-9, 1993*. Eds. D.W. Love, J.W. Hawley, B.S. Kues, J.W. Adams, G.S. Austin, and J.M. Barker. Roswell, NM: New Mexico Geological Society. 18-19.

Kraus, K.A. 1956. "Hydrolytic Behavior of the Heavy Elements," *Proceedings of the International Conference on the Peaceful Uses of Atomic Energy, Geneva, August 8-20, 1955*. New York, NY: United Nations. Vol. 7, 245-257.

Lambert, S.J. 1987. *Feasibility Study: Applicability of Geochronologic Methods Involving Radiocarbon and Other Nuclides to the Groundwater Hydrology of the Rustler Formation, Southeastern New Mexico.* SAND86-1054. Albuquerque, NM: Sandia National Laboratories.

Lambert, S.J. 1991. Chapter 5: "Isotopic Constraints on the Rustler and Dewey Lake Groundwater Systems," *Hydrogeochemical Studies of the Rustler Formation and Related Rocks in the Waste Isolation Pilot Plant Area, Southeastern New Mexico*. Eds. M.D. Siegel, S.J. Lambert, and K.L. Robinson. SAND88-0196. Albuquerque, NM: Sandia National Laboratories. 5-1 through 5-79.

Lambert, S.J. 1992. "Geochemistry of the Waste Isolation Pilot Plant (WIPP) Site, Southeastern New Mexico, U.S.A.," *Applied Geochemistry*. SAND91-0612. Vol. 7, no. 6, 513-531.

Lambert, S.J., and J.A. Carter. 1987. *Uranium-Isotope Systematics in Groundwaters of the Rustler Formation, Northern Delaware Basin, Southeastern New Mexico. I. Principles and Preliminary Results.* SAND87-0388. Albuquerque, NM: Sandia National Laboratories.

Lambert, S.J., and D.M. Harvey. 1987. *Stable-Isotope Geochemistry of Groundwaters in the Delaware Basin of Southeastern New Mexico*. SAND87-0138. Albuquerque, NM: Sandia National Laboratories.

Lambert, S.J., and J.W. Mercer. 1978. *Hydrologic Investigations of the Los Medaños Area, Southeastern New Mexico, 1977.* SAND77-1401. Albuquerque, NM: Sandia National Laboratories.

Lambert, S.J., and K.L. Robinson. 1984. *Field Geochemical Studies of Groundwater in Nash Draw, Southeastern New Mexico*. SAND83-1122. Albuquerque, NM: Sandia National Laboratories.

Lang, W.B. 1935. "Upper Permian Formation of Delaware Basin of Texas and New Mexico," *American Association of Petroleum Geologists Bulletin*. Vol. 19, no. 2, 262-270.

Lang, W.B. 1939. "Salado Formation of the Permian Basin," *American Association of Petroleum Geologists Bulletin*. Vol. 23, no. 10, 1569-1572.

Lang, W.B. 1942. "Basal Beds of Salado Formation in Fletcher Potash Core Test Near Carlsbad, New Mexico," *American Association of Petroleum Geologists Bulletin*. Vol. 26, no. 1, 63-79.

Lappin, A.R. 1988. *Summary of Site-Characterization Studies Conducted From 1983 Through 1987 at the Waste Isolation Pilot Plant (WIPP) Site, Southeastern New Mexico*. SAND88-0157. Albuquerque, NM: Sandia National Laboratories.

Lappin, A.R., R.L. Hunter, D.P. Garber, P.B. Davies, R.L. Beauheim, D.J. Borns, L.H. Brush, B.M. Butcher, T. Cauffman, M.S.Y. Chu, L.S. Gomez, R.V. Guzowski, H.J. Iuzzolino, V. Kelley, S.J. Lambert, M.G. Marietta, J.W. Mercer, E.J. Nowak, J. Pickens, R.P. Rechard, M. Reeves, K.L. Robinson, and M.D. Siegel. 1989. *Systems Analysis, Long-Term Radionuclide Transport, and Dose Assessments, Waste Isolation Pilot Plant (WIPP), Southeastern New Mexico; March 1989.* SAND89-0462. Albuquerque, NM: Sandia National Laboratories.

Laul, J.C., and M.R. Smith. 1988. "Disequilibrium Study of Natural Radionuclides of Uranium and Thorium Series in Cores and Briny Groundwaters from Palo Duro Basin, Texas," *Radioactive Waste Management and the Nuclear Fuel Cycle*. Vol. 11, no. 2, 169-225.

LaVenue, A.M., and B.S. RamaRao. 1992. *A Modeling Approach To Address Spatial Variability within the Culebra Dolomite Transmissivity Field.* SAND92-7306. Albuquerque, NM: Sandia National Laboratories.

LaVenue, A.M., A. Haug, and V.A. Kelley. 1988. *Numerical Simulation of Ground-Water Flow in the Culebra Dolomite at the Waste Isolation Pilot Plant (WIPP) Site: Second Interim Report*. SAND88-7002. Albuquerque, NM: Sandia National Laboratories.

LaVenue, A.M., T.L. Cauffman, and J.F. Pickens. 1990. *Ground-Water Flow Modeling of the Culebra Dolomite. Volume I: Model Calibration*. SAND89-7068/1. Albuquerque, NM: Sandia National Laboratories.

LaVenue, A.M., A. Haug, and V.A. Kelley. 1988. *Numerical Simulation of Ground-Water Flow in the Culebra Dolomite at the Waste Isolation Pilot Plant (WIPP) Site: Second Interim Report*. SAND88-7002. Albuquerque, NM: Sandia National Laboratories.

Leslie, A., A. Kendall, and G. Harwood. 1993. "The Castile Formation: A Continuing Paradox," *Carlsbad Region, New Mexico and West Texas, New Mexico Geological Society, Forty-fourth Annual Field Conference, October 6-9, 1993*. Eds. D.W. Love, J.W. Hawley, B.S. Kues, J.W. Adams, G.S. Austin, and J.M. Barker. Roswell, NM: New Mexico Geological Society. 13-14.

Lieser, K.H., B. Gleitsmann, S. Peschke, and T. Steinkopff. 1986a. "Colloid Formation and Sorption of Radionuclides in Natural Systems," *Radiochimica Acta*. Vol. 40, no. 1, 39-47.

Lieser, K.H., B. Gleitsmann, and T. Steinkopff. 1986b. "Sorption of Trace Elements or Radionuclides in Natural Systems Containing Groundwater and Sediments," *Radiochimica Acta*. Vol. 40, no. 1, 33-37.

Lieser, K.H., A. Ament, R. Hill, R.N. Singh, U. Stingl, and B. Thybusch. 1990. "Colloids in Groundwater and Their Influence on Migration of Trace Elements and Radionuclides," *Radiochimica Acta*. Vol. 49, no. 2, 83-100.

Lloyd, M.H., and R.G. Haire. 1978. "The Chemistry of Plutonium in Sol-Gel Processes," *Radiochimica Acta*. Vol. 25, no. 3-4, 139-148.

Lowenstein, T.K. 1988. "Origin of Depositional Cycles in a Permian 'Saline Giant': The Salado (McNutt Zone) Evaporites of New Mexico and Texas," *Geological Society of America Bulletin*. Vol. 100, no. 4, 592-608.

Lucas, S.G., and O.J. Anderson. 1993a. "Stratigraphy of the Permian-Triassic Boundary in Southeastern New Mexico and West Texas," *Carlsbad Region, New Mexico and West Texas, New Mexico Geological Society, Forty-fourth Annual Field Conference, October 6-9, 1993*. Eds. D.W. Love, J.W. Hawley, B.S. Kues, J.W. Adams, G.S. Austin, and J.M. Barker. Roswell, NM: New Mexico Geological Society. 219-230.

Lucas, S.G., and O.J. Anderson. 1993b. "Triassic Stratigraphy in Southeastern New Mexico and Southwestern Texas," *Carlsbad Region, New Mexico and West Texas, New Mexico Geological Society, Forty-fourth Annual Field Conference, October 6-9, 1993*. Eds. D.W. Love, J.W. Hawley, B.S. Kues, J.W. Adams, G.S. Austin, and J.M. Barker. Roswell, NM: New Mexico Geological Society. 231-235.

Lyklema, J. 1978. "Surface Chemistry of Colloids in Connection with Stability," *The Scientific Basis of Flocculation*. Ed. K.J. Ives. NATO Advanced Study Institutes Series, Series E, Volume E 27. Alphen aan den Rijn: Sijthoff & Noordhoff. 3-36.

Lynch, A.W., and R.G. Dosch. 1980. *Sorption Coefficients for Radionuclides on Samples from the Water-Bearing Magenta and Culebra Members of the Rustler Formation*. SAND80-1064. Albuquerque, NM: Sandia National Laboratories.

Lyon, M.L. 1989. *Annual Water Quality Data Report for the Waste Isolation Pilot Plant*. DOE/WIPP 89-001. Carlsbad, NM: Westinghouse Electric Corporation.

Machette, M.N. 1985. "Calcic Soils of the Southwestern United States," *Soils and Quaternary Geology of the Southwestern United States*. Ed. D.L. Weide. Special Paper 203. Denver, CO: Geological Society of America. 1-21.

Mackay, D.M., D.L. Freyberg, P.V. Roberts, and J.A. Cherry. 1986. "A Natural Gradient Experiment on Solute Transport in a Sand Aquifer. 1: Approach and Overview of Plume Movement," *Water Resources Research*. Vol. 22, no. 13, 2017-2029.

Maiti, T.C., M.R. Smith, and J.C. Laul. 1989. "Colloid Formation Study of U, Th, Ra, Pb, Po, Sr, Rb, and Cs in Briny (High Ionic Strength) Groundwaters: Analog Study for Waste Disposal," *Nuclear Technology*. Vol. 84, no. 1, 82-87.

Matijevi, E. 1973. "Colloid Stability and Complex Chemistry," *Journal of Colloid and Interface Science*. Vol. 43, no. 2, 217-245.

McCarthy, J.F., and C. Degueldre. 1993. "Sampling and Characterization of Colloids and Particles in Ground Water for Studying Their Role in Contaminant Transport," *Environmental Particles*. Eds. J. Buffle and H.P. van Leeuwen. IUPAC Environmental Analytical and Physical Science Series Vol. 2. Chelsea, MI: Lewis Publishers, Inc. 247-315.

McDonald, M.G., and A.W. Harbaugh. 1988. *A Modular Three-Dimensional Finite-Difference Ground-Water Flow Model.* United States Geological Survey Open File Report 83-875. Reston, VA: United States Geological Survey.

McDonald, M.G., A.W. Harbaugh, B.R. Orr, and D.J. Ackerman. 1991. *A Method of Connecting No-Flow Cells to Variable-Head Cells for the U.S. Geological Survey Modular Finite-Difference Ground-Water Flow Model.* United States Geological Survey Open File Report 91-536. Reston, VA: United States Geological Survey.

McDowell-Boyer, L.M., J.R. Hunt, and N. Sitar. 1986. "Particle Transport Through Porous Media," *Water Resources Research*. Vol. 22, no. 13, 1901-1921.

McNeal, R.P. 1965. "Hydrodynamics of the Permian Basin," *Fluids in Subsurface Environments*. AAPG Memoir 4. Tulsa, OK: American Association of Petroleum Geologists. 308-326.

Mercer, J.W. 1983. *Geohydrology of the Proposed Waste Isolation Pilot Plant Site, Los Medaños Area, Southeastern New Mexico*. Water-Resources Investigations Report 83-4016. Albuquerque, NM: U.S. Geological Survey.

Mercer, J.W. 1987. *Compilation of Hydrologic Data From Drilling the Salado and Castile Formations Near the Waste Isolation Pilot Plant (WIPP) Site in Southeastern New Mexico*. SAND86-0954. Albuquerque, NM: Sandia National Laboratories.

Mercer, J.W. 1990. *Basic Data Report for Drillholes at the H-11 Complex (Waste Isolation Pilot Plant-WIPP)*. SAND89-0200. Albuquerque, NM: Sandia National Laboratories.

Mercer, J.W., and B.R. Orr. 1979. *Interim Data Report on the Geohydrology of the Proposed Waste Isolation Pilot Plant Site Southeast New Mexico*. Water-Resources Investigations 79-98. Albuquerque, NM: U.S. Geological Survey.

Mercer, J.W., R.L. Beauheim, R.P. Snyder, and G.M. Fairer. 1987. *Basic Data Report for Drilling and Hydrologic Testing of Drillhole DOE-2 at the Waste Isolation Pilot Plant (WIPP) Site*. SAND86-0611. Albuquerque, NM: Sandia National Laboratories.

Mercer, J.W., P. Davis, K.F. Dennehy, and C.L. Goetz. 1981. *Results of Hydrologic Tests and Water-Chemistry Analyses, Wells H-4A, H-4B, and H-4C at the Proposed Waste Isolation Pilot Plant Site, Southeastern New Mexico*. Water-Resources Investigations 81-36. Albuquerque, NM: U.S. Geological Survey.

Miller, D.N. 1955. "Petrology of Pierce Canyon Redbeds; Delaware Basin, Texas and New Mexico." Ph.D. dissertation. Austin, TX: University of Texas.

Miller, D.N. 1966. "Petrology of Pierce Canyon Redbeds, Delaware Basin, Texas and New Mexico," *American Association of Petroleum Geologists Bulletin*. Vol. 50, no. 2, 383-307.

Mitchell, J.F.B. 1989. "The 'Greenhouse' Effect and Climate Change," *Reviews of Geophysics*. Vol. 27, no. 1, 115-139.

Molecke, M.A. 1983. *A Comparison of Brines Relevant to Nuclear Waste Experimentation*. SAND83-0516. Albuquerque, New Mexico: Sandia National Laboratories.

Myers, J., P. Drez, and P. James. 1991. "Chapter 6: The Redox State and the Occurrence and Influence of Organics in the Culebra," *Hydrogeochemical Studies of the Rustler Formation and Related Rocks in the Waste Isolation Pilot Plant Area, Southeastern New Mexico*. Eds. M.D. Siegel, S.J. Lambert, and K.L. Robinson. SAND88-0196. Albuquerque, NM: Sandia National Laboratories. 6-1 through 6-35.

Neill, R.H., J.K. Channell, L. Chaturvedi, M.S. Little, K. Rehfeldt, and P. Spiegler. 1983. *Evaluation of the Suitability of the WIPP Site*. EEG-23. Santa Fe, NM: Environmental Evaluation Group.

Neuman, S.P., and P.A. Witherspoon. 1969a. "Theory of Flow in a Confined Two-Aquifer System," *Water Resources Research*. Vol. 5, no. 4, 803-816.

Neuman, S.P., and P.A. Witherspoon. 1969b. "Applicability of Current Theories of Flow in Leaky Aquifers," *Water Resources Research*. Vol. 5, no. 4, 817-829.

Newell, N.D., J.S. Bradley, A.J. Whiteman, A.G. Fischer, and J.E. Hickox. 1953. *The Permian Reef Complex of the Guadalupe Mountains Region, Texas and New Mexico--A Study in Paleoecology*. San Francisco, CA: W.H. Freeman & Co.

Nicholson, A., Jr., and A. Clebsch, Jr. 1961. *Geology and Ground-Water Conditions in Southern Lea County, New Mexico*. Ground-Water Report 6. Socorro, NM: New Mexico Bureau of Mines and Mineral Resources, New Mexico Institute of Mining & Technology.

Nitsche, H., K. Roberts, R.C. Gatti, T. Prussin, K. Becraft, S.C. Leung, S.A. Carpenter, and C.F. Novak. 1992. *Plutonium Solubility and Speciation Studies in a Simulant of Air Intake Shaft Water from the Culebra Dolomite at the Waste Isolation Pilot Plant*. SAND92-0659. Albuquerque, NM: Sandia National Laboratories.

Novak, C.F. 1992. *An Evaluation of Radionuclide Batch Sorption Data on Culebra Dolomite for Aqueous Compositions Relevant to the Human Intrusion Scenario for the Waste Isolation Pilot Plant*. SAND91-1299. Albuquerque, NM: Sandia National Laboratories.

Nowak, E.J. 1980. *Radionuclide Sorption and Migration Studies of Getters for Backfill Barriers*. SAND79-1110. Albuquerque, NM: Sandia National Laboratories.

Nuttall, H.E., R. Jain, and Y. Fertelli. 1991. "Radiocolloid Transport in Saturated and Unsaturated Fractures," *High Level Radioactive Waste Management, Proceedings of the Second Annual International Conference, Las Vegas, NV, April 28-May 3, 1991*. New York, NY: American Society of Civil Engineers. Vol. 2, 189-196.

Overbeek, J.T.G. 1982. "Colloids, a Fascinating Subject: Introductory lecture," *Colloidal Dispersions*. J.W. Goodwin. Special Publication No. 43. London: Royal Society of Chemistry. 1-21.

Popielak, R.S., R.L. Beauheim, S.R. Black, W.E. Coons, C.T. Ellingson, and R.L. Olsen. 1983. *Brine Reservoirs in the Castile Formation, Waste Isolation Pilot Plant (WIPP) Project, Southeastern New Mexico*. WTSD-TME-3153. Albuquerque, NM: D'Appolonia Consulting Engineers, Inc.

Powers, D.W., and R.M. Holt. 1990. "Sedimentology of the Rustler Formation near the Waste Isolation Pilot Plant (WIPP) Site," *Geological and Hydrological Studies of Evaporites in the Northern Delaware Basin for the Waste Isolation Pilot Plant (WIPP), New Mexico, Field Trip #14 Guidebook, Geological Society of America 1990 Annual Meeting, Dallas, TX, October 29-November 1, 1990*. Leaders: D.W. Powers, R.M. Holt, R.L. Beauheim, and N. Rempe. Dallas, TX: Dallas Geological Society. 79-106.

Powers, D.W. and R.M. Holt. 1993. "The Upper Cenozic Gatuna Formation of Southeastern New Mexico, Carlsbad Region, New Mexico and West Texas," *New Mexico Geological Society, Forty-fourth Annual Field Conference, October 6-9, 1993*. Eds. D.W. Love, J.W. Hawley, B.S. Kues, J.W. Adams, G.S. Austin, and J.M. Barker. Roswell, NM: New Mexico Geological Society. 271-282.

Powers, D.W., and D.V. LeMone. 1987. "A Summary of Ochoan Stratigraphy, Western Delaware Basin," *Geology of the Western Delaware Basin, West Texas and Southeastern New Mexico, El Paso Geological Society Guidebook 18*. Eds. D.W. Powers and W.C. James. El Paso, TX: El Paso Geological Society. 63-68.

Powers, D.W., and D.V. LeMone. 1990. "A Summary of Ochoan Stratigraphy of the Western and Northern Delaware Basin," *Geological and Hydrological Studies of Evaporites in the Northern Delaware Basin for the Waste Isolation Pilot Plant (WIPP), New Mexico, Field Trip #14 Guidebook, Geological Society of America 1990 Annual Meeting, Dallas, TX, October 29-November 1, 1990*. Leaders: D.W. Powers, R.M. Holt, R.L. Beauheim, and N. Rempe. Dallas, TX: Dallas Geological Society. 27-32.

Powers, D.W., S.J. Lambert, S-E. Shaffer, L.R. Hill, and W.D. Weart, eds. 1978. *Geological Characterization Report, Waste Isolation Pilot Plant (WIPP) Site, Southeastern New Mexico*. SAND78-1596. Albuquerque, NM: Sandia National Laboratories,

Powers, D.W., R. Holt, R.L. Beauheim, and N. Rempe. 1990. "Geological and Hydrological Studies of Evaporites in the Northern Delaware Basin for the Waste Isolation Pilot Plant (WIPP), New Mexico," *Geological and Hydrological Studies of Evaporites in the Northern Delaware Basin for the Waste Isolation Pilot Plant (WIPP), New Mexico, Field Trip #14 Guidebook, Geological Society of America 1990 Annual Meeting, Dallas, TX, October 29-November 1, 1990*. Leaders: D.W. Powers, R.M. Holt, R.L. Beauheim, and N. Rempe. Dallas, TX: Dallas Geological Society. 1-5.

Rai, D., and J.L. Swanson. 1981. "Properties of Plutonium (IV) Polymer of Environmental Importance," *Nuclear Technology*. Vol. 54, no. 1, 107-112.

Ramey, D.S. 1985. *Chemistry of Rustler Fluids*. EEG-31. Santa Fe, NM: Environmental Evaluation Group.

Randall, W.S., M.E. Crawley, and M.L. Lyon. 1988. *1988 Annual Water Quality Data Report for the Waste Isolation Pilot Plant*. DOE/WIPP-88-006. Carlsbad, NM: Westinghouse Electric Corporation.

Rasmuson, A., and I. Neretnieks. 1986. "Radionuclide Transport in Fast Channels in Crystalline Rock," *Water Resources Research*. Vol. 22, no. 8, 1247-1256.

Reeves, M., V.A. Kelley, and J.F. Pickens. 1987. *Regional Double-Porosity Solute Transport in the Culebra Dolomite: An Analysis of Parameter Sensitivity and Importance at the Waste Isolation Pilot Plant (WIPP) Site*. SAND87-7105. Albuquerque, NM: Sandia National Laboratories.

Reeves, M., G.A. Freeze, V.A. Kelley, J.F. Pickens, D.T. Upton, and P.B. Davies. 1991. *Regional Double-Porosity Solute Transport in the Culebra Dolomite Under Brine-Reservoir-Breach Release Conditions: An Analysis of Parameter Sensitivity and Importance*. SAND89-7069. Albuquerque, NM: Sandia National Laboratories.

Richardson, G.B. 1904. "Report of a Reconnaissance of Trans-Pecos Texas, North of the Texas and Pacific Railway," *Texas University Bulletin 23*.

Richey, S.F. 1986. *Hydrologic-Test Data from Wells at Hydrologic-Test Pads H-7, H-8, H-9, and H-10 Near the Proposed Waste Isolation Pilot Plant Site, Southeastern New Mexico*. Open-File Report 86-413. Albuquerque, NM: U.S. Geological Survey.

Richey, S.F. 1987a. *Preliminary Hydrologic Data for Wells Tested in Nash Draw, Near the Proposed Waste Isolation Pilot Plant Site, Southeastern New Mexico*. Open-File Report 87-37. Albuquerque, NM: U.S. Geological Survey.

Richey, S.F. 1987b. *Water-Level Data from Wells in the Vicinity of the Waste Isolation Pilot Plant, Southeastern New Mexico*. Open-File Report 87-120. Albuquerque, NM: U.S. Geological Survey.

Richey, S.F. 1989. *Geologic and Hydrologic Data for the Rustler Formation Near the Waste Isolation Plant, Southeastern New Mexico*. Open-File Report 89-32. Albuquerque, NM: U.S. Geological Survey.

Robinson, J.Q., and D.W. Powers. 1987. "A Clastic Deposit Within the Lower Castile Formation, Western Delaware Basin, New Mexico," *Geology of the Western Delaware Basin, West Texas and Southeastern New Mexico*. Eds. D.W. Powers and W.C. James. El Paso Geological Society Guidebook 18. El Paso, TX: El Paso Geological Society. 69-79.

Robinson, T.W., and W.B. Lang. 1938. "Geology and Ground-Water Conditions of the Pecos River Valley in the Vicinity of Laguna Grande de la Sal, New Mexico, with Special Reference to the Salt Content of the River Water," *Twelfth and Thirteenth Biennial Reports of the State Engineer of New Mexico*. Santa Fe, NM: State Engineer. 77-118.

Rosholt, J.N., and C.R. McKinney. 1980. *Uranium Series Disequilibrium Investigations Related to the WIPP Site, New Mexico. Part II. Uranium Trend Dating of Surficial Deposits and Gypsum Spring Deposit Near WIPP Site, New Mexico*. Open-File Report 80-879. Denver, CO: U.S. Geological Survey.

Roswell Geological Society. 1977. *The Oil and Gas Fields of Southeastern New Mexico*. Roswell, NM: Roswell Geological Society.

Rundberg, R.S., A.J. Mitchell, I.R. Triay, and N.B. Torstenfelt. 1988. "Size and Density of a ^{242}Pu colloid," *Scientific Basis for Nuclear Waste Management XI, Materials Research Society Symposia Proceedings, Boston, MA, November 30-December 3, 1987*. Eds. M.J. Apted and R.E. Westerman. Pittsburgh, PA: Materials Research Society. Vol. 112, 243-248.

Sandia National Laboratories and D'Appolonia Consulting Engineers. 1983. *Basic Data Report for Drillhole AEC 8 (Waste Isolation Pilot Plant - WIPP)*. SAND79-0269. Albuquerque, NM: Sandia National Laboratories.

Sandia National Laboratories and US Geological Survey. 1981. *Basic Data Report for Drillhole WIPP 33 (Waste Isolation Pilot Plant - WIPP)*. SAND80-2011. Albuquerque, NM: Sandia National Laboratories.

Sandia WIPP Project. 1992. *Preliminary Performance Assessment for the Waste Isolation Pilot Plant, December 1992. Volume 3: Model Parameters*. SAND92-0700/3. Albuquerque, NM: Sandia National Laboratories.

Sato, T., and R. Ruch. 1980. *Stabilization of Colloidal Dispersions by Polymer Adsorption*. New York, NY: Marcel Dekker, Inc.

Saulnier, G.J., Jr. 1987. *Analysis of Pumping Tests of the Culebra Dolomite Conducted at the H-11 Hydropad at the Waste Isolation Pilot Plant (WIPP) Site*. SAND87-7124. Albuquerque, NM: Sandia National Laboratories.

Saulnier, G.J., Jr., and J.D. Avis. 1988a. *Interpretation of Hydraulic Tests Conducted in the Waste-Handling Shaft at the Waste Isolation Pilot Plant (WIPP) Site*. SAND88-7001. Albuquerque, NM: Sandia National Laboratories.

Saulnier, G.J., Jr., G.A. Freeze, and W.A. Stensrud. 1987. *WIPP Hydrology Program, Waste Isolation Pilot Plant, Southeastern New Mexico, Hydrologic Data Report #4*. SAND86-7166. Albuquerque, NM: Sandia National Laboratories.

Schiel, K.A. 1988. "The Dewey Lake Formation; End Stage Deposit of a Peripheral Foreland Basin." M.S. thesis. El Paso, TX: University of Texas.

Schiel, K.A. 1994. "A New Look at the Age, Depositional Environment and Paleogeographic Setting of the Dewey Lake Formation (Late Permian)," *West Texas Geological Society Bulletin*. Vol. 33, no. 9, 5-13.

Schlesinger, M.E., and J.F.B. Mitchell. 1987. "Climate Model Simulations of the Equilibrium Climatic Response to Increased Carbon Dioxide," *Reviews of Geophysics*. Vol. 25, no. 4, 760-798.

Serne, R.J., D. Rai, M.J. Mason, and M.A. Molecke. 1977. *Batch Kd Measurements of Nuclides to Estimate Migration Potential at the Proposed Waste Isolation Pilot Plant in New Mexico*. PNL-2448. Richland, WA: Battelle Pacific Northwest Laboratories.

Sewards, T. 1991. *Characterization of Fracture Surfaces in Dolomite Rock, Culebra Dolomite Member, Rustler Formation*. SAND90-7019. Albuquerque, NM: Sandia National Laboratories.

Sewards, T., R. Glenn, and K. Keil. 1991. *Mineralogy of the Rustler Formation in the WIPP-19 Core*. SAND87-7036. Albuquerque, NM: Sandia National Laboratories,

Siegel, M.D., and S. Anderholm. 1994. "Geochemical Evolution of Groundwater in the Culebra Dolomite near the Waste Isolation Pilot Plant, Southeastern New Mexico, USA," *Geochimica et Cosmochimica Acta*. Vol. 58, no. 10, 2299-2323.

Siegel, M.D., and S.J. Lambert. 1991. "Chapter 1: Summary of Hydrogeochemical Constraints on Groundwater Flow and Evolution in the Rustler Formation," *Hydrogeochemical Studies of the Rustler Formation and Related Rocks in the Waste Isolation Pilot Plant Area, Southeastern New Mexico*. Eds. M.D. Siegel, S.J. Lambert, and K.L. Robinson. SAND88-0196. Albuquerque, NM: Sandia National Laboratories. 1-1 through 1-109.

Siegel, M.D., S.J. Lambert, and K.L. Robinson, eds. 1991a. *Hydrogeochemical Studies of the Rustler Formation and Related Rocks in the Waste Isolation Pilot Plant Area, Southeastern New Mexico*. SAND88-0196. Albuquerque, NM: Sandia National Laboratories.

Siegel, M.D., S.L. Robinson, and J. Myers. 1991b. "Solute Relationships in Groundwaters from the Culebra Dolomite and Related Rocks in the Waste Isolation Pilot Plant Area, Southeastern New Mexico," *Hydrogeochemical Studies of the Rustler Formation and Related Rocks in the Waste Isolation Pilot Plant Area, Southeastern New Mexico*. Eds. M.D. Siegel, S.J. Lambert, and K.L. Robinson. SAND88-0196. Albuquerque, NM: Sandia National Laboratories. 2-1 through 2-164.

Siemers, W.T., J.W. Hawley, C. Rautman, and G. Austin. 1978. *Evaluation of the Mineral Potential (Excluding Hydrocarbons, Potash, and Water) of the Waste Isolation Pilot Plant Site, Eddy County, New Mexico*. Open File Report 87. Socorro, NM: New Mexico Bureau of Mines and Mineral Resources.

Sipes, Williamson & Aycock, Inc. 1976. *Hydrocarbon Evaluation, Proposed Southeastern New Mexico Radioactive Material Storage Site, Eddy Country, New Mexico*. SAND77-7033. Albuquerque, NM: Sandia National Laboratories. Vols. 1-2.

Snyder, R.P. 1985. *Dissolution of Halite and Gypsum, and Hydration of Anhydrite to Gypsum, Rustler Formation, in the Vicinity of the Waste Isolation Pilot Plant, Southeastern New Mexico*. USGS-OFR-85-229. Denver, CO: U.S. Geological Survey.

Stensrud, W.A., M.A. Bame, K.D. Lantz, A.M. LaVenue, J.B. Palmer, and G.J. Saulnier, Jr. 1987. *WIPP Hydrology Program, Waste Isolation Pilot Plant, Southeastern New Mexico, Hydrologic Data Report #5*. SAND87-7125. Albuquerque, NM: Sandia National Laboratories.

Stensrud, W.A., M.A. Bame, K.D. Lantz, T.L. Cauffman, J.B. Palmer, and G.J. Saulnier, Jr. 1988a. *WIPP Hydrology Program, Waste Isolation Pilot Plant, Southeastern New Mexico, Hydrologic Data Report #6*. SAND87-7166. Albuquerque, NM: Sandia National Laboratories.

Stensrud, W.A., M.A. Bame, K.D. Lantz, J.B. Palmer, and G.J. Saulnier, Jr. 1988b. *WIPP Hydrology Program, Waste Isolation Pilot Plant, Southeastern New Mexico, Hydrologic Data Report #7*. SAND88-7014. Albuquerque, NM: Sandia National Laboratories.

Stensrud, W.A., M.A. Bame, K.D. Lantz, J.B. Palmer, and G.J. Saulnier, Jr. 1990. *WIPP Hydrology Program, Waste Isolation Pilot Plant, Southeastern New Mexico, Hydrologic Data Report #8*. SAND89-7056. Albuquerque, NM: Sandia National Laboratories.

Stout, D.L., and S.A. Carroll. 1993. *A Literature Review of Actinide-Carbonate Mineral Interactions*. SAND92-7328. Albuquerque, NM: Sandia National Laboratories.

Swift, P.N. 1993. "Long-Term Climate Variability at the Waste Isolation Pilot Plant, Southeastern New Mexico, USA," *Environmental Management*. SAND91-7055. Vol. 17, no. 1, 83-97.

Swift, P.N., B.L. Baker, K. Economy, J.W. Garner, J.C. Helton, and D.K. Rudeen. 1994. *Incorporating Long-Term Climate Change in Performance Assessment for the Waste Isolation Pilot Plant*. SAND93-2266. Albuquerque, NM: Sandia National Laboratories,

Theng, B.K.G. 1979. *Formation and Properties of Clay-Polymer Complexes*. Developments in Soil Science Vol. 9. New York, NY: Elsevier Scientific Publishing Co.

Tien, P-L., F.B. Nimick, A.B. Muller, P.A. Davis, R.V. Guzowski, L.E. Duda, and R.L. Hunter. 1983. *Repository Site Data and Information in Bedded Salt: Palo Duro Basin, Texas*. NUREG/CR-3129, SAND82-2223. Albuquerque, NM: Sandia National Laboratories.

Tiller, C.L., and C.R. O'Melia. 1993. "Natural Organic Matter and Colloidal Stability: Models and Measurements," *Colloids in the Aquatic Environment. Colloids and Surfaces A: Physicochemical and Engineering Aspects*. Eds. T.F. Tadros and J. Gregory. London: Elsevier Applied Science. Vol. 73, 89-102.

Tipping, E. 1993. "Modelling Ion Binding by Humic Acids," *Colloids in the Aquatic Environment. Colloids and Surfaces A: Physicochemical and Engineering Aspects*. Eds. T.F. Tadros and J. Gregory. London: Elsevier Applied Science. Vol. 73, 117-131.

Tóth, J. 1963. "A Theoretical Analysis of Groundwater Flow in Small Drainage Basins," *Journal of Geophysical Research*. Vol. 68, no. 16, 4795-4812.

Toth, L.M., H.A. Friedman, and M.M. Osborne. 1981. "Polymerization of Pu(IV) in Aqueous Nitric Acid Solutions," *Journal of Inorganic and Nuclear Chemistry*. Vol. 43, no. 11, 2929-2934.

Triay, I.R., D.E. Hobart, A.J. Mitchell, T.W. Newton, M.A. Ott, P.D. Palmer, R.S. Rundberg, and J.L. Thompson. 1991. "Size Determinations of Plutonium Colloids Using Autocorrelation Photon Spectroscopy," *Radiochimica Acta*. Vol. 52/53, pt. 1, 127-131.

U.S. Department of Energy. 1994a. *Draft Compliance Status Report for the Waste Isolation Pilot Plant. March 1994, Revision 0, Draft*. DOE/WIPP 94-019. Carlsbad, NM: U.S. Department of Energy.

U.S. Department of Energy. 1994b. *Waste Isolation Pilot Plant Transuranic Waste Baseline Inventory Report*. CAO-94-1005. Revision 0, May 1994. Carlsbad, NM: U.S. Department of Energy.

van der Lee, J., G. de Marsily, and E. Ledoux. 1993. "Are Colloids Important for Transport Rate Assessment of Radionuclides?" *High Level Radioactive Waste Management, Proceedings of the Fourth Annual International Conference, Las Vegas, NV, April 26-30, 1993.* New York, NY: American Society of Civil Engineers. 646-652.

van Olphen, H. 1991. *Introduction to Clay Colloid Chemistry.* 2nd ed. New York, NY: Wiley.

Verwey, E.J.W., and J.T.G. Overbeek. 1948. *Theory of the Stability of Lyophobic Colloids. The Interaction of Sol Particles Having an Electric Double Layer.* New York, NY: Elsevier Publishing Company, Inc.

Vilks, P. 1994. *The Role of Colloids and Suspended Particles in Radionuclide Transport in the Canadian Concept for Nuclear Fuel Waste Disposal.* AECL-10280. Pinawa, Manitoba: Whiteshell Laboratories, Atomic Energy of Canada, Ltd.

Vine, J.D. 1963. *Surface Geology of the Nash Draw Quadrangle, Eddy County, New Mexico.* Geological Survey Bulletin 1141-B. Washington, DC: U.S. Government Printing Office.

Vlassopoulos, D., S.A. Wood, and A. Mucci. 1990. "Gold Speciation in Natural Waters: II. The Importance of Organic Complexing—Experiments with Some Simple Model Ligands," *Geochimica et Cosmochimica Acta.* Vol. 54, no. 6, 1575-1586.

Washington, W.M., and G.A. Meehl. 1984. "Seasonal Cycle Experiment on the Climate Sensitivity Due to a Doubling of CO_2 With an Atmospheric General Circulation Model Coupled to a Simple Mixed-Layer Ocean Model," *Journal of Geophysical Research.* Vol. 89, no. D6, 9475-9503.

Weber, W.J., Jr., P.M. McGinley, and L.E. Katz. 1991. "Sorption Phenomena in Subsurface Systems: Concepts, Models and Effects on Contaminant Fate and Transport," *Water Research.* Vol. 25, no. 5, 499-528.

Wilson, C.A., and J.F.B. Mitchell. 1987. "A Doubled CO_2 Climate Sensitivity Experiment With a Global Climate Model Including a Simple Ocean," *Journal of Geophysical Research.* Vol. 92, no. D11, 13,315-13,343.

WIPP PA (Performance Assessment) Department. 1992-1993. *Preliminary Performance Assessment for the Waste Isolation Pilot Plant, December 1992. Volumes 1,2,4,5.* SAND92-0700/1,2,4,5. Albuquerque, NM: Sandia National Laboratories.

WIPP PA (Performance Assessment) Division. 1991. *Preliminary Comparison with 40 CFR Part 191, Subpart B for the Waste Isolation Pilot Plant, December 1991. Volume 3: Reference Data.* Eds. R.P. Rechard, A.C. Peterson, J.D. Schreiber, H.J. Iuzzolino, M.S. Tierney, and J.S. Sandha. SAND91-0893/3. Albuquerque, NM: Sandia National Laboratories.

APPENDIX A: EVOLUTION OF PATTERNS OF REGIONAL GROUNDWATER FLOW IN SOUTHEASTERN, NEW MEXICO; RESPONSE TO POST-PLEISTOCENE CHANGES IN CLIMATE. THOMAS F. CORBET, SANDIA NATIONAL LABORATORIES, ALBUQUERQUE, NEW MEXICO, PRESENTED AS A POSTER SESSION, 1994 ANNUAL MEETING OF THE GEOLOGICAL SOCIETY OF AMERICA, SEATTLE, WASHINGTON, OCT. 24 - 27, 1994

Appendix A: Evolution of Patterns of Regional Groundwater Flow in Southeastern, New Mexico; Response to Post-Pleistocene Changes in Climate. Thomas F. Corbet, Sandia National Laboratories, Albuquerque, New Mexico, presented as a poster session, 1994 Annual Meeting of the Geological Society of America, Seattle, Washington, Oct. 24 - 27, 1994

Introduction

The Waste Isolation Pilot Plant (WIPP) is a potential repository for transuranic wastes generated by defense programs of the U.S. Department of Energy. The repository site is located 42 km east of the city of Carlsbad, New Mexico in a thick, Permian-age deposit of bedded salt. One consideration in evaluating the performance of the repository is that a future society might inadvertently penetrate the repository with one or more drill holes. Given certain circumstances, these holes could provide a pathway for contaminated brine to move upward into relatively permeable strata located above the bedded salt. There is concern that flowing groundwater could then transport radionuclides laterally to the sub-surface portion of the accessible environment, currently defined by the disposal regulations as the region more than 5 kilometers from the radioactive waste. The simulations presented here are part of a numerical modeling study of the possible impact that a change in climate over the next 10,000 years could have on the pattern of groundwater flow and, consequently, on the migration of radionuclides in strata overlying the repository.

One previous modeling study has examined the long-term response of this hydrologic system to changes in climate. Davies (1989) used a cross-sectional model to simulate the transient response assuming an elevated initial water table and zero recharge over a 20,000 year period. His results confirmed that it is possible that this system drains slowly enough that it could sustain transient flow from the Pleistocene to the present without additional recharge.

In this study, we expand on the work of Davies by simulating flow in large three-dimensional region and by using rigorous free-surface and seepage-face boundary conditions. We assume that changes in climate influence regional groundwater flow by modifying the rate at which moisture percolates through the unsaturated zone to arrive at the water table. Once moisture reaches the water table, it recharges the saturated zone until the water table rises to the land surface. Moisture in excess of the amount required to maintain the water table at the land surface is removed by evapotranspiration or surface runoff.

We simulate the effects of climate on regional flow by treating the model region as a series of contiguous groundwater basins in which the water table moves in response to imbalance between the rate of recharge and the rate at which groundwater flows away from the water table. The model region encompasses multiple groundwater basins because the lateral boundaries separating these basins can move, or possibly be generated or destroyed, during the course of the simulations. The lateral boundaries of the model region follow the closest groundwater divides that we believe could be stationary for entire period of time simulated.

The simulations presented here suggest that the position and shape of the water table, and consequently the entire flow system above the salt, is sensitive to changes as small as a few hundredths of a centimeter per year in the rate of recharge to the saturated zone. If recharge is sufficient to maintain the water table near the surface, flow in confined units at depth follows the slope of local topography. Smaller recharge rates result in a deeper, flatter water table and flow in confined units is along the same direction as the regional slope of the land surface.

Flow rates and directions in confined units, however, respond too slowly to changes in recharge to remain in equilibrium with the current recharge rate. Instead, flow in these units probably remains in a transient state of adjustment to long-term changes in climate.

Two steady-state calculations were performed to demonstrate the sensitivity of the flow field to the assumed recharge rate. The calculations contrast flow conditions for rates of maximum potential recharge of 0.1 and 0.01 cm/yr.

The larger recharge rate is sufficient to maintain the water table at the land surface except in the regions where the land surface is at high elevation. Figure 11 shows that the depth of the water table is zero over most of the model region and 40 to 80 meters under topographic highs. Consequently, the water table (Figure 12) reflects local features of the land surface. In contrast, the depth to the water table, if recharge is 0.01 cm/yr (Figure 13), is more than 80 meters over more than half of the model region. The water table at this recharge rate (Figure 14) is a flatter and smoother surface which slopes north-to-south along the regional topographic gradient.

The shape of the water table exerts a clear control on potentiometric surfaces of confined units at depth. The potentiometric surface of the Culebra dolomite, for example, is similar to that of the water table. Figures 15 and 16 show the potentiometric surface of the Culebra dolomite for recharge rates of 0.1 and 0.01 cm/yr respectively.

The sensitivity of the flow field to the amount of recharge has implications for the performance of the WIPP repository. Figures 17 and 18 show vectors of flow in the Culebra for the two steady- state calculations. Given a recharge rate of 0.1 cm/yr, flow from the vicinity of the WIPP is toward the west. A recharge rate of 0.01 cm/yr results in flow toward the south.

Steady-state calculations demonstrate that the modeled flow system is sensitive to the amount of recharge but do not provide information about the time required for the flow system to respond to changes in recharge. We performed a transient calculation to simulate the change in recharge shown in Figure 10. The highest and lowest recharge rates used for the transient calculation are the same as those for the steady-state calculations. We assumed a compressibility of 5×10^{-9} Pa^{-1} and a specific yield of 0.05 for all hydrostratigraphic units.The initial condition is the steady-state flow field calculated for a recharge rate of 0.1 cm/yr.

Figures 19, 20, and 21 show how the simulated potentiometric surface of the Culebra dolomite changed with time. The potentiometric surface drops and flow directions rotate toward the south as the recharge rate declines during the 6,000 year period starting 14,000 years ago. This trend continues at an accelerated rate over the following 8,000 years during which the recharge rate remains constant at 0.01 cm/yr.

The simulated potentiometric surface at the present time, however, is still considerably different from the potentiometric surface calculated for steady-state flow with recharge equal to 0.01 cm/yr (Figure 16). The present-day potentiometric surface would continue to become more similar to Figure 16 if the period of constant recharge at a rate of 0.01 cm/yr were extended. The difference between these two potentiometric surfaces represents degree to which the simulated present-day flow field remains out of equilibrium with the 0.01 cm/yr recharge rate.

The recharge rate was increased over the final 2,000 years of the simulation. During this period, the potentiometric surface started to rise and flow rotated back toward the west, demonstrating the reversible nature of changes in the flow field.

The simulated depth to the water table (Figure 22) and the flow vectors (Figure 23) for the present time provide additional insight into the changes that occurred over the first 14,000 years of the simulation. The water table dropped by as much as 55 meters over much of the model region during this period of time. The area of greatest change in flow directions and rates is within and to the south of the WIPP-site boundary.

Summary

A series of simulations, including the examples presented here, have improved our conceptual understanding of long-term regional groundwater flow in strata overlying the bedded salt that encloses the WIPP repository. The simulations suggest that the position and shape of the water table, and consequently entire flow system above the salt, is sensitive to small changes in the rate of recharge to the saturated zone. A recharge rate of 0.1 cm/yr is sufficient to maintain the water table near the surface. In this case, flow in confined units at depth follows the slope of local topography. A smaller recharge rate of 0.01 cm/yr results in a deeper, flatter water table and flow in confined units is along the same direction as the regional slope of the land surface.

The groundwater flow system, however, responds very slowly to changes in recharge occurring over time periods that are thought to be representative of climate change since the end of the Pleistocene. During the transient simulation presented here, an 8,000 year period of recharge at a constant rate of 0.01 cm/yr was not long enough to allow the flow field to adjust to that recharge rate. This result suggests that groundwater flow within the region represented by these simulations is always in a transient state of adjustment to long-term changes in climate. Modern flow might, for example, be more representative of past climate conditions than those observed today.

Acknowledgements

This work is sponsored by the U.S. Department of Energy under contract number DE-ACO4-94AL85000. Pat Knupp developed the numerical model used for these simulations and provided the description of SECO-3D used for this presentation. Ellen Dombroski assisted in software implementation of the algorithm. Mike Wallace and Steve Askew helped perform and interpret the simulations. The graphics programming was performed by Rebecca Blaine using IDL, a commercial software package. Bob Holt and Roy Courtright compiled the stratigraphy of the model region. Bob Holt also identified the zones used to assign a hydraulic conductivity distribution to the hydrostratigraphic units. Tina Johnson and Sally Woerner prepared the poster display.

References

Bear, J. and Verruijt, A., 1987, Modeling groundwater flow and pollution: D. Reidel Publishing Company, 414 p.

Corbet, T. and Wallace, M., 1993, Post-Pleistocene patterns of shallow groundwater flow in the Delaware Basin, southeastern New Mexico and west Texas: New Mexico Geological Society Guidebook, 44th Field Conference, Carlsbad Region, New Mexico and west Texas, p. 321-325.

Davies, P. B., 1989, Variable-density ground-water flow and paleohydrology in the Waste Isolation Pilot Plant (WIPP) region, southeastern New Mexico: U.S. Geological Survey Open-File Report 88-490, 139 p.

Hunter, R. L. 1985, A regional water balance for the Waste Isolation Pilot Plant (WIPP) site and surrounding area: SAND84-2233. Sandia National Laboratories, Albuquerque, New Mexico.

Knupp, P., 1995, A moving mesh algorithm for 3D groundwater flow calculations with a water table and seepage face: submitted for location.

Powers, D. W., and Holt, R. M., 1990, Sedimentology of the Rustler Formation near the Waste Isolation Pilot Plant (WIPP) site: geological and hydrological studies of evaporites in the northern Delaware Basin for the Waste Isolation Pilot Plant (WIPP), New Mexico, Geological Society of America Field Trip 14, 1990 Annual Meeting, Dallas, Texas.

Swift, P. N., 1993, Long-term climate variability at the Waste Isolation Pilot Plant, southeastern New Mexico, USA: Environmental Management, v. 17. p. 83-97.

Vine, J. D., 1963, Surface geology of the Nash Draw Quadrangle, Eddy County, New Mexico: U. S. Geological Survey Bulletin 1141-B.

General Description and Capabilities

The SECO-3D (Knupp, 1995) code was specifically designed for both steady-state and transient regional groundwater flow calculations involving interactions between a free-surface water-table and a realistic topography.

SECO-3D solves the rigorous free-surface equations (i.e., the kinematic or phreatic boundary condition).

The equations solved by SECO-3D are an ordered approximation, therefore the code may be verified through grid convergence testing.
SECO-3D uses a finite volume discretization to achieve second-order spatial accuracy. A fully-implicit first-order accurate time-stepping algorithm is used; there are no restrictions on time-step size due to stability requirements. A steady-state algorithm, developed as the limiting case of the transient algorithm, permits simulation of steady conditions.

The code was designed for simulations that involve strongly heterogeneous and geometrically complicated stratigraphies. The use of 'inactive' cells permits simulations with complicated geometries. Recharge can be time-varying.

The code presently uses a line-SOR solver to handle the 2000-to-1 cell aspect ratios used in this study. Future plans include installation of a three-dimensional multi-grid solver.

Seepage Condition

The kinematic condition is applied wherever the water-table elevation is below the land surface. If the water-table elevation is the same as the land surface, the kinematic condition may need to be converted to a seepage face. The seepage boundary condition is

$$h(x, y, z_{wt}, t_{wt}) = z_{LS}(x, y)$$

where z_{LS} is the local land surface elevation and t is the time at which the water-table encounters the land-surface. To determine whether the kinematic or the seepage boundary condition should be applied, the vertical speed of the water-table,

$$\frac{\partial z_{wt}}{\partial t},$$

is computed. The algebraic sign of the quantity indicates whether or not the water-table is rising or falling. If the water-table at a particular location is rising, the seepage condition is enforced there. If the water-table is falling, the kinematic condition is applied.

Picard Iteration

The numerical algorithm consists of an intra-time-step Picard iteration having the following steps:

The stencil coefficients of the discrete system are calculated from the provisional water-table solution.

The linearized equations are relaxed until the scaled residual is less than the user-specified tolerance.

An outer-residual for the water-table boundary condition is computed.

A 'convergence' test is applied to the outer and scaled residuals. If the tolerances are not satisfied, the water-table position is updated from the boundary conditions and the intra-time-step iteration continues. Otherwise, the calculation proceeds to the next time-step.

The Governing Equations

Mass conservation requires that on the interior of the domain

$$\nabla \cdot K \nabla h = S_s \frac{\partial h}{\partial t}$$

with hydraulic head h as the dependent variable, K, a spatially-dependent conductivity tensor, and S the specific storage. No-flow boundary conditions are imposed on the bottom and vertical sides of the domain, while the following pair of conditions are imposed on the top boundary representing the free-surface:

$$h(x, y, z_{wt}, t) = z_{wt}(x, y, t)$$

$$(K \cdot \nabla h + N) \cdot \nabla (h - z) = S_y \frac{\partial z_{wt}}{\partial t}$$

where z is the elevation of the water-table, N is the normal flux due to recharge and/or evapotranspiration, and S is the specific yield.

The Moving Mesh

The code uses a moving mesh to track the location of the free-surface. The main advantage of the moving mesh is that a finite volume discretization can be used that is second-order spatially accurate even on the boundary. The principle disadvantage of the moving mesh is that it is difficult to maintain grid alignment with stratigraphic layers; SECO-3D addresses this problem by keeping the computational mesh aligned with the stratigraphy except near the water-table surface. Another disadvantage of the moving mesh is that when the water-table position is updated, material properties must be interpolated from the stratigraphic database onto the computational mesh. Because the interpolations are one-dimensional they are not expensive.

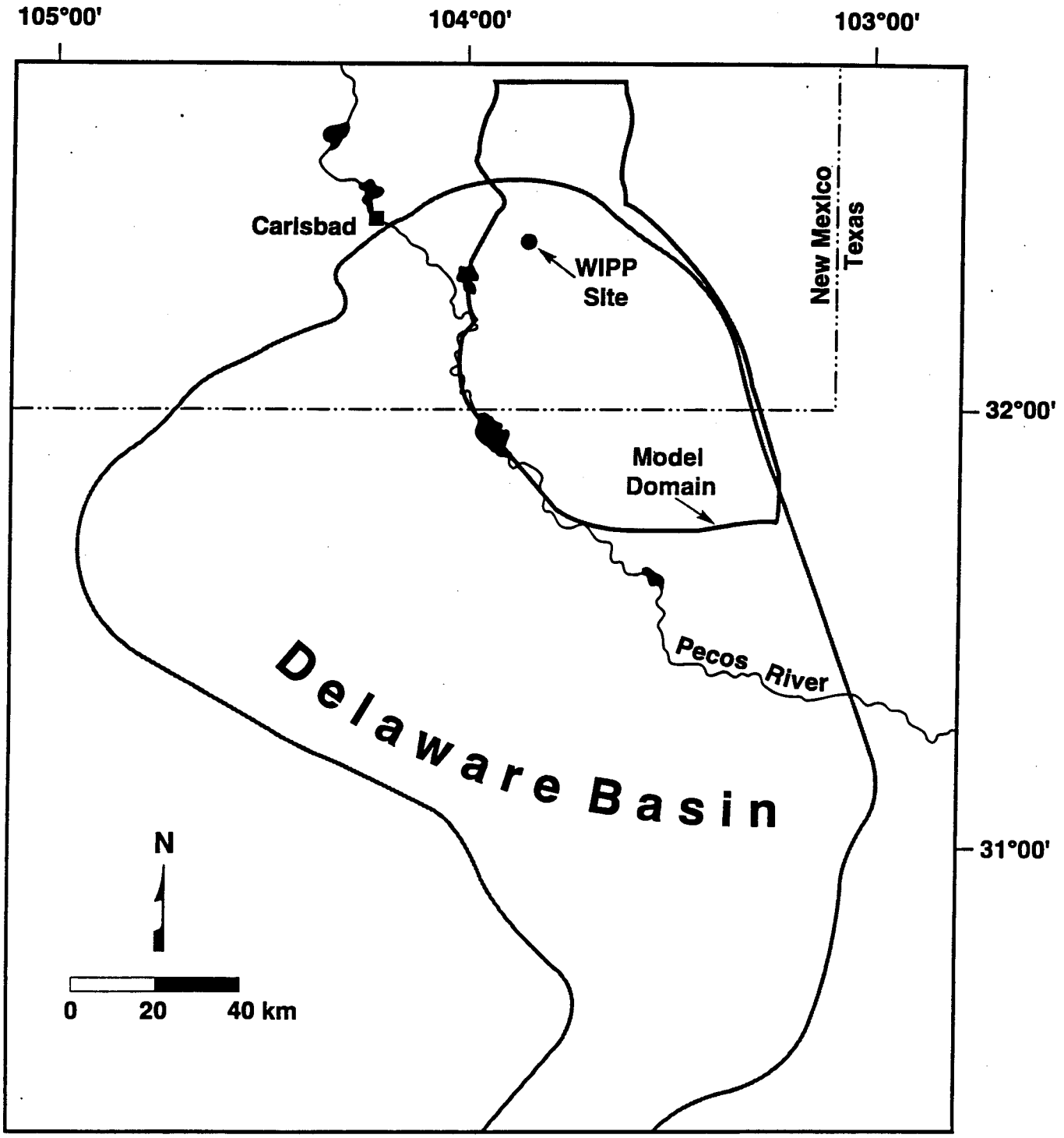

Figure 1

The WIPP repository is located in the Salado Formation, a 600 m thick deposit of bedded salt, in the northern portion of the Delaware Basin (green line). The boundaries of our numerical model (red line) enclose about 6000 square kilometers.

2430-0

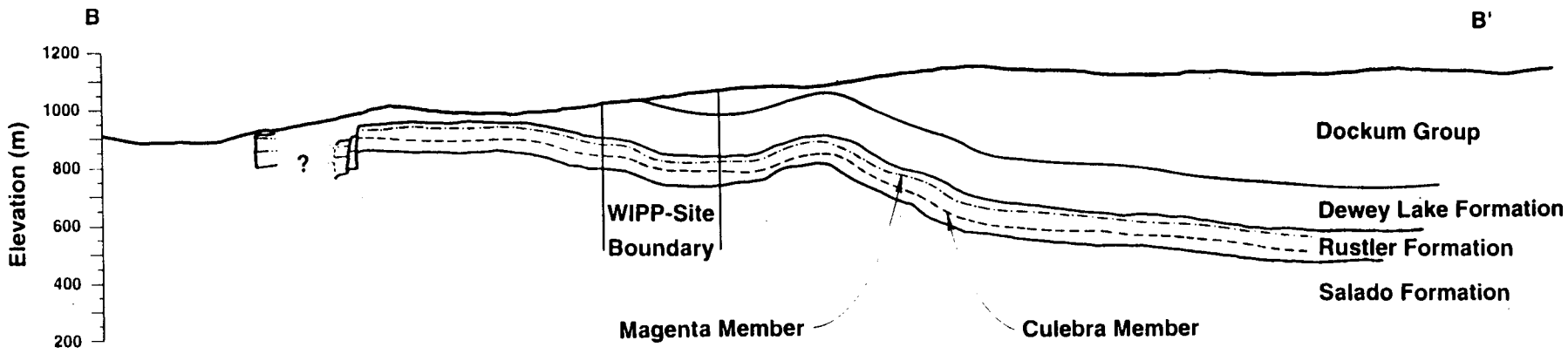

Figure 2

Cross section showing the strata above the Salado Formation. The location of this section is shown on Figure 3. Dissolution of the upper Salado Formation along the west end of the section has disrupted stratigraphic continuity.

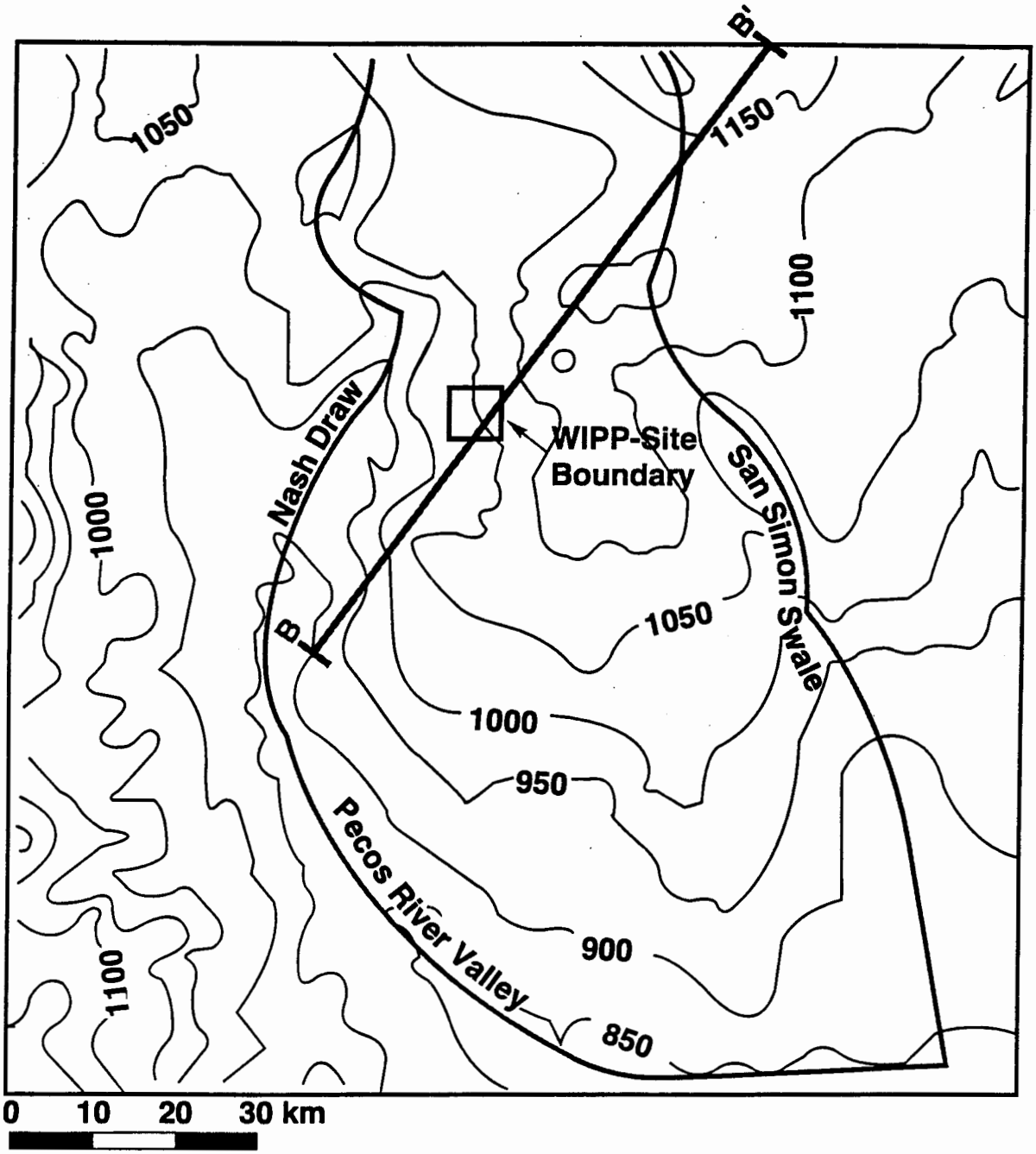

Figure 3

This figure shows the topography of land surface and the lateral boundary of the numerical model (red line). The contour interval for the elevation of the land surface is 50 meters. The model boundary follows groundwater divides that we believe are valid for the entire period of time simulated. It follows major topographic depressions such as Nash Draw and the Pecos River valley to the west and south and the San Simon Swale to the east. The boundary continues up drainages and dissects topographic highs in the northern part of the model region. We use a no-flow boundary condition along the entire length of the lateral boundary to represent groundwater divides.

2432-0

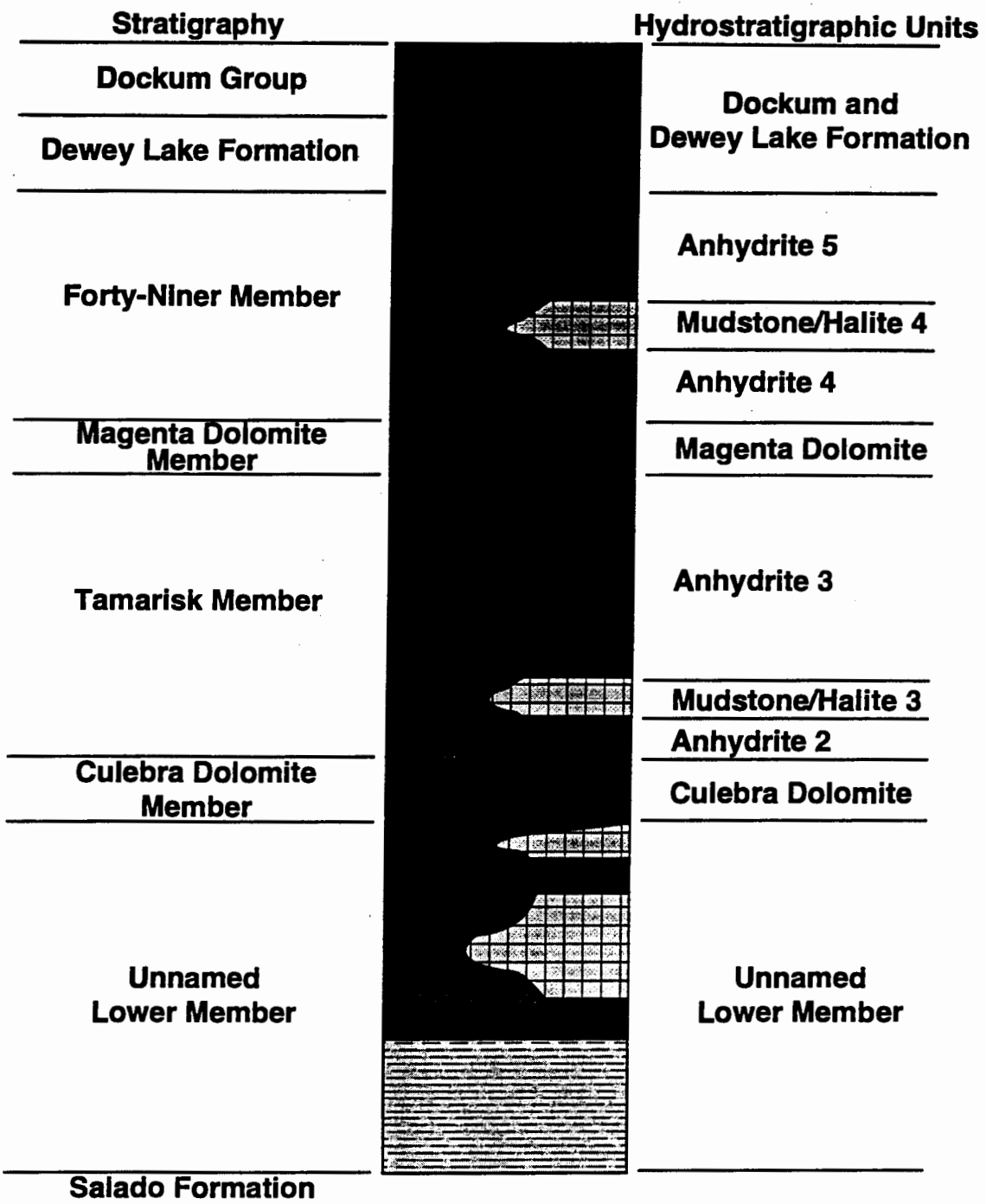

Figure 4

The Rustler Formation is a 100 meter thick sequence of dolomite, anhydrite, mudstone, and halite. The dolomite members are the most permeable units in the formation. We divided the Rustler into nine hydrostratigraphic units for these simulations. The Dewey Lake Formation and the Dockum Group were combined as one additional hydrostratigraphic unit. This unit ranges in thickness from 0 meters in Nash Draw where it has been removed by erosion, to 600 meters in a graben that runs along the southern portion of the eastern model boundary. [Modified from Powers and Holt (1990); original stratigraphy from Vine (1963)].

2433-0

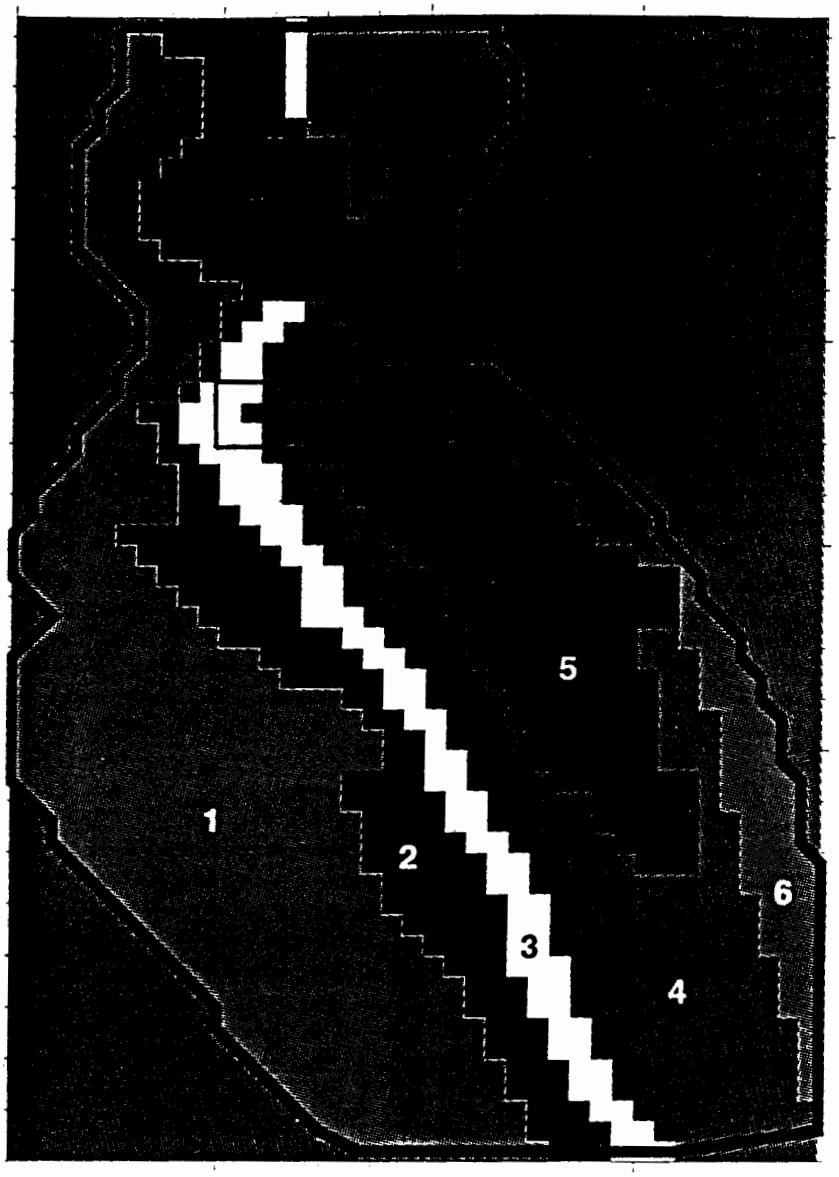

Figure 5

We used a zonation approach to assign a hydraulic conductivity distribution to each model layer in order to represent the effects of depositional setting and post-depositional processes. Zone 1 is a region in which dissolution of the upper Salado has fractured and disrupted overlying strata to the extent that stratigraphic layering is not preserved over long distances. In Zone 2, dissolution of the upper Salado is thought to have fractured the Rustler, but did not disrupt layering. Fractures that pre-date dissolution of the upper Salado are mostly filled with gypsum. These fracture fillings have been removed in Zone 3. Zone 4 represents intact strata. The region occupied by the halite facies of the mudstone/halite layers is indicated by Zone 5. A Permian-age graben structure is shown as Zone 6.

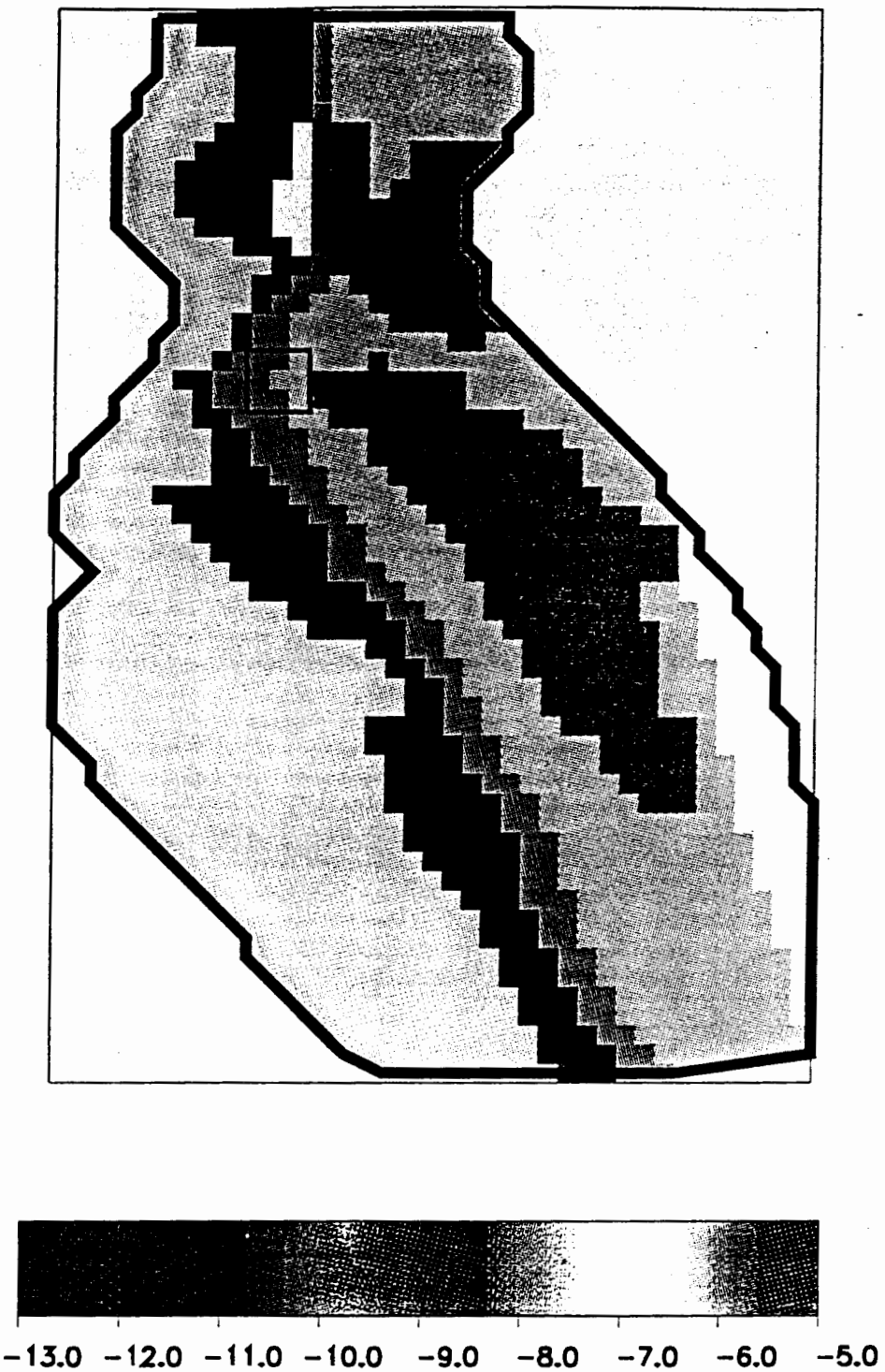

Figure 6

Distribution of Log of Hydraulic Conductivity (meters/second) Used for the Culebra Dolomite

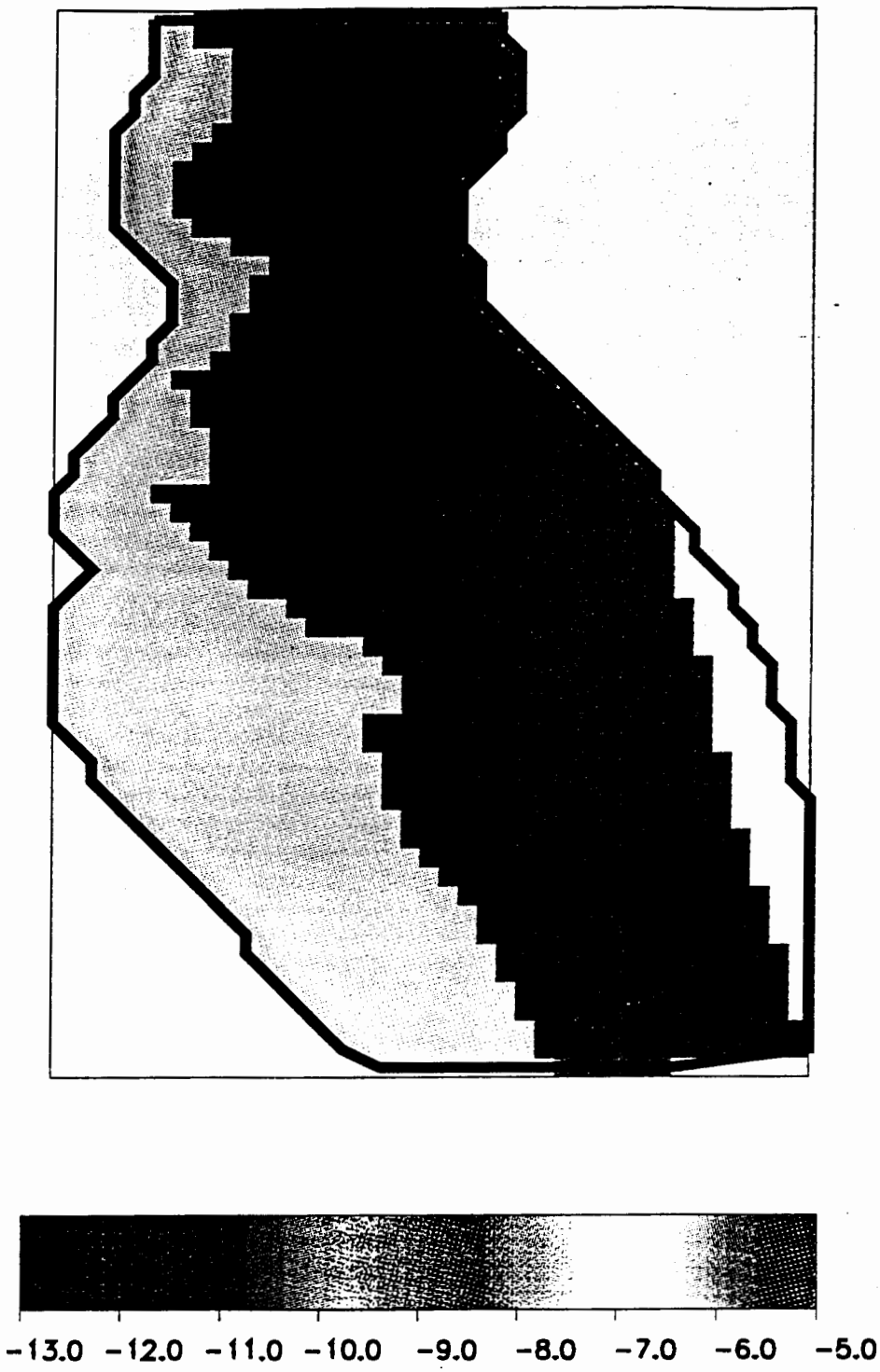

Figure 7

Distribution of Log of Hydraulic Conductivity (meters/second) Used for the Anhydrite Units

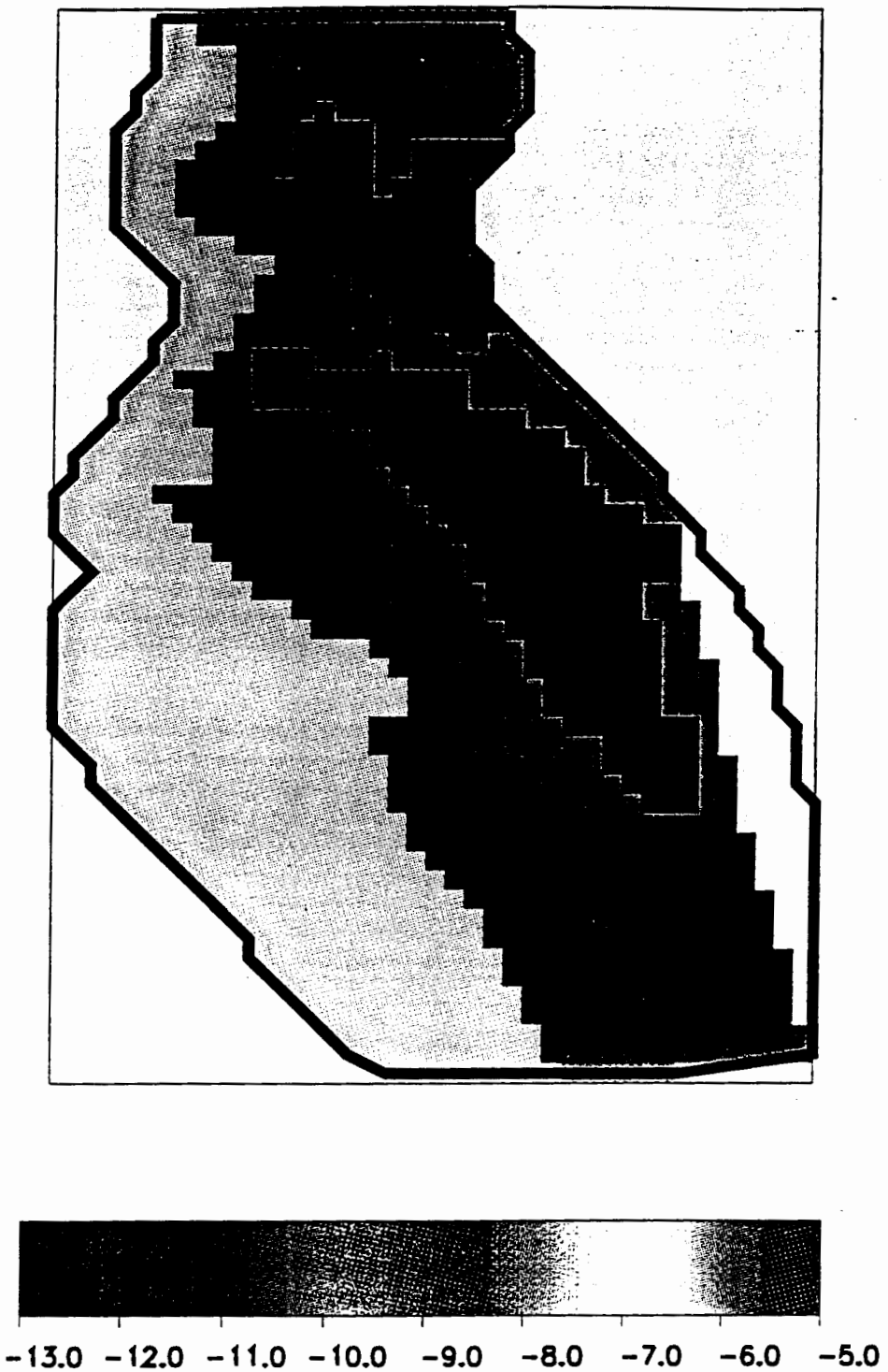

Figure 8

Distribution of Log of Hydraulic Conductivity (meters/second) Used for the Mudstone/Halite Units

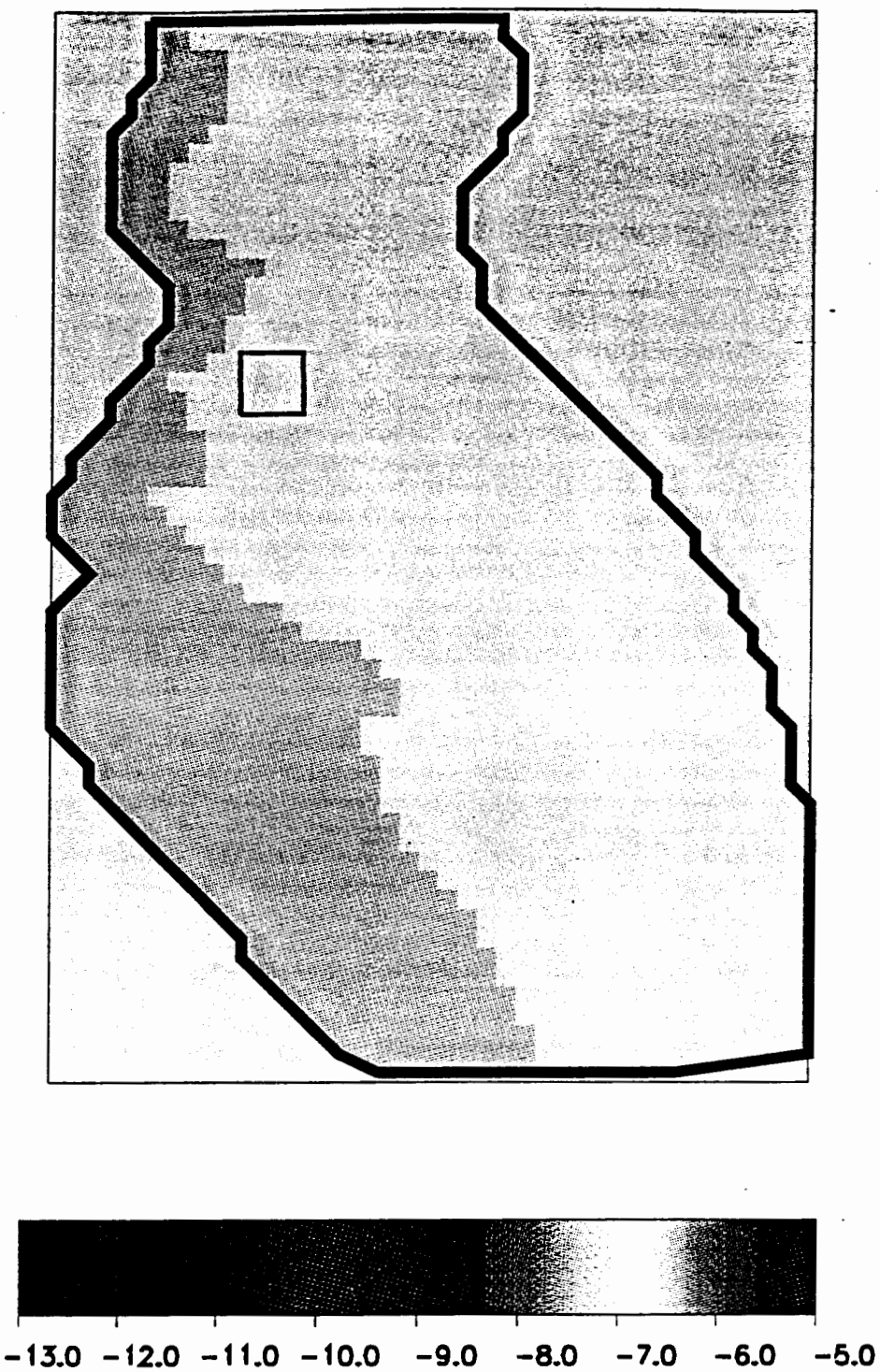

Figure 9

Distribution of Log of Hydraulic Conductivity (meters/second) Used for the Combined Dewey Lake Formation and Dockum Group

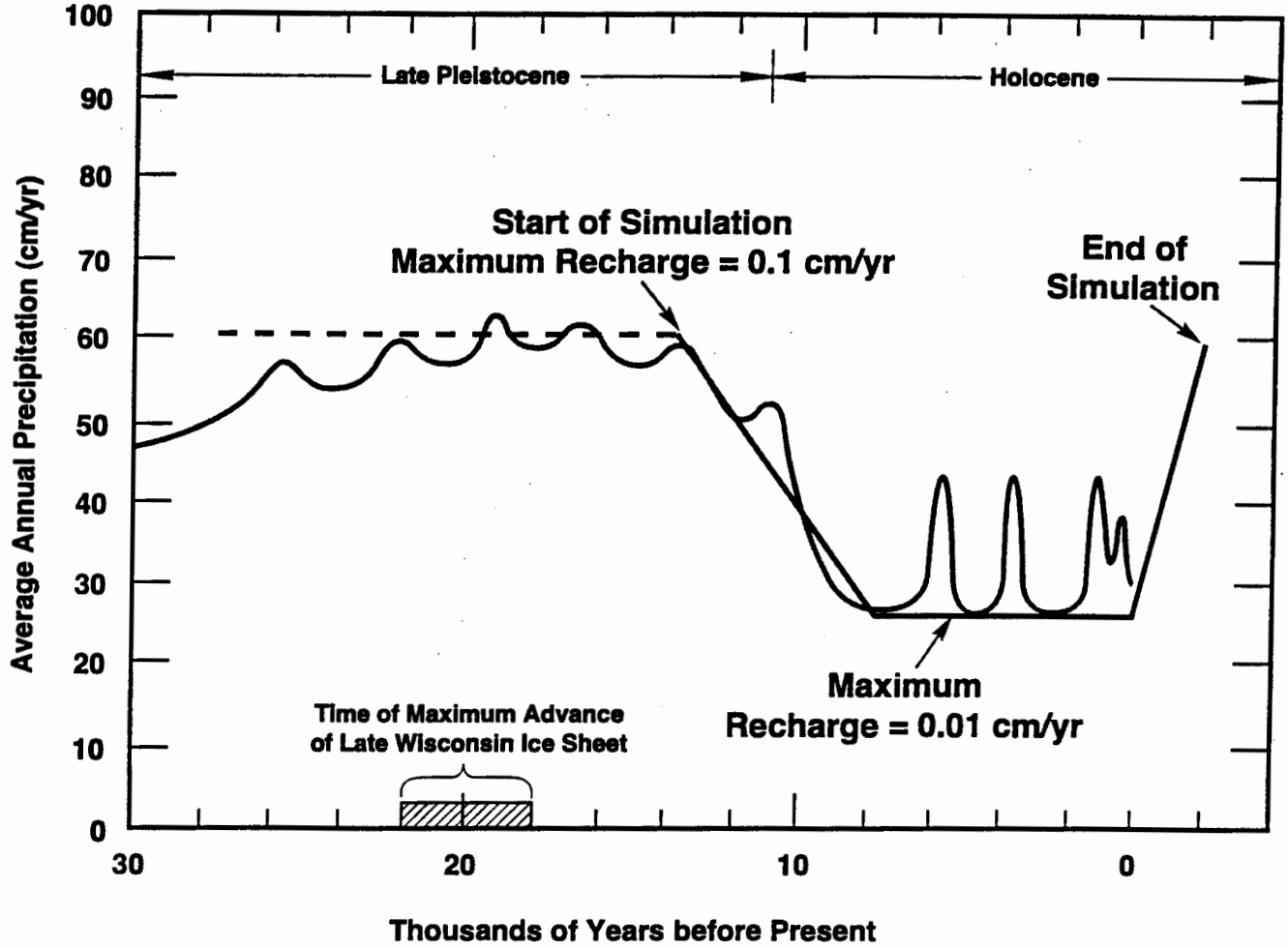

Figure 10

The present-day climate at the WIPP is arid to semi-arid. The mean annual precipitation is estimated to be between 28 and 34 cm/yr (Hunter, 1985). This figure shows the estimated mean annual precipitation at the WIPP (blue line) during the past 30,000 years (Swift, 1993). The simulations presented here are designed to represent the drying of the climate that is thought to have occurred over the period from 14,000 to 8,000 years before the present.

We don't have a reliable method to correlate mean annual precipitation with the rate at which the groundwater system is recharged. In these simulations we used rates of maximum potential recharge ranging from 0.01 to 0.1 cm/yr (red line) to represent the change in climate over the past 14,000 years. The larger rate of recharge is more than sufficient to maintain the water table close to the land surface. The smaller rate results in hydraulic heads in the Rustler Formation that are similar to those observed today. In addition to representing the past climate, we have added a rapid increase in recharge to examine the impact of a hypothetical sharp increase in precipitation over the next several thousand years.

2431-0

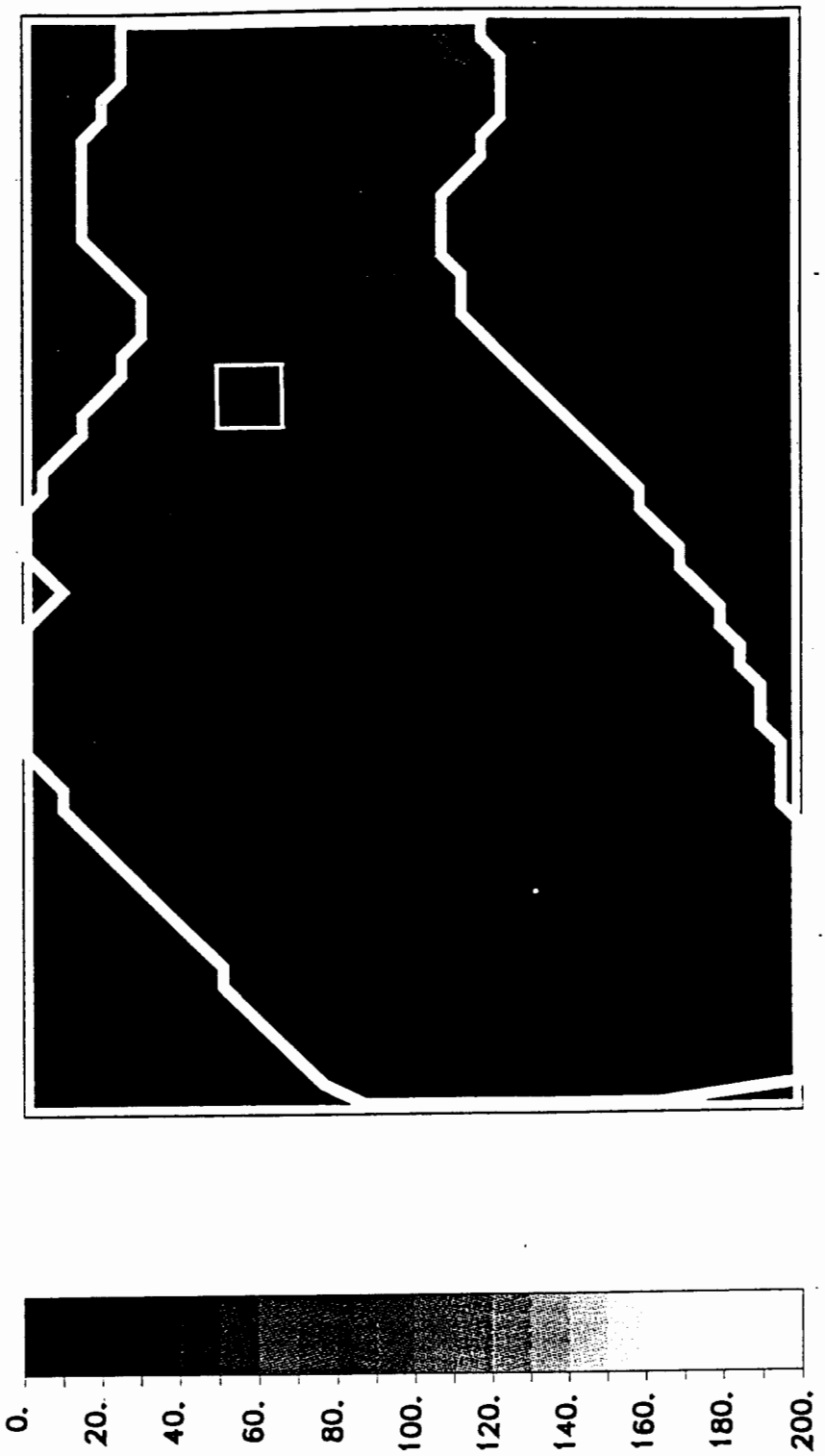

Figure 11

Steady-State Depth to the Water Table (meters)
Maximum Potential Recharge = 0.1 cm/yr

Figure 12

Steady-State Water Table (meters)
Maximum Potential Recharge = 0.1 cm/yr

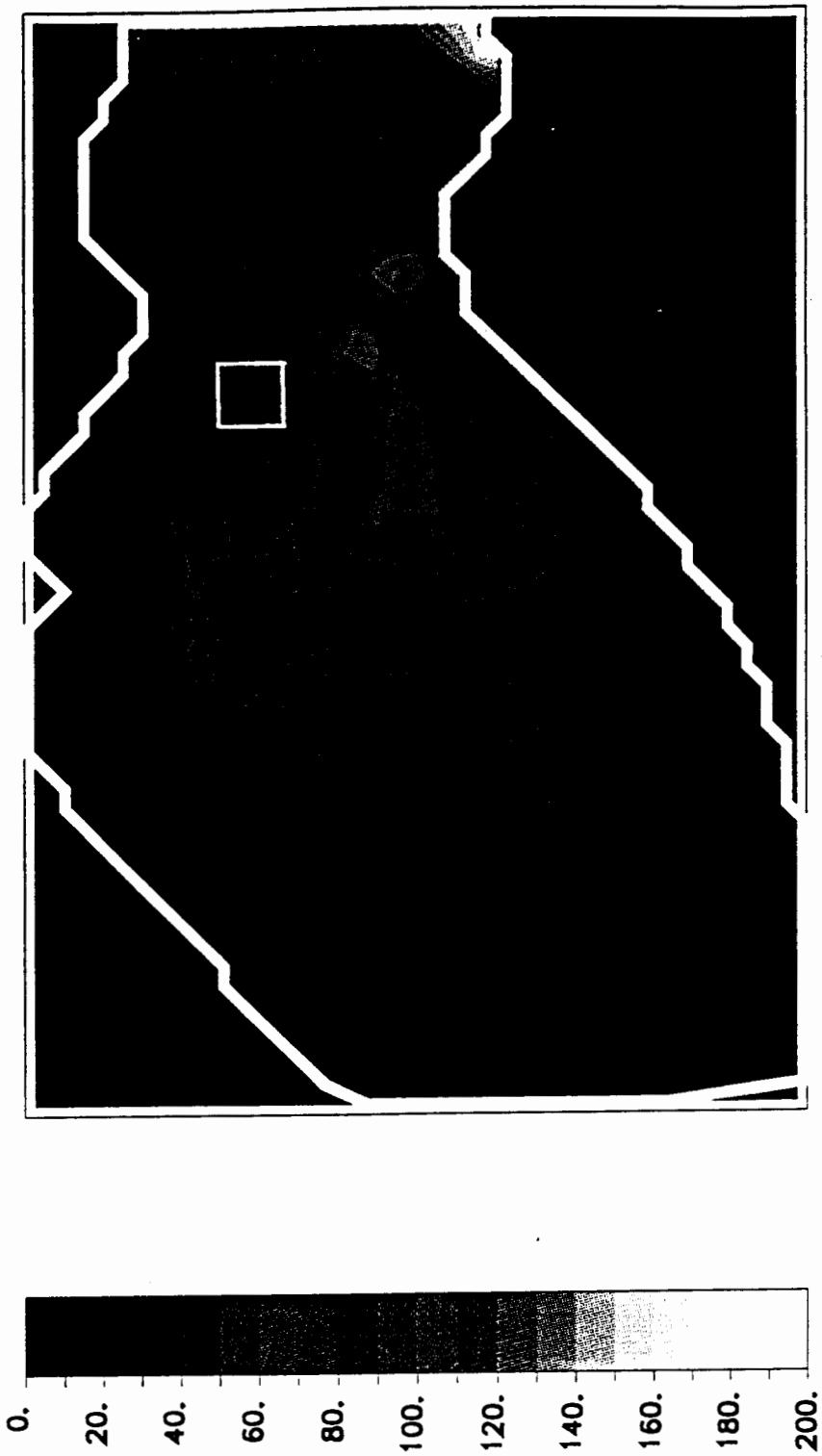

Figure 13

Steady-State Depth to the Water Table (meters)
Maximum Potential Recharge = 0.01 cm/yr

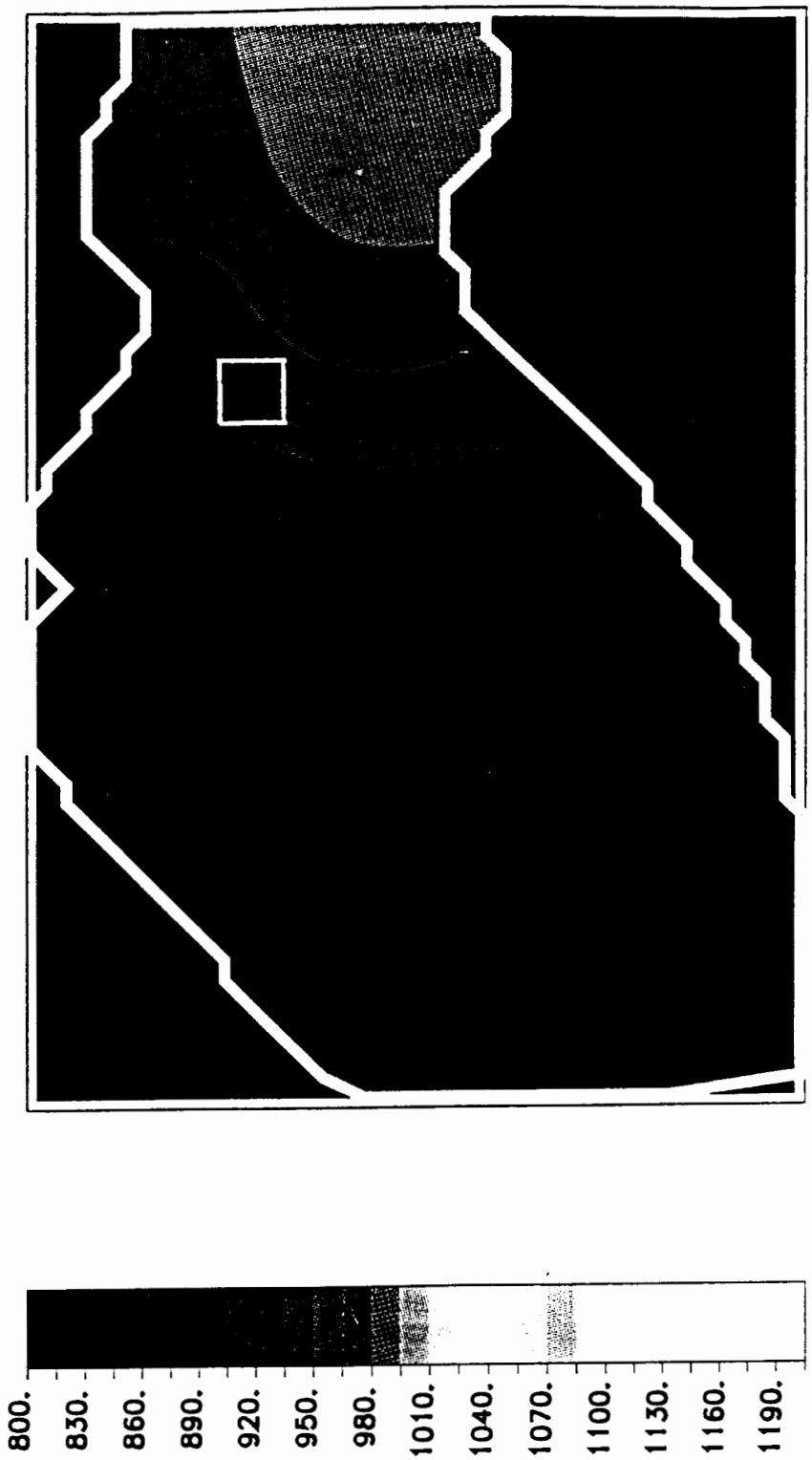

Figure 14

Steady-State Water Table (meters)
Maximum Potential Recharge = 0.01 cm/yr

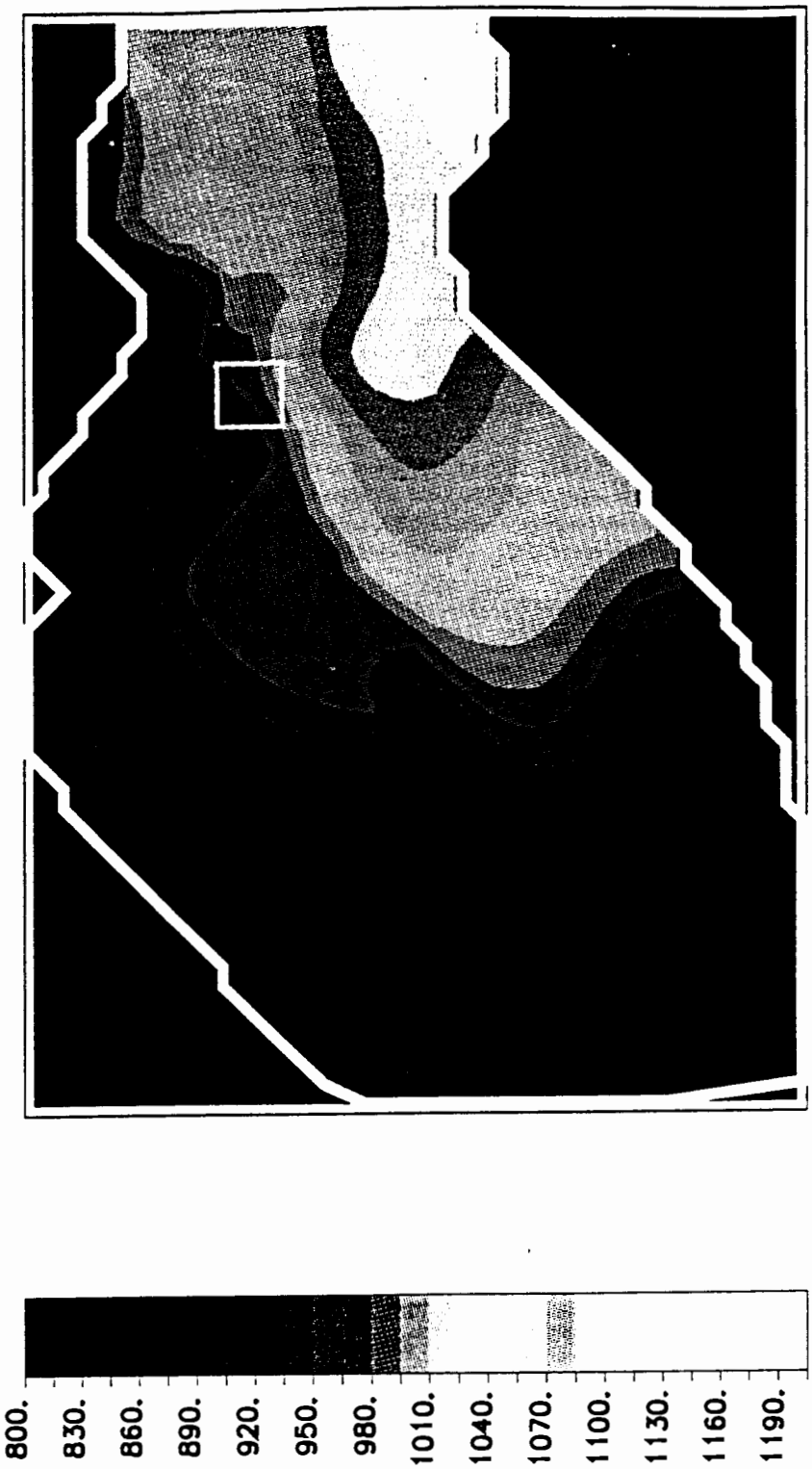

Figure 15

Steady-State Hydraulic Head in the Culebra (meters
Maximum Potential Recharge = 0.1 cm/yr

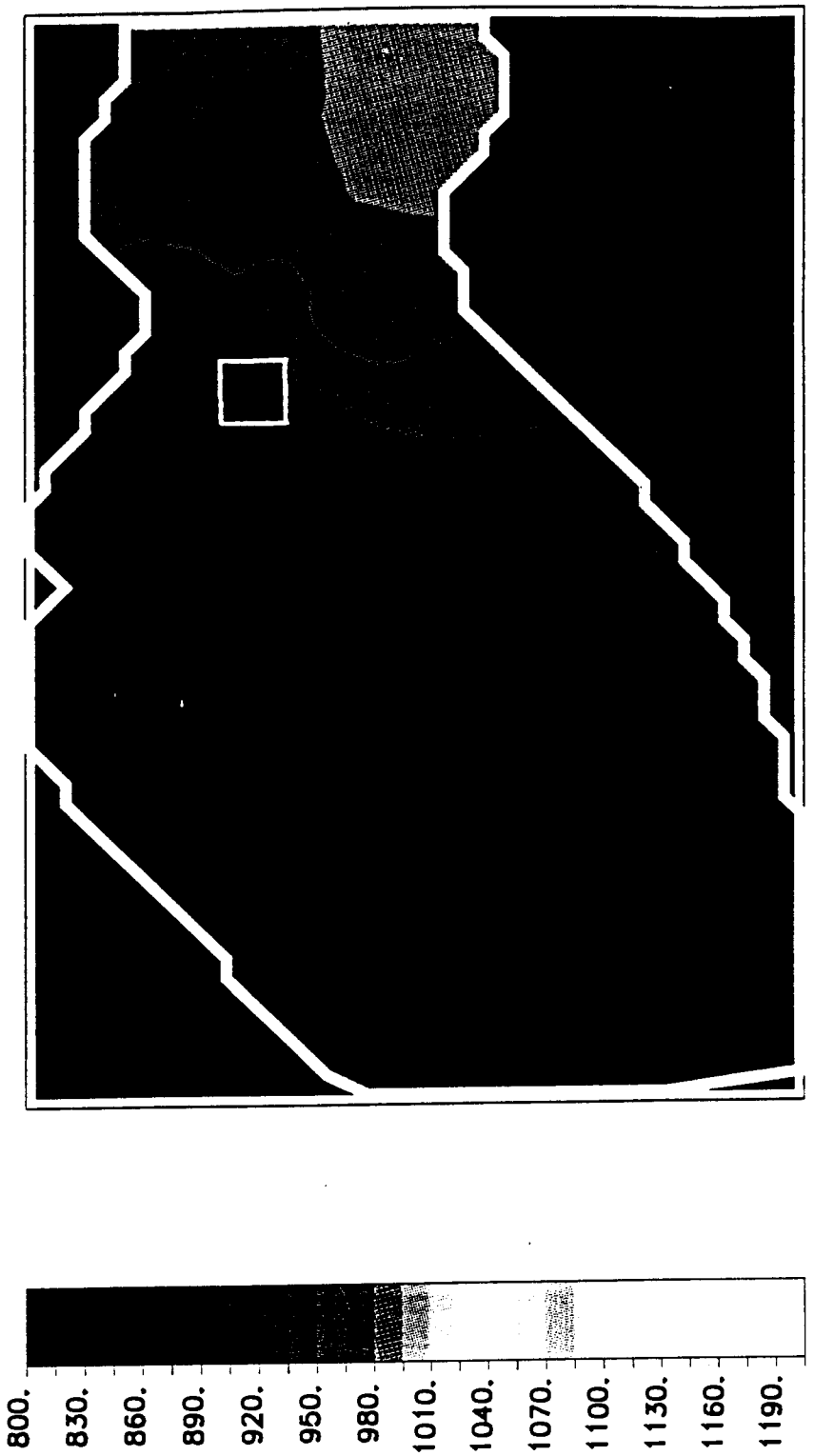

Figure 16

Steady-State Hydraulic Head in the Culebra (meters)
Maximum Potential Recharge = 0.01 cm/yr

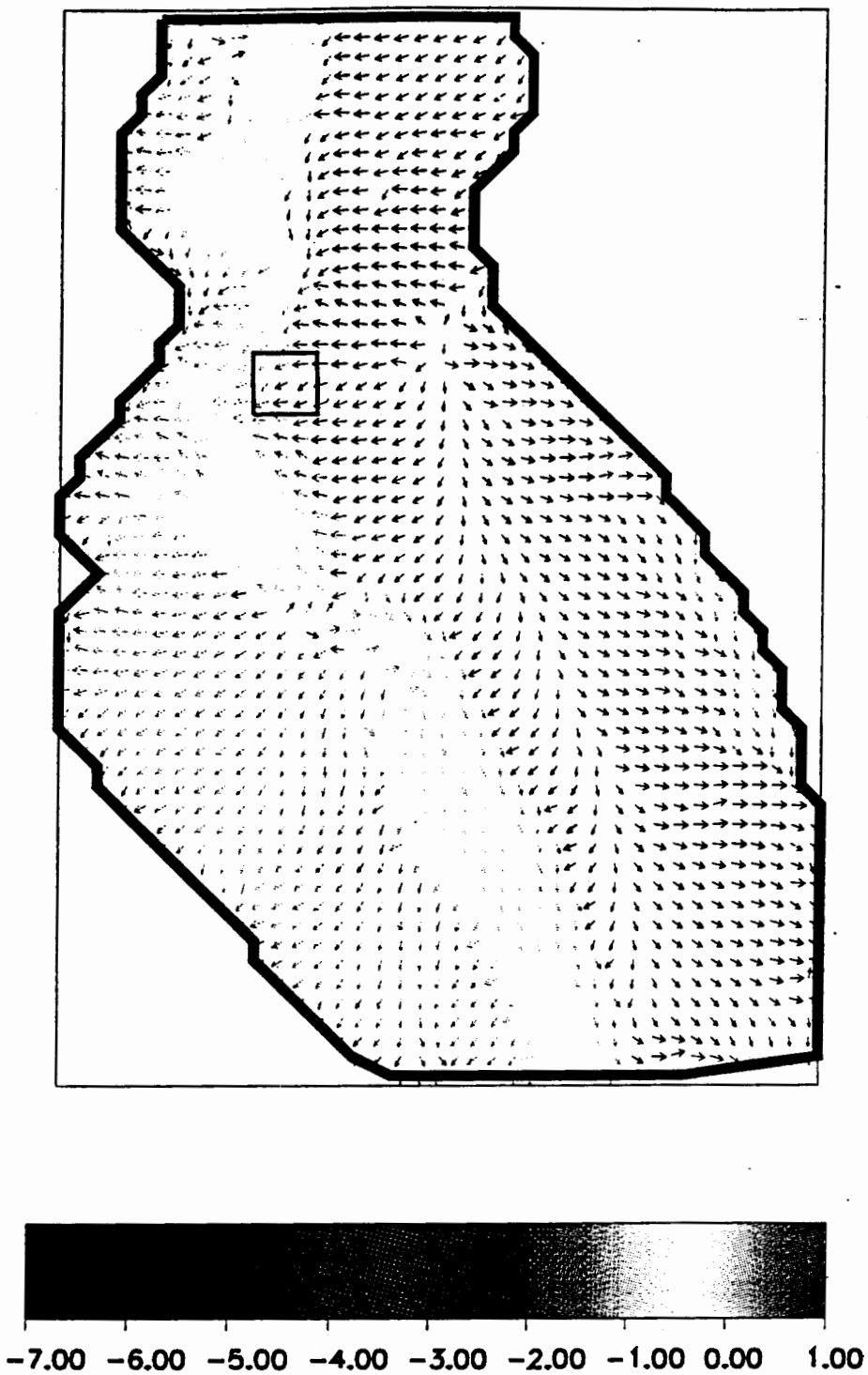

Figure 17

Log of Steady-State Specific Discharge in the Culebra (meters/year
Maximum Potential Recharge = 0.1 cm/yr

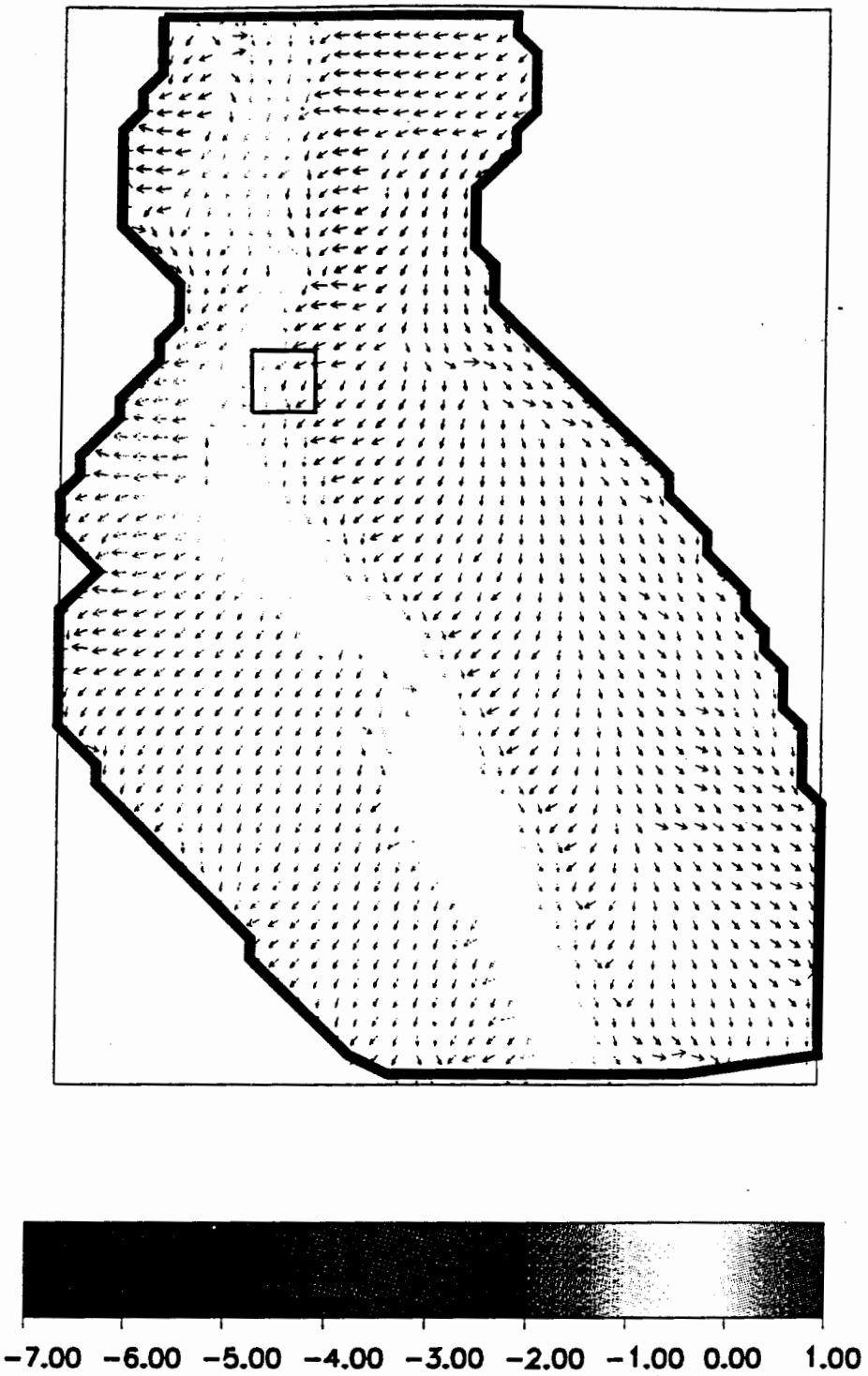

Figure 18

Log of Steady-State Specific Discharge in the Culebra (meters/year)
Maximum Potential Recharge = 0.01 cm/yr

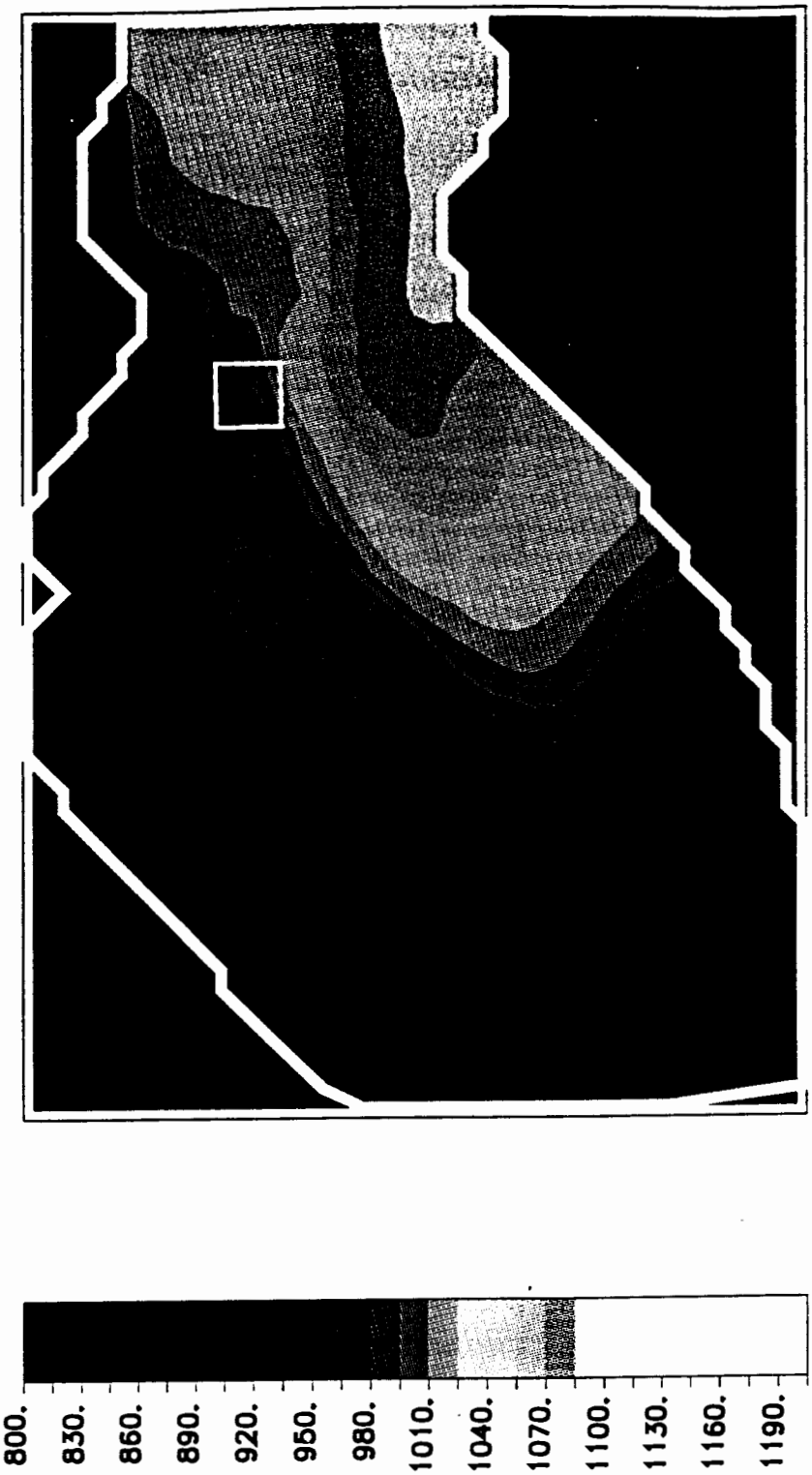

Figure 19

Hydraulic Head in the Culebra (meters) at 8,000 Years Before Present

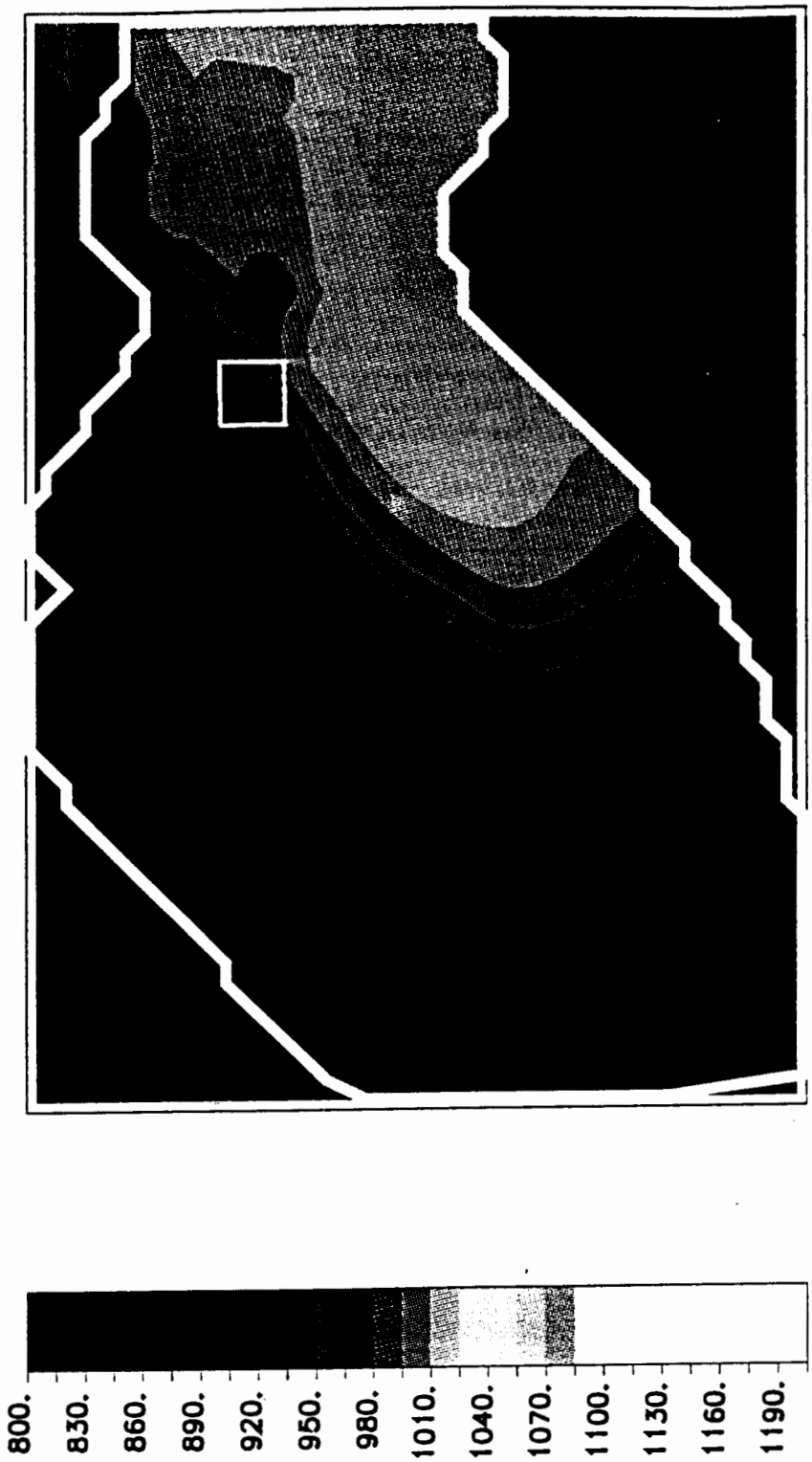

Figure 20

Hydraulic Head in the Culebra (meters) at the Present Time

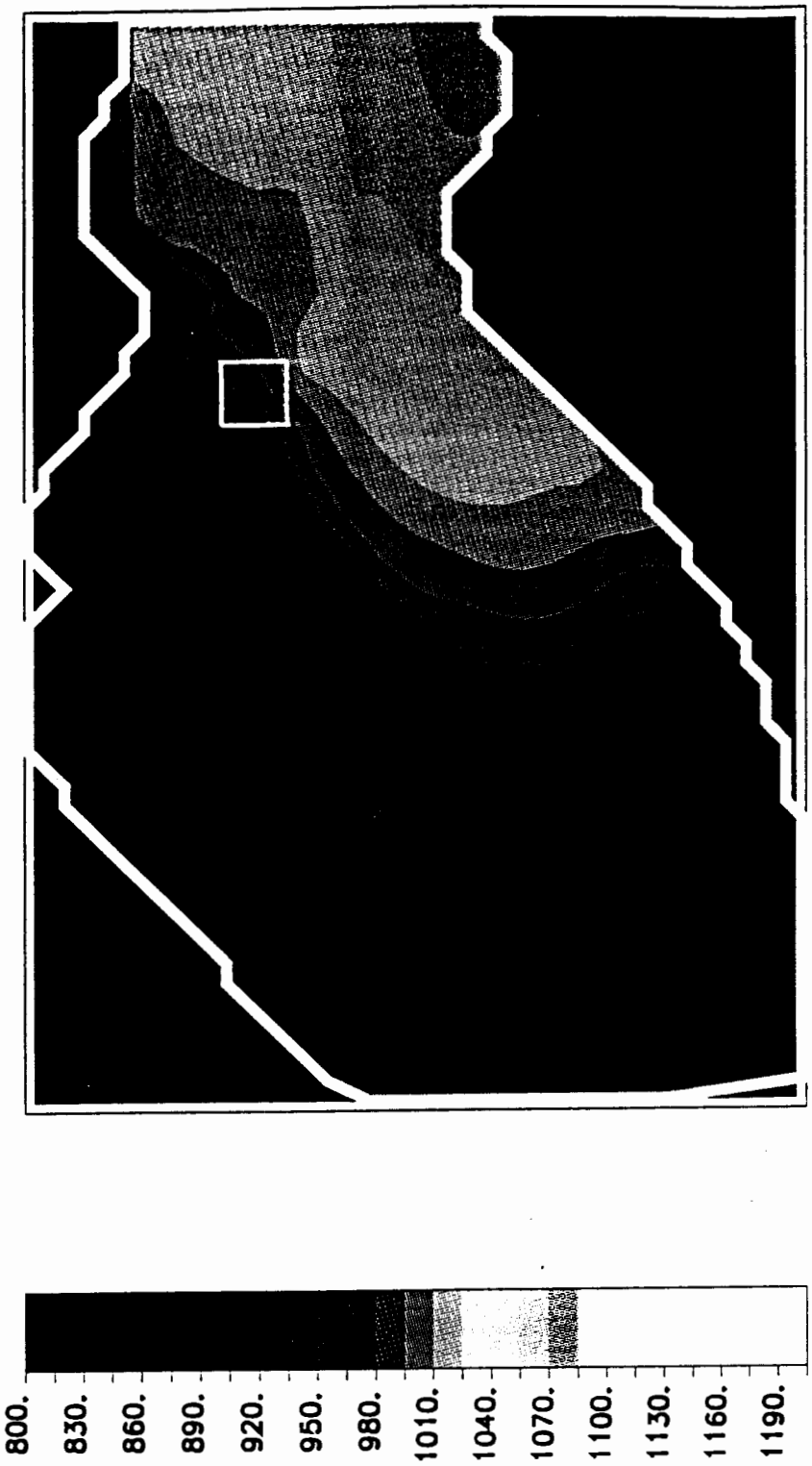

Figure 21

Hydraulic Head in the Culebra (meters) at 2,000 Years in the Future

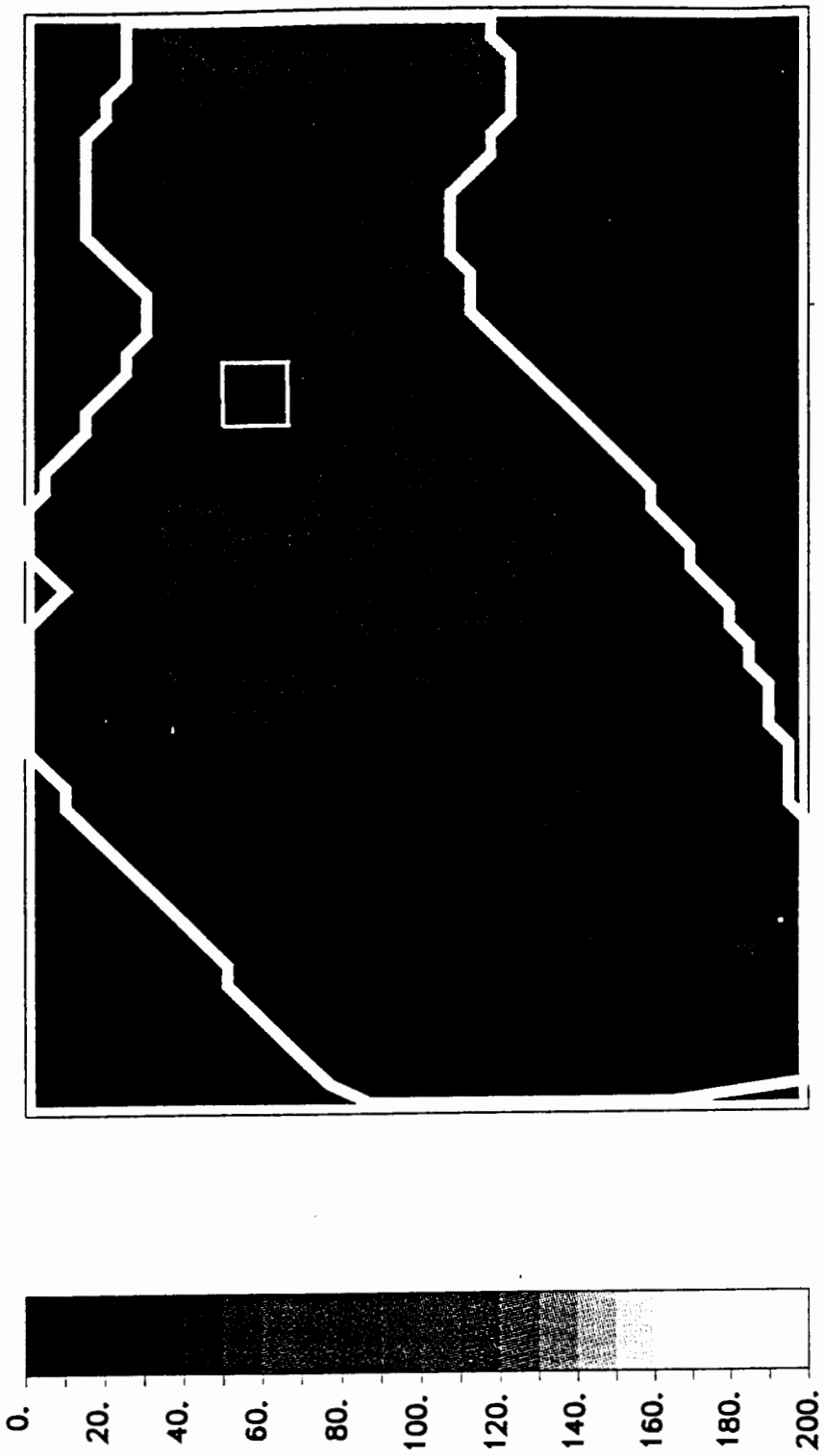

Figure 22

Depth to the Water Table (meters) at the Present Time

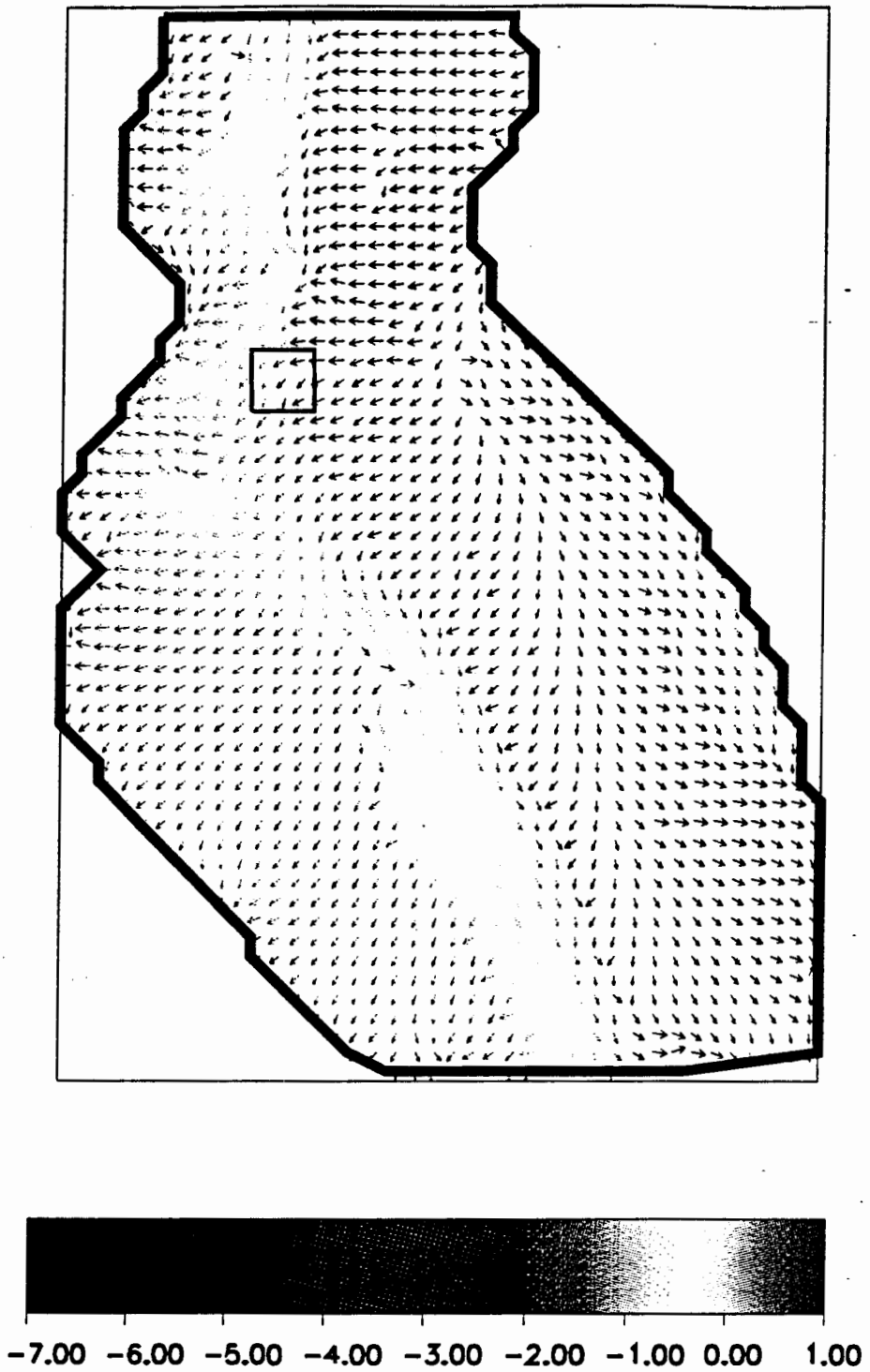

Figure 23

Log of Specific Discharge in the Culebra (meters/year) at the Present Time